Methanol Carbonylation

with Metal/Zeolite Catalysts

G. P. FULLER

A thesis submitted in partial fulfilment of the requirements of
The Nottingham Trent University for the degree of Doctor of Philosophy

This research programme was carried out in collaboration with BP Chemicals Ltd.

January 2002

Abstract

The industrial production of acetic acid currently uses a homogeneous methanol carbonylation process that requires the presence of a halide promoter. The commercially viable formation of further products, e.g. ethanol, via this route is restricted by the halide impurities in the intermediate acetic acid. Considering the growing importance of methanol, as a feedstock from natural gas, over that of the established petrochemical resources, there is an incentive for the development of a halide free acetic acid process. Heterogeneous catalysts, especially protonated zeolites incorporating copper, have previously been reported to produce acetic acid by methanol carbonylation, in the absence of a halide promoter, and these form the basis of this work.

The carbonylation of methanol, has been carried out here in a fixed bed reactor under conditions typically of 350°C, 8 bar gauge and a CO : methanol ratio of 8.8 : 1.

The two main aims of the work have been to determine (i) the role of copper and (ii) the effect of the zeolite's pore structure.

Mordenite zeolites of different silica/alumina ratios were studied both in their proton and copper forms. Copper was introduced using several techniques, including ion-exchange, impregnation and solid state exchange. It was found that copper significantly promoted the proton form only when it was introduced by ion-exchange.

Examples of zeolites with different framework structures, e.g. ZSM-5, theta, and beta, were similarly studied in both their proton and copper forms. It was confirmed that the unique pore structure of mordenite, large pores containing narrow side pockets, was the most productive for methanol carbonylation.

On comparing the reactivity of the different catalysts tested, this work concludes that the carbonylation of methanol occurs at Bronsted acid sites and is therefore in direct competition with hydrocarbon formation.

Furthermore, if the Bronsted acid sites are isolated from each other, e.g. in the narrow channels of H/theta, then the carbonylation reaction is promoted. Conversely, high concentrations of methanol activated in the channel intersections of H/ZSM-5 or H/beta cause the preferential formation of hydrocarbons.

Acknowledgments

Thanks to everyone, who has been involved in any small way with this project.

Contents

CHAPTER 1

METHANOL CARBONYLATION

The product acetic acid, its uses and manufacture

Acetic acid is a major product of the chemicals industry. BP Chemicals Ltd., holds a leading position in the manufacture of acetic acid from methanol, currently producing over 2 million tonnes annually[1]. The majority of the acetic acid becomes the feedstock in further chemical processes, e.g. for production of the esters: ethyl acetate, n-butyl acetate and iso-propyl acetate. The final products have a wide range of applications, e.g. for the polymers used in paints and printing inks.

The first commercial homogeneous process[2] for the production of acetic acid from methanol, introduced by BASF in 1960, used a cobalt species that required a halide promoter under severe operating conditions (250°C, 680 bar) to produce a 90% methanol selectivity to acetic acid.

In 1970, the cobalt species was replaced by a rhodium one in the Monsanto process, which under less severe conditons (150-200°C, 30-60 bar) gives 99% methanol selectivity to acetic acid, but still with the halide promoter. BP Chemicals bought the exclusive licensing rights to the Monsanto process in 1986. The catalytic cycle for the rhodium species in the Monsanto process is illustrated[3] below in Figure 1.1.

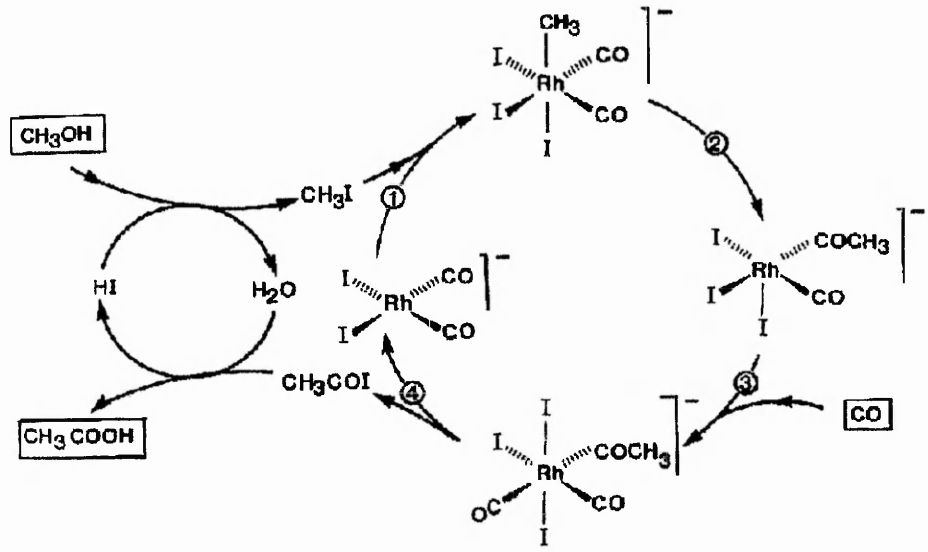

Figure 1.1 The catalytic cycle for the Monsanto Process, reproduced from reference 3.

The mechanism, for carbon monoxide insertion into methanol by rhodium, has been studied by high pressure infra red studies[2]. Rhodium, normally introduced as rhodium (III) iodide, readily converts under the reaction conditions to the active rhodium (I) species $[RhI_2(CO)_2]^-$. Methyl iodide, the preferred promoter, has to be present in excess to give viable conversion rates. Using acetic acid, as the solvent, prevents the formation of dimethyl ether from methanol. The reaction, first order in both rhodium and methyl iodide, is independent of the methanol concentration. Methyl acetate is readily formed from methanol and the acetic acid solvent, methyl iodide then forms by the reaction of the methyl acetate with hydrogen iodide. Oxidative addition (step 1) of methyl iodide, to the active rhodium (I) species $[RhI_2(CO)_2]^-$, is the rate determining step. The rhodium methyl complex is not observed because the methyl migration (step 2), being driven by the insertion of carbon monoxide (step 3), occurs rapidly to form the rhodium acyl species. Reductive elimination (step 4) of acetyl iodide, forming acetic acid and hydrogen iodide in the presence of water, regenerates the active rhodium species. However, to maintain the reaction rate and prevent the loss of rhodium by precipitation, the Monsanto process requires a high water concentration in the reactor. Productivity is limited by the necessity for multiple distillation columns, to retain the high water concentration within the reactor, and by the drying columns required for further purification of the product stream.

In 1996, BP Chemicals Ltd. replaced the rhodium for a similar iridium species, with the introduction of the Cativa™ process[4]. Capable of being fitted to the existing carbonylation plants, the Cativa™ process operates at lower water concentrations than the Monsanto process. The necessity for one of the distillation columns is therefore removed. The 'debottle-necking' of the existing plants and a significant reduction in operating costs, are currently supporting the introduction of new and larger capacity plants[5]. The stability of the iridium species, in the low water concentrations, is more intricate and therefore its mechanism shall not be discussed further here. Workers at Monsanto found iridium to be active[2], for methanol carbonylation, at the time rhodium was being developed. But, the dependence of iridium on low water concentrations prevented its commercialisation at that time.

DEVELOPMENTS ON THE HOMOGENEOUS PROCESS

Supported rhodium in the liquid phase

A major problem, encountered when operating the Monsanto process, has been the loss of the active homogeneous rhodium species during product separation.
Attempts, to overcome catalyst loss, have concentrated on supporting the rhodium species in the presence of the halide promoter.
By 1992, according to the review[2] by M. Howard et al., the supports tested in the liquid phase reaction were either polymer resins or activated carbons. In both cases, pendant phosphine groups linked rhodium to the support. However, there is little presented evidence for the rhodium being immobilised on the support[6]. The observed activity was probably, analagous to the Monsanto process, due to a liquid phase rhodium species.
To date, other supports tested for rhodium in the liquid phase have included (i) silica with pyridine pendant groups[7], (ii) zirconia[8], and (iii) hydrotalcite[9]. In the first two cases leaching is openly reported, but in (iii), no clear evidence is presented to confirm the supported metallic rhodium particles are the active catalyst.

Supported rhodium in the vapour phase

The use of a heterogeneous catalyst allows easier product separation, especially if the reactants are maintained in the vapour phase. At the time of the review[2] by M. Howard et al., the only example of a polymer resin was under the mild conditions of 100°C and atmospheric pressure. The conditions, being limited by the resins poor thermal stability, although productive would be unfavourable on a commercial scale because of the slow rate (0.04 h^{-1}) of product formation.
Rhodium supported on several polyvinylpyrrolidone (PVP) polymers[10,11] has recently been found to be productive, in the presence of iodide, and retained on the support even under the more severe vapour phase conditions.
Rhodium supported on activated carbon was found to be productive by Monsanto[2] under vapour phase conditions, but not for long enough periods to be commercially viable. A large number of the available activated carbons[12], including pyrolysed PVP polymers[13], have subsequently been studied. Although productive, leaching is still a major problem for these catalysts.
Although not recently studied, vapour phase carbonylation, in the presence of iodide,

has been carried out using rhodium on inorganic oxide supports. It is thought[2], a neutral Rh(I) dicarbonyl species is present on silica, but an anionic Rh(I) dicarbonyl species is present on alumina and silica-alumina. A rapid loss of rhodium was observed from the silica support. The catalytic activity observed, for the strongly held anionic species, was attributed to the acid-base character of both alumina and silica-alumina.
Similarly, zeolites as supports for the rhodium system have not been studied since the review of M. Howard et al. Certain rhodium exchanged zeolites are active for methanol carbonylation. Rh/NaY, being analogous to silica, forms a neutral dicarbonyl species that is inactive, while Rh/NaX, similar to the homogeneous catalyst, forms an active anionic rhodium species.

Different supported metal species

Under the more severe vapour phase reaction conditions, supported metal species other than rhodium have been tested. Replacement of the rhodium, with a less expensive but productive alternative, is one solution to overcome the loss of the expensive catalyst component. One widely studied catalyst, has been nickel supported on activated carbon[2,14], which in the presence of iodide and under similar conditions, gives a rate one third of that for Rh/C. However, a major problem above 200°C is the competitive formation of inert nickel carbide[15]. Furthermore, nickel supported on other common supports, such as silica or alumina, favours dissociative chemisorption of carbon monoxide followed by hydrogenation, rather than the desired non-dissociative chemisorption and subsequent carbonylation[2]. Attempts to overcome these problems have included the incorporation of additional metal species, e.g. tin[16] and palladium[2], to control the dispersion of nickel on the activated carbon. Tin and palladium, when separately supported on activated carbon, show low levels of carbonylation activity that, as for nickel, is understood to arise from the active carbon support. The conducting support decreases the band gap, between the metal's oxidised and reduced states, to promote the reductive elimination of the acetyls product. The rate determining step for these supported catalysts is the insertion of carbon monoxide. In contrast, the slow step in the homogeneous rhodium process is the oxidative addition of methyl iodide, where once formed the methylated species can not be isolated.
Iridium on activated carbon[17] has a similar activity to supported rhodium and, as for supported nickel, the rate is independent of the methyl iodide concentration.

REMOVAL OF THE HALIDE PROMOTER

The successful replacement of rhodium by iridium, as described above, indicates further replacement, of the homogeneous process, is not economically viable solely for the production of acetic acid and its ester derivatives.

However, increasing the versatility of methanol, a C_1 feedstock readily produced from methane, is extremely desirable considering the growing world resources of methane. For the further products possible from the intermediate acetic acid, e.g. ethanol, a total absence of the iodide promoter would be required to prevent poisoning the downstream hydrogenating catalyst. The controlled formation of a single carbon-carbon bond from the C_1 feedstock, in the complete absence of a halide promoter, is therefore of both academic and commercial interest.

The formation of methyl iodide is the established route to cleave the strong carbon-oxygen bond of methanol. The iodide species is unique, in its ability to act both as a good nucleophile and leaving group, which explains its use to promote the carbonylation of methanol for the range of different catalysts described. Activation of the carbon-oxygen bond requires an increase in charge separation, with the electron density preferably moving towards the oxygen. One alternative for activating the carbon-oxygen bond, in the absence of the iodide as a nucleophile, is to protonate the oxygen.

Homogeneous carbonylation by strong acids

The formation of tertiary carboxylic acids, in the presence of strong acids e.g. phosphoric acid, occurs at high pressures (> 200 bar) by the carbonylation of alkenes in the Koch[18] reaction. G. Olah[19] using superacids such as HF-BF_3 has reported the homogeneous carbonylation of methanol in the absence of halide.

In the presence of strong acids the carbonylation of olefins and alcohols, via the Koch reaction, under mild conditions (25°C, 1 bar) occurs readily in the presence of Cu(I) carbonyl catalysts[20]. The species $[Cu(CO)]^+$ detected by FT IR and ^{13}C NMR is relatively stable in acidic solutions[21]. However, at high acid concentrations under carbon monoxide, the active species $[Cu(CO)_n]^+$ (where n = 3 or 4) is formed. The strong acid conditions create a carbenium ion, from the olefin, that undergoes carbon monoxide insertion from the unstable $[Cu(CO)_n]^+$ species to produce alkanoic acids.

Heterogeneous carbonylation by non-zeolitic acid catalysts

Strong heterogeneous acid catalysts, tested for vapour phase methanol carbonylation, have included sulfated zirconia[22] and sulfided cobalt/molybdenum catalysts supported on activated carbon[23]. The presence of the activated carbon support was found to be necessary, under the optimum conditions (250°C, 1 bar abs., 5% methanol), for methyl acetate formation.

The other promising catalyst, under similar conditions (225°C, 1 bar abs.), for producing methyl acetate from methanol is the heteropoly acid[24] of formula $Ir[W_{12}PO_{40}]$ supported on silica. It is proposed that the polyoxometalate anion is similar to the halide in providing the activation of the carbon-oxygen bond.

However, these alternatives need an increase in productivity by at least an order of magnitude[2], before they can be considered as replacements for the current acetic acid process.

Heterogeneous carbonylation by acidic zeolites

Acidic zeolites have been studied for the halide free carbonylation of methanol. The first reported zeolites[22] were tested under moderate conditions (200-300°C, 10 bar) with an equimolar ratio of carbon monoxide to methanol. In all cases dimethyl ether was the major product and the acetyls productivity increased in the order Y < mordenite < ZSM-5. It was also reported, ion-exchanged copper further promoted the formation of the acetyls. At higher pressures (258-375°C, 70 bar) it was independently reported[25] that H/ZSM-5, especially when copper ion-exchanged, was superior to H/mordenite. Subsequent work[26] in BP Chemicals Ltd. tested similar zeolites in greater detail, by varying their silica to alumina ratios and metal contents, under a set of typical conditions (350°C, 25 bar) with 4 – 8 times the excess of carbon monoxide. Under these conditions, the proton form of mordenite was more productive than H/ZSM-5. The results also confirmed that a high level of copper loading, especially in a mordenite of lower alumina content, increased the maximum acetyls yield.

In the absence of iodide, rhodium and iridium exchanged into the proton form of mordenite[26] were found to have no significant promoting effect. Furthermore, catalysts prepared by supporting copper on both amorphous alumina and silica were also unreactive under similar testing conditions.

Typical productivity profiles[27] for a mordenite zeolite, in Figure 1.2 below, show the promoting effect of ion-exchanged copper when compared with the proton form.

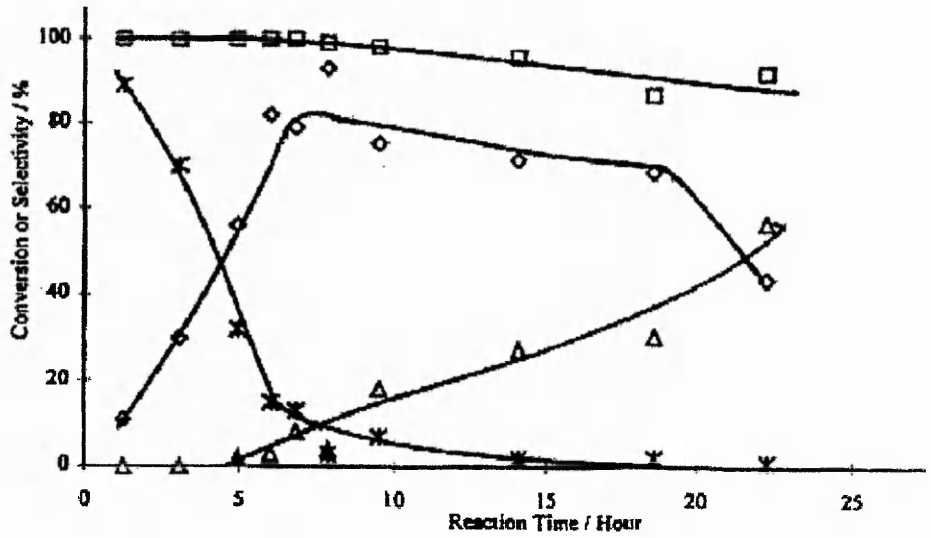

(a) Cu/H/MOR (SAR 20)

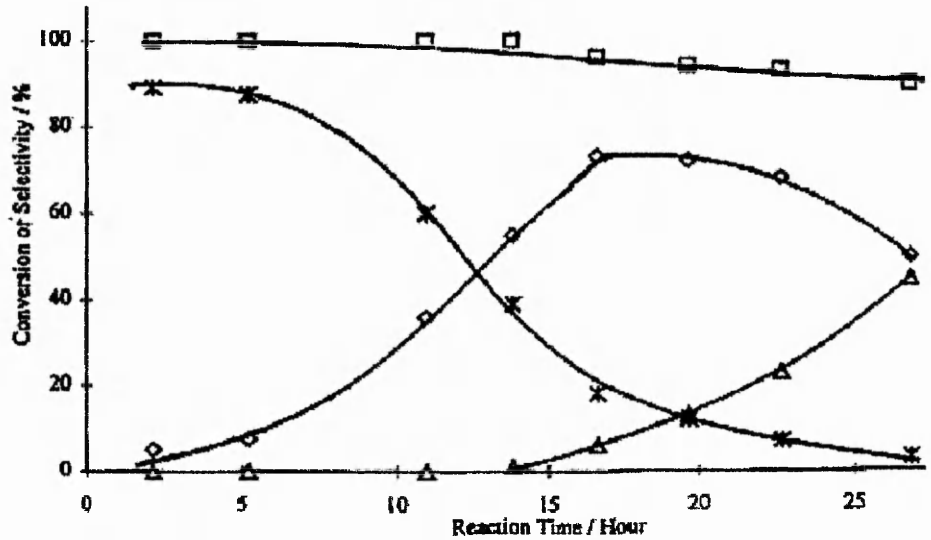

(b) H/MOR (SAR 20)

Figure 1.2 The promoting effect of 3.4 wt% copper on H/mordenite (SAR 20), under typical conditions (350°C, 10 bar, CO : methanol = 10 : 1, GHSV = 3000 h^{-1}). Symbols: % methanol conversion □, selectivity to hydrocarbons ✱, dimethyl ether △, & acetyls ◇ (acetic acid + methyl acetate). Reproduced from reference 27.

There are three clear regions where the different selectivities dominate in turn. Initially the hydrocarbons dominate, but they rapidly decrease to allow the formation of the acetyls that are then replaced by dimethyl ether. The presence of copper reduces the initial period of hydrocarbon selectivity and favourably prolongs the period of acetyls formation.

The copper containing mordenite catalysts were characterised[27] using x-ray photoelectron spectroscopy (XPS) before, during and after the period of acetyls productivity. Initially, the isolated copper (II) cations introduced by ion-exchange are deep within the zeolite crystallites and undetected by XPS. By the point of maximum productivity, XPS detects the copper as large metallic particles presumably at the crystallite surface. However, corresponding infra red spectroscopy studies of adsorbed carbon monoxide indicate that a proportion of the copper, undetected by XPS, is present as isolated copper (I) ions and possibly copper (II) oxide species.

The two main aims of the current project are to determine (i) the role of copper and (ii) the effect of the zeolite's pore structure.

There is supporting evidence for the Koch reaction[28] occurring over protonated ZSM-5 from *in situ* ^{13}C solid state Nuclear Magnetic Resonance (NMR) spectroscopy. Under mild conditions (21-100°C), the coadsorption of carbon monoxide with butyl alcohol yields trimethylacetic acid, via the adsorbed tertiary cation intermediate.

ZEOLITES AS HETEROGENEOUS CATALYSTS

Background

The Swedish mineralogist Baron Axel Cronstedt, in 1756, gave the name *Zeolites* to a small class of naturally occurring aluminosilicate minerals after observing that they appeared to boil on heating[29] (Greek; *zeo* - to boil and *lithos* - stone). Approximately 40 natural zeolite structures have subsequently been identified, with hundreds more having been prepared synthetically[30], especially since the 1960's.

Structure and application

The primary building unit, of the zeolite structure[29], is a silicon or aluminium coordinated to a tetrahedron of oxygens, illustrated in Figure 1.3a. An open three-dimensional framework is formed by each tetrahedron sharing at least two of its corner oxygens with its neighbours. The open framework creates uniform channels and/or cavities, of molecular dimensions, throughout the crystallite. The large number of possible connecting sequences for the tetrahedra gives rise to the many different framework structures so far identified, in Figure 1.3b mordenite is given as an example. The number of tetrahedra forming the major channels is used in this work to classify the frameworks e.g. the 12-T ring channel of mordenite.

One limitation on the structure is the aluminium can only be coordinated, via the oxygens, to silicons in the framework, as empirically defined by Lowenstein's Rule. Each negative charge on the framework, introduced by the trivalent aluminium being tetrahedrally coordinated, is balanced by cations located within the channel structure. The cations, usually univalent metals e.g. sodium, are hydrated until the zeolite is thermally treated. The hydrated cations, mobile within the porous structure, give rise to the application of zeolites as ion-exchanging media e.g. in water purification.

As illustrated in Figure 1.3c, if a zeolite containing ammonium ions is heated sufficiently, ammonia is released and the framework retains the protons as bridging hydroxyl groups [Si-OH-Al]. The aluminium content of the framework, presented here in terms of the silica to alumina ratio (SAR), therefore determines the concentration of the Bronsted acid sites.

Further heating, in excess of 500°C, causes dehydroxylation of the Bronsted acid sites with the formation of Lewis acid sites.

(a) The primary building unit (b) The open framework

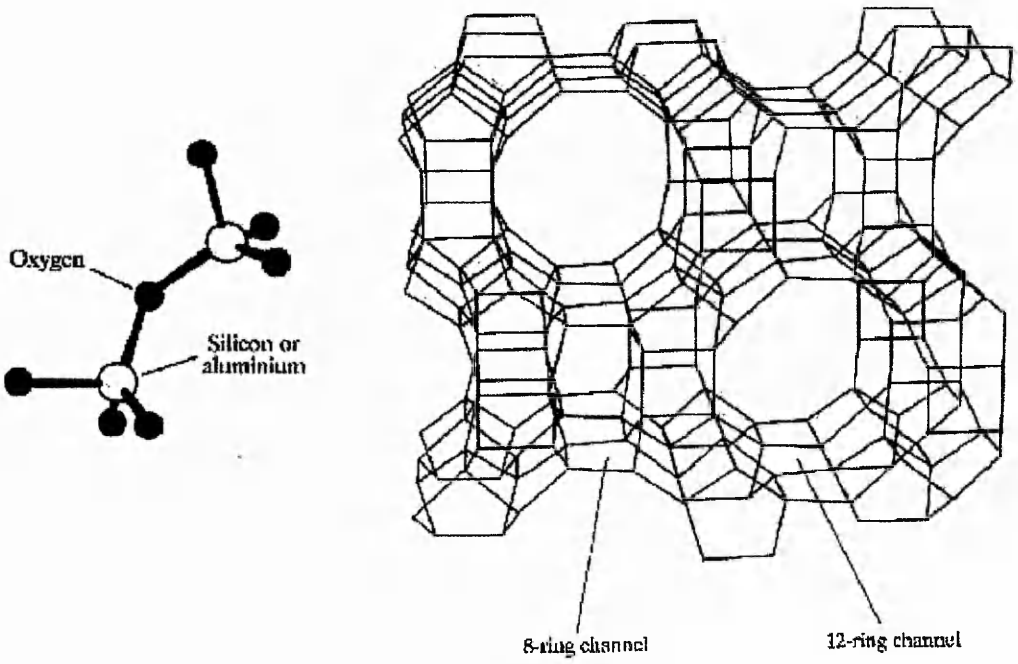

(c) The formation of Bronsted and Lewis acid sites in zeolites

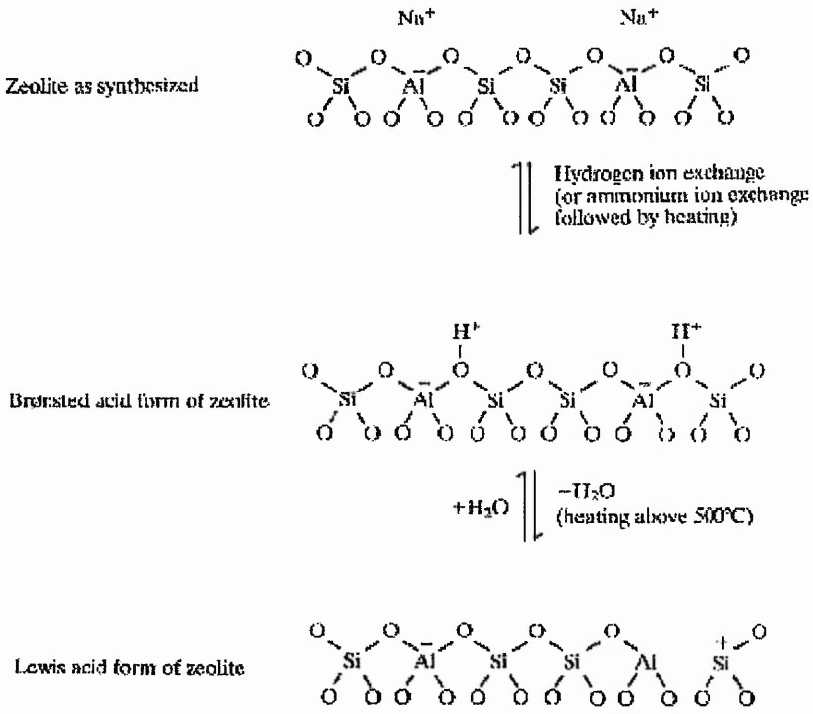

Figure 1.3(a) The primary building unit of the zeolite framework (b) Mordenite, as an example of a framework structure. The vertices correspond to the T-atoms and the lines represent the bridging T-O-T. (c) The incorporation of acid sites into the framework. Reproduced from reference 29.

The application of zeolites, as heterogeneous catalysts, especially in the fine chemicals sector is growing in importance[31]. Zeolites as solid acids are well established[32], in the petrochemical industry, for the production of gasoline grade hydrocarbons from the combined cracking and isomerisation of heavier oil fractions.

The catalytic activity of a zeolite, as a heterogeneous acid, depends[33] on (i) the concentration of acid sites, and (ii) the structure of the framework.

For the zeolites used in the petrochemical industry, e.g. zeolite Y and ZSM-5, the Bronsted acid sites are strong enough to protonate hydrocarbons to form carbocation intermediates[34]. The success of zeolites[35] partly arises from the restricting channel structure inducing a high level of selectivity on (a) the reactants, (b) the final product, or (c) the transition state for a reaction, as illustrated in Figure 1.4.

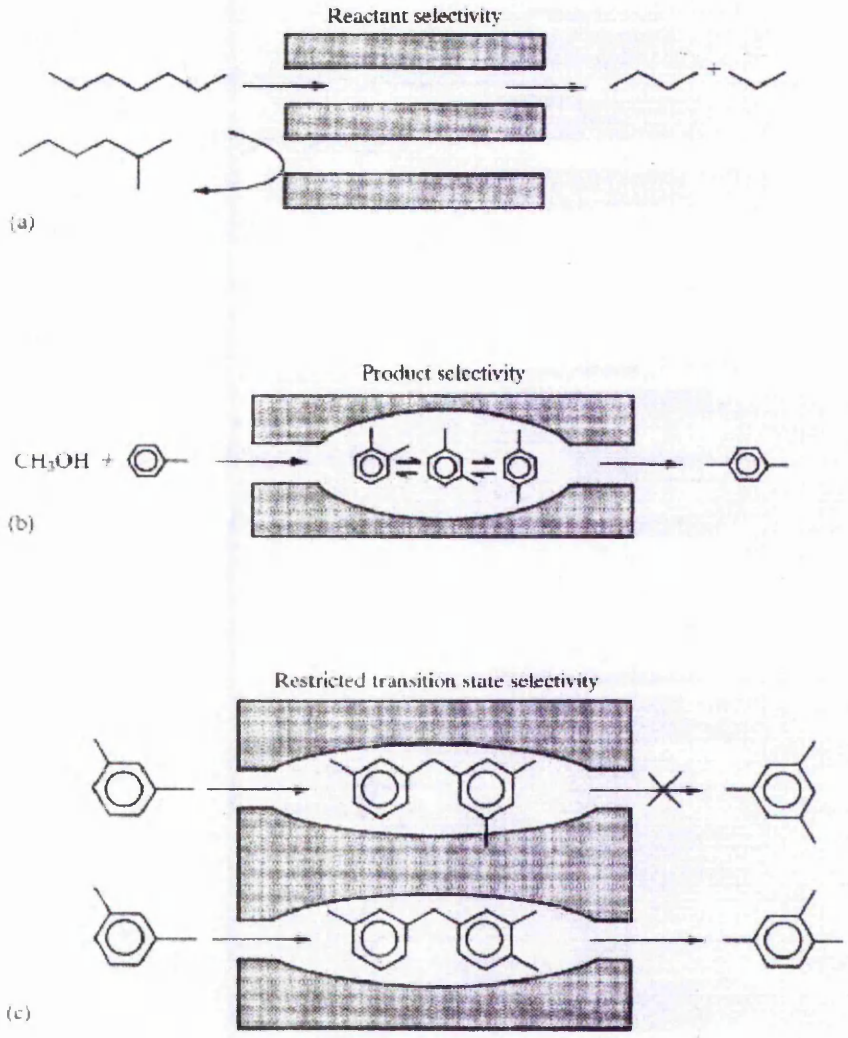

Figure 1.4 The three possible forms of selectivity induced, by the zeolite framework, on catalytic activity. Reproduced from reference 29.

The modification of zeolites

In addition to the variation of both the aluminium content and framework structure, for freshly prepared zeolites, further post-synthesis procedures for 'tailoring' the potential catalysts are also possible[36].

Introducing different cations, e.g. sodium or calcium, into the proton form can change the character of the catalyst[37]. The reduction in the concentration of Bronsted acid sites is coupled with the introduction of the Lewis acidic metal cations. Furthermore, multi valent cations, e.g. copper, can introduce sites with REDOX functionality into the catalyst[38].

The concentration of Bronsted acid sites can be reduced by the dealumination of the framework. As the framework aluminium content is reduced, the number of Bronsted acid sites decreases. The acid strength of the remaining Bronsted acid sites increases to a maximum that corresponds to all their 'next nearest neighbours' being silicons[39,40,41]. The acid strength increases because the remaining negative charges on the framework are localised at the isolated sites. Further aluminium removal decreases the concentration of the remaining sites.

Additionally, the removal of framework atoms opens up the structure, to make the remaining sites more accessible, which helps to prevent the 'coking' of the zeolite with carbonaceous byproducts[42].

Two methods of framework dealumination, used separately or in combination, are (i) 'steaming' the zeolite under hydrothermal conditions[43], and (ii) acid-refluxing the zeolite[44].

Reducing the Bronsted acid concentration, by any of the modifications, produces a multi-functional catalyst, the catalytic activity of which is difficult to predict[45] and catalytic testing is therefore required.

Methanol to gasoline chemistry

One industrial application of Bronsted acid zeolites, closely related to methanol carbonylation, is the formation of hydrocarbons from methanol. Mobil first reported[46] the conversion of methanol to gasoline (MTG) using the proton form of ZSM-5 in the late 1970's. Subsequently in 1979, New Zealand adopted the process[47] to produce gasoline from their extensive Maui gas field. By 1986, the MTG plant produced one

third of New Zealand's gasoline supply (600 000 ton annually). However, the rising price of methanol, in comparison to oil, caused the MTG plant to be shut down.
The MTG reaction, as shown in Figure 1. 5, occurs in three phases: (i) The dehydration of methanol to dimethyl ether, (ii) the formation of olefins, and (iii) the formation of gasoline range (C_2 - C_{10}) hydrocarbons and coke.

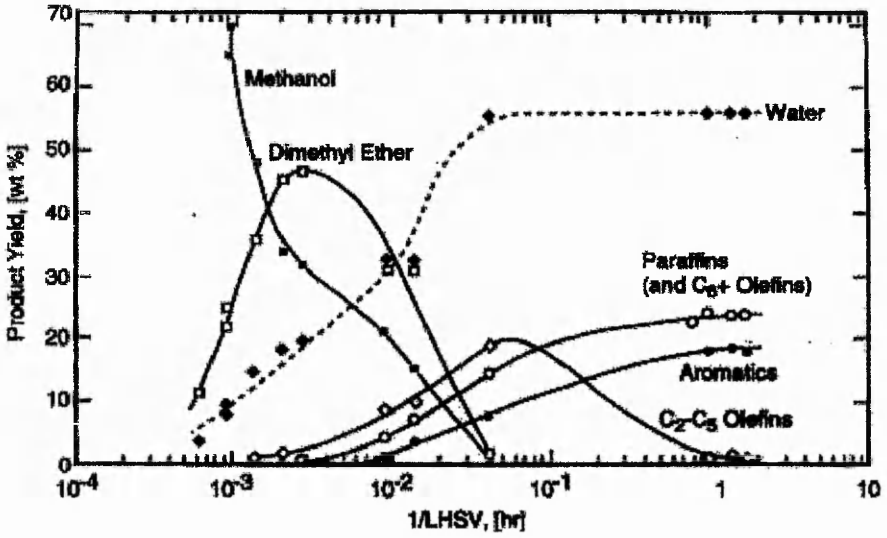

Figure 1. 5 The product distribution of the MTG process, reproduced from reference 46.

The interaction of methanol with the Bronsted acid sites of zeolites has been widely studied[48] using increasingly complex levels of theoretical modelling. It has generally been concluded[48,49] that the interaction is dependent on the level of methanol coverage. Up to coverages of one methanol per acid site the methanol is physisorbed and not protonated, but at higher coverages the Bronsted acid site can donate its proton to a cluster of hydrogen bonded methanol molecules. There is still a debate[49,50] as to whether the interaction is framework dependent.
The formation of dimethyl ether has been shown, both experimentally[51] and theoretically[52], to occur by the interaction of a hydrogen bonded cluster of two or more methanol molecules at a single Bronsted acid site.

$$2CH_3OH + [Si\text{-}OH\text{-}Al] = CH_3OCH_3 + H_2O + [Si\text{-}OH\text{-}Al]$$

At the typical reaction temperatures (300-400°C) methanol is in equilibrium with dimethyl ether and water, and the two molecules can be considered as equivalent

reactants[53]. However, it has not been conclusively determined[54] whether the dimethyl ether formation is required for the subsequent reaction steps to occur. The formation of DME regenerates the Bronsted acid sites that have been shown[55], by varying the extent of dealumination of H/ZSM-5, to be required for the further steps. There is IR[56] and C^{13} MAS NMR[57] evidence that indicates the methanol, or dimethyl ether, is initially protonated at the Bronsted acid sites. The exact requirements for dissociative adsorption of methanol, or dimethyl ether, to leave a bridging [Si-OCH_3-Al] group[58], are not fully understood[59].

As recently reviewed[47] by M. Stocker, the formation of the first carbon – carbon bond has been studied extensively, both experimentally and theoretically. The majority of the postulated mechanisms assume the initial formation of the [Si-OCH_3-Al] species. The direct formation of a carbon – carbon bond via this species would require a nucleophilic carbon species, which is unlikely under typical reaction conditions. One mechanism, that has both experimental[60] and theoretical[54] support, involves a negatively charged ylide species (or surface bound carbene) formed by the loss of a proton to a neighbouring framework oxygen. The methyl group of a second methanol reacts with the ylide to form ethene and water. The theory[61] supports this mechanism if both methanols are initially adsorbed at the Bronsted site to form a cyclic transition state. Since the development[62] of *in-situ* ^{13}C MAS NMR greater insight into the mechanism of the MTG mechanism has been possible especially when in combination with on-line gas chromatography[63]. A wide range of olefin products has been observed within H/ZSM-5 giving support to a 'carbon pool' mechanism[64], which assumes the presence of a high concentration of reactive carbonaceous species, adsorbed within the zeolite pore structure.

References

1. http://www.bpamocochemicals.com/ (2000)
2. Howard, M.J., Jones, M.D., Roberts, M.S., Taylor, S.A., *Catal. Today,* 1993, **18,** 325-354.
3. Elschenbroich, Ch., Salzer, A., *Organometallics: A Concise Introduction,* VCH, Rev. 2nd Ed., 1992, 433.
4. Sunley, G.J., Watson, D.J., *Catal. Today,* 2000, **58,** 293-307.
5. (i) *Chem. Br.,* 1996, **32,** 7. (ii) *Chem. Ind.,* July 1996, 483.
6. Halttunen, M.E., Niemela, M.K., Krause, A.O.I., Vuori, A.I., *J. Mol. Catal. A-Chem.,* 1996, **109(3),** 209-217.
7. Capka, M., Schubert, U., Heinrich, B., Hjortkjaer, J., *Collect. Czech. Chem. Commun.,* 1992, **57(12),** 2615-2621.
8. De Blasio, N., Wright, M.R., Tempesti, E., Mazzocchia, C., Cole-Hamilton, D.J., *J. Organometal. Chem., 1998,* **551(1-2),** 229-234.
9. Kapoor, M.P., Matsumura, Y., *J. Chem. Soc. Chem. Commun.,* 2000, **1,** 95-96.
10. Wang, Q., Liu, H.F., Han, M., Li, X.G., Jiang, D.Z., *J. Mol. Catal. A-Chem.,* 1997, **118(2),** 145-151.
11. De Blasio, N., Tempesti, E., Kaddouri, A., Mazzocchia, C., Cole-Hamilton, D.J., *J. Catal.,* 1998, **176(1),** 253-259.
12. Bodis, J., Zsako, J., Nemeth, C., Mink, J., *Vib. Spectrosc.,* 1995, **9(2),** 197-202.
13. Jiang, H., Liu, Z.Y., Pan, P.L., Yuan, G.Q., *J. Mol. Catal. A-Chem.,* 1999, **148(1-2),** 215-225.
14. Merenov, A.S., Nelson, A., Abraham, M.A., *Catal. Today,* 2000, **55(1-2),** 91-101.
15. Merenov, A.S., Abraham, M.A., *Catal. Today,* 1998, **40(4),** 397-404.
16. Liu, T.C., Chiu, S.J., *Appl. Catal. A-Gen.* 1994, **117(1),** 17-27.
17. Zehl, G., Bischoff, S., Lucke, B., *Catalysis Lett.,* 1993, **19(2-3),** 247-255.
18. March, J., *Advanced Organic Chemistry,* J. Wiley, 4th Ed., 1992, 808-809.
19. Bagno, A., Bukala, J., Olah, G.A., *J. Org. Chem.,* 1990, **55,** 4284-4289.
20. Xu, Q., Souma, Y., *Topics in Catal.,* 1998, **6,** 17-26.
21. Souma, Y., Iyoda, J., Sano, H., *Inorg. Chem.,* 1976, **15(4),** 968-970.
22. Fujimoto, K., Shikada, T., Omata, K., Tominaga, H., *Chem. Lett.,* 1984, 2047-2050.
23. Calafat, A., Laine, J., *Catalysis Lett.,* 1994, **28(1),** 69-77.
24. Wegman, R.W., *J. Chem. Soc. Chem. Commun.,* 1994, 947-948.
25. Feitler, D., USP 4 612 387.
26. Smith, W.J., BP Chemicals Ltd, EP 596 632 A1 (1993).
27. Ellis, B., Howard, M.J., Joyner, R.W., Reddy, K.N., Padley, M.B., Smith, W.J., *Stud. Surf. Sci. Catal.,* 1996, **101,** 771-779.

28. Stepanov, A.G., Luzgin, M.V., Romannikov, V.N., Sidelnikov, V.N., Zamaraev, K.I., *J. Catal.*, 1996, **164**, 411-421.

29. Smart, L., Moore, E., Solid State Chemistry: An Introduction, Chapman & Hall, 1992, 183-209.

30. Szostak, R., Handbook of Molecular Sieves, Van Nostrand Reinhold, 1992,

31. Tanabe, K., Holderich, W.F., *Appl. Catal. A-Gen.*, 1999, **181**, 399-434.

32. Abbot, J., Guerzoni, F.N., *Appl. Catal. A-Gen.*, 1992. **85**, 173-188.

33. Largo, R.M., Haag, W.O., Mikovsky, R.J., Olson, D.H., Hellring, S.D., Schmitt, K.D., Kerr, G.T., *Proceedings, 7th International Zeolite Conference*, Murakami, Y., Iijima, A., Ward, J.W., (Eds.) Kodansha Ltd, Tokyo, 1986, 677-684.

34. Ashton, A.G., Batmanian, S., Clark, D.M., Dwyer, J., Fitch, F.R., Hinchcliffe, A., Machado, F.J., *Catalysis by Acid and Bases,* Imelik, B., et.al. (Eds.), 1985, 101-109.

35. Ribeiro, F.R., Alvarez, F., Henriques, C., Lemo, F., Lopes, J.M., Ribeiro, M.F., *J. Molec. Cat. A-Chem.*, 1995, **96**, 245-270.

36. Perot, G., Guisnet, M., *J. Molec. Cat.* 1990, **61**, 173-196.

37. Torre-Abreu, C., Ribeiro, M.F., Henriques, C., Ribeiro, F.R., *Appl. Catal. B-Env.*, 1997, **13**, 251-264.

38. Sarkany, J., Sachtler, W.M.H., *Zeolites,* 1994, **14**, 7-11.

39. Stach, H., Janchen, J., *Zeolites.*, 1992, **12**, 152-154.

40. Teraishi, K., Akanuma, K., *J. Phys. Chem. B,* 1997, **101**, 1298-1304.

41. Trung Tran, M., Gnep, N.S., Szabo, G., Guisnet, M., *J. Catal.*, 1998, **174**, 185-190.

42. Fernandes, L.D., Bartl, P.E., Monteiro, J.L.F., daSilva, J.G., deMenezes, S.C., Cardoso, M.J.B., *Zeolites*, 1994, **14**, 533-540.

43. Meyers, B.L., Fleisch, T.H., Ray, G.J., Miller, J.T., Hall, J.B., *J. Catal,* 1988, **110**, 82-95.

44. Sawa, M., Niwa, M., Murakami, Y., *Appl. Catal.*, 1989 **53** 169-181.

45. Corma, A., Garcia, H., *Catal. Today*, 1997, **38**, 257-308.

46. Chang, D., Silvestri, A.J., *J. Catal.*, 1977, **47**, 249-259.

47. Stocker, M., *Microporous Mesoporous Mat.*, 1999, **29**, 3-48.

48. Schwarz, K., Nusterer, E., Blochl, P.E., *Catal. Today*, 1999, **50**, 501-509.

49. Haase, F., Sauer, J., *Chem. Phys. Lett.*, 1997, **266**, 397-402.

50. Shah, R., Gale, J.D., Payne, M.C., *J. Phys. Chem.*, 1996, **100**, 11688-11697.

51. Hunger, M., Horvath, T., *J. Am. Chem. Soc.*, 1996, **118**, 12302-12308.

52. Blaszkowski, S.R., van Santen, R.A., *J. Am. Chem. Soc.*, 1996, **118**, 5152-5153.

53. Fougerit, J.M., Gnep, N.S., Guisnet, M., *Microporous Mesoporous Mat.*, 1999, **29**, 79-89.

54. Hutchings, G.J., Watson, G.W., Willock, D.J., *Microporous Mesoporous Mat.*, 1999, **29**, 67-77.

55. Campbell, S.M., Jiang, X.Z., Howe, R.F., *Microporous Mesoporous Mat.*, 1999, **29**, 91-108.

56. Jiang, X.Z., *J. Molec. Cat. A-Chem.*, 1997, **121**, 63-68.

57. Ivanova, I.I., Corma, A., *J. Phys. Chem. B.*, 1997, **101**, 547-551.

58. Ono, Y., Mori, T., *J. Chem. Soc., Faraday Trans. 1*, 1981, **77**, 2209-2221.

59. Stich, I., Gale, J.D., Terakura, K., Payne, M.C., *J. Am. Chem. Soc.*, 1999, **121**, 3292-3302.

60. Hunter, R., Hutchings, G.J., *J. Chem. Soc., Chem. Commun.*, 1985, 886-887.

61. Sinclair, P.E., Catlow, C.R.A., *J. Phys. Chem. B.*, 1997, **101(3)**, 295-298.

62. Anderson, M.W., Klinowski, J., *Nature*, 1989, **339**, 200-203.

63. Seiler, M., Schenk, U., Hunger, M., *Catalysis Letters*, 1999, **62**, 139-145.

64. Dahl, I.M., Kolboe, S., *J. Catal.*, 1996, **161**, 304-309.

CHAPTER 2

CATALYST PREPARATION

The zeolite frameworks

The zeolites tested were either supplied by BP Chemicals Ltd. (Sunbury-on-Thames), or purchased from Catal Ltd. (Sheffield).

Two parent mordenite frameworks with different initial silica/alumina ratios (SAR) were studied:

(i) Na/MOR (SAR 12.8) originally supplied by PQ-Zeolites.

(ii) H/MOR (SAR 20) supplied directly by Catal Ltd. (Product Code CT 406).

The other frameworks: H/Theta-1 (SAR 54.5) and Cu/H/MCM-22 (SAR 36) were synthesised within BP Chemicals Ltd. The H/Beta (SAR 25) was originally supplied by PQ-Zeolites whilst the H/ZSM-5 (SAR 50), was supplied by Catal Ltd. (PC CT 411).

As outlined in the introduction, the target reaction for this work is the carbonylation of methanol to the products, acetic acid and methyl acetate. It had previously been shown[1] that the mordenite zeolite was promoted for this reaction by the presence of copper. The frameworks listed above were therefore tested for their catalytic activity towards the carbonylation of methanol in both their proton form and after the introduction of copper. To determine whether the method of copper introduction affected the catalytic activity, a range of techniques including: ion-exchange[2,3], impregnation and solid state exchange[4], were studied.

A summary, of all the catalyst samples prepared and tested, is given in Table 2.1. The sample designation assigned in the table is to be used throughout the work. Unless otherwise stated, the copper has been introduced by ion-exchange of the proton form. The SAR value is given in the designation in brackets only where confusion between samples could occur. The values for the two ratios (SAR, Cu/Al_2) and the percent weight of copper were determined by X-ray fluorescence (XRF) at BP (Sunbury). The copper weight percent values in brackets were determined by Atomic Absorption (AA) of dilute nitric acid solutions prepared from solid lithium borate fusions of the calcined samples. In the table, N/A means 'Not Applicable' and a – indicates 'not available'.

Designation	Source	SAR*	Cu wt%*,†	Cu/Al_2*
H/MOR(12.8)	Na/MOR(12.8) PQ	-	N/A	N/A
Cu/H/MOR BP	BP (Sunbury)	12.8‡	3.5‡	Not quoted
Cu/Na/MOR 0.9	Na/MOR(12.8) PQ	14.0	0.96 (0.96)	0.18
Cu/Na/MOR 3.4	Na/MOR(12.8) PQ	14.9	3.40 (3.51)	0.66
Na/MOR(20)	H/MOR(20) Catal	-	N/A	N/A
H/MOR(20)	H/MOR(20) Catal	-	N/A	N/A
Cu/MOR SE1	H/MOR(20) Catal	18.6	2.20	0.47
Cu/MOR SE2	H/MOR(20) Catal	18.8	2.59	0.56
Cu/MOR SE3	H/MOR(20) Catal	-	(2.45)	-
Cu/MOR HP1	H/MOR(20) Catal	18.3	0.32	0.06
Cu/MOR HP2	H/MOR(20) Catal	18.7	0.70	0.14
Cu/MOR HP3	H/MOR(20) Catal	18.0	1.27	0.26
Cu/MOR HP4	H/MOR(20) Catal	-	(2.40)	-
Cu/MOR HP5	H/MOR(20) Catal	-	(4.96)	-
Cu/MOR IMP	H/MOR(20) Catal	-	-	-
Cu/MOR [1M]	H/MOR(20) Catal	-	(2.80)	-
Cu/MOR SS	H/MOR(20) Catal	-	(4.24)	-
BP 1ST	Na/MOR(12.8) PQ	13.9	N/A	N/A
BP 1ST&AW	Na/MOR(12.8) PQ	19.6	N/A	N/A
BP 2ST	Na/MOR(12.8) PQ	19.5	N/A	N/A
BP 2ST&AW	Na/MOR(12.8) PQ	-	N/A	N/A
NTU1 500C	Na/MOR(12.8) PQ	-	N/A	N/A
NTU2 200C	Na/MOR(12.8) PQ	-	N/A	N/A
NTU3 NC	Na/MOR(12.8) PQ	-	N/A	N/A
DOW	H/MOR(20) Catal	-	N/A	N/A
H/Theta	BP (Sunbury)	54.5	N/A	N/A
Cu/Theta SE	H/Theta BP (Sunbury)	54.6	0.10 (0.12)	0.06
Cu/Theta HP	H/Theta BP (Sunbury)	79.4	1.82	2.58
Cu/Theta SS	H/Theta BP (Sunbury)	-	(4.54)	-
H/ZSM-5	H/ZSM-5 Catal	50.0‡	N/A	N/A
Cu/ZSM-5 SE	H/ZSM-5 Catal	-	(1.23)	-
H/Beta	H/Beta PQ	25.0‡	N/A	N/A
Cu/Beta SE	H/Beta PQ	-	(1.43)	-
Cu/Beta HP	H/Beta PQ	5.5	2.60 (2.67)	0.19
Cu/MCM-22	BP (Sunbury)	35.7	5.90	2.80

Table 2.1 Summary of all the samples prepared and tested as detailed in this chapter

*Values from XRF by BP (Sunbury)

†Values in brackets determined by AA from dilute nitric acid solutions of lithium borate fusions.

‡Value quoted when supplied.

Introduction of copper by ion-exchange

Preparation procedures from the literature were initially followed to produce two samples of Na/MOR (SAR 12.8), one with a low copper loading[2] (0.9 wt%) the other with a high copper loading[3] (3.5 wt%). Copper was introduced into the zeolite by ion-exchange of either its ammonium or H-form, with aqueous copper nitrate (Aldrich Analar grade) solution, at room temperature overnight. The general procedure adopted is outlined here.

Initially, 5 g of the zeolite was suspended in 100 ml of distilled water by continuous stirring. When fully dispersed, 100 ml of aqueous copper nitrate solution were slowly added to the suspended zeolite. The copper concentration in the total volume of 200 ml is the one quoted. After filtering, the zeolite was washed with at least 1 L of distilled water to remove the nitrate counter-anion and any residual copper. The zeolite was then dried, either at room temperature overnight or at 200°C in air for at least 2 hours. To achieve further different copper loadings, either the initial copper nitrate concentration was varied or the exchange procedure was repeated with fresh copper nitrate solution.

Introduction of copper by pH controlled ion-exchange

To achieve high levels of copper loading into an H-Beta zeolite, Holmen's group in Trondheim Norway[5] modified the above conventional procedure, by the addition of ammonium hydroxide solution to the initial copper and zeolite suspension. The following is a further extension of this pH-modified procedure in which alliquots of ammonium hydroxide are added during the ion-exchange process.

5 g of the zeolite, in the H-form, were suspended by stirring in 100 ml of distilled water at room temperature. The pH of the zeolite suspension was increased from its initial 5.5 to 7.5 by the careful addition of ammonium hydroxide solution (3.5 % v/v). The amount of copper acetate (BDH Analar grade) required to give the desired loading was dissolved in 100 ml of distilled water and its initial pH of ~6.0 was raised, by the drop wise addition of ammonium hydroxide, to give a final pH of 7.5. The solution of copper acetate was then continuously added to the suspended zeolite over a period of two minutes. The pH of the mixture steadily decreased, to a stable value of ~5.5, within a period of 10 minutes. When the pH had stabilised, a further aliquot of ammonium hydroxide solution was added. The resulting rise in pH was followed by another steady decrease. Ammonium hydroxide solution was added, until no subsequent pH decrease

was evident. The process was completed well within 4 hours. On stopping the stirring, the suspended zeolite settled out to give a colourless solution, indicating that no copper remained in solution. A further test during the filtering, of having concentrated ammonium hydroxide in the Buchner flask, gave no deep violet copper ammonium complex in the supernatant. The blue zeolite was washed with 1 L of distilled water without pH modification and then dried as before.

Copper introduced by impregnation

5 g of the H/MOR (SAR 20) zeolite were impregnated with 0.27 g of copper nitrate (Aldrich Analar grade) dissolved in 4.0 ml of distilled water. The resulting thick paste was dried at 110°C overnight.

Copper introduced by solid state exchange

1 g of the ammonium exchanged zeolite was thoroughly mixed with 0.06 g of copper (II) oxide (BDH Analar grade) by grinding, in a mortar and pestle, for at least 10 minutes. The resulting physical mixture was uniformly grey in colour. The mixture was then packed, between silica wool plugs, into a silica tube (internal diameter 20 mm) within a horizontal furnace. Helium (100 ml min^{-1}) was flowed through the material during heating to 600°C at 10°C min^{-1}. The catalyst was held at 600°C for four hours and allowed to cool to room temperature, still under the helium flow.

Dealumination of the mordenite framework

Na/MOR (SAR 12.8) samples were subject to three different sets of dealuminating conditions to reduce the Bronsted acid site density.

(1) Hydrothermal treatment using BP's steaming apparatus followed by acid washing.

(2) Hydrothermal treatment using NTU's steaming apparatus followed by acid washing.

(3) Acid washing followed by calcination according to a DOW patent[6].

(1a) Hydrothermal treatment using BP's steaming apparatus.

The Na/MOR (SAR 12.8) catalyst was initially pelleted to produce a 0.6 – 1.0 mm fraction. At least 30 ml (~15 g) of the pelleted catalyst, held between silica wool plugs in a silica reactor tube, was loaded into a vertical furnace. The temperature of the catalyst bed was controlled by a thermocouple held at the external surface of the silica tube. The space above the catalyst bed was filled with silica boiling chips, into which the needle from a syringe of distilled water was placed. Nitrogen (100 ml min^{-1}) was used as the carrier gas for the water vapour. The catalyst bed was heated to 600°C at 20°C min^{-1} under flowing nitrogen. When the temperature had stabilised at 600°C the water flow (10 ml h^{-1}), controlled by a syringe pump, was started. The pump was stopped after three hours and the catalyst was allowed to cool to room temperature under the flowing nitrogen.

(1b) Acid washing of the steamed catalyst.

Half of the steamed catalyst was refluxed for 2 hours in concentrated nitric acid, diluted 1:1 with water (7.7 M nitric acid). The volume of nitric acid used was 20 ml per gram of catalyst refluxed. The catalyst was then filtered and washed with 1 L of distilled water and dried in an oven at 110°C for 2 hours.

(2) Hydrothermal treatment using a steaming apparatus at NTU.

The above process was replicated on a smaller scale steaming apparatus built at NTU. A smaller (2-5 g) catalyst bed was held in a horizantal furnace with helium as the carrier gas. All the other conditions were similar. The acid washing process was as in (1b).

(3) Preparation of the DOW dealuminated mordenite.

20 g of Na/MOR (SAR 12.8) was ammonium exchanged at room temperature overnight using 1 M ammonium nitrate solution. After filtering, washing and drying, the ammonium mordenite was calcined at 550°C for 2 hours to give the H-form. 5 g of the freshly prepared H-form was refluxed for 2 hours in 6 M nitric acid (concentrated nitric acid, diluted 2:3 with distilled water). 20 ml of nitric acid was used per gram of catalyst refluxed. After washing in 1 L of distilled water, the catalyst was dried at 90°C in a tube furnace under static air for 2 hours. The tube furnace temperature was then raised to 700°C at 5°C min^{-1} and held for 2 hours to calcine the catalyst under static air.

CATALYST REACTOR STUDIES

Preparation of the catalysts for reactor testing

The catalysts, in their dry powder form, were calcined in a muffle furnace at 550°C under static air for 4 hours. The catalysts were then pressed, using a standard 25 mm diameter infrared dye, under 5 tonnes for 3 minutes (Pressure of 9.99×10^7 N m^{-2}). Enough powdered sample was used to ensure the resulting disc was at least 0.6mm thick. The disc was then screened through stainless steel sieves, with the 0.6 – 1.0 mm fraction being taken for the reactor testing. Figure 2.1 shows the X-ray diffraction (XRD) traces, before and after the pressing of Na/MOR (SAR 12.8), to illustrate that the framework crystallinity was not modified significantly by these pelleting conditions.

(a) Na/MOR (SAR 12.8) As Supplied

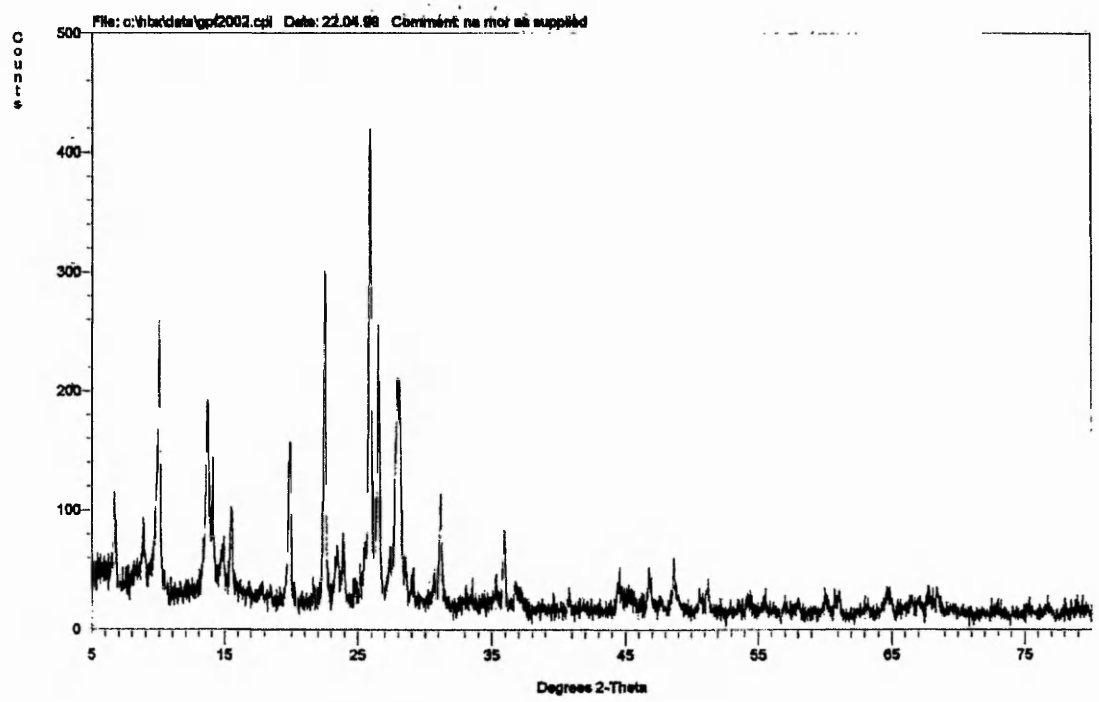

(b) Na/MOR (SAR 12.8) After Pelleting

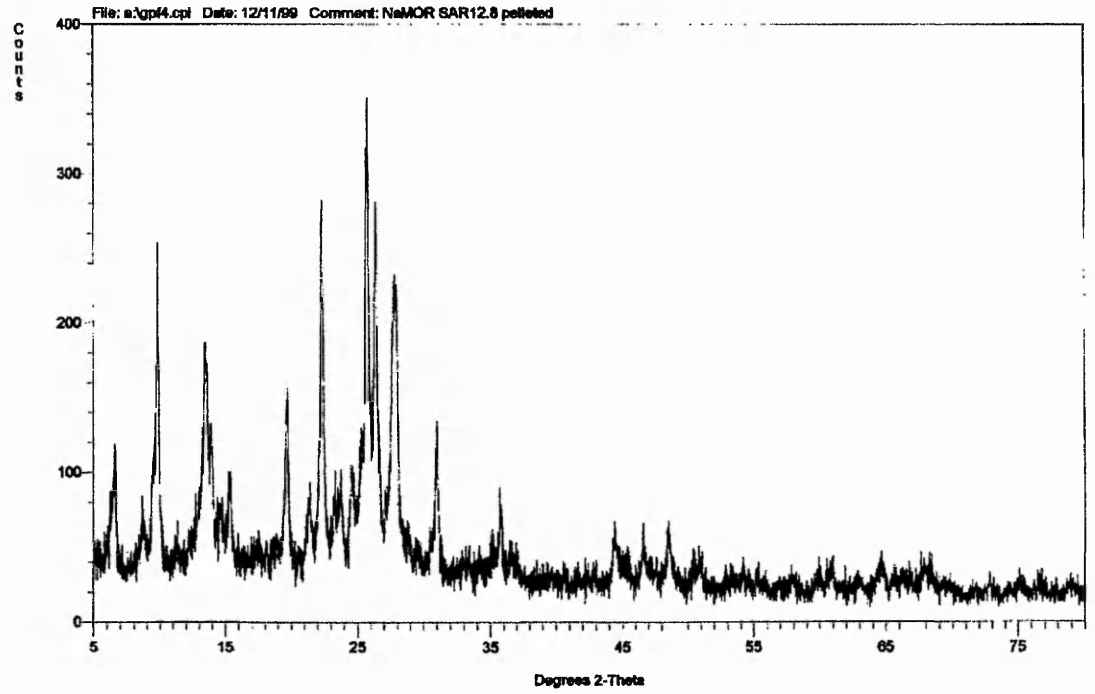

Figure 2.1 XRD Traces confirming that the framework crystallinity was retained after pressing

The reactor

A schematic diagram of the catalytic reactor system is shown in Figure 2.2. The reactor was configured with the catalyst bed horizontal and trace heating tapes (Isopad ITH series) were used to maintain both the reactants and products in the vapour phase either side of the reactor furnace (Carbolite tube furnace).

Flowrates of the gaseous reactants, carbon monoxide and nitrogen, were controlled by mass flow controllers (Brookes 5850 TR series), whilst the liquid phase methanol (Aldrich HPLC grade) was introduced using a HPLC pump (Kontron 420 series) and vaporised in a heated region before mixing with the gaseous feed.

A fixed volume of 1.0 ml of the pelleted catalyst was used to form the catalyst bed, held between silica wool plugs, within the ½ inch stainless steel reactor tube. The temperature of the catalyst bed was maintained by an external thermocouple connected to a temperature controller (Eurotherm).

A pressure of 8 bar gauge was maintained within the reactor by a back pressure regulator (Veriflo) protected from reactor fines by an in-line filter. The composition of the vapour phase, downstream of this regulator, at atmospheric pressure, was determined using on-line gas chromatography (Varian GC 4000 series) with two Porapaq QS columns, the first connected to a flame ionisation detector (FID), and the second to a thermal conductivity detector (TCD).

The FID, calibrated quantitatively was used to determine the vapour phase organic composition whilst the TCD gave a semi-quantitative indication of whether water and carbon dioxide were present. For the separation, and detection by the FID, of dimethyl ether and methanol the column oven was held at 60°C for 10 minutes followed by a temperature ramp of 30°C min^{-1} to 180°C which was then held. This temperature program prevented the simultaneous sampling of vapour to the FID and TCD, so the consumption of carbon monoxide could not be determined. The flow rate of the permanent gases through the reactor was measured by using a bubble meter downstream of the GC.

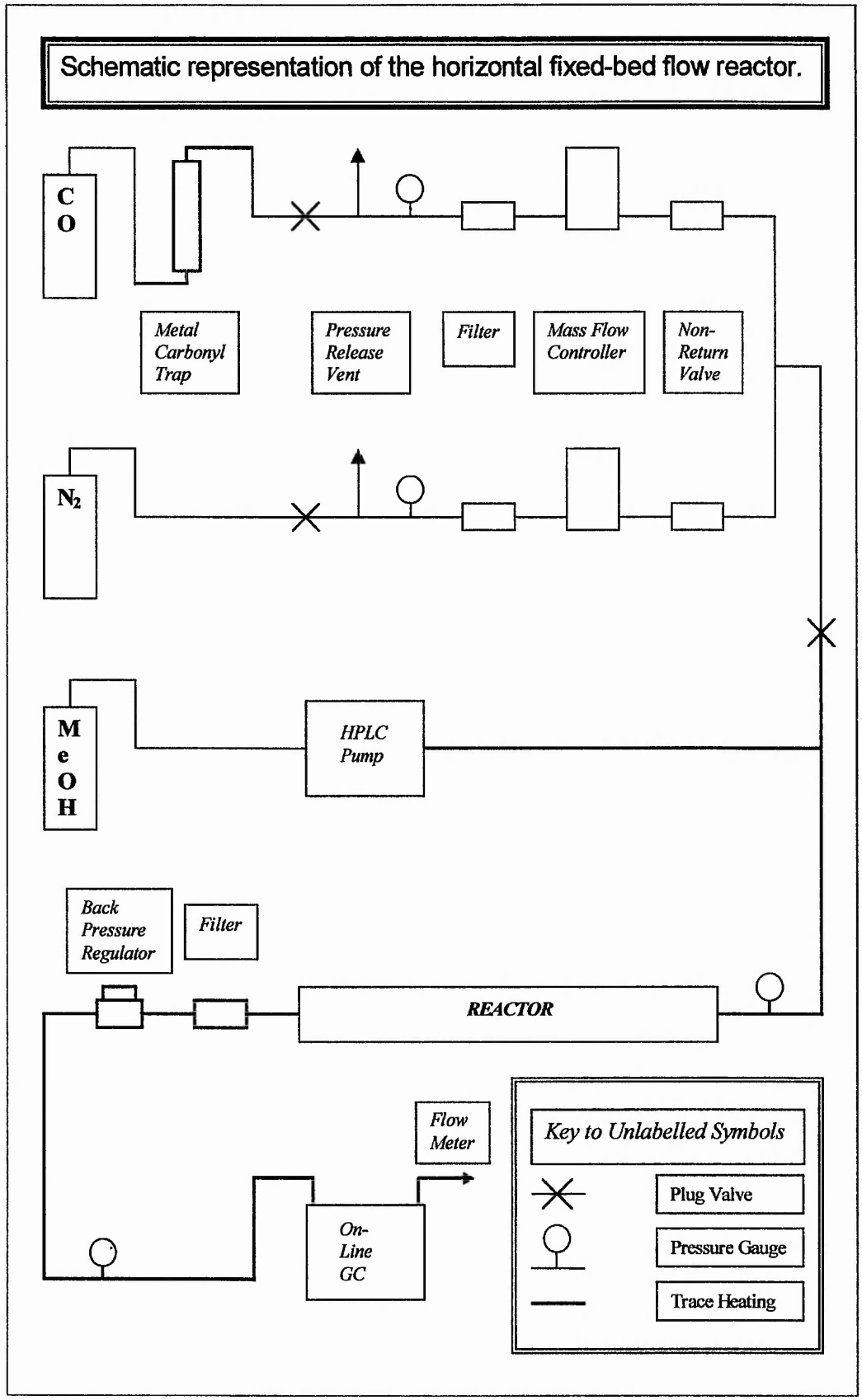

Figure 2.2 A Schematic Representation of the Reactor

The catalyst testing conditions

All the catalysts were initially tested for methanol carbonylation activity using the conditions summarised below in Table 2.2.

Summary of Catalyst Testing Conditions	
Temperature	350°C
Pressure	8 bar gauge
Methanol LHSV Calculated GHSV	0.9 h^{-1} 543 h^{-1}
CO GHSV	4800 h^{-1}
TOTAL GHSV	5343 h^{-1}
Methanol : CO Ratio Methanol %	1 : 8.8 10.2%
Catalyst bed	Pelleted 0.6 - 1.0 mm Volume 1.0 ml
Pretreatment	CO, 500°C, 1 bar, 4h, 4800 h^{-1}
Product Sampling	On-line GC FID & TCD every 1h

Table 2.2 Summary of the catalyst testing conditions

The temperature 350°C was chosen, following the previous work[1,2] and 8 bar gauge was the maximum delivery pressure that was safe for the carbon monoxide supply. The liquid methanol flow of 0.015 ml min^{-1} was limited to the lowest recommended stable flow rate for the HPLC pump. The low methanol flow was necessary to produce the ratio of carbon monoxide to methanol, used in the earlier work, without creating a pressure build-up through the restriction of the GC sample loop. To prevent the catalyst bed moving during experiments it was found necessary to restrict the bed volume to 1.0ml. As a result of the smaller bed volume, the GHSV is approximately twice that of the earlier work. The activation of the catalyst was carried out in carbon monoxide rather than in an inert carrier gas to ensure that the methanol contacted the catalyst in the presence of carbon monoxide.

REACTOR CALIBRATION

On-line analysis of catalyst performance

The reactor was commissioned to study the performance of catalysts for the conversion of methanol to the products, acetic acid and methyl acetate. Under the conditions of testing, the reactants and desired products were maintained in the vapour phase and detected by on-line GC analysis of the reactor effluent. On-line analysis minimizes the time lag between the vapour exiting the catalyst bed and the determination of its composition. It was assumed in this work, that any vapour phase reactions occurring after the vapour leaving the catalyst bed and before its detection were negligable. It was only possible to quantify vapour phase products as a function of time. The products deposited on the catalyst as coke were determined by separate CHN analysis after the period of testing.

Composition of the reactor feed

The reactor feed was periodically calibrated by using the catalyst testing conditions and feeding methanol through the reactor tube in the absence of a catalyst bed. Averaging over all these empty tube runs, the carbon monoxide flow measured with the bubble meter at room temperature was 80 ± 4 ml min^{-1}.

Pumping the methanol (density 0.791 g ml^{-1}) as a liquid at 0.015 ml min^{-1} represents a rate of 3.703×10^{-4} moles min^{-1}. Assuming that methanol behaves as an ideal gas (obeys $PV = nRT$) the calculated methanol vapour flow rate is 9.05 ml min^{-1} at room temperature and atmospheric pressure. The volume of methanol vapour had to be estimated by calculation rather than be measured directly because the liquid within the bubble meter dissolved the methanol, and any other soluble vapour. This was clearly evident from the lack of a measurable change in flow rate on the introduction of methanol, confirmed by GC, into the carbon monoxide. It was assumed the total vapour flow entering the catalyst bed was the sum of the carbon monoxide flow measured at room temperature and the calculated methanol flow (total flow 89 ± 4 ml min^{-1}), giving a methanol composition of $10.2 \pm 0.4\%$ by volume.

Calibration of the GC sample loop

It was further assumed that the composition of the reactor feed remained constant as a function of temperature and pressure and therefore that methanol occupied 10.2% of the sample loop volume.

In the empty tube calibration runs, the methanol injected from the sample loop generated $7.58 \pm 0.4 \times 10^6$ counts (averaged over 80 data points).

Independent, constant volume (1 μL), syringe injections of methanol, with water as the solvent, made directly onto the GC column gave the calibration graph shown below in Figure 2.3, and lead to the equation: -

$$\text{moles methanol injected} = \text{methanol counts} \times (1.20 \times 10^{-13} \text{ moles count}^{-1})$$

Using the above calibration equation, 7.58×10^6 counts corresponds to 9.06×10^{-7} moles of methanol contained within the sample loop. Assuming therefore that 9.06×10^{-7} moles of methanol occupy 10.2% of the sample loop volume, the sample loop has a total vapour capacity of 8.93×10^{-6} moles under the operating conditions of the GC (180°C).

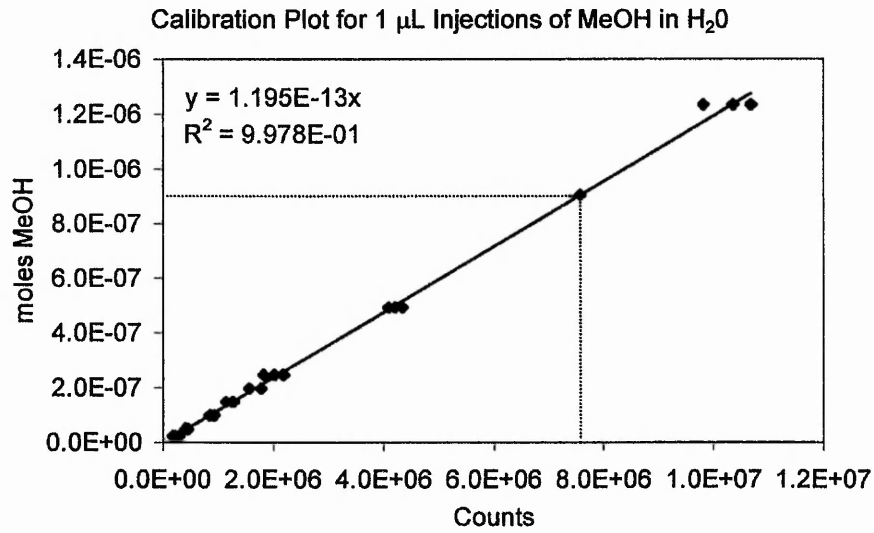

Figure 2.3. Calibration plot for 1 μL syringe injections of methanol diluted in water. The point highlighted by (·····) is the single calibration point from the sample loop injections when running methanol through the empty reactor tube.

Calibration of the detected products

To have complete confidence in the data from an on-line GC, the calibration of potential products should be carried out under conditions identical to those used when on-line to the reactor. For this case, the calibration mixtures should have been passed through the reactor to the GC. Unfortunately the desired products, acetic acid and methyl acetate, were not compatible with the HPLC pump. Additionally both are extremely volatile and so problems were encountered with their stability on dilution.

The solution adopted, for all the liquid phase products, was to build an injection loop to allow manual syringe injections of constant volume (1 μL) directly onto the column. Water or methanol was normally used as the solvent, measured by volume, for at least five different concentrations over the required range. Fresh solutions were made for each injection and each concentration repeated until consistent results were obtained. From these injections, calibration plots for moles of product injected versus GC detector counts gave calibration coefficients with units of (mol $count^{-1}$). This calibration is independent of the sample loop of the reactor. To account for the sample loop volume, each value for the moles of product manually injected was divided by the molar volume of the sample loop, as determined above (8.93×10^{-6} moles), to give an effective mole fraction of the sample loop equivalent to the manual injection. This fraction as a percentage, termed the percentage volume of the sample loop, was then used for the calibration plots to give a calibration coefficient, with units (%Vol $count^{-1}$), related directly to the sample loop. As everything in the sample loop is in the vapour state, a mole percent is equivalent to a volume percent of the sample loop.

It had to be assumed that the operating conditions for the manual injections were identical to those for the reactor's sample loop. This assumption is supported by two findings. Firstly the retention times were closely matched, indicating the flow rates and temperatures for the two different methods were equivalent. Secondly, and more conclusively, the calibration coefficient from the manual injections of methanol (1.34×10^{-6} %Vol $count^{-1}$) was identical to the single point calibration coefficient for the sample loop injections from the empty reactor tube, as highlighted in Figure 2.3 in the previous section.

In summary, for each product, identified by its retention time, multiplying the GC counts obtained by the independantly determined volume percent calibration coefficient gives the percentage volume of the sample loop occupied by that product.

Calibration for the gaseous products dimethyl ether and methane was done through the reactor with injections from the sample loop, changing the flow rate of the inert carrier gas, nitrogen, to vary the concentration.

The C2 – C4 products were calibrated and the methane checked at a single concentration, using commercial calibration mixtures (SCOTTY II) injected via the sample loop.

For each product, it was assumed that for every CHn group formed one methanol molecule was consumed. The amount of methanol converted into the product was therefore expressed as an effective methanol percentage volume, obtained by multiplying the volume percent of product by the number of CHn groups in the product. The acetyl groups were assumed to arise from carbon monoxide, as under nitrogen no acetyls were detected. These effective methanol percentage volumes are the values used in the following calculations.

The treatment of the GC data

The performance of the catalysts was compared using the three expressions below based only on the vapour composition as determined by the GC.

(I) The amount of methanol consumed, determined as the percent conversion of methanol: -

$$\%\ \text{methanol conversion} = \frac{\text{methanol feed} - \text{unreacted methanol}}{\text{methanol feed}} \times 100$$

(II) The amount of methanol converted to each detected product, expressed as a percent selectivity to that product: -

$$\%\ \text{selectivity to product (a)} = \frac{\text{amount of product (a) detected}}{\text{total of detected products}} \times 100$$

(III) The rate of formation of the desired products, acetic acid and methyl acetate, determined in terms of their space time yield: -

$$\text{space time yield (STY)} = \text{g acetyls product / g catalyst / hour}$$

The undetected products

In the presence of a catalyst it was often found that the total amount of detected methanol, the sum of unreacted methanol and detected products, was less than the methanol feed. Given the known tendency of methanol to form coke on similar materials, this is not surprising. The amount of methanol feed detected has been expressed as a methanol carbon balance: -

$$\text{Methanol carbon balance} = \frac{\text{total carbon from methanol detected}}{\text{carbon from methanol feed}} \times 100$$

Calibration for dimethyl ether (DME)

It was often observed that dimethyl ether (DME) was a significant product of the reaction, particularly after long times on stream. DME is a gas at room temperature, so the following approach was adopted to check its calibration in the presence of a catalyst. Dimethyl ether was generated *in situ* over Na/MOR (SAR 20) by the dehydration of methanol, a reaction which is known to be highly selective to DME over weakly acidic materials. Figure 2.4 shows the low conversion of methanol, averaging 20%. The major product, as shown in Figure 2.5, is DME with a selectivity of greater than 95%. The hydrocarbon impurities detected are methane and propene, which are also present at similar levels during the empty tube calibrations. It can therefore be assumed that the sole product over Na/MOR (SAR 20) is DME. The corresponding carbon balance in Figure 2.4 is 90%. It can be assumed that the DME calibration is reasonable, as explained below.

A low methanol conversion of 20% indicates 80% of the feed is detected as unreacted methanol. Therefore, 80% of the 90% carbon balance is solely due to unreacted methanol. Of the 20% methanol converted, only 10% is detected as DME to give the 90% carbon balance. Assuming that the DME was being under represented would require its calibration coefficient to be modified by a factor of two to account for the remaining 10% methanol. However, the normal high conversion conditions of 90% methanol conversion, combined with a 60% selectivity to DME, confirm that at least 50% of the methanol introduced is converted to DME. Applying the modified calibration coefficient from the low conversion case above would indicate that over 100% of the methanol introduced formed DME, which is clearly not the case.

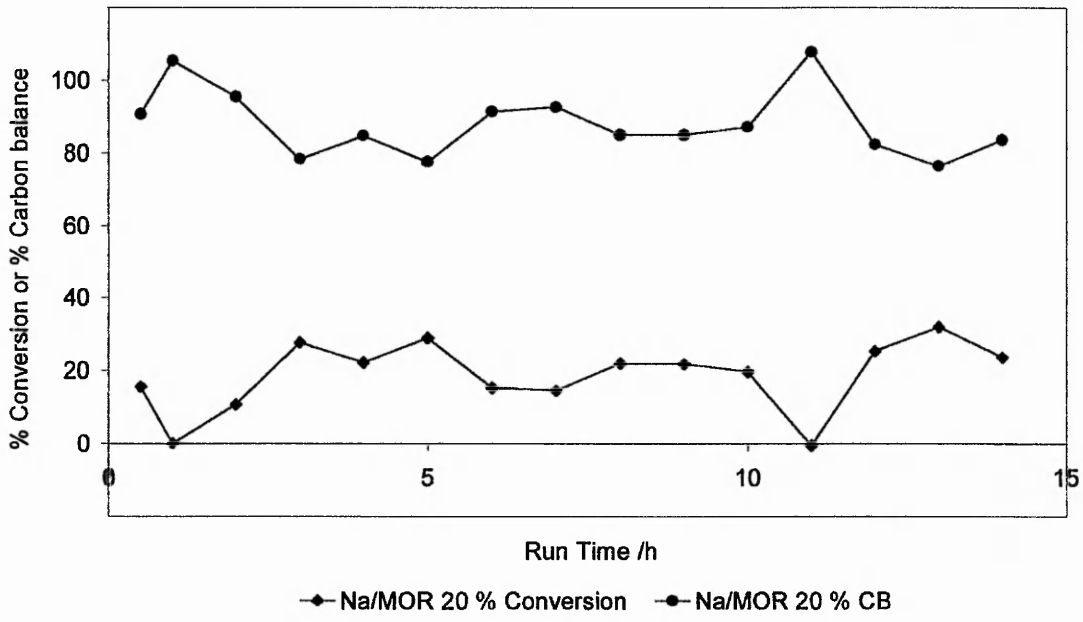

Figure 2.4 Percentage conversion & carbon balance for Na/MOR (SAR 20)

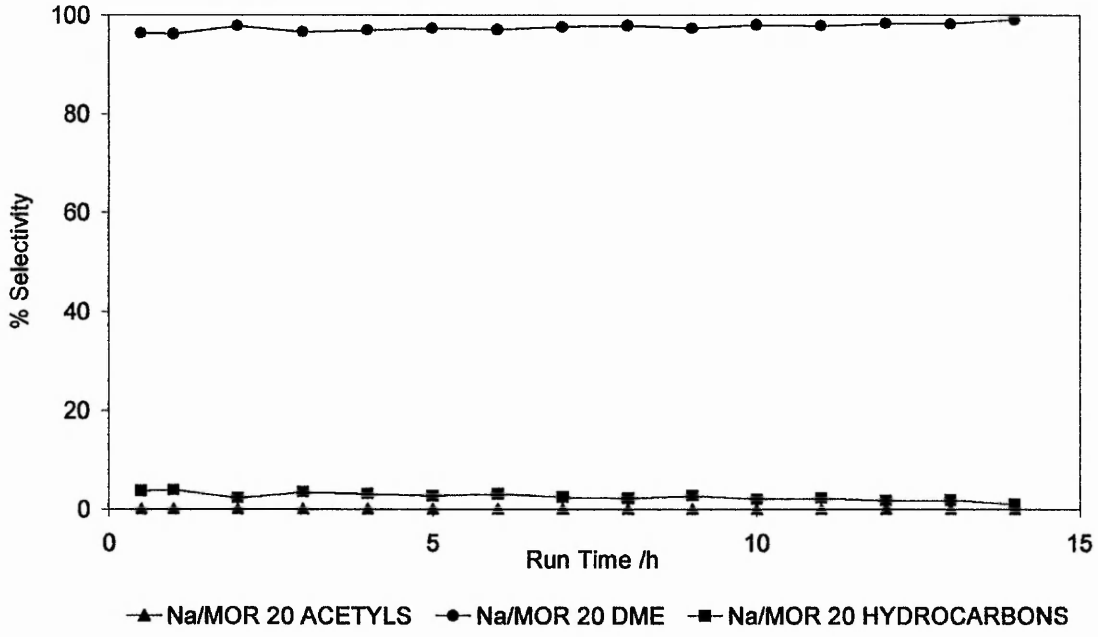

Figure 2.5 Percentage selectivities for Na/MOR (SAR 20)

The modification of the calibration coefficient would cause the carbon balance for the high conversion experiment to rise from the detected 60% to well over 100%. The confidence in the DME calibration, shown in Figure 2.6, is higher than that obtained by modifying the calibration coefficient.

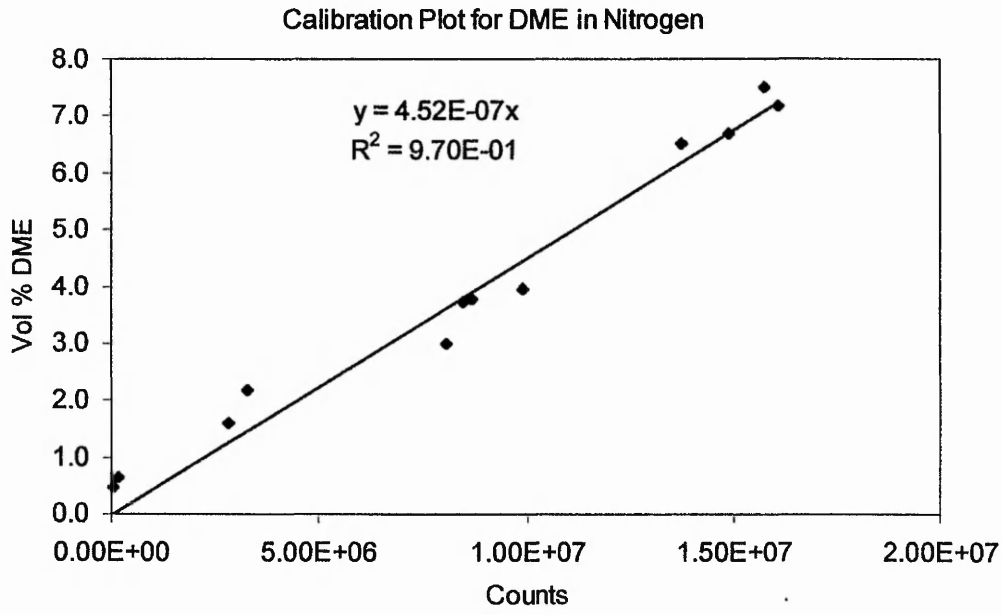

Figure 2.6 The calibration plot for DME diluted in nitrogen carrier gas

Bearing the losses of detected methanol in mind, the low concentration of unreacted methanol detected indicates that the level of conversion is normally high. The product selectivities and yields are determined directly from their independent calibrations and therefore are not affected directly by the low carbon balances detected. A comparison of catalytic activity in terms of product selectivity and yield can therefore be made from the data obtained.

Confirmation of the reactors performance

Before screening the freshly prepared catalyst samples, two further checks made on the reactor are detailed here.

(1) Previously prepared sample

The reproducibility of both the reactor's performance and of the previous work's results were confirmed, using a previously prepared sample of copper ion-exchanged mordenite Cu/H/MOR BP (SAR 12.8) with a copper loading of 3.5 wt%. Figures 2.7-9 compare two sets of results obtained for this sample under the standard testing conditions. Only the aspects concerning the reproducibility of the reactor are discussed here. Figure 2.7(a) shows the initial methanol conversion to be virtually 100%, after only 3 hours it has dropped to 80% but is still at 65% after 20 hours on stream.

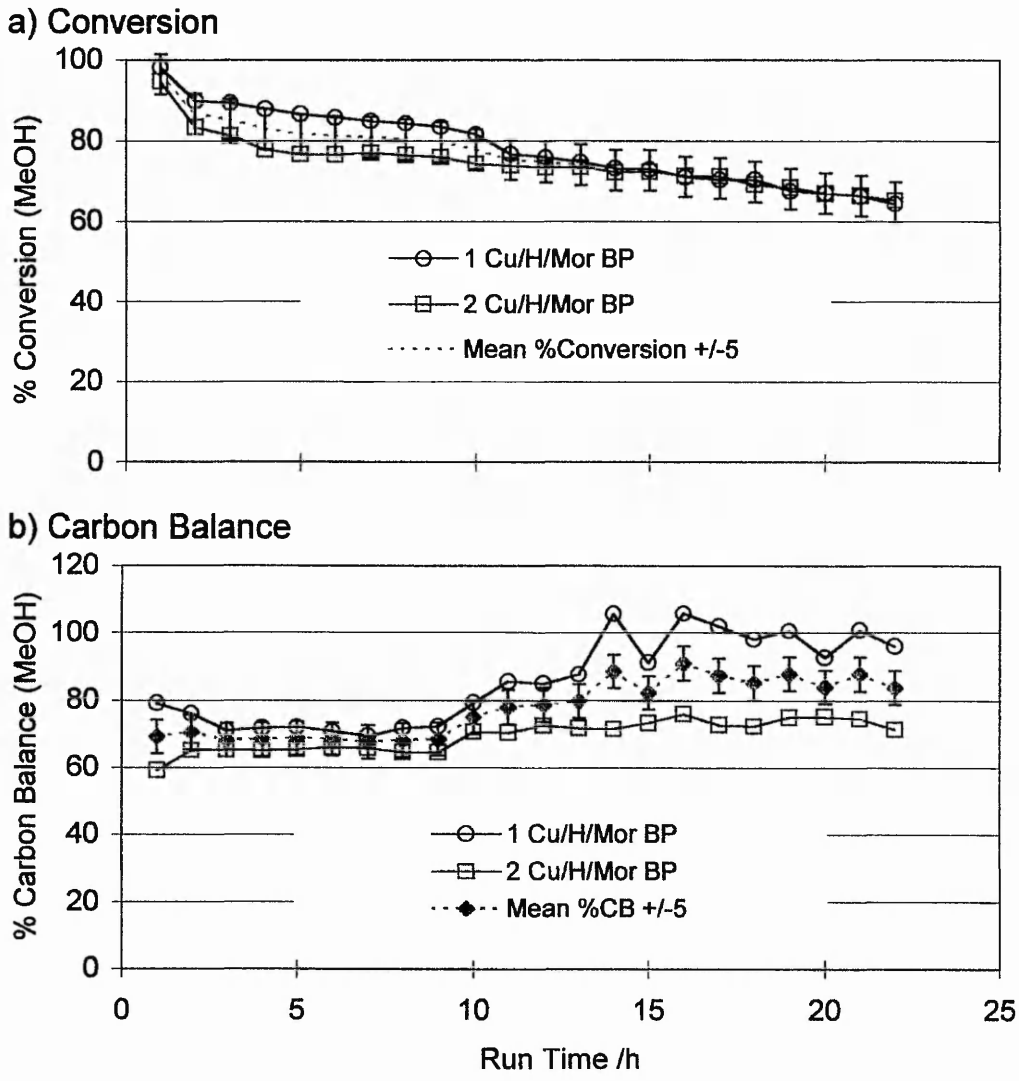

Figure 2.7 Reproducibility of the (a) Conversions and (b) Carbon Balances for Cu/H/MOR BP

The conversions are within an error of ±5% from their mean. The carbon balances, shown in Figure 2.7(b), but for the first point, lie within the ±5% margin until they diverge after 10 hours on stream. The mean carbon balances for the first 10 hours being constantly around 70%.

After 14 hours the carbon balance for reaction 1 approaches 100%, this has been assigned to the reactor becoming blocked by the deposition of heavy hydrocarbon byproducts. At the pressure gauge, between the back pressure regulator and the GC sample loop (see Figure 2.2 page 26), an increase from atmospheric pressure was observed, indicating that the exit line of the reactor was blocked. A blockage causes the pressure to rise in the sample loop, effectively increasing the number of molecules sampled, assuming an ideal gas (PV = nRT).

The calculations (see page 31) assume a constant methanol concentration (10.2 % methanol) and sampling size (8.93 $x10^{-6}$ moles). A larger sample contains a larger amount of unreacted methanol, and the level of conversion is reduced, as can be seen by the 5% drop at 11 hours for reaction 1.

The selectivites for three groups of products, (i) the desired acetyls, (ii) the major byproduct DME and (iii) the remaining detected volatiles, labelled as hydrocarbons, respectively are shown in Figure 2.8a-c. It can be seen for the two reactions, reproducibility of the selectivity to acetyls lies within the error margin of ±5 % for the entire period of testing. The reactor blocking after 14 hours has a negligible effect on the selectivity to the desired acetyls products. The selectivity to DME, lies on the edges of the error margin of ±5 % for the entire time, and follows the same rising trend, with or without the reactor blocking. The selectivity for the summation of all the other detected products is the most affected by the increase in sample size in reaction 1. The mean value is less than 20% and constant for the period of testing, the two runs lie on the edges of the ±5% error margin. After 14 hours for reaction 1, the selectivity jumps from 10% to 20%, and then oscillates as the pressure varies in the blocking reactor. The increase in pressure, through the sample loop, is assumed to be more prone to increasing the proportion of the hydrocarbons sampled, because the average number of methanols consumed per heavy hydrocarbon formed is taken as six. Only a small increase in the proportion of hydrocarbons detected would be required to significantly increase the calculated amount of methanol (carbon balance) consumed.

The reproducibility of the acetyls yields for the Cu/H/MOR BP sample is shown in Figure 2.9. The yields are reproducible in both trend and normalised values within the error of ±0.05 g acetyls /g catalyst /hour. As for the selectivities, the yields do not appear to be affected by the pressure build up that occurred after 11 hours in reaction 1. The variations in experimental reproducibility observed can be assumed to arise from the differences in pretreatment history for the catalyst samples.

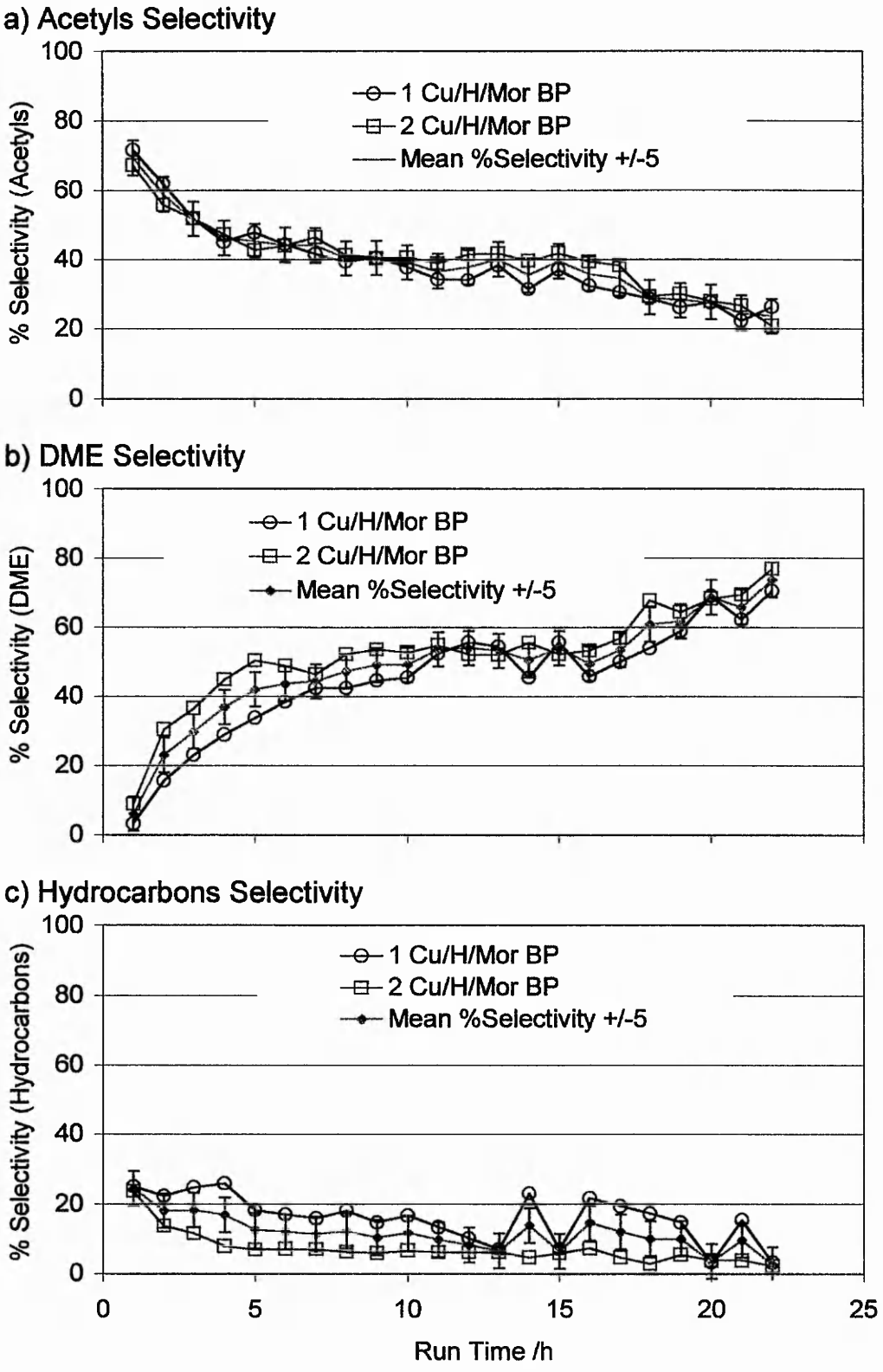

Figure 2.8 Reproducibility of the Selectivities to (a) Acetyls, (b) DME and (c) Hydrocarbons for Cu/H/MOR BP

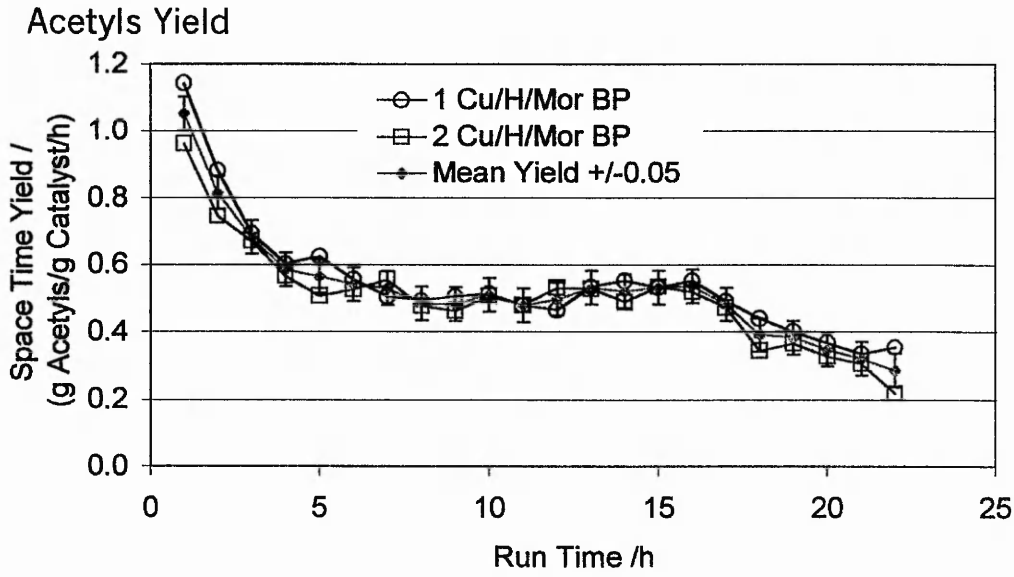

Figure 2.9 Reproducibility of the Acetyls Space Time Yields for Cu/H/MOR BP

(2) A silica liner in the reactor tube

A silica liner was sealed into the stainless steel reactor tube, because of evidence in the literature that suggests carbon monoxide forms iron carbonyl clusters in the presence of steel[7,8]. It was therefore thought to be a possible concern in this stainless steel system. As indicated in the systematic diagram of the reactor (Figure 2.2 page 26) a heated column containing molecular sieve 13X was commisioned to trap any iron carbonyl clusters formed under the high pressure within the steel carbon monoxide cylinder. Without the trap in place, a metallic deposit was found to form on the silica liner in front of the catalyst bed.

Figures 2.10-12 compare the results obtained with and without the silica liner, for the same Cu/H/MOR BP sample, in the absence of any reactor fouling.

The convention adopted for the figures, from here on, lists the new sample first, labelled throughout by the crosses, and is compared directly with a previous sample labelled by the filled squares.

The methanol conversions, shown in Figure 2.10a, in the presence of the silica liner are reduced by 40%, throughout the 20 hours of testing, compared to when no silica liner is present. The trends in the carbon balances, shown in Figure 2.10b, are however similar with a steady rise of 10% in the 20 hours, the silica liner being constantly higher by a maximum of 20%.

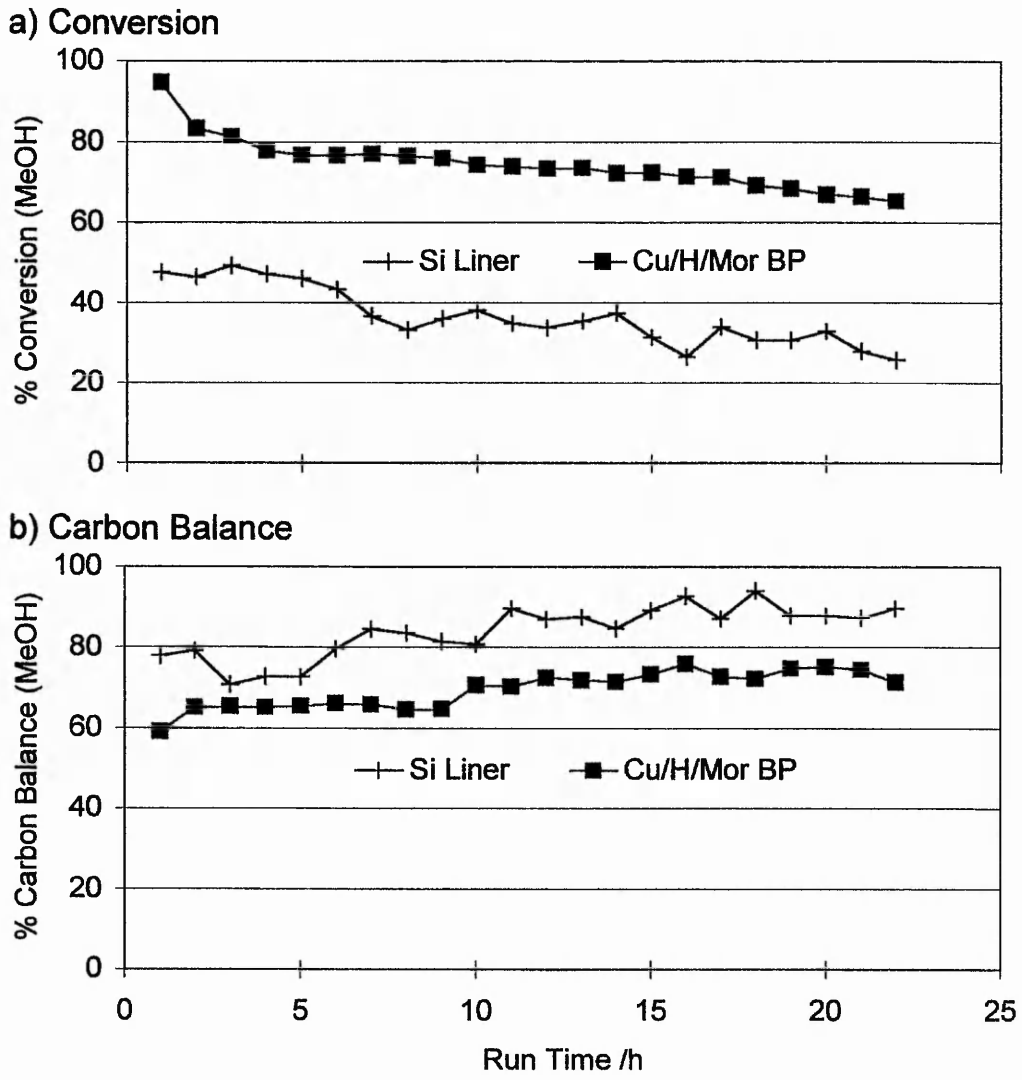

Figure 2.10 The effect of a Silica Liner on (a) % Conversion and (b) % Carbon Balance for Cu/H/MOR BP

There are significant differences in the selectivities, as shown in Figure 2.11(a-c). In the presence of a silica liner the selectivities to the acetyls and DME are reversed, with that to the acetyls dominating, at a constant 40% higher than for no liner. The trend of a steady decrease by 10% every 10 hours, is found to occur for both reactions, suggesting that similar chemistry is occurring. In the presence of the silica liner, DME is only a minor product, not reaching a selectivity of 20% until after 20 hours. In contrast, with no liner, DME selectivity has reached 50% after only 5 hours, which is maintained over a stable period of 10 hours before rising again. The selectivities to hydrocarbons are seen to be identical, being less than 10% throughout, except for an initial period for no liner where the selectivity drops from 20%.

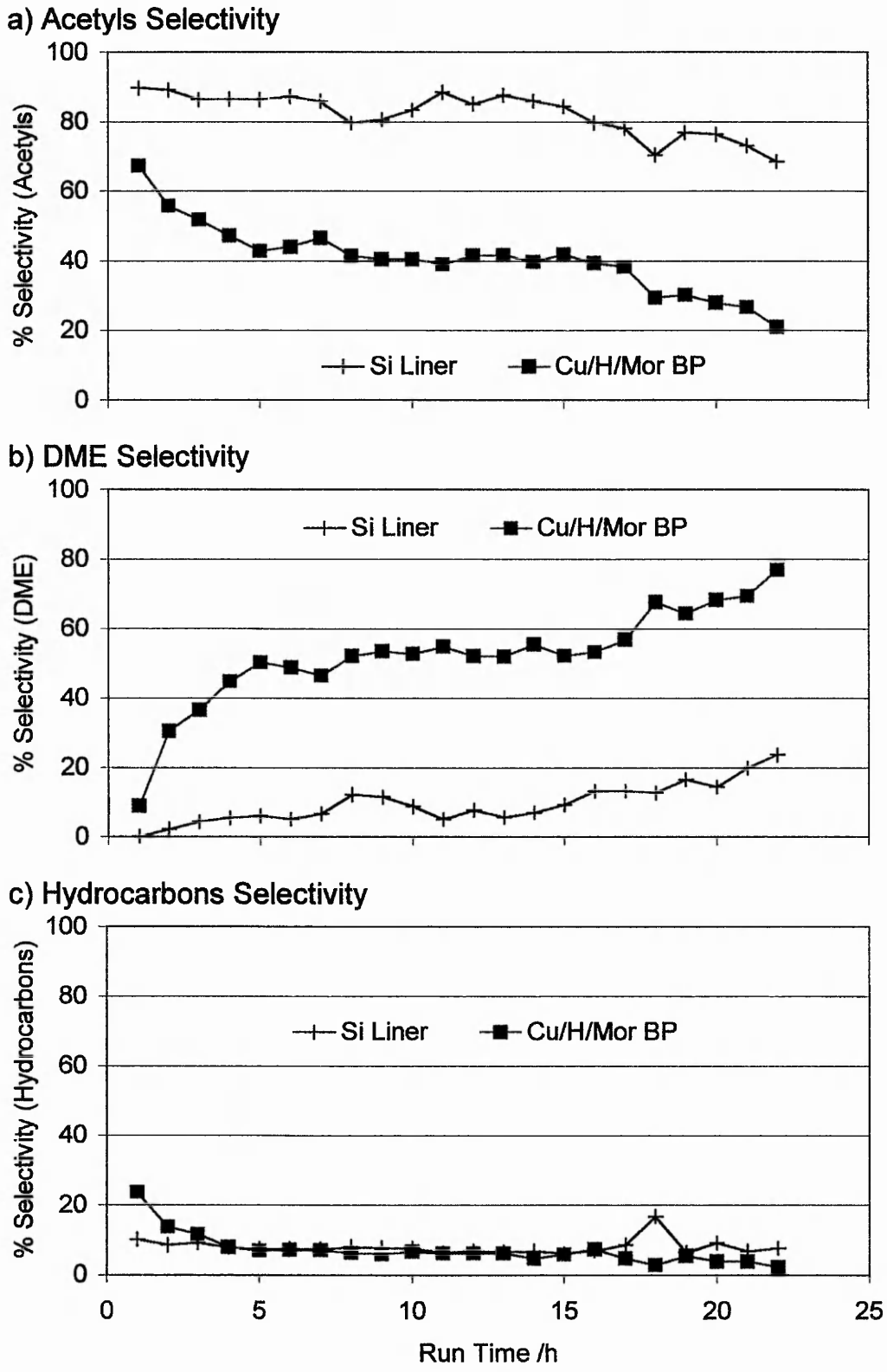

Figure 2.11 The effect of a Silica Liner on the % Selectivities to (a) Acetyls, (b) DME and (c) Hydrocarbons for Cu/H/MOR BP

Figure 2.12(a) shows the combined yield of acetyls for the two systems. It is clearly seen that, except for the first 3 hours, the yields of acetyls are comparable. This is interesting, considering the total methanol conversion with the liner present is significantly lower, but that the corresponding selectivity to acetyls is higher. A lower level of conversion, coupled with an equivalent selectivity to hydrocarbons, also suggests that the actual yield of hydrocarbons is lower in the presence of a liner. Therefore, the main effect of the silica liner is to reduce the conversion of methanol to DME and the other byproducts, but it does not effect the conversion to acetyls.
On comparing the yields of acetic acid and methyl acetate in Figure 2.12(b&c), it is noticeable that the acetic acid is not affected, to any significant degree, by the presence of the silica liner. However, the amount of methyl acetate, is initially significantly lower in the presence of the silica liner. Under the initial conditions of very low DME concentrations (less than 10%), acetic acid is the favoured product.
The standard reactor conditions included operating at a constant gas hourly space velocity (GHSV), by maintaining a 1.0 ml bed volume of pelleted catalyst and a constant flow rate of reactants. Modifying the bed shape, by the insertion of a silica liner, caused a dramatic reduction in both the level of methanol conversion and the formation of DME. The constant residence time through the catalyst bed implies that the stainless steel reactor tube causes the formation of DME. However, no formation of DME was found during the empty tube calibration runs.
The temperature of the reactor was controlled externally and set constantly at 350°C. It could be assumed the presence of the silica liner, reduced the bed temperature resulting in the reduced conversion of methanol.
To determine the temperature drop across the reactor tube a thermocouple was inserted into the catalyst bed. A drop in the order of ten degrees was observed for the open tube. However, under the reaction conditions, use of the K-type thermocouple within the reactor tube, led to the preferential disproportionation of carbon monoxide by the Bouduard reaction, which resulted in the reactor line rapidly becoming blocked by the deposition of carbon.

Although the silica liner results are encouraging, it could not be confirmed that under the operating conditions, the silica liner remained sealed to the stainless steel reactor tube. Therefore, to ensure continuity with the earlier work, the silica liner was not routinely used in this work.

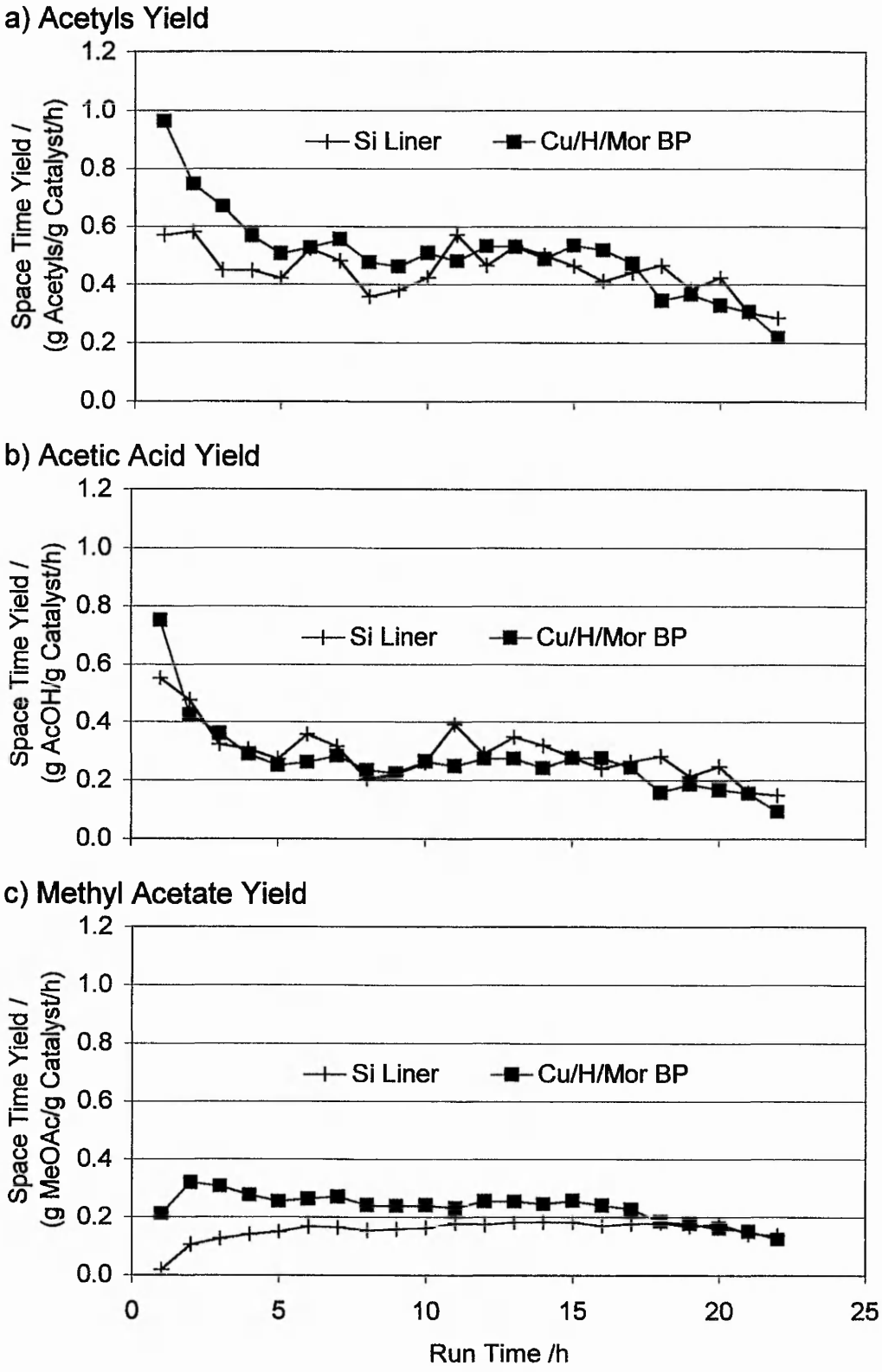

Figure 2.12 The effect of a Silica Liner on the Space Time Yield of (a) Acetyls, (b) Acetic Acid and (c) Methyl Acetate for Cu/H/MOR BP

Evidence for acetyls sticking or an effect of low methanol concentration

On stopping the methanol flow after testing a catalyst, after a period of 2 hours the reactor was clear of all products except acetic acid. Therefore, the reactor had to be cleared between each reaction, by continuing the flow of carbon monoxide through the post reactor line, for several hours after stopping the methanol.

To determine the effect, on the measured productivity, of the acetic acid remaining resident in the line, the methanol flow was stopped for 3 hours during the stable period of acetyls formation from Cu/MOR SE2. In addition to the normal cleaning procedure mentioned above, to ensure the reactor was clean before starting the reaction, carbon monoxide alone was passed through, at a pressure of 8 bar, for 2 hours before introducing the methanol. To prevent the HPLC pump from stalling, 8 bar of carbon monoxide in the absence of methanol was avoided under the normal operating conditions. The results, presented from the point when the methanol was first turned on, are compared to the 2 Cu/MOR BP reaction. The methanol was interrupted immediately after the injection at 16 hours, to allow 1 hour for the reactor to clear before the injection at 17 hours. The methanol flow was then restarted, similarly, straight after the injection at 19 hours.

It can be seen that from starting the methanol flow at the HPLC pump, 1 hour elapsed before the products were detected at the GC. All the results to be presented throughout this work therefore start at 1 hour, the methanol being turned on at zero hours.

Figure 2.13a shows for both reactions the level of conversion is initially 100% and falls to around 80% after a total run time of 3 hours, from when it remains constant. On stopping the methanol after 16 hours, the level of conversion rises within the hour to 100% indicating that no unreacted methanol, and hence no methanol feed, was present for the 3 hours. Restarting the methanol causes the conversion level to fall back towards 80%, as the unreacted methanol is detected.

Before starting the methanol flow, the carbon balance should be zero. The following explanation is given as to why the initial carbon balance, shown in Figure 2.13b, is actually 30%. To ensure that the HPLC pump did not stall, it was disconnected from the reactor and the heated zone was purged with fresh liquid methanol. After loading the sample, and reconnecting the heated zone, the system was pressurised to 8 bar of flowing carbon monoxide. While the temperature stabilised for two hours, methanol was able to migrate from the heated zone into the reactor, giving rise to the 30%

methanol carbon balance, by the time the pump was started.

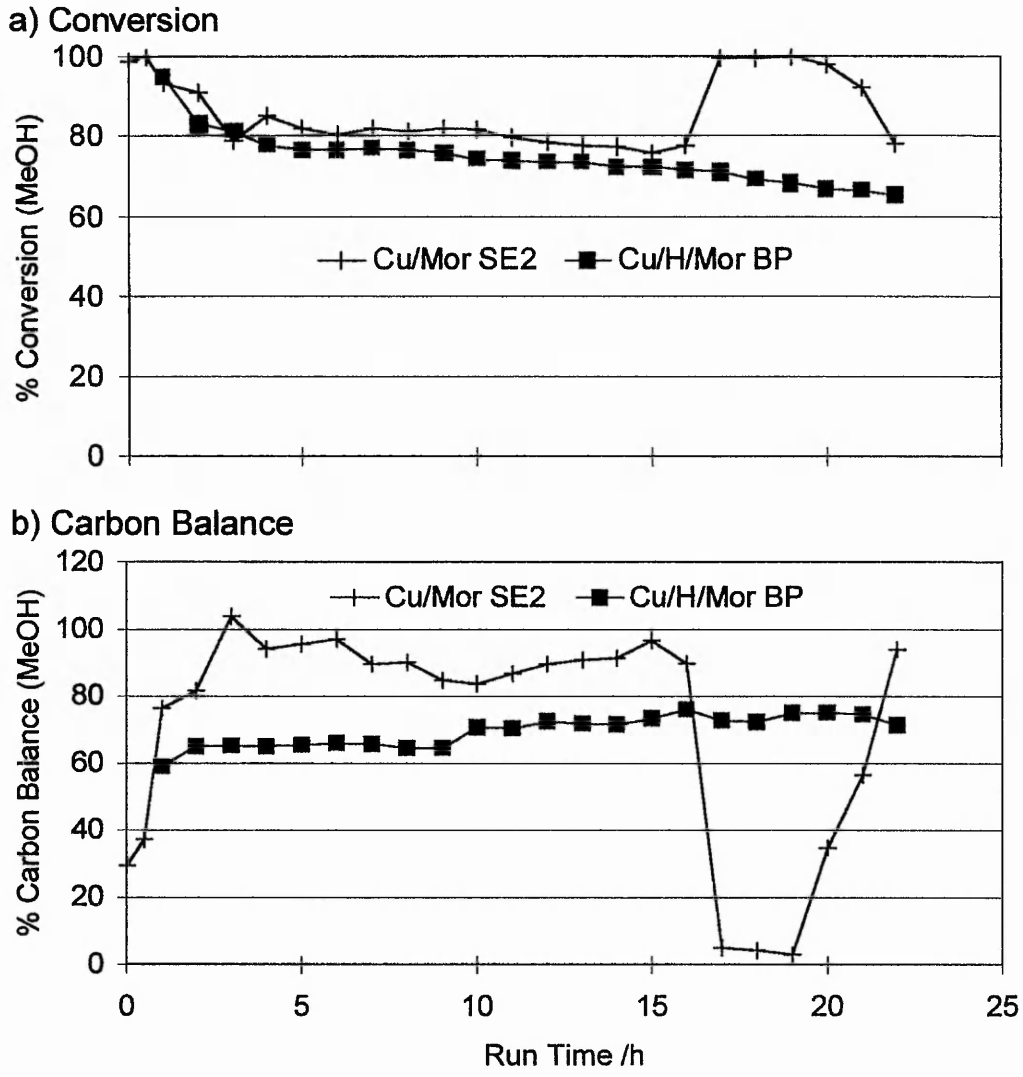

Figure 2.13 The effect of the acetyls sticking on (a) the Conversion and (b) the Carbon Balance on stopping the methanol flow

On starting the methanol flow, the carbon balance rapidly rises and has reached 80% after 2 hours, it being maintained until the methanol is stopped. Within the first hour of stopping the methanol, the carbon balance has fallen to approximately 5%, and decreases further with time. On restarting the methanol, the carbon balance rises again to 80%, at a similar rate as to when the reaction was started.

When the methanol flow is off, the selectivity to the acetyls is 90%, as shown in Figure 2.14, with hydrocarbons as the remainder. The initial high selectivity to acetyls decreases rapidly, as the methanol concentration increases. However, as the methanol concentration increases, the DME selectivity is also seen to increase.

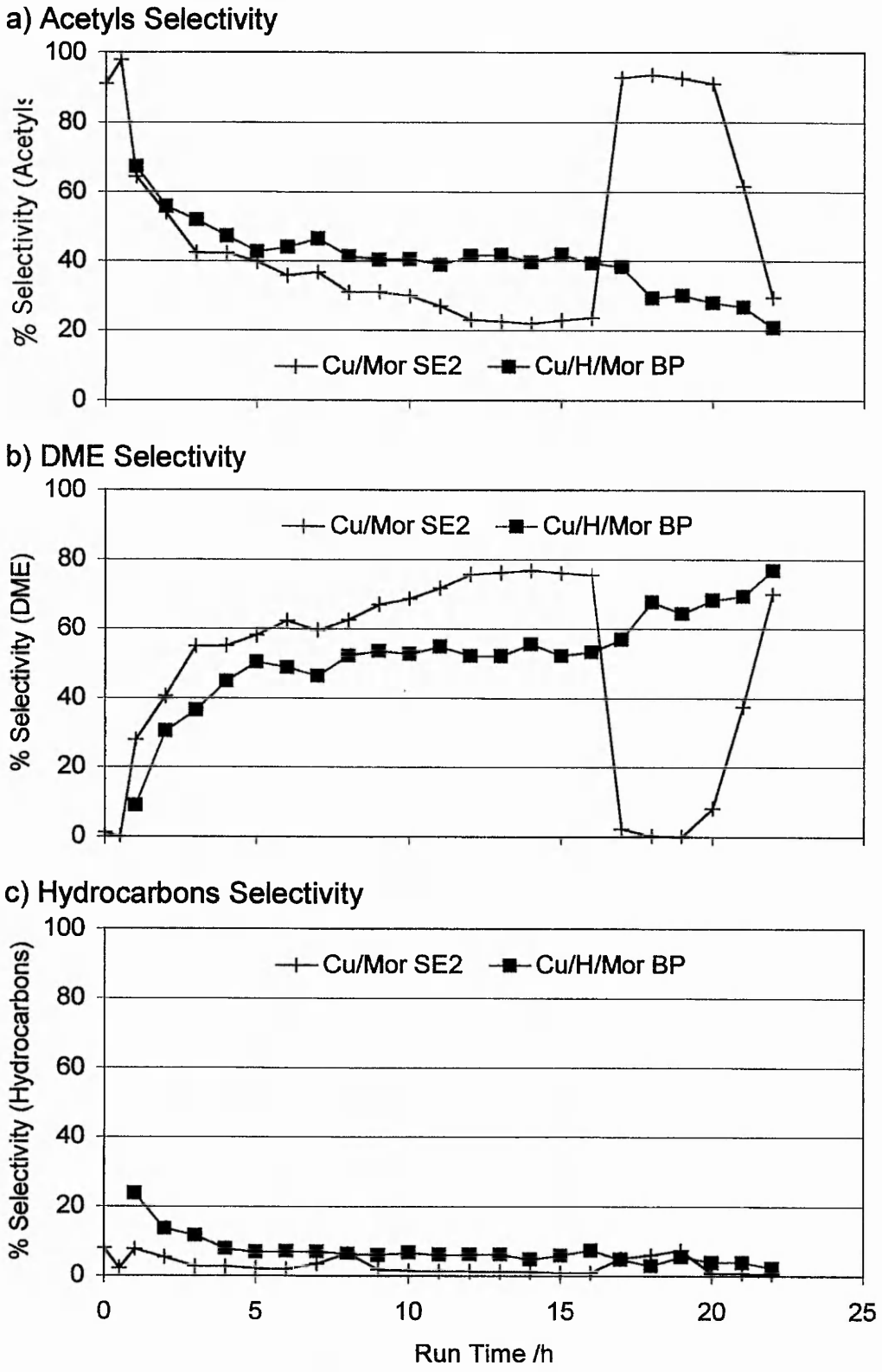

Figure 2.14 The effect of the acetyls sticking on the selectivities to (a) Acetyls, (b) DME and (c) Hydrocarbons

By 10 hours, the selectivities to acetyls and DME are stable at 20% and 80% respectively, with a carbon balance of over 80%. On stopping the methanol, the high DME selectivity falls to zero within the hour, whilst the acetyls selectivity rises to 80% again. In the presence of methanol the hydrocarbon selectivity is virtually zero and rises to 10% in the absence of methanol. However it has to be remembered, the rise in hydrocarbon selectivity does not take into account, the significant drop in the total concentration of detected species.

The initial combined acetyls yield is an incredible 7.5 g/g/h, as shown in Figure 2.15a, and is virtually a 1:1 ratio of acetic acid and methyl acetate. It could therefore be possible to obtain a high acetyls yield, from very low methanol concentrations. Work to confirm this unfortunately failed, because of the practical limitations encountered for maintaining stable pressures under flow rates higher than the 100 ml min^{-1} reported here. In the first 2 hours, the yield rises further to a maximum of 1.4 g/g/h, due mainly to a substantial rise in methyl acetate. Afterwards the yield falls, and by 10 hours it maintains a stable 0.5 g/g/h. On stopping the methanol flow, within the hour the acetyls yield has dropped to 0.1 g/g/h, entirely due to the loss of methyl acetate. The yield of acetic acid appears to be unaffected by the stopping of the methanol flow, and is explained by two possible causes. Firstly, the formation of acetic acid is favoured, under the lower concentrations of methanol. Secondly, because the acetic acid becomes trapped within the post reactor line, the substantial increase in the residence time causes acetic acid to still be released from the reactor, even after 3 hours.

A point of extreme importance should be stressed here. On restarting the methanol, the initial combined acetyls yield, regains its initial value of at least 0.8 g/g/h. Again, there are two possible explanations. Firstly, the formation of acetyls is more favoured under the initial low concentrations of methanol, or secondly, restarting the methanol releases the acetic acid sticking in the reactor by converting it to methyl acetate. The second explanation is plausible because both the acetic acid and methyl acetate yields increase by approximately the same extent.

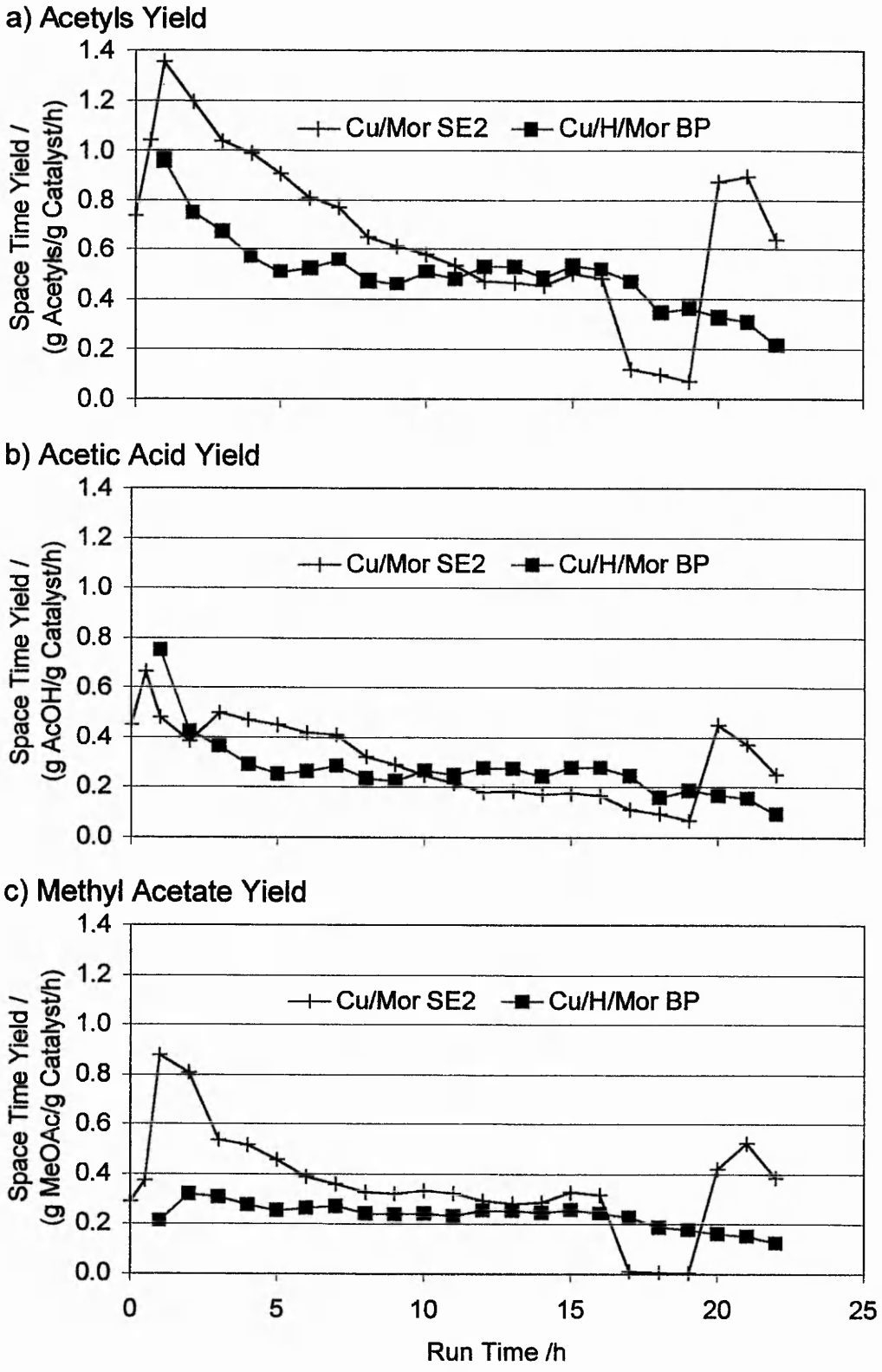

Figure 2.15 The effect of acetyls sticking on the Space Time Yields of (a) Acetyls, (b) Acetic Acid and (c) Methyl Acetate

References

1. Ellis, B., Howard, M.J., Joyner, R.W., Reddy, K.N., Padley, M.B., Smith, W.J., *Stud. Surf. Sci. Catal.*, 1996, **101**, 771-779.
2. Smith, W.J., BP Chemicals Ltd, EP 596 632 A1 (1993).
3. Kuroda, Y., Kotani, A., Uemura, A., Yoshikawa, Y., Morimoto, T., *J. Chem. Soc. Chem. Commun.*, 1989, 1631-1632.
4. Schay, Z., Knozinger, H., Guczi, L., Pal-Borbely, G., *Appl. Catal. B-Env.*, 1998, **18**, 263-271.
5. Jensen, S.F., Catalytic decomposition of NO over metal exchanged zeolites., thesis, University of Trondheim, NTH, Trondheim (1998)
6. Garces, J.M., The DOW Chemical Co. US Patent 4 891 448 (1990)
7. Xu, L.Q., Zholobenko, V.L., Kustov, L.M., Sachtler, W.M.H, *J. Molecular Catal.*, 1993, **83**, 391-395.
8. Ziethen, H.M., Trautwein, A.X., *Zeolites as Catalysts, Sorbents and Detergent Builders*, Karge, H.G., Weitkamp, J., (Eds.) Elsevier Science Publishers B.V., Amsterdam, 1989, 789-800.

CHAPTER 3

THE MORDENITE FRAMEWORK

Introduction – aims of the chapter

In this chapter, the results from the mordenite catalysts are presented. Starting with the mordenite containing a single cation species, and then the effect of the silica to alumina ratio (SAR). The following experiments highlight the effect of introducting copper into the system. As described in Chapter 1, the presence of copper has been found to promote the carbonylation of methanol over the mordenite framework. Here, attempts are made to determine the influence of the copper loading. Finally, the results of framework modification by dealumination are reported.

The implications of all these results are discussed further in Chapter 4.

Introduction – the presentation of results

A standard presentation format, for all the catalytic results, is maintained throughout the following chapters.

The four measurements are,

(i) The percentage methanol conversion.

(ii) The percentage carbon balance for methanol.

(iii) The percentage selectivity to (a) acetyls, (b) dimethyl ether (DME) and (c) hydrocarbons.

(iv) The space time yields for the acetyls, acetic acid and methyl acetate.

The results are based only on the composition of the volatile components detected, the calculations for which are described in Chapter 2. The results for two different reactions, plotted as a function of reaction time, are compared directly. The data points are crosses for the first series and filled squares for the second.

Carbonylation activity of mordenite in the Na and H forms

The first sample, Na/MOR (SAR 20), prepared from the supplied proton form by multiple ion exchanges with sodium nitrate, is compared with the supplied H/MOR (SAR 20), under the standard reaction conditions described in Chapter 2.

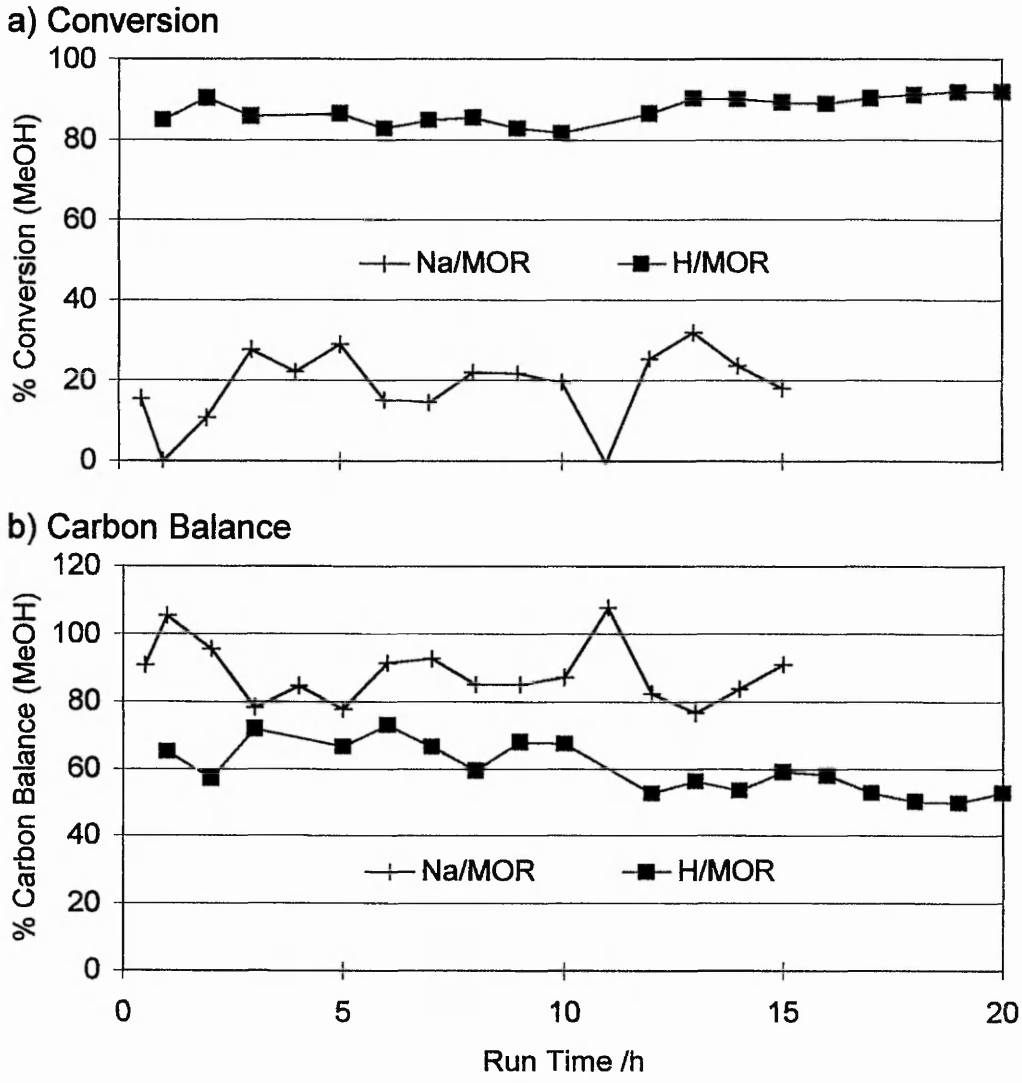

Figure 3.1 The Comparison of (a) the Conversion and (b) the Carbon Balance for Na and H mordenite SAR 20

Figure 3.1a shows the methanol conversion for the sodium form is typically 20%, compared to the proton form being over 80% throughout. Figure 3.1b shows for the sodium form, the carbon balance is above 80% throughout. Whereas, the carbon balance for the proton form is lower, initially at 70% it decreases to 50% after 20 hours of testing.

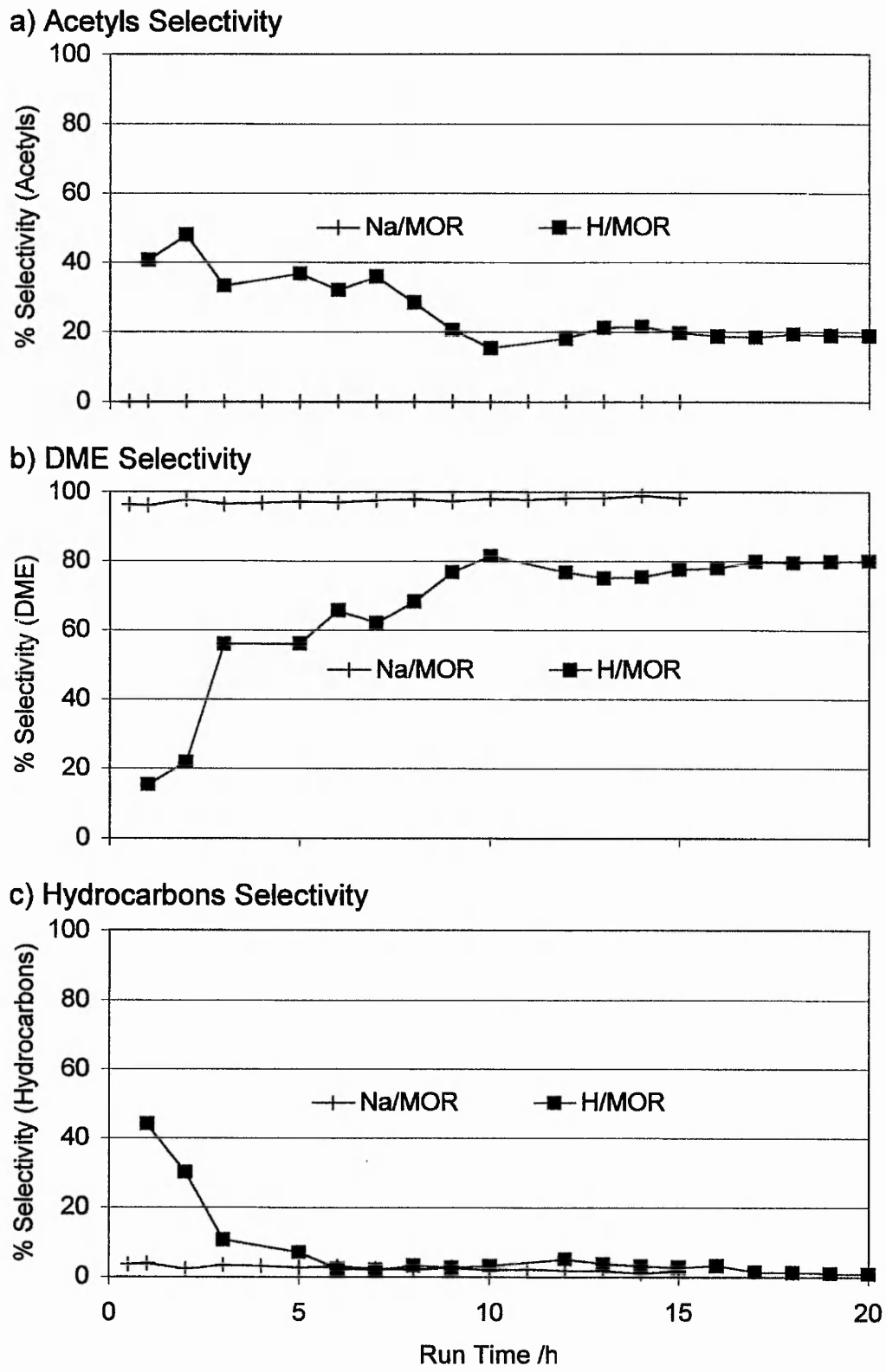

Figure 3.2 The Comparison of the Selectivities to (a) Acetyls, (b) DME and (c) Hydrocarbons for Na and H mordenite SAR 20

The selectivities to the three groups of products are shown in Figure 3.2a-c. As described previously in Chapter 2, the single product from the sodium form is DME, with only 20% of the methanol converted. In contrast, the proton form shows an initial acetyls selectivity of 40%, which after 10 hours has stabilised at 20%. Selectivity to the hydrocarbons, initially 40%, has dropped virtually to zero after 5 hours. DME dominates the selectivity by 3 hours on stream, it then continues to rise, reaching a stable selectivity of 80% after 10 hours.

The initial 40% selectivity to acetyls, corresponds to a space time yield of approximately 0.8 g acetyls/ g catalyst /h (g/g/h), which after 10 hours has halved to between 0.4-0.3 g/g/h, as shown below in Figure 3.3.

Clearly the proton form, having a higher overall reactivity compared to the sodium form, converts a larger proportion of the methanol, primarily to DME, but also to the desired acetyls and the initial hydrocarbon byproducts. The proton form of mordenite, initially produces a relatively high yield of acetyls that then drops by half, to what appears to be a steady state, under the experimental conditions adopted.

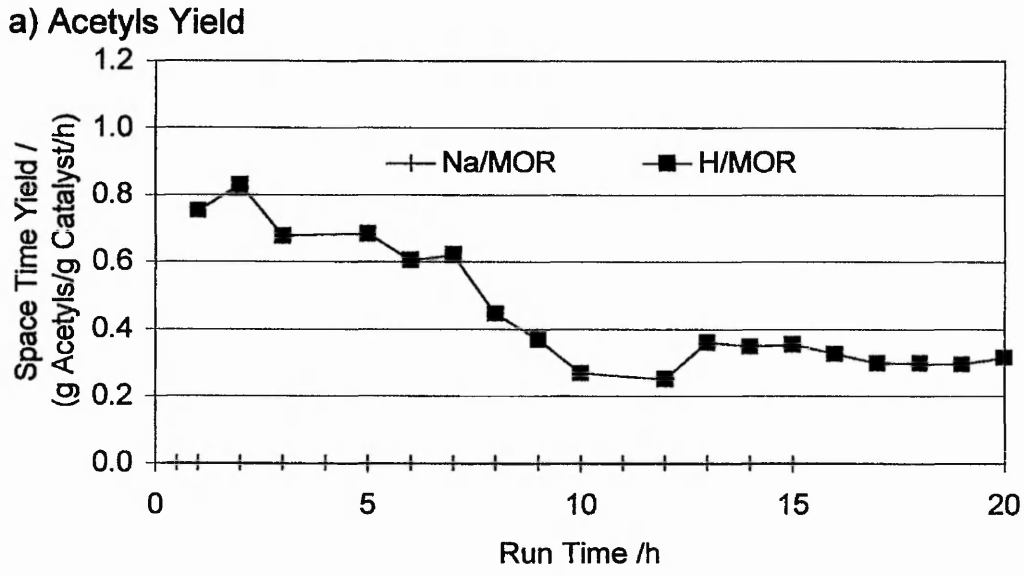

Figure 3.3 The Comparison of the Acetyls Space Time Yields for Na and H mordenite SAR 20

The effect of the silica to alumina (SAR) ratio

As outlined in Chapter 1, the reactivity of zeolite catalysts can be modified in a number of ways e.g., (i) varying their aluminium content & (ii) exchanging their counter cations. The reactivity of mordenite is dependent on the aluminium content of the framework, represented by the silica to alumina ratio (SAR). It is therefore of interest, to compare this proton form of mordenite with a similar one of higher aluminium content (lower SAR).

Below in Figure 3.4-6, the results are presented for two frameworks, the H/MOR (SAR 20) is compared with H/MOR (SAR 12.8).

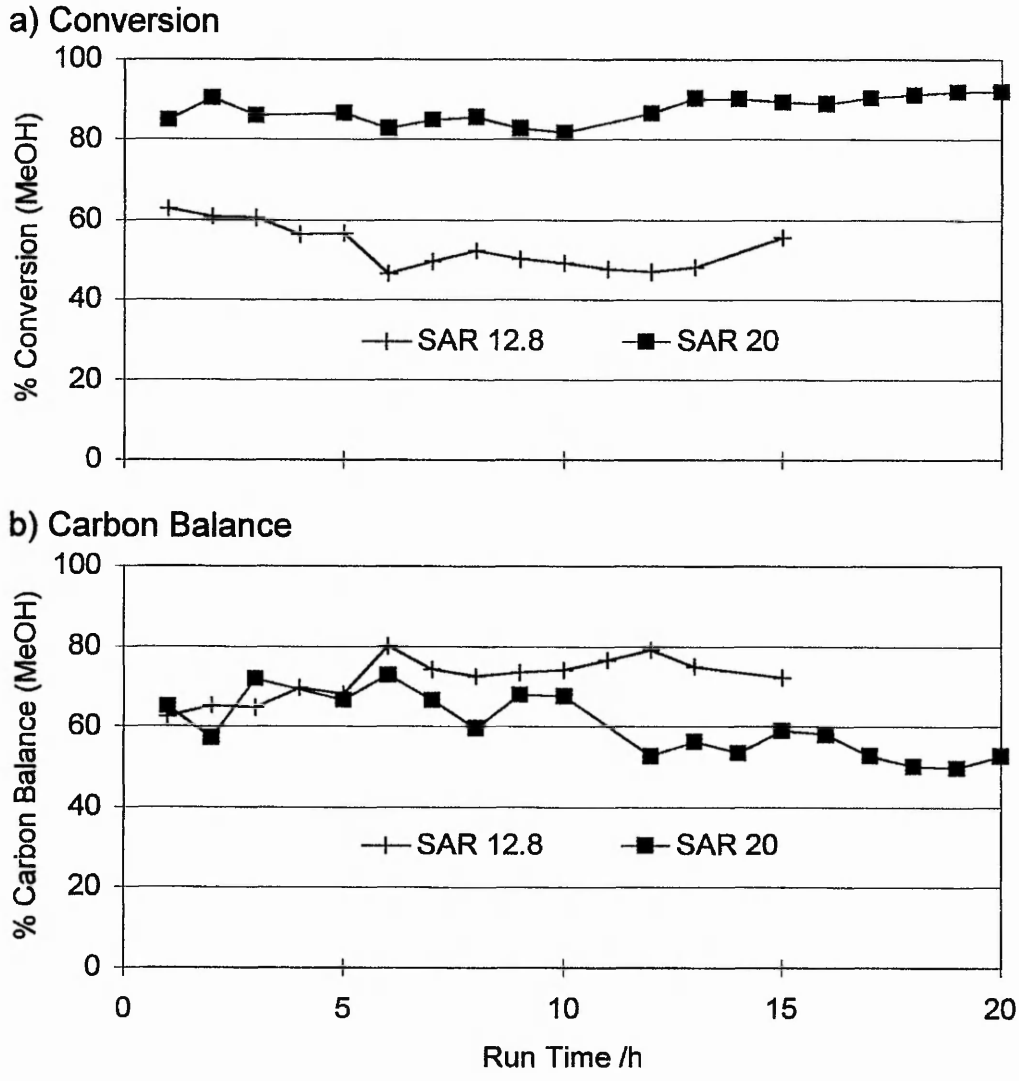

Figure 3.4 The effect of the Silica/Alumina Ratio (SAR) on (a) the Conversion and (b) the Carbon Balance for H/MOR

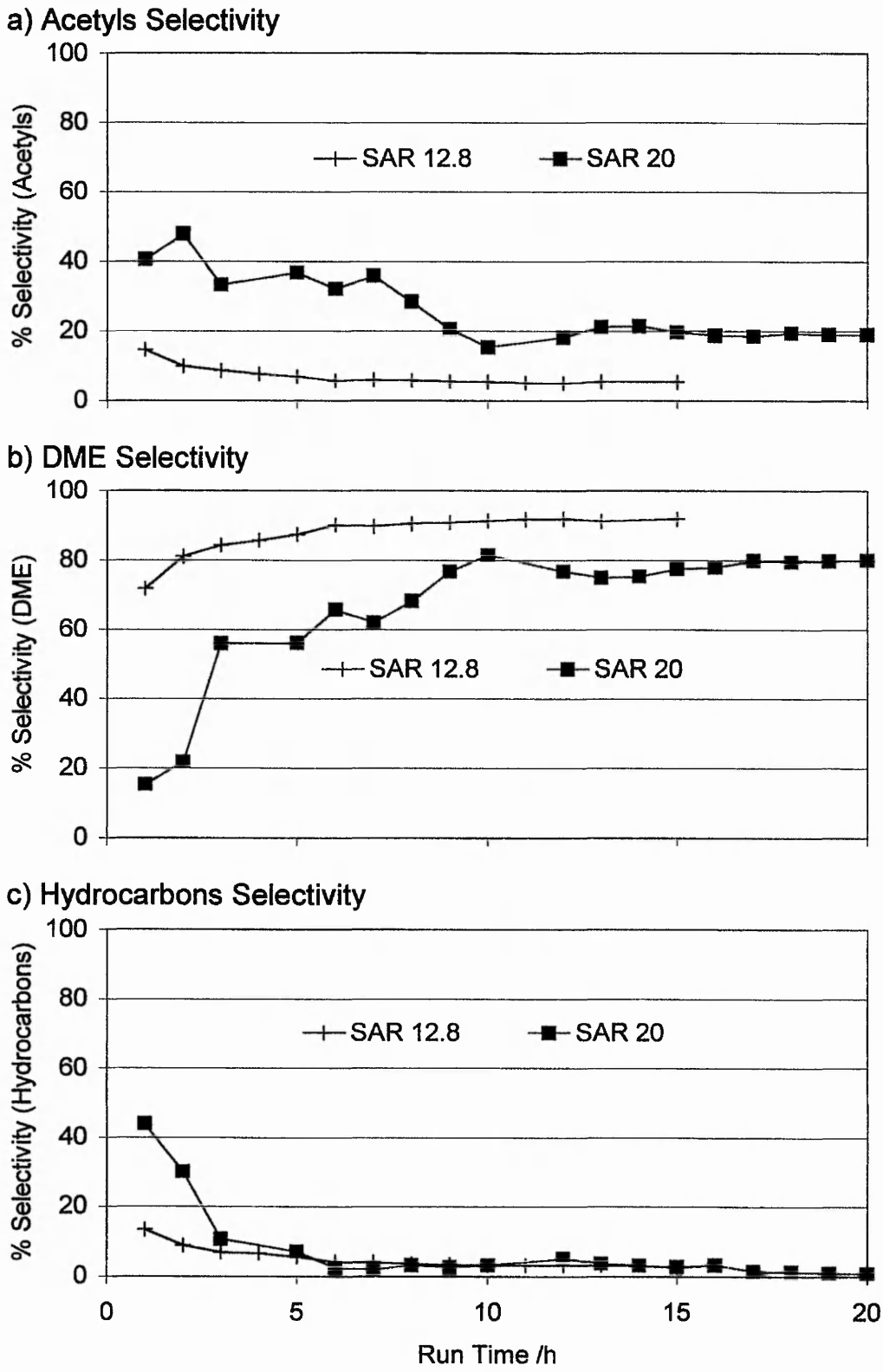

Figure 3.5 The effect of the Silica/Alumina Ratio (SAR) on the Selectivities to (a) Acetyls, (b) DME and (c) Hydrocarbons for H/MOR

The methanol conversion over the framework of SAR20 is consistently higher than for the SAR12.8 framework. The conversion level for the SAR20 framework is 80 ±5%, whereas, for the SAR12.8 framework it steadily decreases from its initial 60%, by 10% over the 15 hours. The reaction was terminated early due to the reactor blocking.
The carbon balance for the two frameworks is initially around 70%, for SAR20 it gradually decreases to 50% by 20 hours on stream, while for SAR12.8 it rises to around 80% after 15 hours. The SAR20, even at the higher levels of conversion, compared to SAR12.8 gives twice the acetyls selectivity, as shown in Figure 3.5.
As shown below in Figure 3.6, both the higher conversion and acetyls selectivity for SAR20, result in a maximum acetyls space time yield (0.8 g/g/h) greater than four times that for SAR12.8.

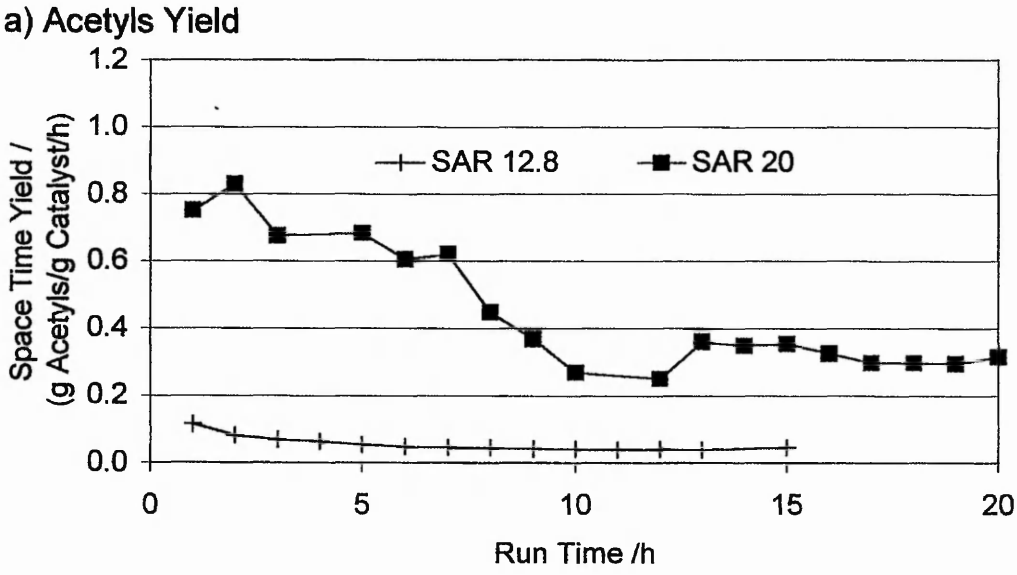

Figure 3.6 The effect of the Silica/Alumina Ratio (SAR) on the Acetyls yield for H/MOR

The promotional effect of ion-exchanged copper

As previously reported (see Chapter 1), the introduction of copper by ion-exchange, into the proton form of mordenite, promotes the conversion of methanol to the desired acetyls by both, (i) increasing the yield and (ii) prolonging the period of acetyls formation. The relevant results obtained in this work are presented in Figure 3.7-9, H/MOR (SAR20) is compared to Cu/MOR SE1, the proton form of the SAR20 with an ion-exchanged copper loading of 2.2 wt%.

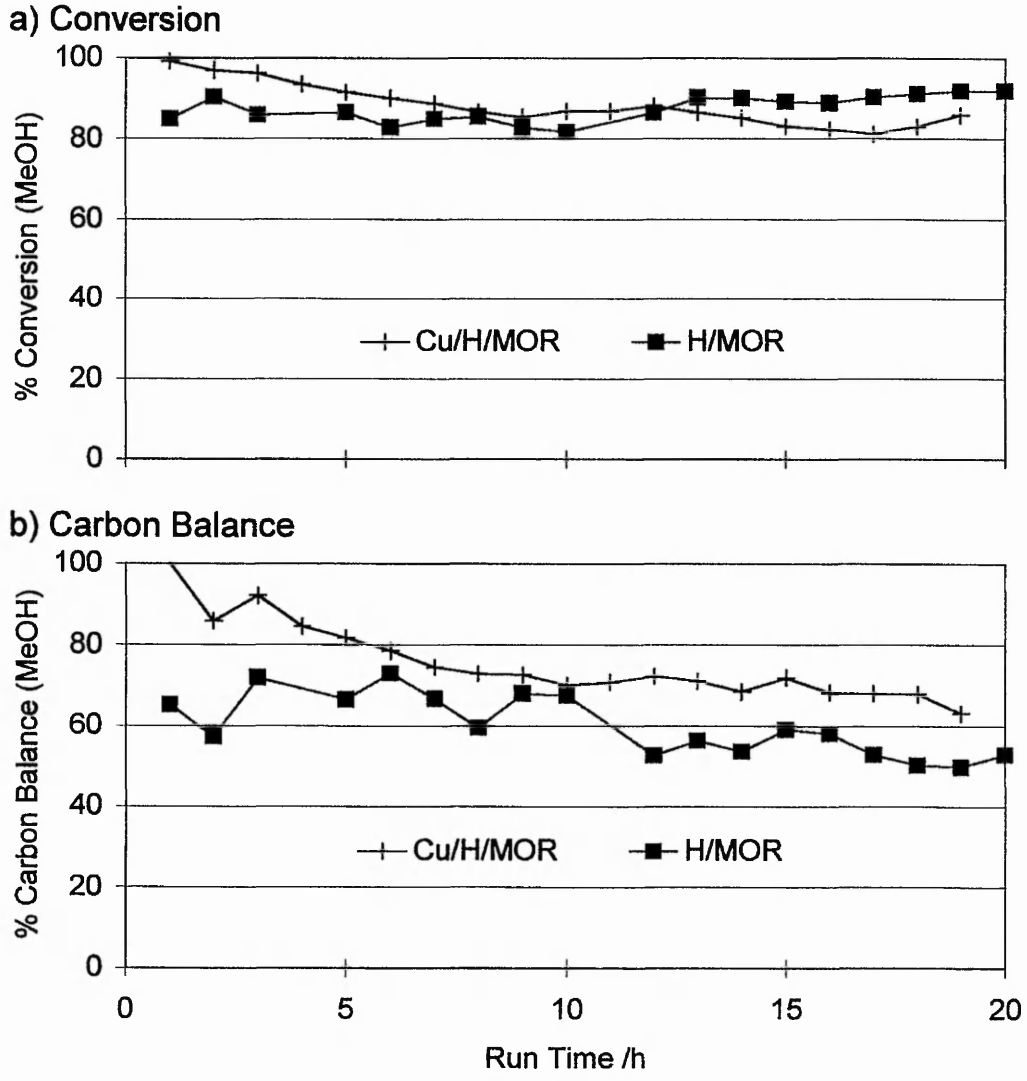

Figure 3.7 The effect of ion-exchanged copper on (a) the Conversion and (b) the Carbon Balance for H/MOR SAR20

It can be seen from Figure 3.7a, that the introduction of copper into the proton form does not affect the degree of methanol conversion. However, Figure 3.7b shows that the carbon balance is modified by the presence of copper. Initially, for the proton form the carbon balance is 70% and decreases further to 50%, after 20 hours on stream. Whereas, for the copper form the initial carbon balance is 100%, indicating that all the methanol is being converted and detected. With time, the carbon balance is seen to decrease, reaching a value of 70% after 18 hours.

For the copper form, the initial 100% conversion is supported by a selectivity to the acetyls of 80%, which steadily drops to 40% by 18 hours. In sharp contrast, the proton form shows an initial acetyls selectivity of only 40%, which after 10 hours has fallen further to 20%. In both catalysts, the decrease in acetyls selectivity, is mirrored by a steadily rising selectivity to DME. For the copper form, the DME selectivity dominates at 50%, but only after 13 hours. While for the proton form, DME has become the dominant product by 3 hours, and by 10 hours has stabilised at 80%.

The hydrocarbon selectivity for both catalysts dies off to below 10% after 5 hours.

Figure 3.9 shows for the copper form, the initial high acetyls yield corresponds to a space time yield of 1.8 g acetic acid /g catalyst /hour. As the acetic acid declines, it is replaced by the rising methyl acetate yield. The combined yield of 1.0 g/g/h after 6 hours is of equal parts acetic acid and methyl acetate. The combined effect of these two yields produces the largest STY of acetyls seen throughout this work.

In comparison, the lower yield for the proton form is due to a very low acetic acid yield. However, the two samples are producing very similar yields of methyl acetate after the initial 3 hours.

In summary, the copper form is initially dominated, by virtually complete conversion of methanol to acetyls, whilst the proton form converts less methanol, at an initial 50:50 selectivity of acetyls to hydrocarbons. With time, both catalysts lose their reactivity towards acetyls, in favour of the formation of DME.

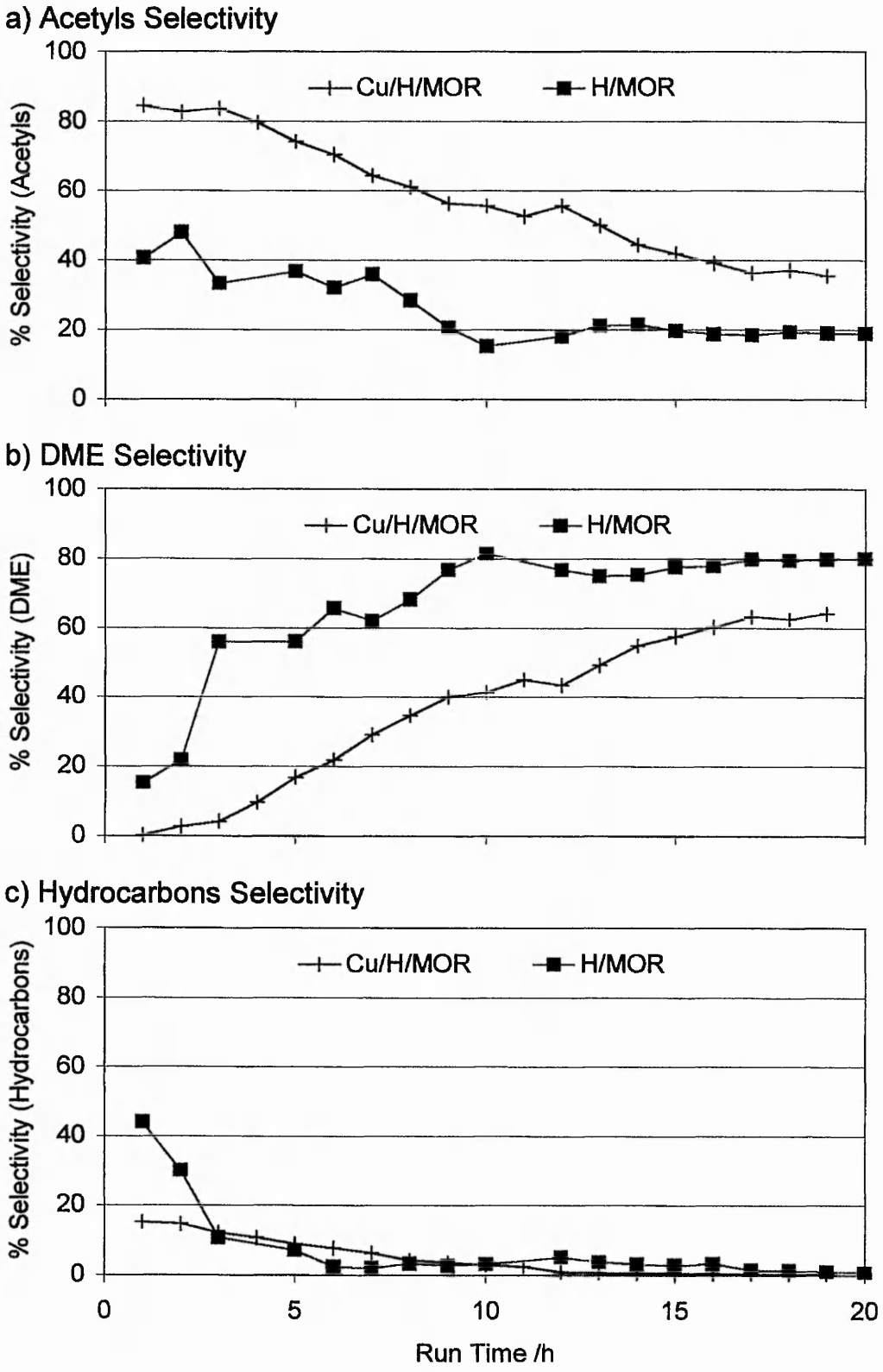

Figure 3.8 The effect of ion-exchanged copper on the Selectivities to (a) Acetyls, (b) DME and (c) Hydrocarbons for H/MOR SAR 20

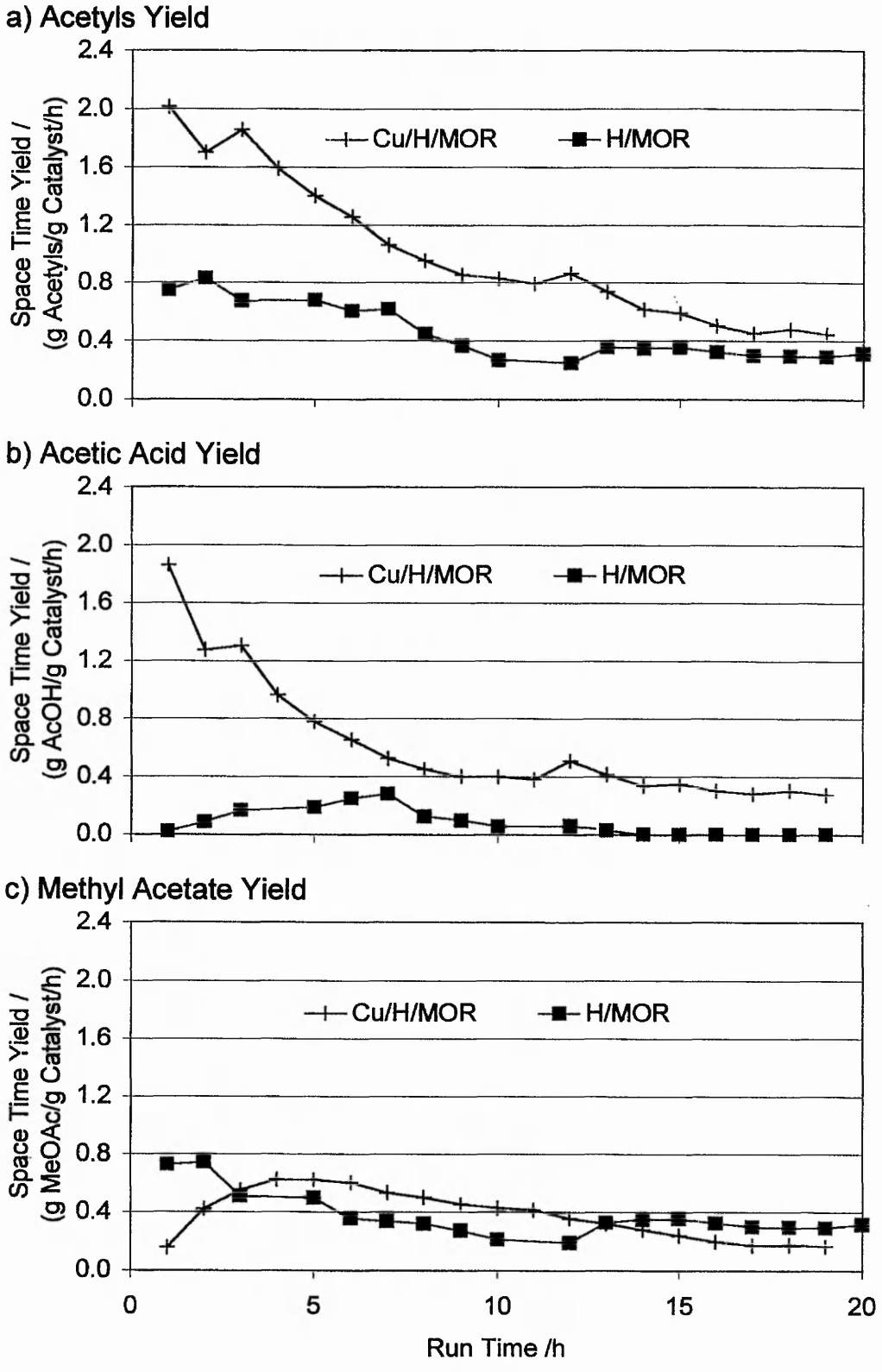

Figure 3.9 The effect of ion-exchanged copper on the Space Time Yields of (a) Acetyls, (b) Acetic Acid and (c) Methyl Acetate for H/MOR SAR 20

Active sites due to copper

The previous section clearly shows the increase in the acetyls yield, following the introduction of copper, by ion-exchange, into the proton form of mordenite.
An attempt, to determine whether the copper creates independent sites, or works synergistically with the proton sites, was made by directly copper ion-exchanging Na/MOR (12.8). In Figure 3.10-12, the results for Cu/Na/MOR 0.9 and Cu/Na/MOR 3.4 are shown.

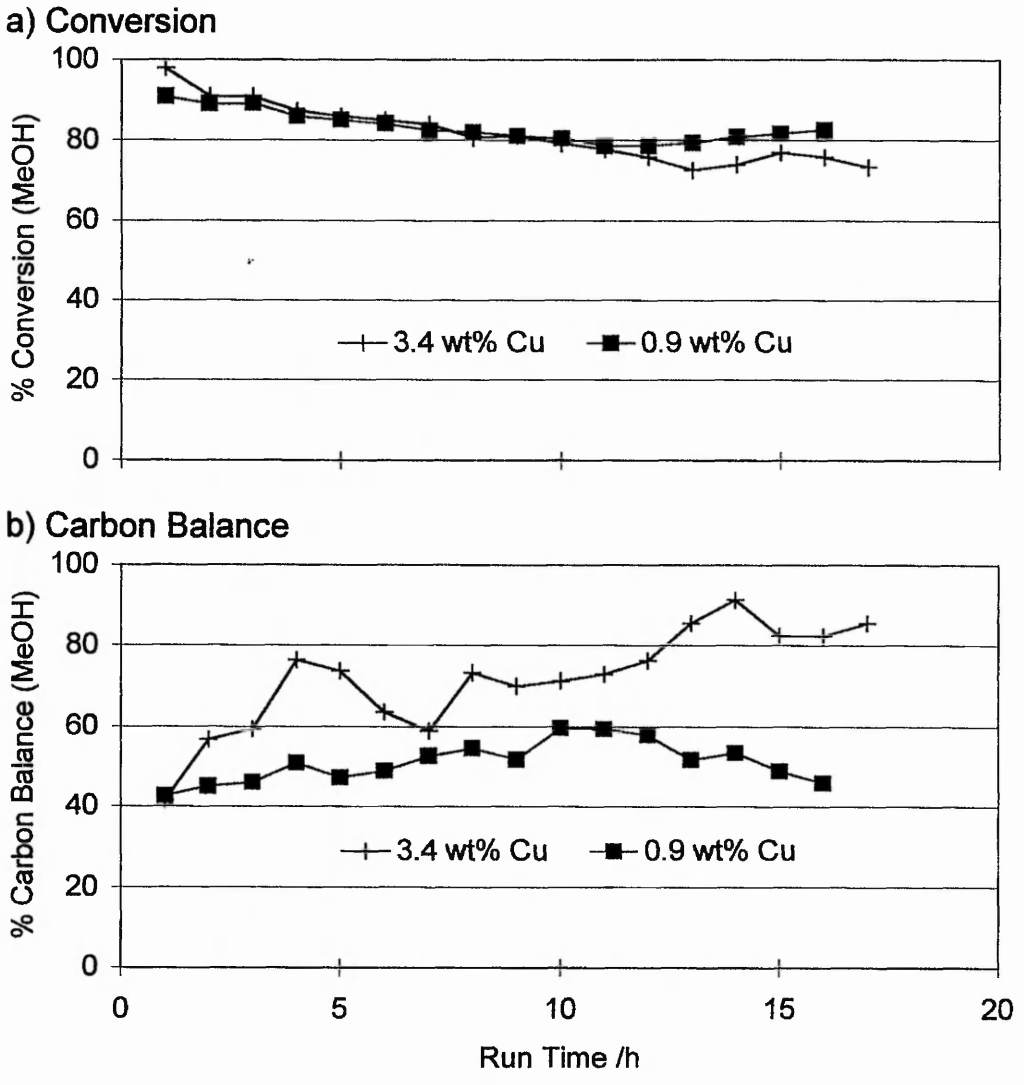

Figure 3.10 The effect of copper loading on (a) the Conversion and (b) the Carbon Balance for Cu/Na/MOR SAR12.8

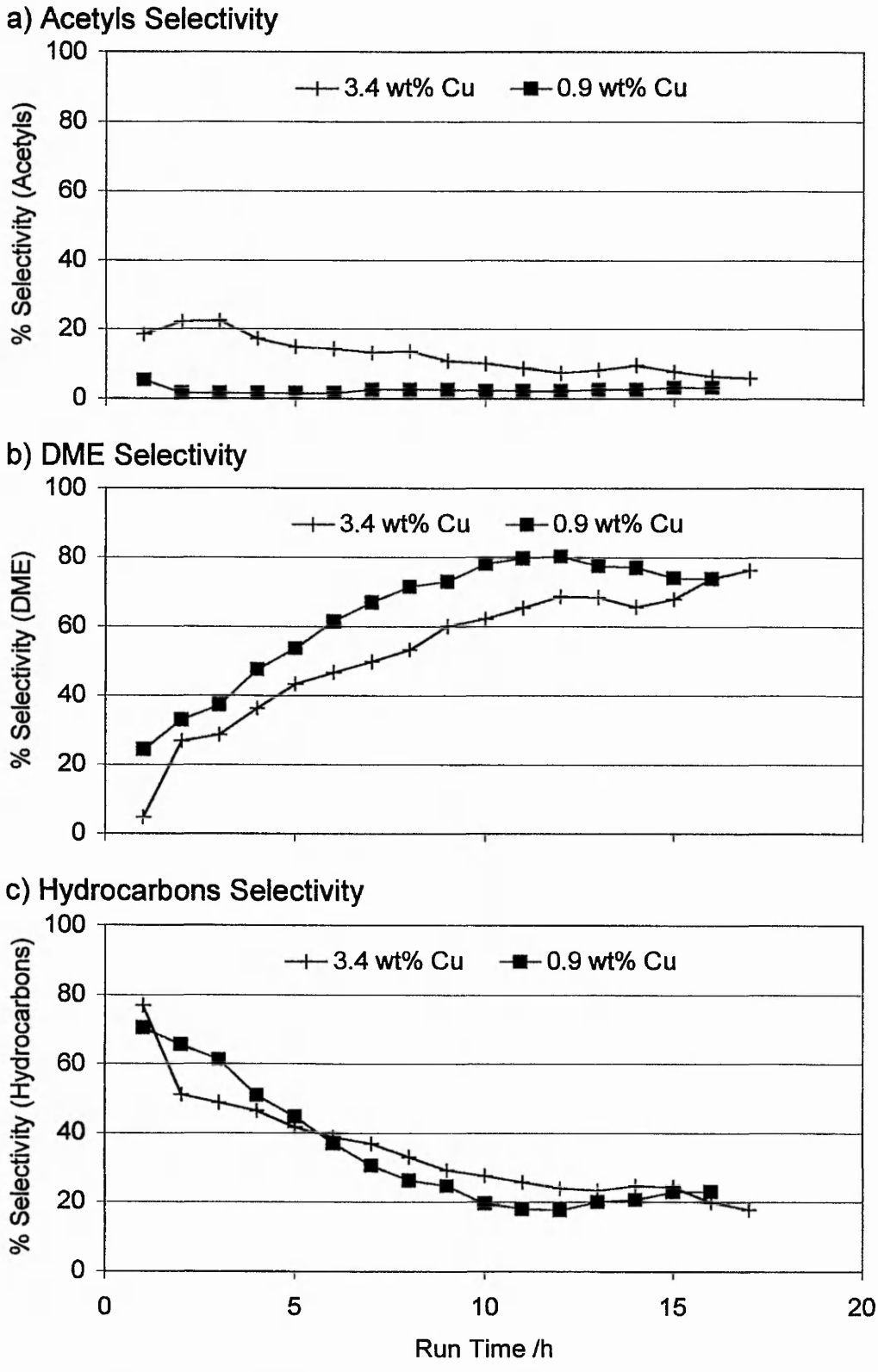

Figure 3.11 The effect of copper loading on the Selectivities to (a) Acetyls, (b) DME and (c) Hydrocarbons for Cu/Na/MOR SAR12.8

The methanol conversion, for the two copper loadings, is virtually identical throughout, initially 100-90% and falling to 80-70% after 15 hours of reaction. The carbon balances also follow similar trends, both initially being at 40% and rising with reaction time. However, the carbon balance for the 3.4 wt% loading is always greater than for the corresponding value for the 0.9 wt% loading.

Figure 3.11a shows the selectivity to acetyls for the two reactions. The 3.4 wt% copper loading shows an initial acetyls selectivity of 20%, that steadily decreases to 10% after 10 hours of reaction. Although not comparable to the Cu/H/MOR SE of the previous section, the acetyls selectivity of 20% is significant, compared to the virtually zero acetyls selectivity of the 0.9 wt% loading. The selectivity to DME is constantly lower for the 3.4 wt% than for the 0.9 wt% sample. However, their trends are similar, initially zero but rising to 60-70% by 10 hours of reaction. This clearly indicates that a large proportion of the methanol introduced to both samples forms DME.

The selectivity to hydrocarbons for both samples is virtually identical, initially around 70% they fall to a stable 20% level after 10 hours.

The only product from the Na/MOR (SAR 20) reported in the first section was DME. Although not the same sample, the selectivity is assumed to be the same, but the level of conversion may be different. As the copper content is increased from zero to 3.4 wt%, the selectivity towards DME is reduced in favour of, firstly the hydrocarbons at the low copper loading, and then further for the acetyls at the high loading.

The space time yields are shown in Figure 3.12a-c. The initial 20% selectivity to acetyls for the 3.4 wt % sample corresponds to a maximum 0.3 g/g/h yield. Acetic acid forms the major component but decays away steadily, while methyl acetate rises to, and maintains, a stable 0.1 g/g/h yield. For the majority of the time, the acetyls composition is approximately of equal parts acetic acid and methyl acetate. In contrast, the 0.9 wt% sample shows no acetic acid, only a very low 0.02 g/g/h yield of methyl acetate.

These results show that, in the presence of a sufficiently high loading of copper, with sodium as the starting cation, the mordenite framework is able to produce a significant acetyls yield under the adopted reaction conditions.

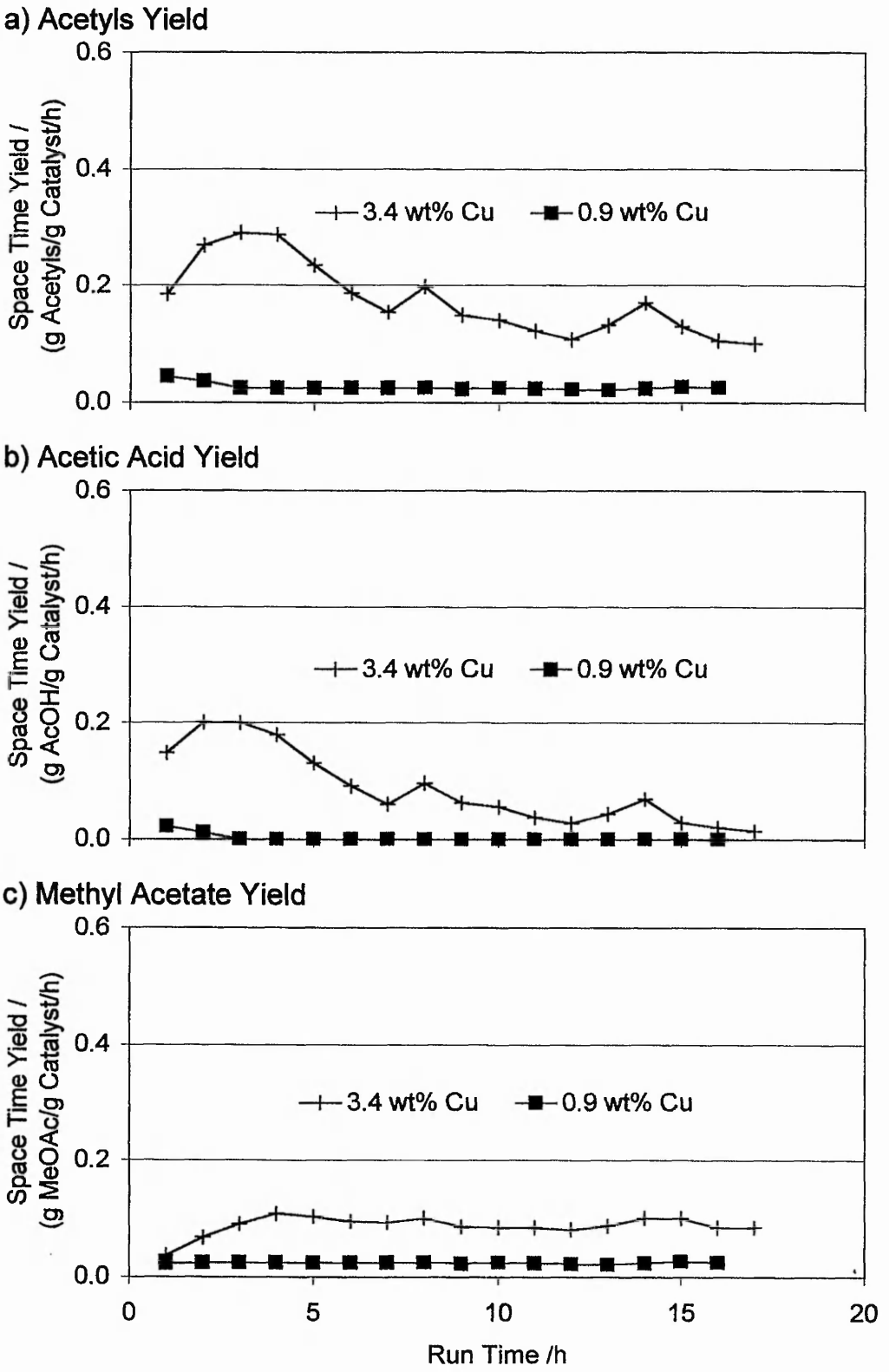

Figure 3.12 The effect of copper loading on the Space Time Yields of (a) Acetyls, (b) Acetic Acid and (c) Methyl Acetate for Cu/Na/MOR SAR 12.8

The effect of the counter-ion

In Figure 3.13-15, to determine if copper promotes the sodium form to the same extent as it does the proton form, the Cu/Na/MOR 3.4 sample is compared to the Cu/H/MOR BP sample which contains 3.5 wt% copper, first reported in Chapter 2.

The level of conversion, over the two copper loaded mordenites, is identical within the experimental error of ±5%. Both samples have an initial conversion around 100% that drops steadily, approaching 75% after 13 hours. Likewise, the carbon balances are equivalent within the experimental error.

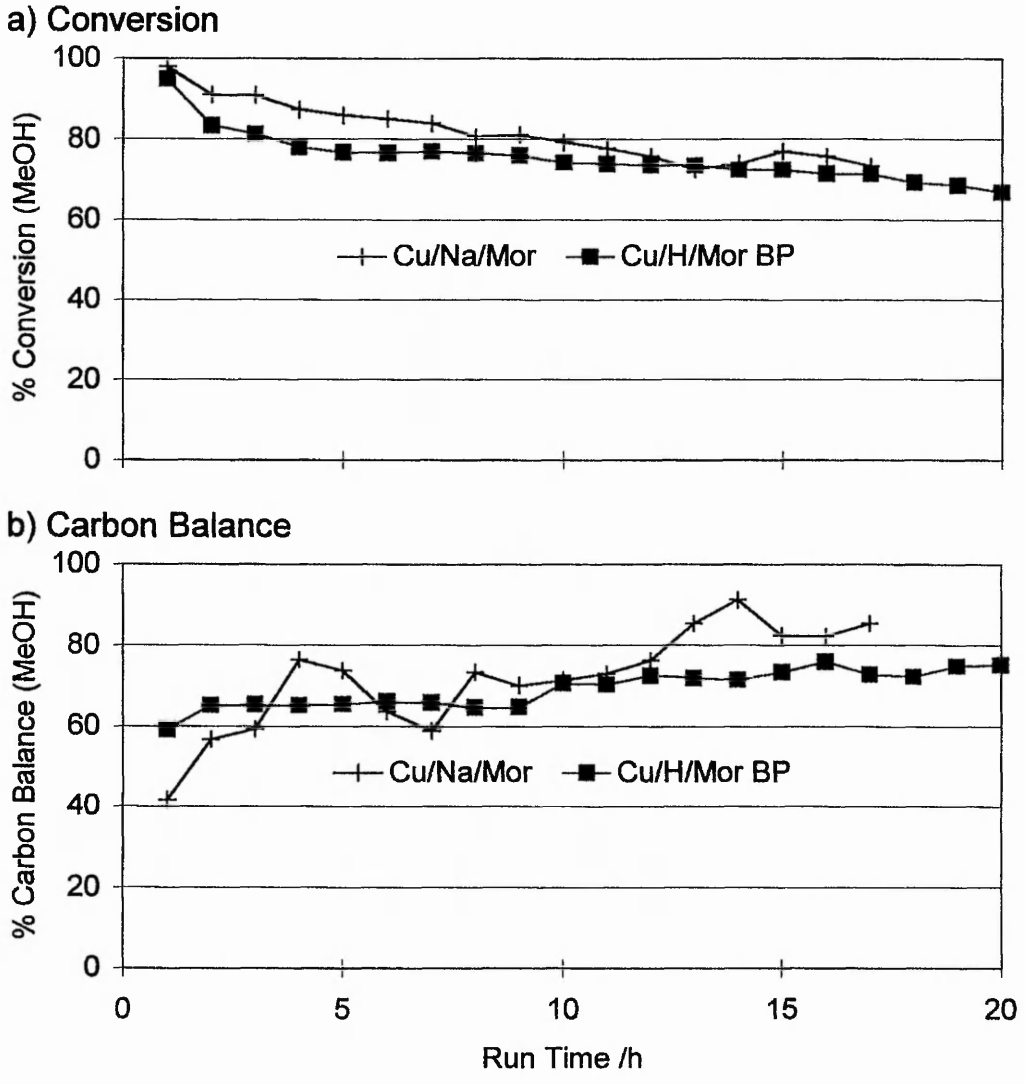

Figure 3.13 The effect of the counter-ion on (a) the Conversion and (b) the Carbon Balance for Cu/MOR SAR 12.8

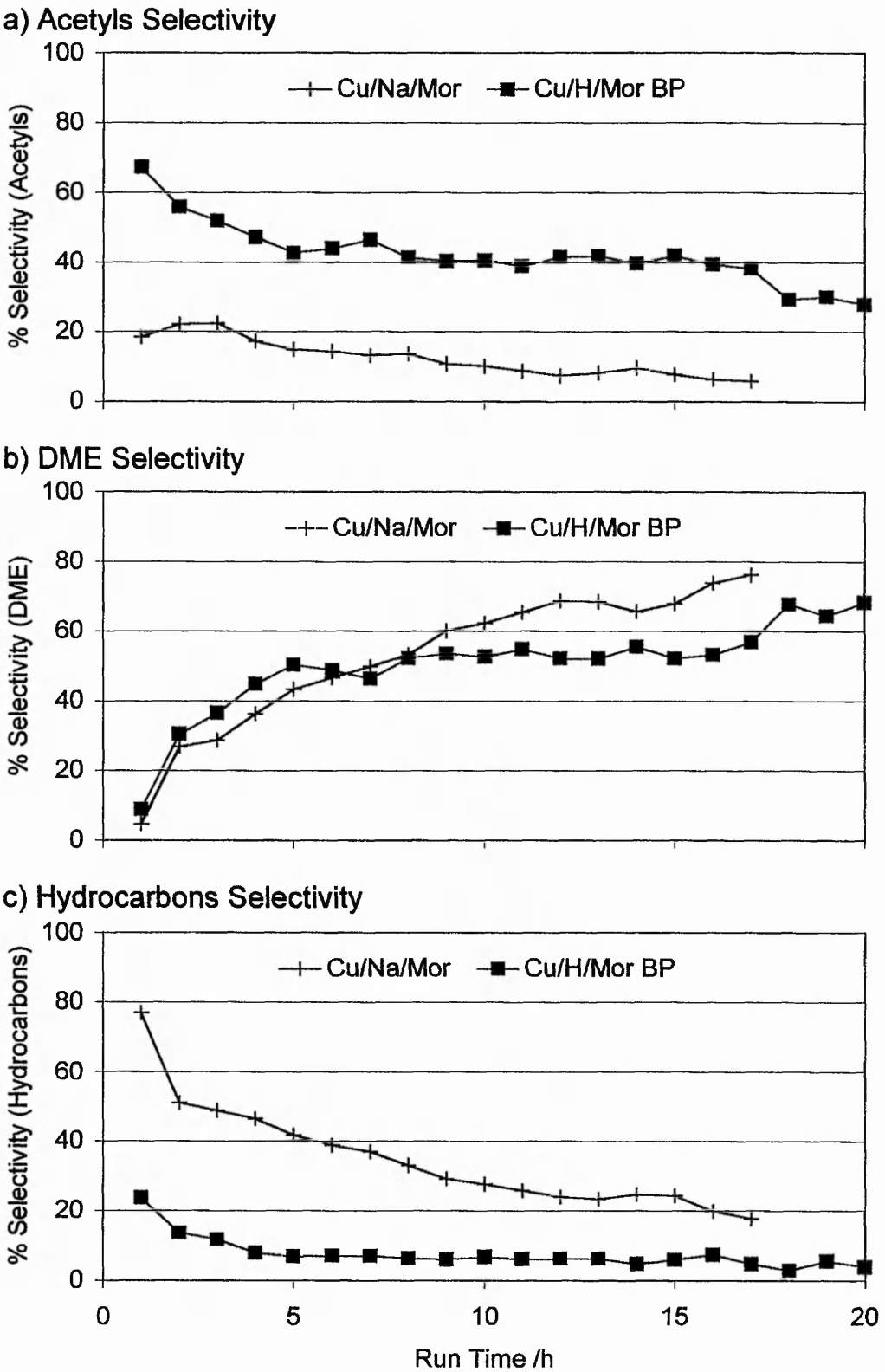

Figure 3.14 The effect of the counter-ion on the Selectivities to (a) Acetyls, (b) DME and (c) Hydrocarbons for Cu/MOR SAR12.8

It can be seen in Figure 3.14a, that the acetyls selectivity is enhanced markedly in the case of the proton form. The initial acetyls selectivity of 70% for the proton form is in contrast to the 20% for the sodium form. However, the selectivity towards DME can be seen to follow the same trend for both reactions. The difference therefore, in acetyls selectivity, is due to a greater selectivity to hydrocarbons for the sodium form.
From the yields, shown in Figure 3.15, the sodium form produces a peak of 0.3 g/g/h acetyls, which then stabilises between 0.2-0.1 g/g/h for the remaining time on stream. In comparison, the yield of acetyls from the proton form is much greater throughout. The initial yield, of nearly 1.0 g/g/h acetyls, is composed purely of acetic acid. The combined yield then decreases, to a stable 0.5 g/g/h of equal parts acetic acid and methyl acetate.
The difference in the acetyls yields is greater than could be expected, solely from the slight variation in copper content.

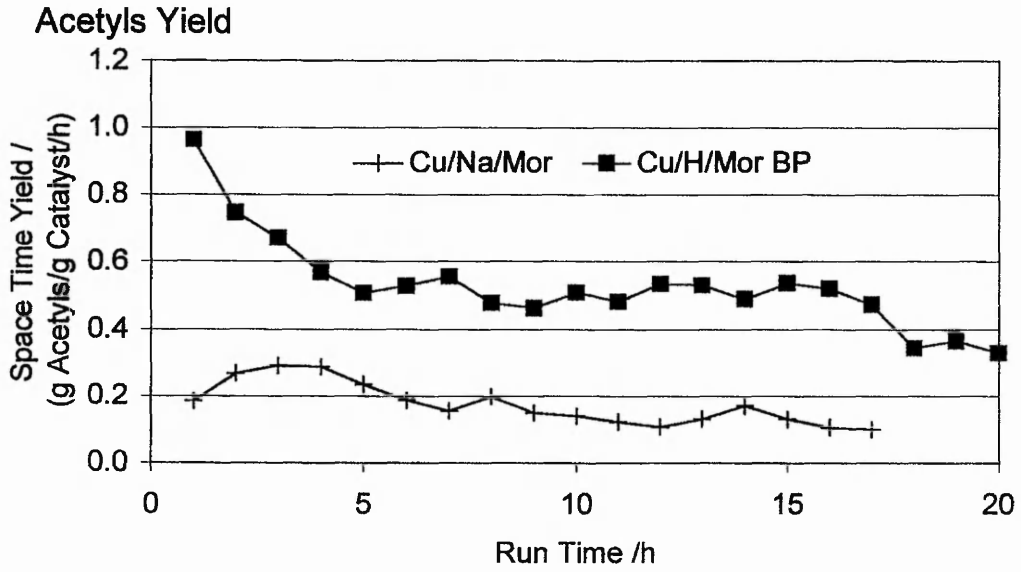

Figure 3.15 The effect of the counter-ion on the Space Time Yield of the Acetyls for Cu/MOR SAR 12.8

Pretreatment in carbon monoxide

The standard conditions included four hours of in situ pretreatment at 500°C, under flowing carbon monoxide at atmospheric pressure, to ensure the sample was activated after being pressed. As detailed in Chapter 2, carbon monoxide was used during activation to ensure methanol contacted the catalyst only in the presence of carbon monoxide. It is known, methanol will readily form hydrocarbons over strong Bronsted acid sites in the absence of carbon monoxide (see Chapter 1 and page 71). Any effect of the pretreatment was determined, using the Cu/H/MOR SE1 sample, directly without any high temperature pretreatment.

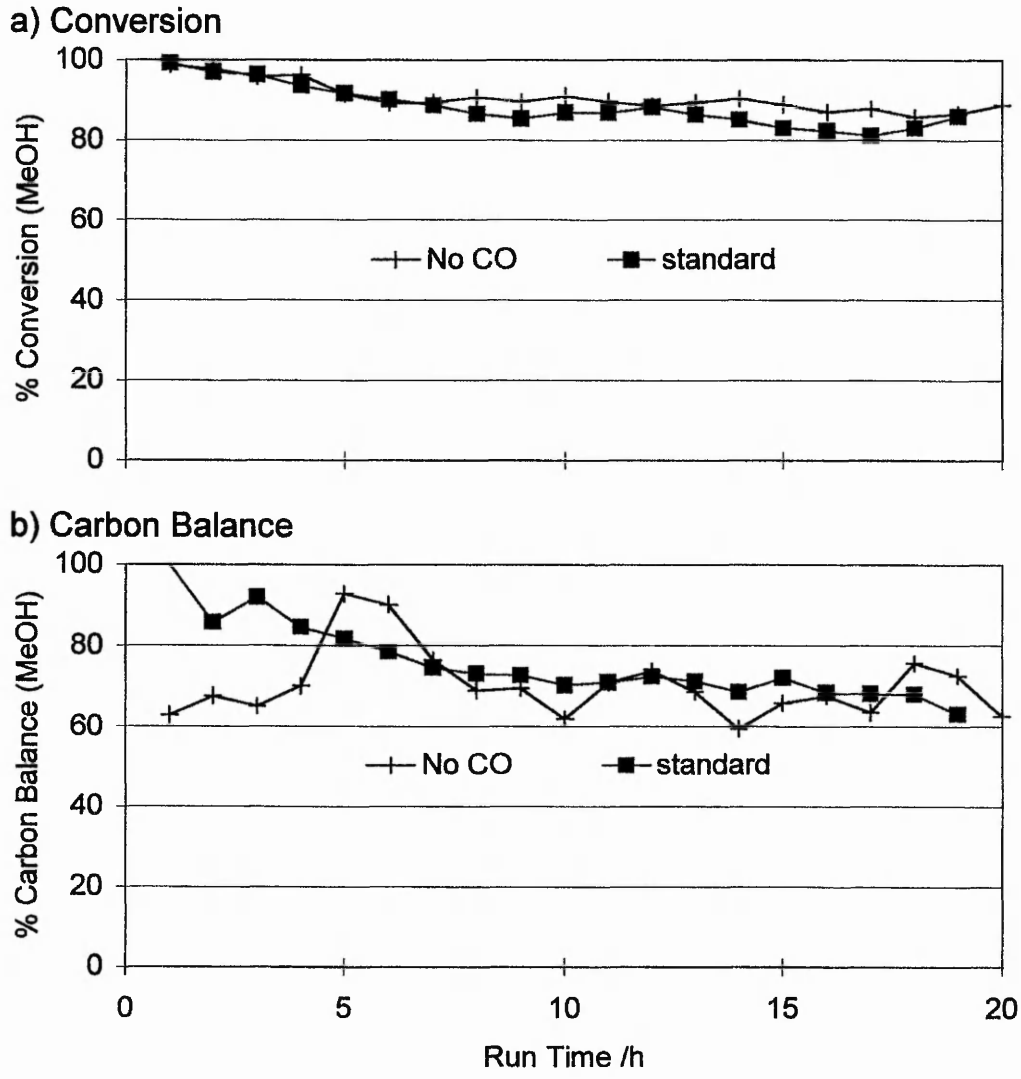

Figure 3.16 The effect of CO pretreatment on (a) the Conversion and (b) the Carbon Balance for Cu/H/MOR SAR20

The level of methanol conversion, in Figure 3.16a, is not modified by the pretreatment. However, Figure 3.16b shows that without pretreatment, the initial carbon balance is only 60% compared to 100% for the standard conditions. After being effectively constant for 4 hours, the carbon balance of the former appears to rise to the same stable level as for the pretreated sample.

The selectivities are on the whole comparable, the major difference being in the first three hours, where the selectivity to acetyls for the untreated sample lies below that of the standard sample. The trends in DME selectivities are equivalent, initially zero and rising to become the major product after 14 hours. The hydrocarbon selectivity, for the standard sample is seen to fall to zero by 12 hours, whilst the untreated sample is seen to maintain a selectivity of 10-15%.

The maximum combined acetyls yield, shown in Figure 3.18a, is 2.0 g/g/h for both samples. However, it takes 6 hours for it to be reached for the untreated sample. Whereas, the standard sample produces it immediately, this corresponds to the difference shown in the initial acetyls selectivity. The untreated sample produces a constant 1.0 g/g/h yield of acetic acid, before dropping to 0.6 g/g/h after the first 6 hours. In comparison, the treated sample produces 2.0 g/g/h of acetic acid immediately, which then decreases smoothly to 0.4 g/g/h by 8 hours. Meanwhile, the methyl acetate yields for the two reactions follow similar trends, rising from zero to a maximum at 5 hours (0.9 g/g/h untreated, 0.6 g/g/h standard), before steadily decreasing again. Therefore the maximum yield, for the untreated sample, arises from the combination of a stable acetic acid yield and the maximum methyl acetate yield. Whereas, the treated sample, gives an initial maximum yield solely of acetic acid.

The average yield of acetic acid, over the first 6 hours, is seen to be 1.1 g/g/h for both treatments. While the average methyl acetate yield, over the same period, for the treated sample is lower at 0.5 g/g/h, compared to 0.7 g/g/h for the untreated one. Therefore the average yield of acetyls, over the intial period, is greater for the untreated sample due to the methyl acetate.

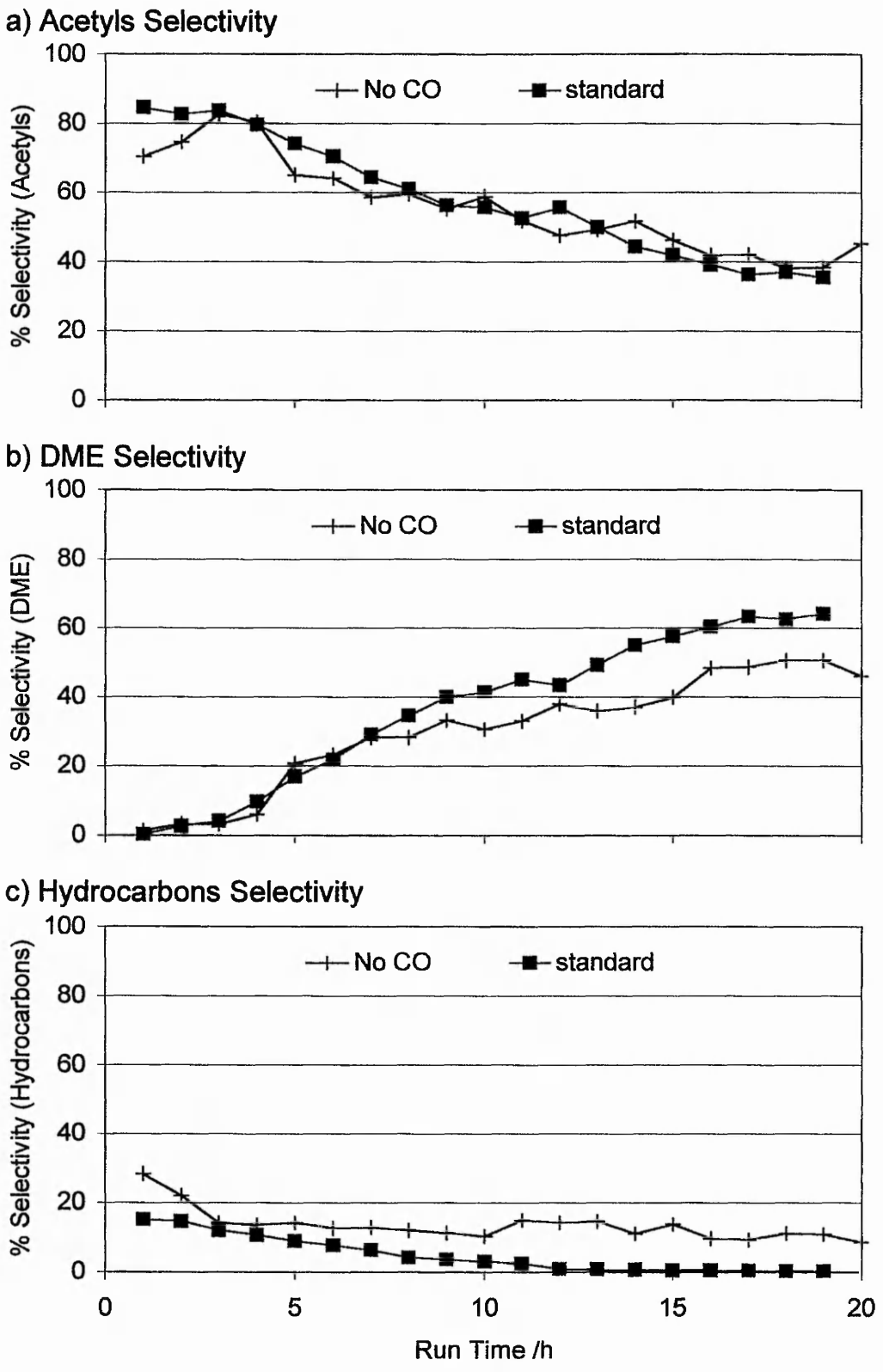

Figure 3.17 The effect of CO pretreatment on the Selectivities to (a) Acetyls, (b) DME and (c) Hydrocarbons for Cu/H/MOR SAR20

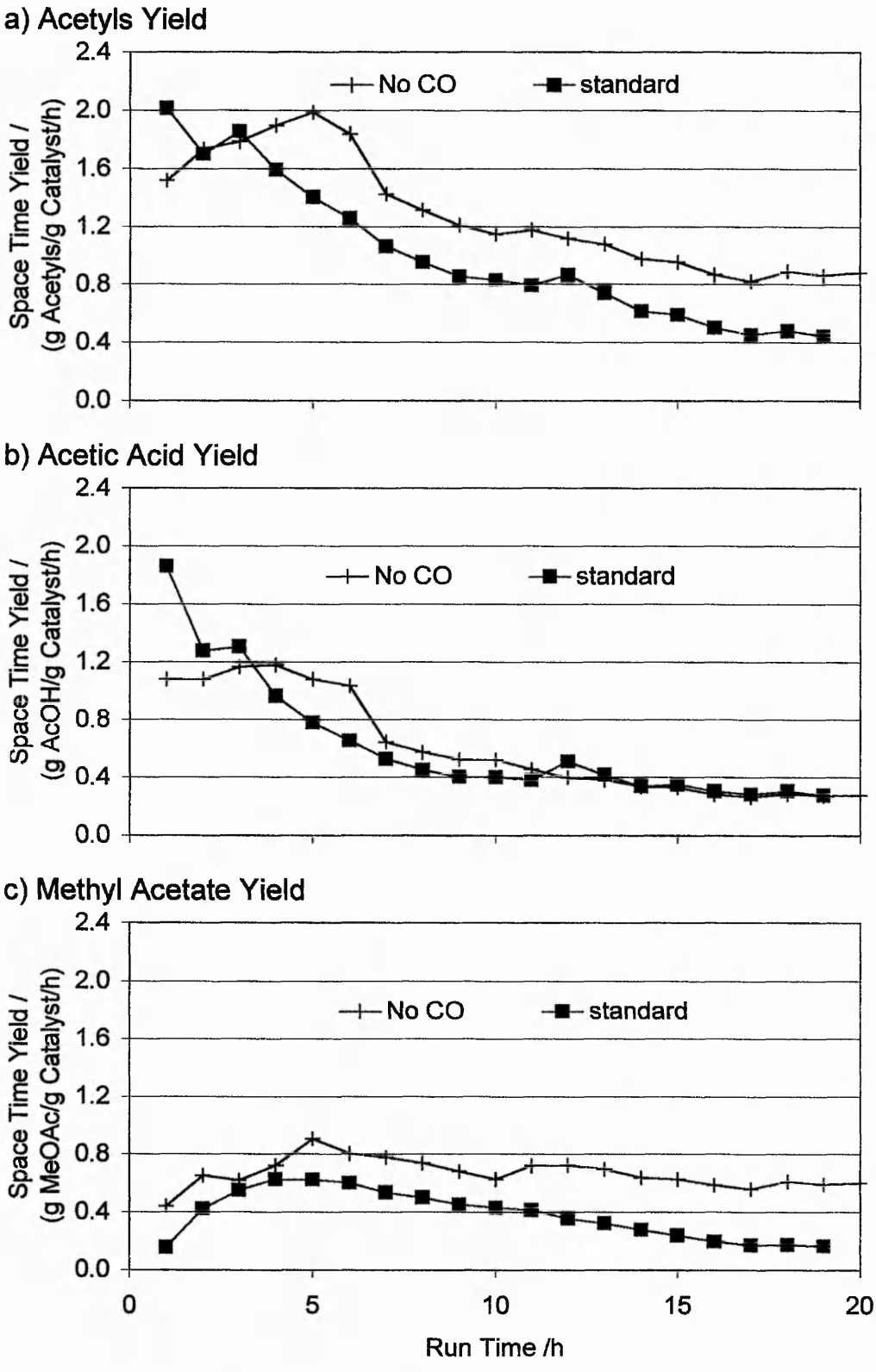

Figure 3.18 The effect of CO pretreatment on the Space Time Yield of (a) Acetyls, (b) Acetic Acid and (c) Methyl Acetate for Cu/H/MOR SAR20

The formation of hydrocarbons

As reviewed in Chapter 1 and mentioned in the previous section, the formation of hydrocarbons from methanol over acidic catalysts is known to occur. Methanol to gasoline (MTG) chemistry has been studied intensively, due to the economic implications arising from the possible formation of gasoline, via synthesis gas or methanol, from methane.

The effect of replacing carbon monoxide with nitrogen

A comparison of the acetyls reactivity is made, for the Cu/H/MOR SAR20 sample, in the presence and absence of carbon monoxide. To ensure equivalent conditions for the MTG reaction, nitrogen replaced carbon monoxide as the carrier gas for methanol. Figure 3.19a shows the conversion of methanol is independent of the co-reactant. For both reactions the conversion, initially 100% has not decreased below 80% after 15 hours. However, as shown in Figure 3.19b, there is a sharp contrast in carbon balances. Under the MTG conditions, the initial carbon balance is zero, but rapidly rises to 40% in 3 hours and reaches 60% after 19 hours. Whereas, for the standard reaction, the initial carbon balance of 100% steadily falls, reaching 70% after 15 hours.

Under the MTG conditions the selectivity to acetyls, in Figure 3.20a, is less than 3% throughout. The initial low carbon balance under MTG conditions corresponds to the zero selectivity to DME, which as for the standard conditions steadily rises, reaching 60% after 15 hours. It therefore appears the co-reactant does not effect the selectivity to DME, for the equivalent levels of conversion obtained.

Initially in the presence of nitrogen, the entire amount of methanol introduced is converted to hydrocarbons. With time, the selectivity to hydrocarbons decreases in favour of DME formation. However, even after 20 hours, there is still a significant level of methanol being converted to hydrocarbons.

For the MTG reaction the constant background level of acetyls selectivity, no greater than 3% throughout, corresponds solely to a space time yield of less than 0.03 g/g/h of methyl acetate. However, it can clearly be stated that no acetic acid is detected in the absence of carbon monoxide, considering for the same sample under carbon monoxide the initial 2.0 g/g/h yield of acetic acid is obtained.

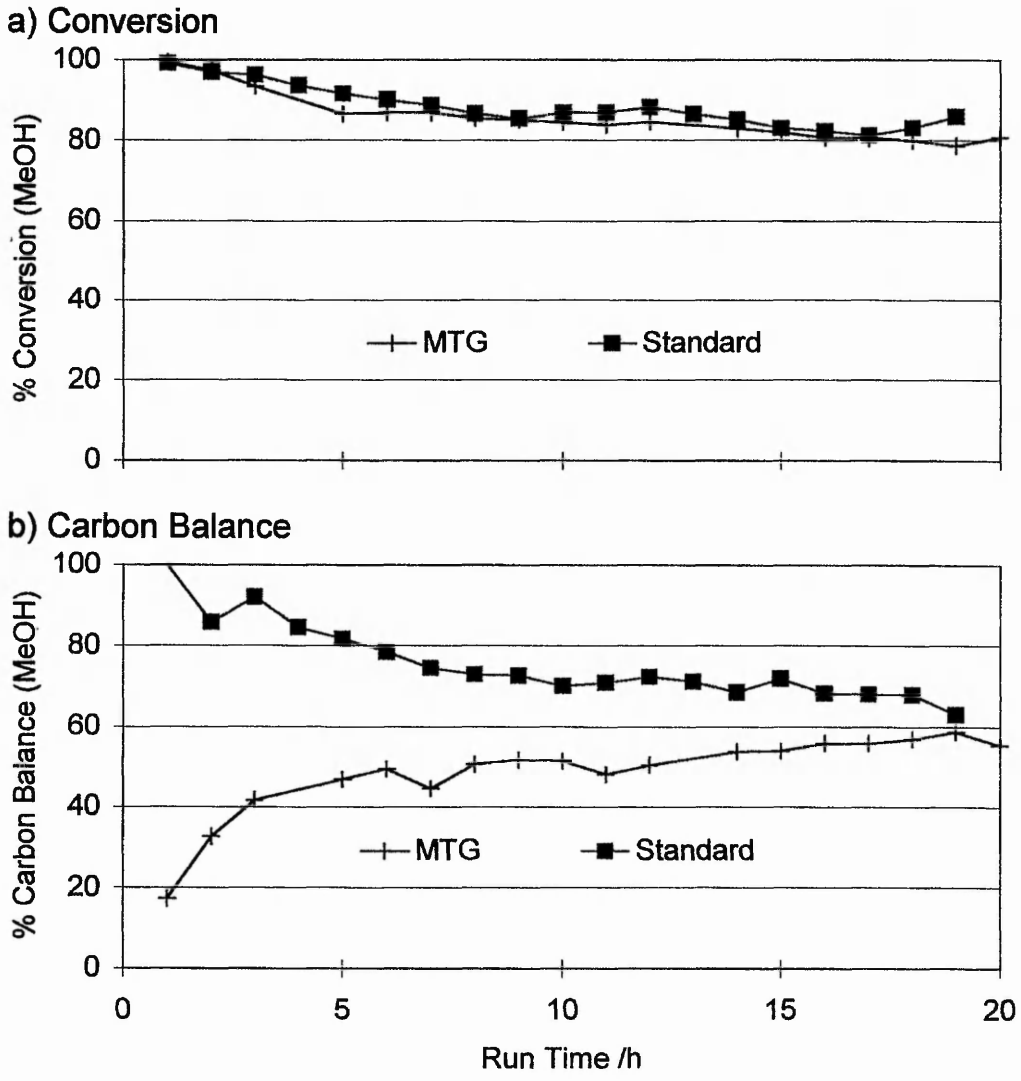

Figure 3.19 The effect of Replacing CO with N2 on (a) the Conversion and (b) the Carbon Balance for Cu/H/MOR SAR20

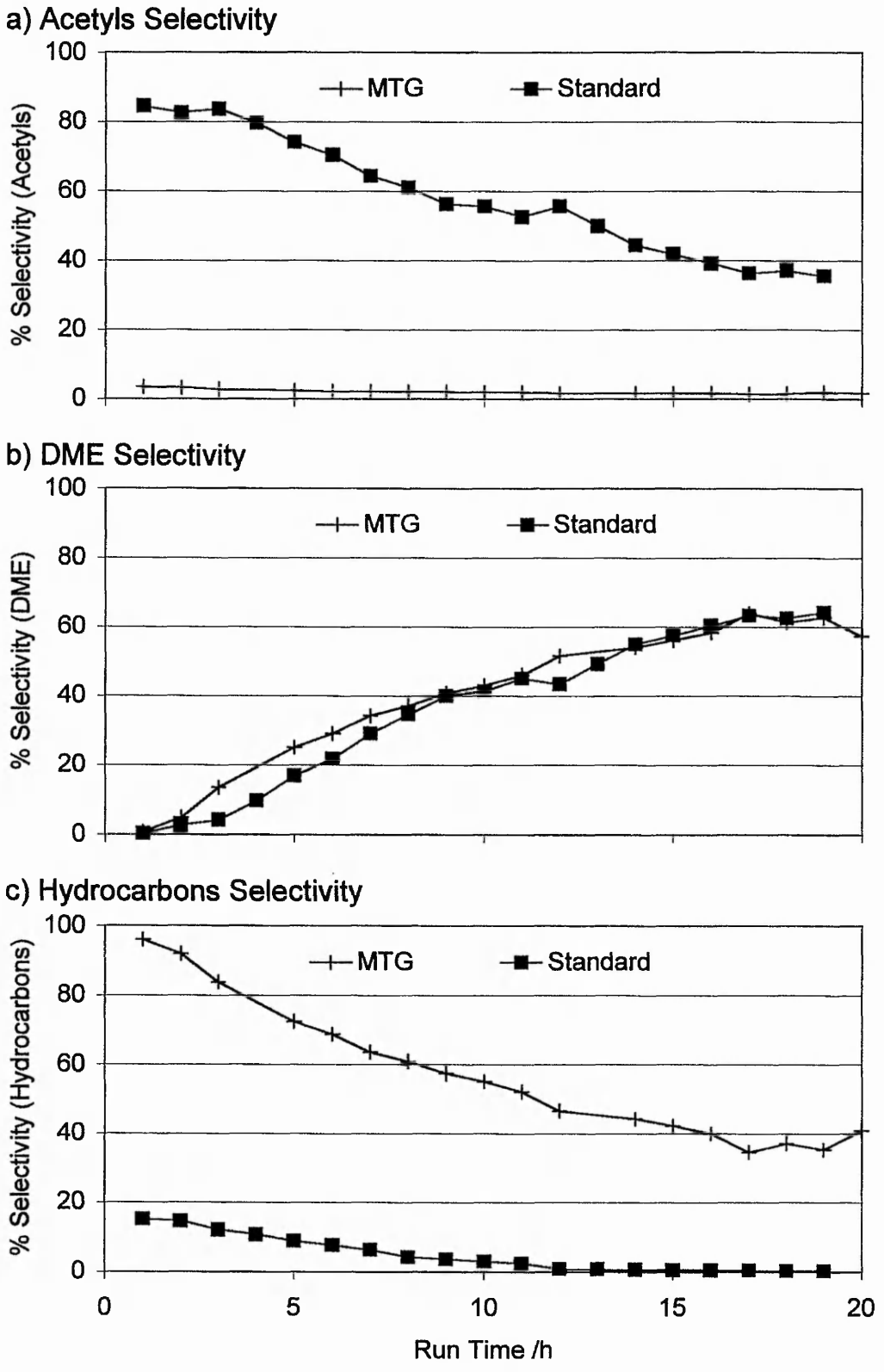

Figure 3.20 The effect of Replacing CO with N2 on the Selectivities to (a) Acetyls, (b) DME and (c) Hydrocarbons for Cu/H/MOR SAR20

The nature of the hydrocarbons formed

Since a wide range of hydrocarbons can be formed, in the presence of nitrogen (MTG) or carbon monoxide (Standard), a detailed comparison of the hydrocarbons produced at 2 hours reaction is made in Figure 3.21. For both sets of conditions, methanol conversion is over 90% and the yield of hydrocarbons is significant. Of the methanol introduced, approximately 30% is detected as hydrocarbons in the MTG compared with 12% in the Standard reaction. The different hydrocarbons are compared as their percentage contribution to the total hydrocarbons detected for the injection. The hydrocarbons are classed in the following groups: C1 (methane), C2 (ethane, ethene), C3 (propane, propene, propyne), C4 (butane, the butenes, isobutane/ene), C6 (all other products detected) and acetone. Acetone was the only additional oxygen functionalised byproduct determined.

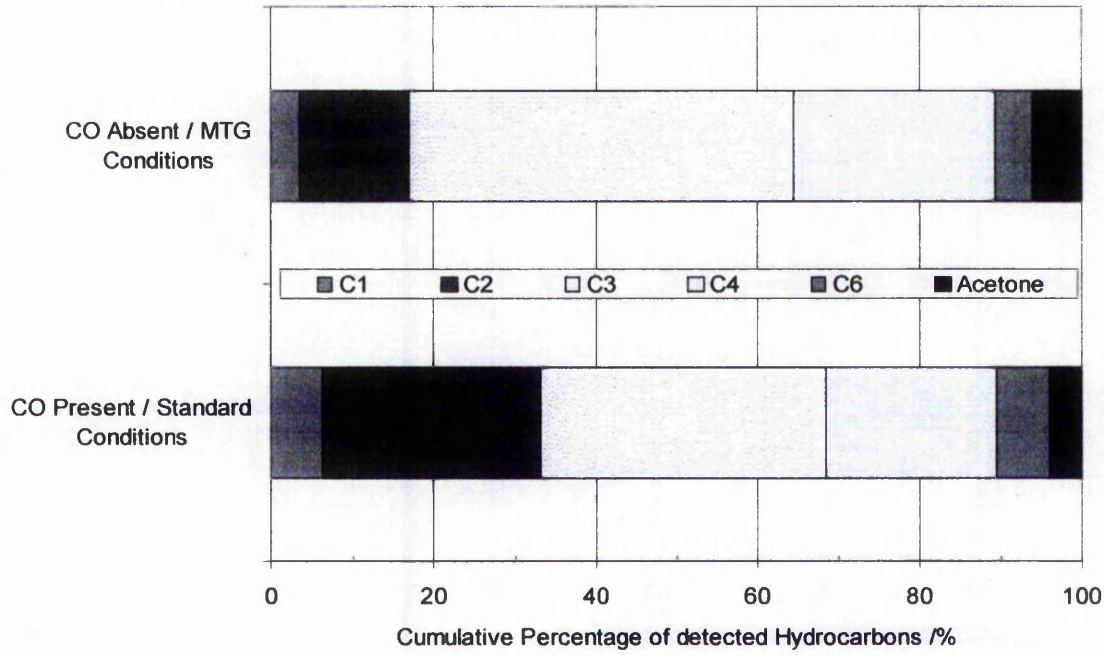

Figure 3.21 The Percentage Composition of the Hydrocarbon Products Detected at 2 Hours for the MTG and Standard Reactions Over Cu/H/MOR SAR20

The total yield of hydrocarbons under nitrogen is approximately double that under carbon monoxide, therefore the moles of methanol converted to C1 and C2 are virtually equivalent. For both reactions, 90% of the hydrocarbons detected are C1-C4, with the C3s being the major constituent. Under MTG conditions the proportion of the C6s is smaller than for the standard conditions. However, the actual yield of the heavier hydrocarbons is greater.

CONTROLLED COPPER EXCHANGE

Background

The ion-exchange procedure, used throughout this work, does not seek to limit the amount of copper introduced into the zeolite framework. The three samples of Cu/H/MOR prepared in this way are all found to have different levels of exchange, see Table 3.1 below. It is therefore interesting to prepare samples, with controlled levels of copper loading.

As detailed in Chapter 2 the procedure adopted, to attempt controlled loading, involved the addition of ammonium hydroxide alliquots to the zeolite suspension. Five samples, Cu/MOR HP(1-5) with increasing levels of copper loading, were prepared from H/MOR (SAR 20).

Table 3.1 below summarizes the copper loadings obtained, along with the initial concentration of the copper solution and where applicable the theoretical copper loadings. The quoted concentration of copper is for the total volume of the solution, once all the copper solution had been added to the suspended zeolite. The volume of ammonium hydroxide added is not taken into account, so that the quoted concentration is equivalent to that for the conventional ion-exchange procedure. The theoretical copper loading values assume that all the copper initially in solution is taken up by the zeolite.

SAMPLE ID	Initial [Cu] of Solution /M	Theoretical Cu Loading /wt%	Cu Loading /wt%
Cu/MOR SE1	0.3	N/A	2.20
Cu/MOR SE2	0.3	N/A	2.59
Cu/MOR SE3	0.3	N/A	(2.45)
Cu/MOR HP1	0.0006	0.32	0.32
Cu/MOR HP2	0.0011	0.65	0.70
Cu/MOR HP3	0.0023	1.28	1.27
Cu/MOR HP4	0.0045	2.51	(2.40)
Cu/MOR HP5	0.0089	4.95	(4.96)

Table 3.1 Summary of the controlled copper loadings of the Cu/H/MOR SAR20 samples

The variation in the copper loading is large for the samples prepared by ion-exchange. The amount of copper introduced is dependent on the equilibrium established between the copper in solution and that exchanged into the framework. The percentage of the initial copper solution, introduced without any modification of conditions, is extremely low. On the contrary, the controlled procedure is seen to incorporate all of the copper from the initial solution into the zeolite framework, as confirmed by comparing the theoretical and actual copper loadings of the samples. Two other experimental observations also support this. Firstly, when the zeolite was allowed to settle out, the resulting solution was seen to be clear and the zeolite a distinct blue colour. Secondly on filtering, the supernatent was added directly to concentrated ammonium hydroxide solution in the Buchner Flask, no formation of the dark blue $Cu(NH_3)_4$ complex was observed. The formation of the $Cu(NH_3)_4$ complex should readily occur for copper(II) ions in the presence of ammonia solution with a pH of 8 or greater.

The effect of controlled copper loading

The results, for the five samples of controlled copper loading Cu/MOR HP(1-5), are compared directly with the H/MOR SAR 20 sample. HP1, the sample with the lowest loading of copper, contains 0.32 wt% copper. Figure 3.22 shows that the low loading of copper does not have any great effect on the level of methanol conversion nor the carbon balance. The results for HP1 lie within the variation of experimental data for H/MOR.

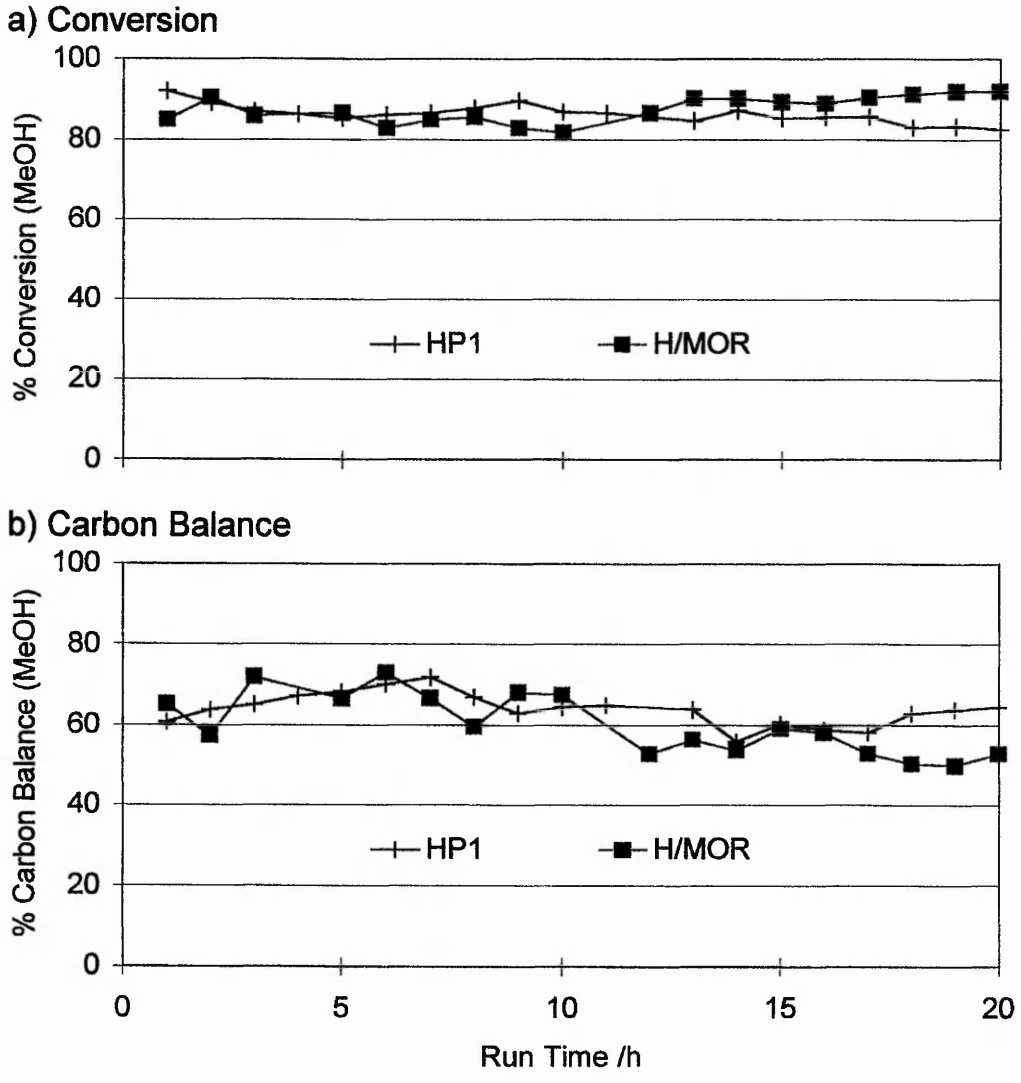

Figure 3.22 The effect on (a) the Conversion and (b) the Carbon Balance of controlled copper loading for sample HP1

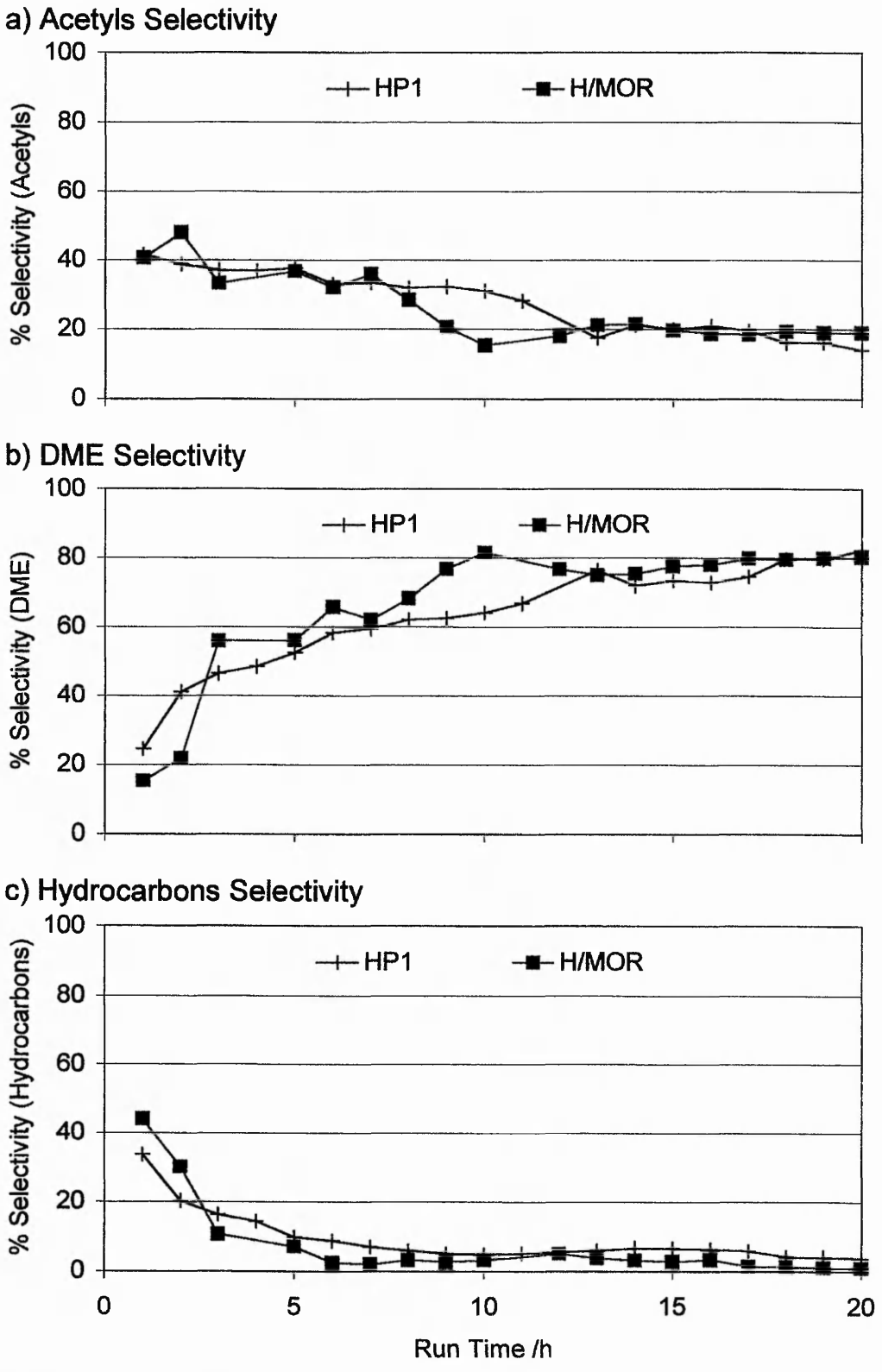

Figure 3.23 The effect on the Selectivities to (a) Acetyls, (b) DME and (c) Hydrocarbons of controlled copper loading for sample HP1

Similarly in Figure 3.23a-c, the overall selectivities to Acetyls, DME and Hydrocarbons are not greatly affected by the presence of only 0.32wt% copper. However in Figure 3.24, the combined yield of acetyls from H/MOR drops quickly, from 0.6 g/g/h after 7 hours to 0.3 g/g/h by 10 hours. Whilst for HP1, the acetyls yield slowly decreases from the 0.6 g/g/h at 7 hours to a stable 0.3 g/g/h by 13 hours. But overall, there is no significant promotional effect by the incorporation of such a low level of copper loading.

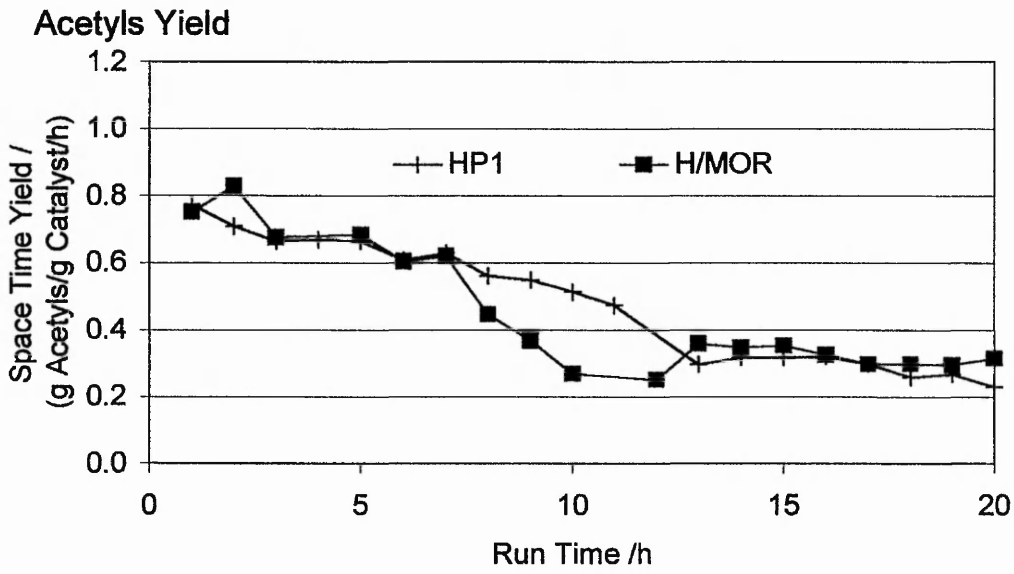

Figure 3.24 The effect on the Space Time Yield of Acetyls of controlled copper loading for sample HP1

HP2 has a copper loading of 0.7 wt%, Figure 3.25a shows that the methanol conversion falls for this loading of copper compared to H/MOR. Initially both are around 85%, but HP2 falls to around 70% by 10 hours, whilst H/MOR maintains at least 85%. In Figure 3.25b the carbon balance, for HP2 is at 70% throughout while, for H/MOR it falls from the initial 70% to 50-60% after 10 hours.

The selectivity to acetyls, Figure 3.26a, is similar for HP2 and H/MOR for the first 7 hours of reaction. However, HP2 maintains a higher value of ~30% compared to only 20% for H/MOR, but both are considered to be stable with time. The selectivity to DME in Figure 3.26b is seen to be generally lower for HP2 compared to H/MOR. For HP2, the proportion of DME rises slowly from 30% to 70%, whereas for H/MOR the intial rise is rapid from 20% to 60%.

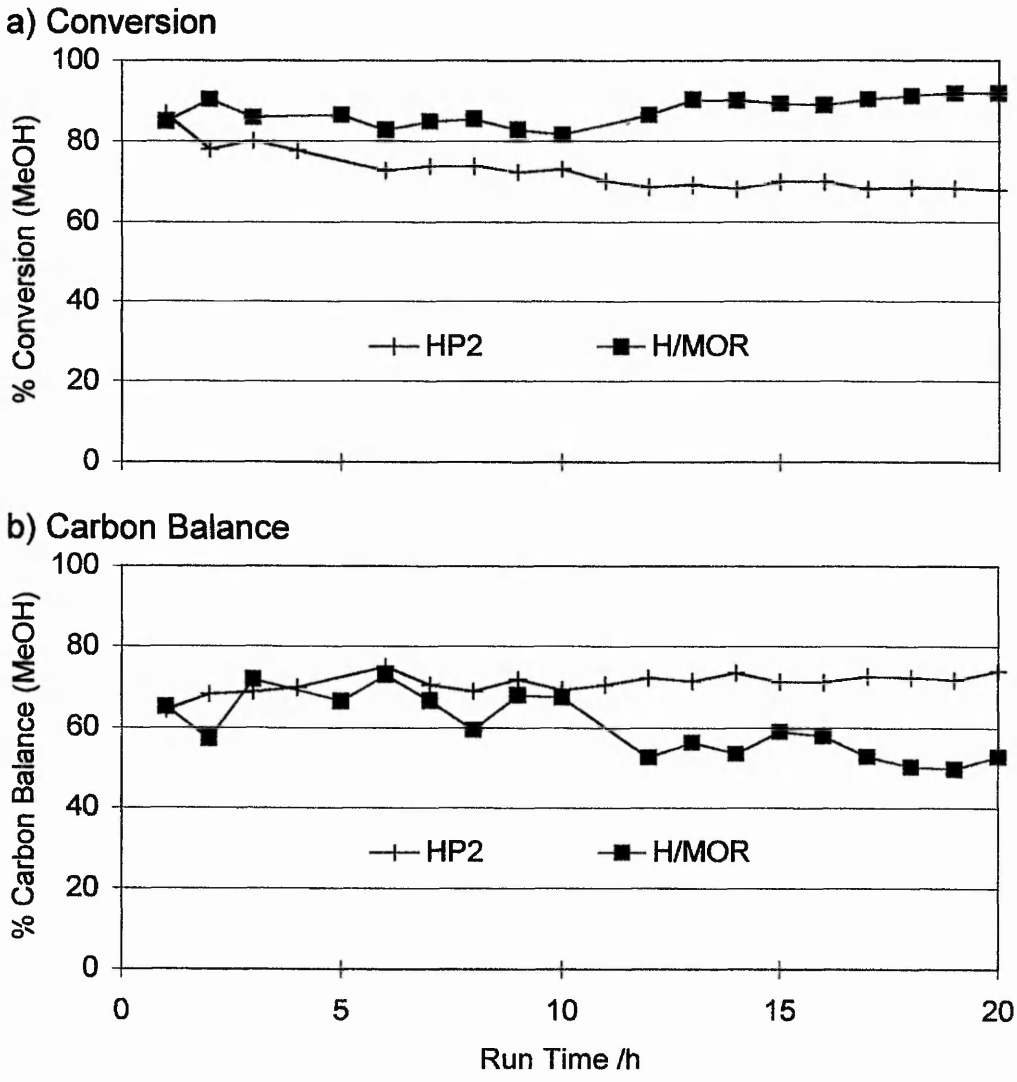

Figure 3.25 The effect on (a) the Conversion and (b) the Carbon Balance of controlled copper loading for sample HP2

The selectivity to hydrocarbons is also different. For HP2, the initial 20% selectivity falls steadily over time to 10% by 15 hours, compared to the initial 40% for H/MOR rapidly falling to below 10% after only 5 hours.

In Figure 3.27, the combined yield of acetyls is seen to be equivalent throughout for the two reactions. The lower conversion observed therefore does not effect the acetyls yield, making the incorporation of this low level of copper produce a more selective catalyst.

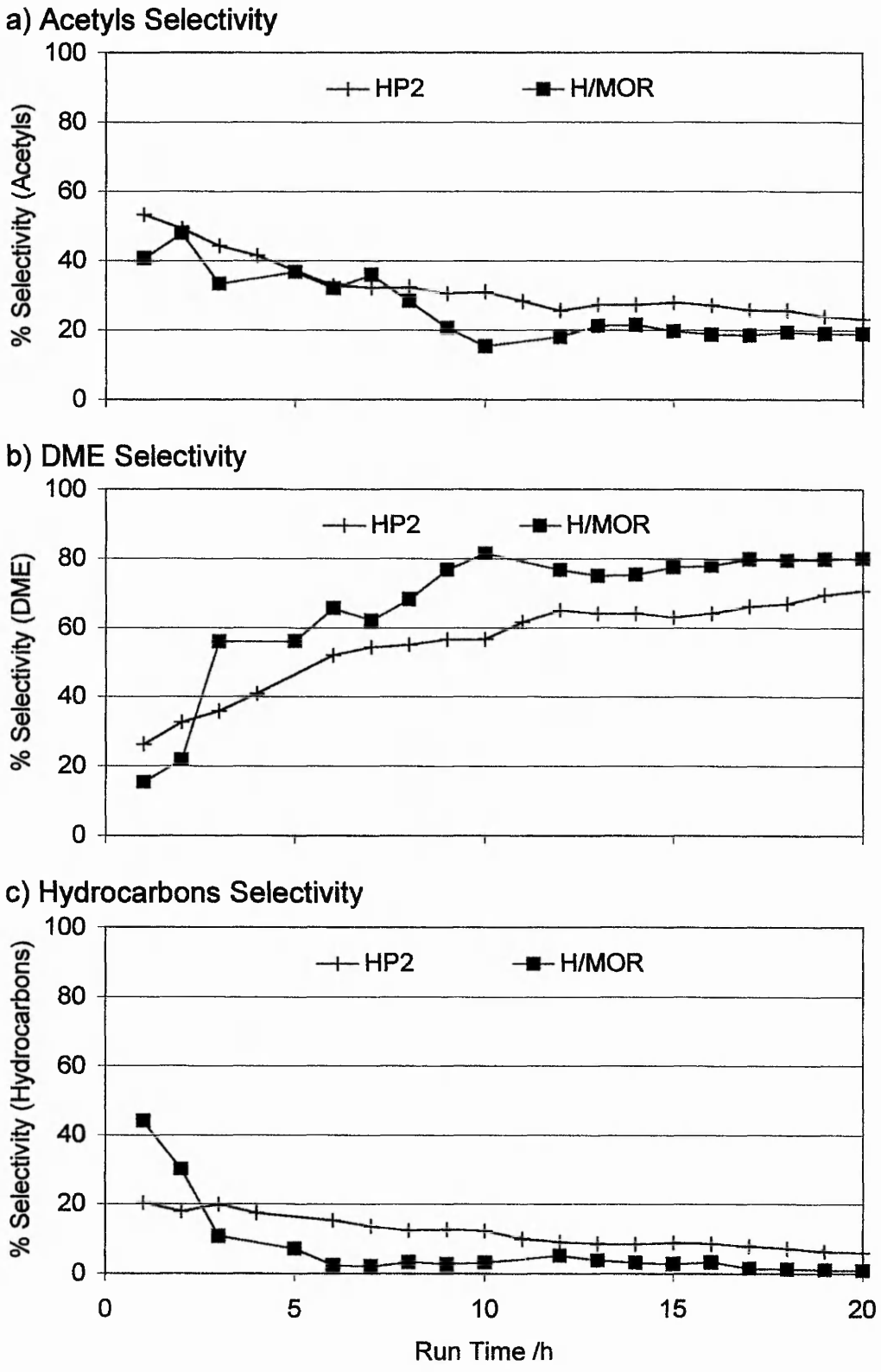

Figure 3.26 The effect on the Selectivities to (a) Acetyls, (b) DME and (c) Hydrocarbons of controlled copper loading for sample HP2

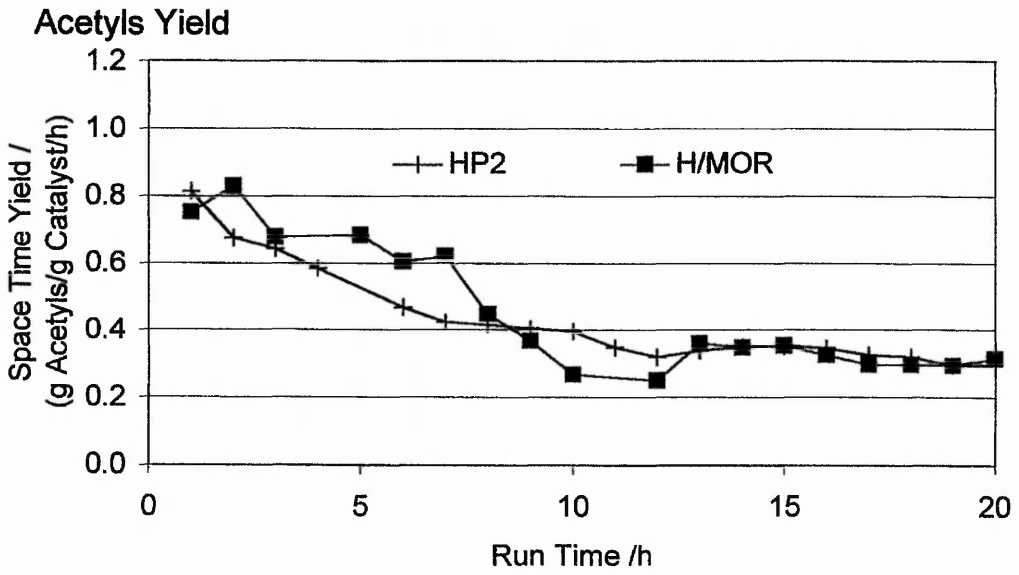

Figure 3.27 The effect on the Space Time Yield of Acetyls of controlled copper loading for sample HP2

The third sample, HP3, contains a copper loading of 1.28 wt%. Unfortunately the reactor becoming blocked disrupted this reaction, after only 16 hours, but the comparison with H/MOR can still be made. Figure 3.28a shows for HP3 the level of conversion is slightly greater than that for H/MOR. Meanwhile the carbon balance, in Figure 3.28b, is equivalent throughout.

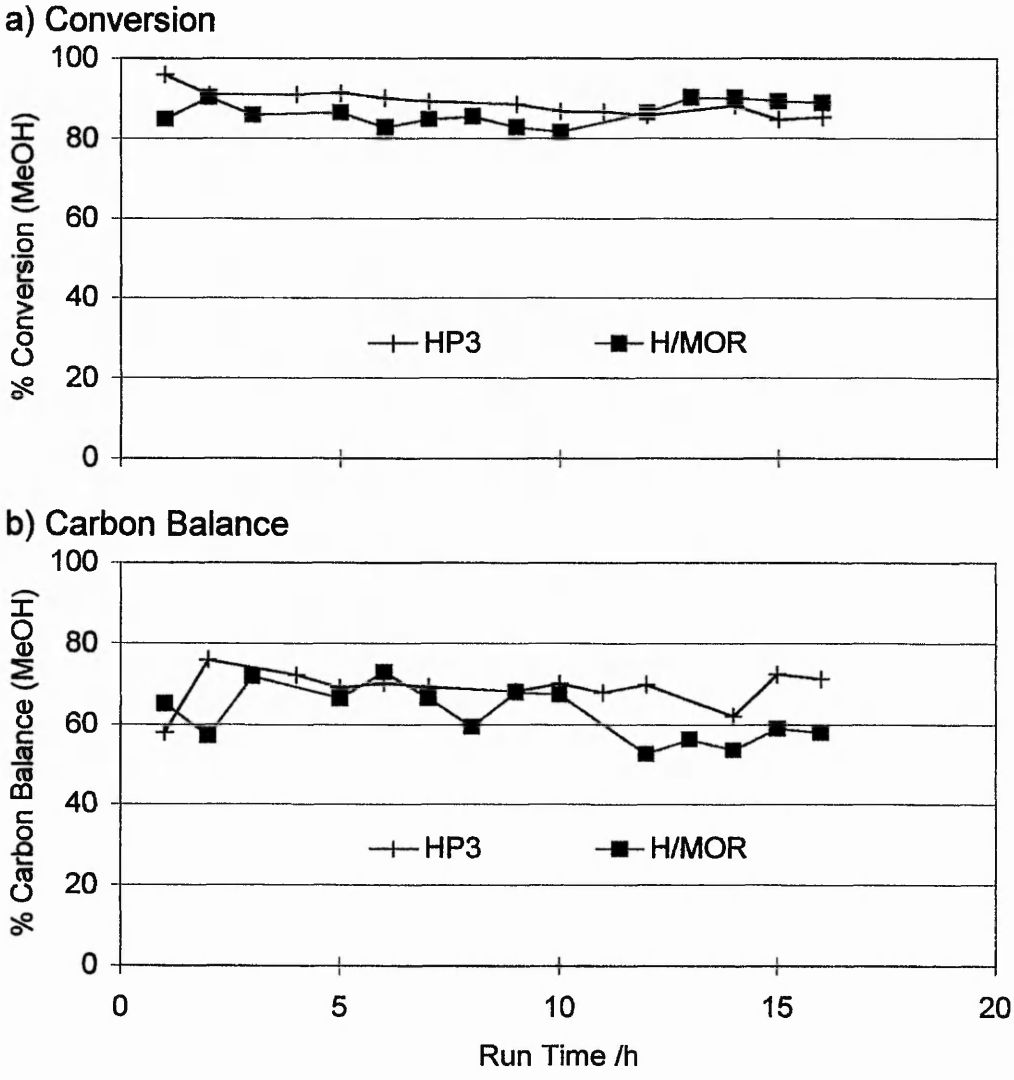

Figure 3.28 The effect on (a) the Conversion and (b) the Carbon Balance of controlled copper loading for sample HP3

The acetyls selectivity, in Figure 3.29a, is greater for HP3 than for H/MOR throughout the reaction. The overall trend is the same, being constantly at least 10% higher for HP3. Although equivalent for the first 2 hours, the selectivity to DME remains significantly lower, by at least 20%, for HP3 compared to H/MOR. For HP3 the overall selectivity to hydrocarbons is low throughout, compared to the initial 40% for H/MOR falling virtually to zero.

For the equivalent levels of conversion, it is evident in Figure 3.30 that the acetyls yield for HP3 is constantly greater, by 0.2 g/g/h, than that of H/MOR. This indicates that the incorporation of 1.28 wt% copper increases the reactivity above that of the H/MOR framework.

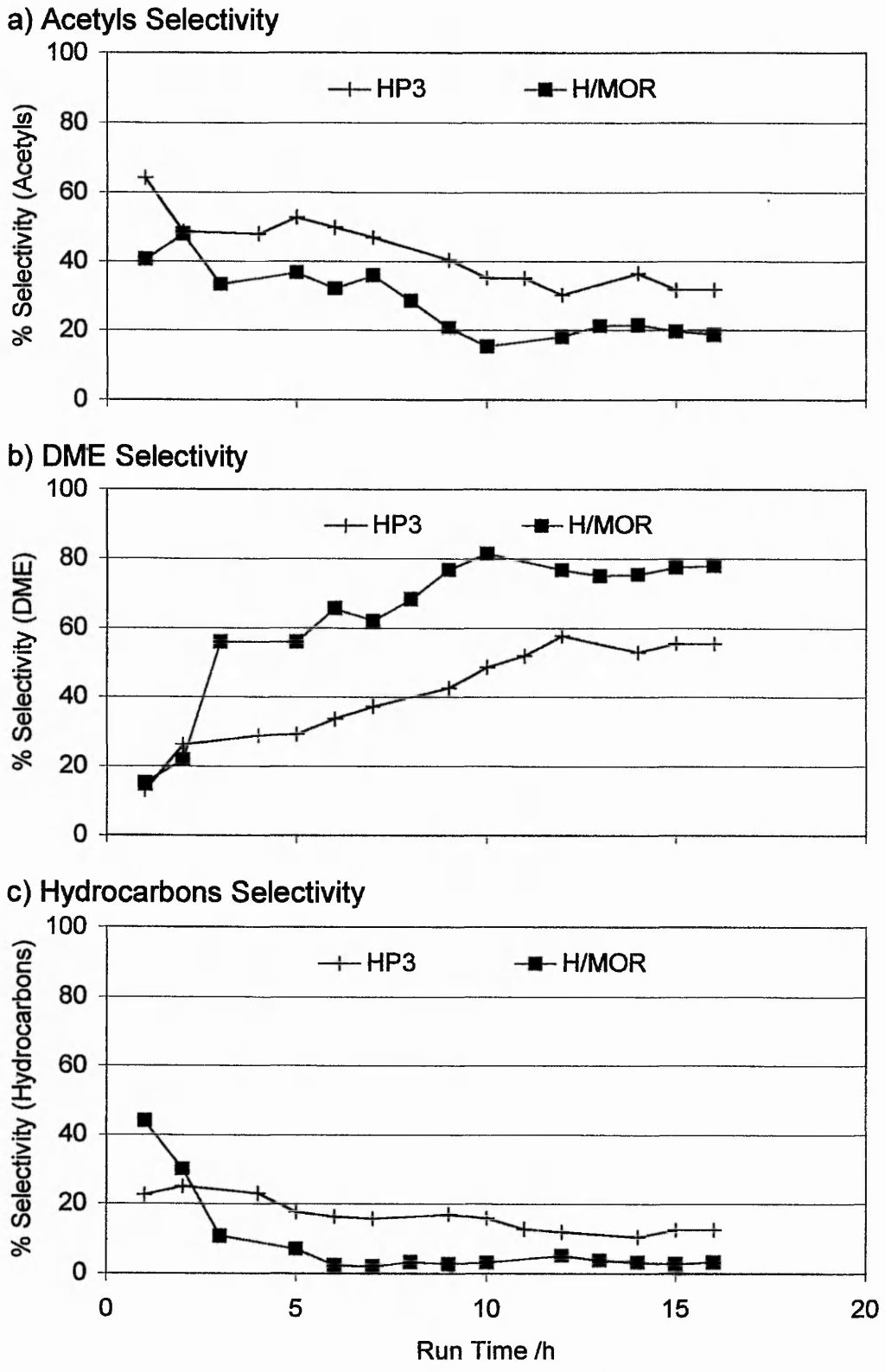

Figure 3.29 The effect on the Selectivities to (a) Acetyls, (b) DME and (c) Hydrocarbons of controlled copper loading for sample HP3

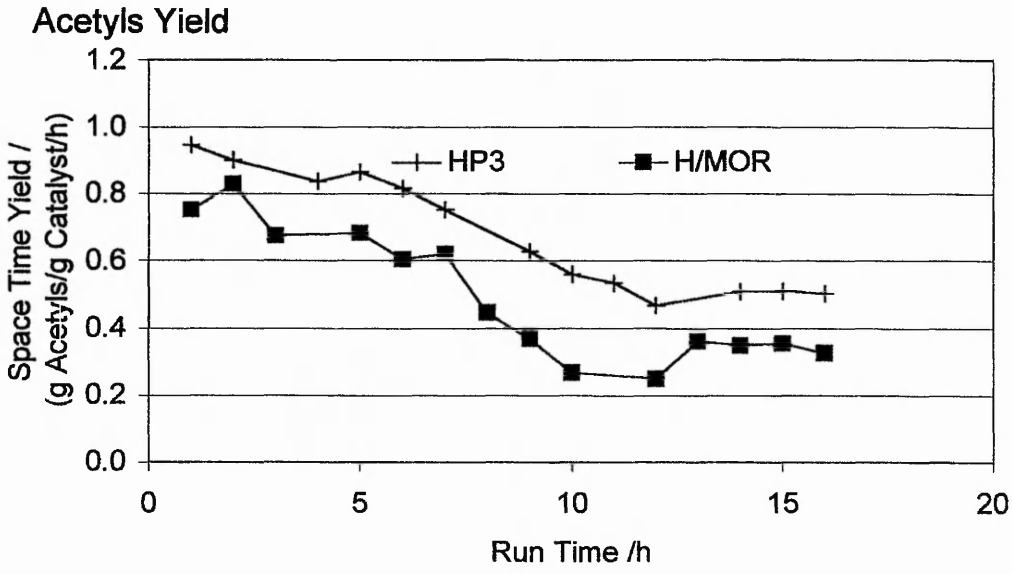

Figure 3.30 The effect on the Space Time Yield of Acetyls of controlled copper loading for sample HP3

The following sample HP4 has a copper loading of 2.4 wt%, which is close to 2.2 wt% for the ion-exchange sample Cu/H/MOR SE2. The level of conversion, shown in Figure 3.31a, for HP4 is initially higher than for H/MOR, and falls smoothly to 80% by 20 hours of reaction. In contrast, initially 85% the conversion over H/MOR rises and by 20 hours has reached 95%. The two curves are seen to cross after 12 hours of reaction. The initial carbon balance for HP4 is similar to that for H/MOR at 60%, remaining stable for the first 10 hours, before rising towards 80% at 20 hours.

The selectivity to acetyls for HP4, in Figure 3.32a, is greater throughout than for H/MOR, although not by a constant amount. Initially at 50%, the selectivity falls to 30% by 10 hours, which it then maintains. In comparison, H/MOR initially 40-50% falls to a stable 20%, again by 10 hours. As for HP3, the DME selectivity for HP4 is equal to that for H/MOR for the first 2 hours, but subsequently remains 20% lower. The selectivity to hydrocarbons is therefore greater for HP4 than for H/MOR, initially 30% it then falls to a stable 10%, and so the hydrocarbon selectivity is also greater than for the HP3.

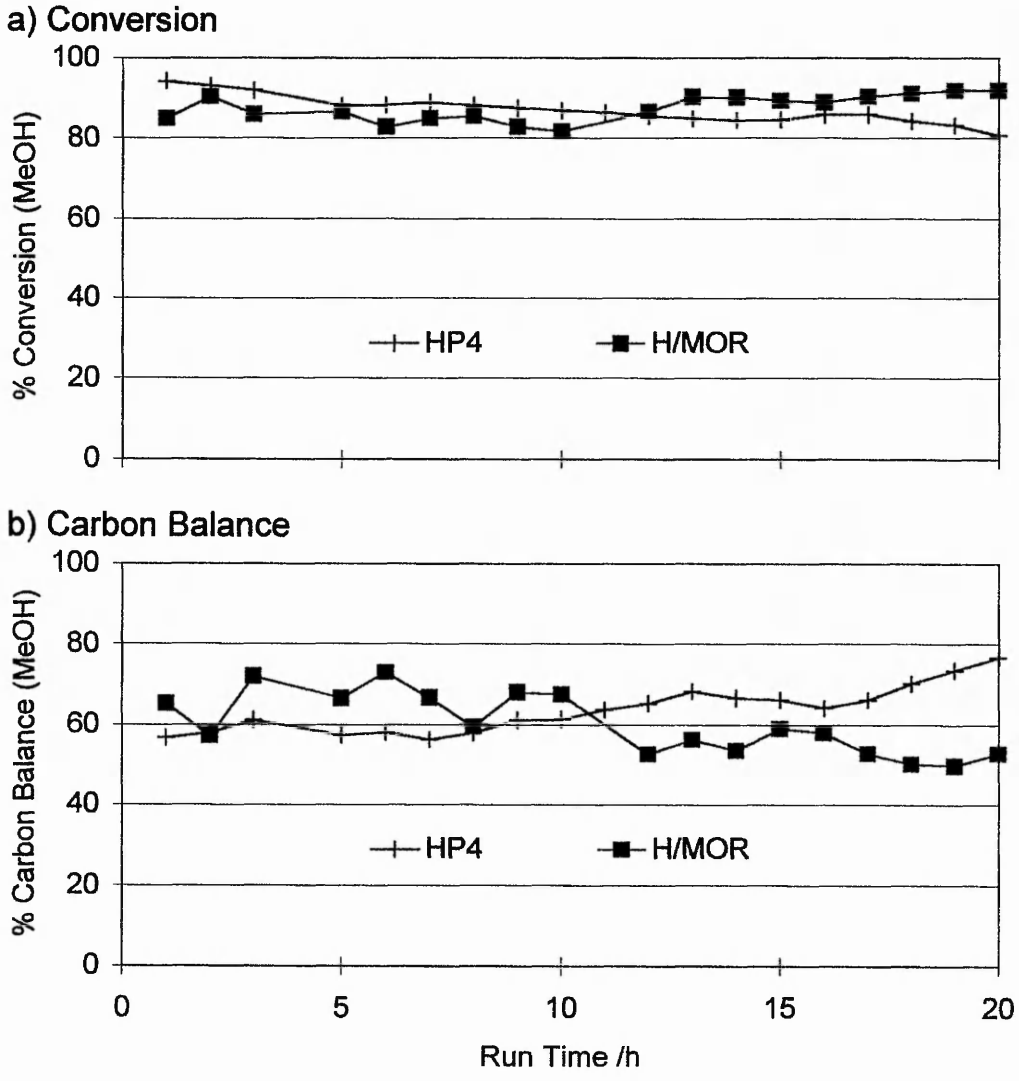

Figure 3.31 The effect on (a) the Conversion and (b) the Carbon Balance of controlled copper loading for sample HP4

The higher methanol conversion and the higher hydrocarbon selectivity, correspond to a yield of acetyls, in Figure 3.33, equal to that for H/MOR over the first 7 hours. But whereas H/MOR deactivates, the acetyls yield of 0.5 g/g/h from the HP4 is maintained for the remaining reaction time. HP4 does not produce the initial high acetyls yield of the ion-exchanged Cu/H/MOR SE2, but does maintain a significant stable yield compared to H/MOR.

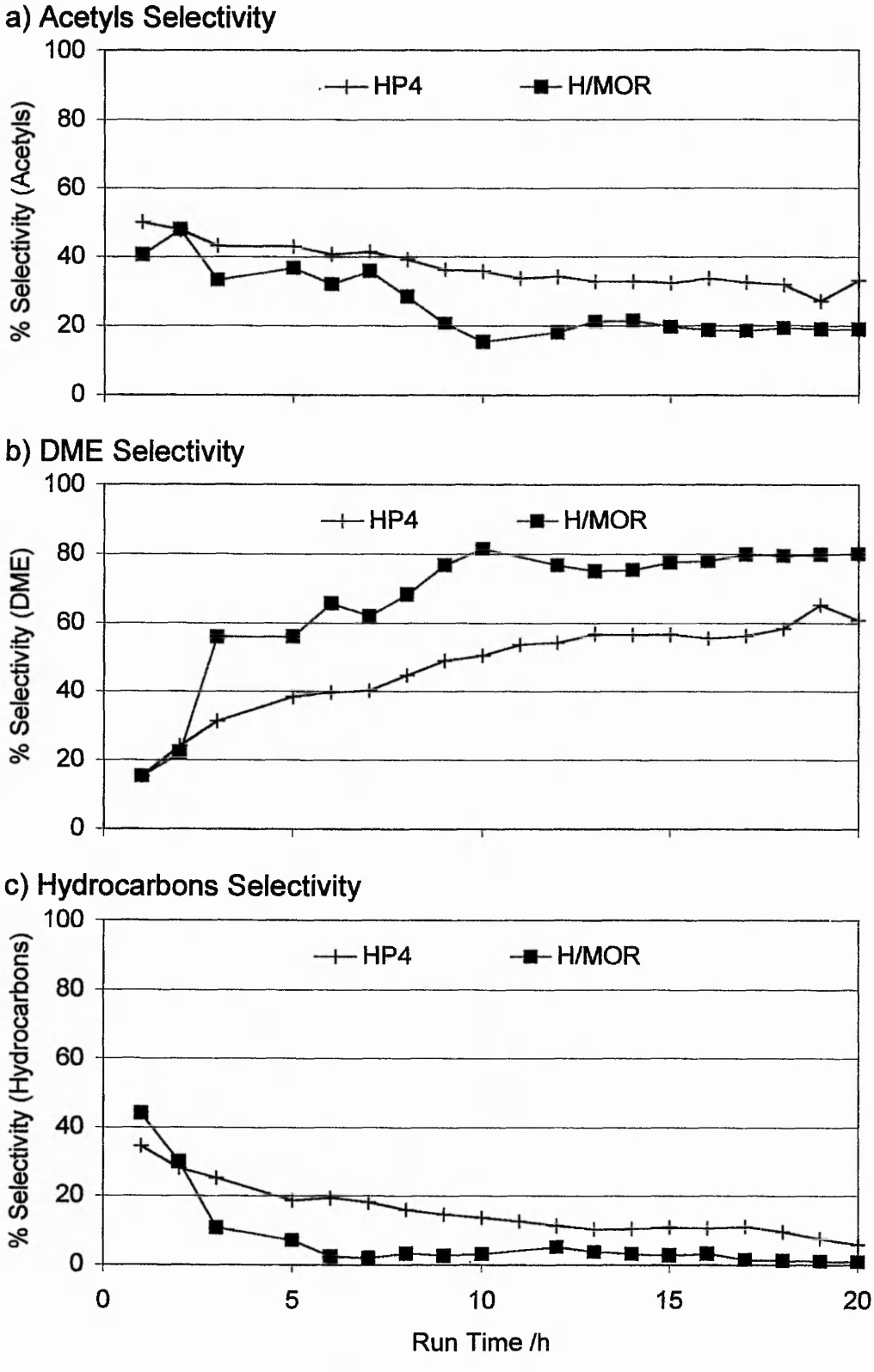

Figure 3.32 The effect on the Selectivities to (a) Acetyls, (b) DME and (c) Hydrocarbons of controlled copper loading for sample HP4

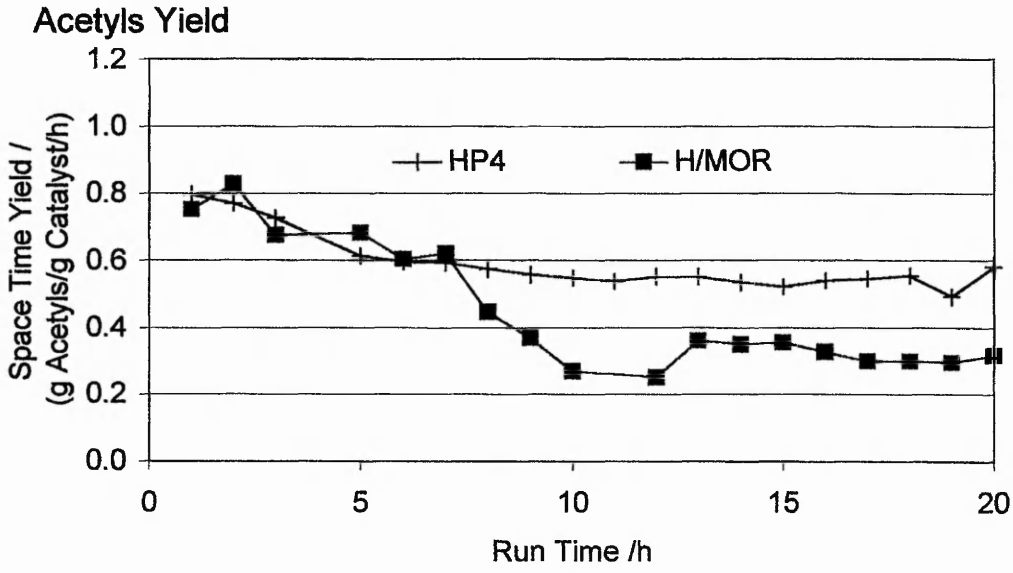

Figure 3.33 The effect on the Space Time Yield of Acetyls of controlled copper loading for sample HP4

The final sample HP5 has a copper loading of 4.96 wt%. The maximum theoretical copper loading is 4.95 wt%, assuming that the copper remains in oxidation state (+2) and each divalent cation exchanges for two available monovalent cations.

In Figure 3.34a, it can be seen that the level of conversion maintains the same trend as for the other controlled copper loading samples. The carbon balance for HP5 is initially 60% and rises to a stable 80%, in contrast to H/MOR for which the initial value of 70% decreases to 50%.

The acetyls selectivity is always greater for HP5 than for H/MOR, as shown in Figure 3.35. The selectivity of HP5 to DME is lower than for H/MOR, but similar to that found for HD3 & HD4. The Hydrocarbon selectivity for HP5 follows a similar trend as for H/MOR, initially at 30% it quickly drops to less than 10%. Considering the similar degree of conversion, the higher selectivity to acetyls corresponds to a higher acetyls yield as shown in Figure 3.36.

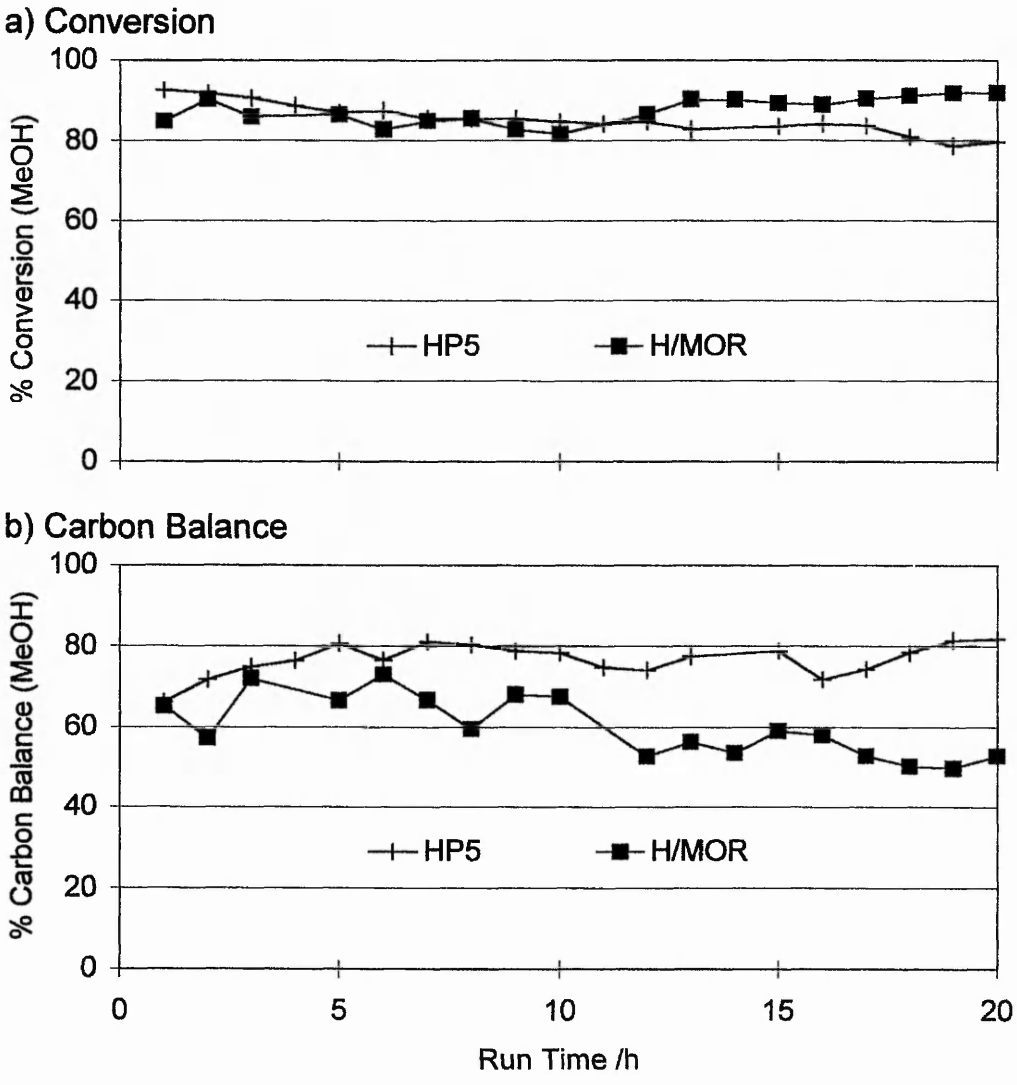

Figure 3.34 The effect on (a) the Conversion and (b) the Carbon Balance of controlled copper loading for sample HP5

The HP5 sample produces a stable acetyls yield of 0.9 g/g/h for 7 hours, but then it falls, over a period of 3 hours, to a stable 0.6 g/g/h yield, which is twice the yield achieved for H/MOR. The effect of the high loading of copper introduced by this technique is to enable a stable yield of 0.6 g/g/h to be maintained, even after 10 hours.

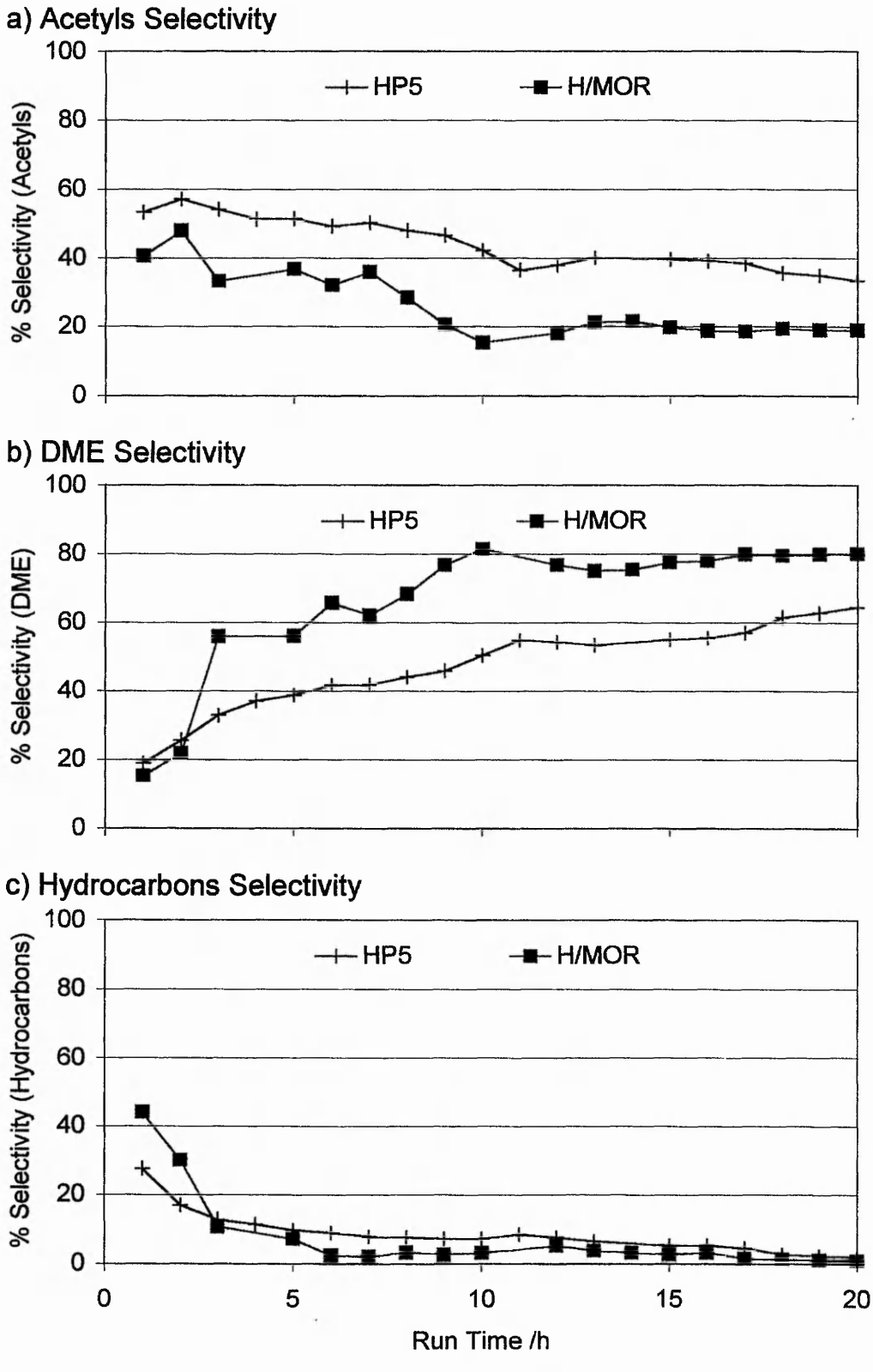

Figure 3.35 The effect on the Selectivities to (a) Acetyls, (b) DME and (c) Hydrocarbons of controlled copper loading for sample HP5

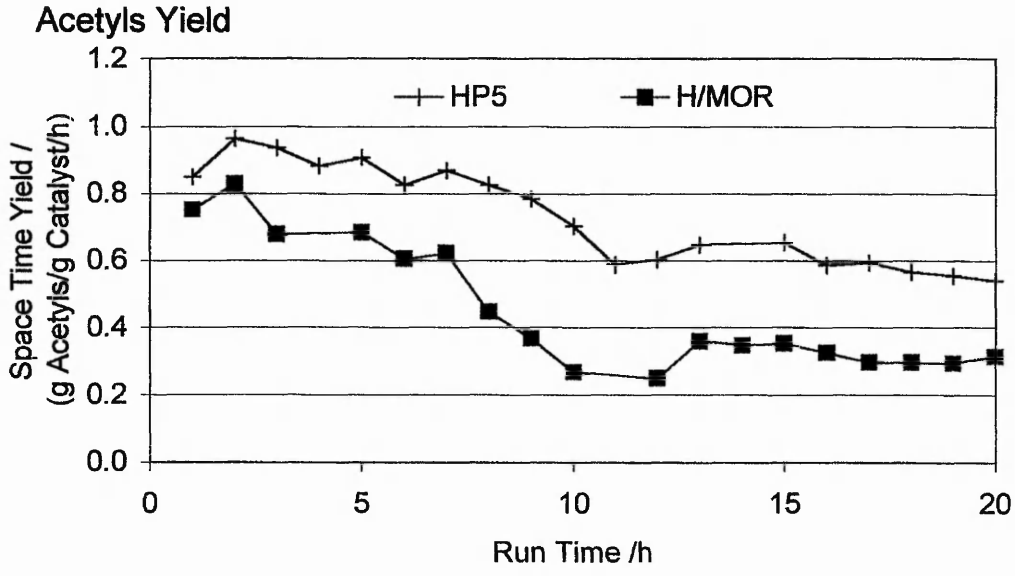

Figure 3.36 The effect on the Space Time Yield of Acetyls of controlled copper loading for sample HP5

Summary

To summarise the effect of the controlled copper loading technique on the productivity of mordenite, Figure 3.37 shows the space time yield of the acetyls for all the five samples and compares them to H/MOR. Although the figure contains a lot of data, the general trends are clear. It can be seen that as the copper loading increases the acetyls yield also increases. In particular, it should be noted that the stable period of reactivity after 10 hours is increased rather than the initial high period, as illustrated in Figure 3.38 where the acetyls yield for HP5 is compared to both H/MOR and to Cu/MOR SE2. Although the initial maximum yield of Cu/MOR SE2 is not achieved for HP5, the stable period occurs by 10 rather than 15 hours, and is maintained at a higher level than for Cu/MOR SE2. For the controlled loading technique it is observed that the acetyls yield stabilises at two distinct levels, H/MOR, HP1 & 2 at 0.3 g/g/h whilst HP3-5 stabilise at 0.6 g/g/h.

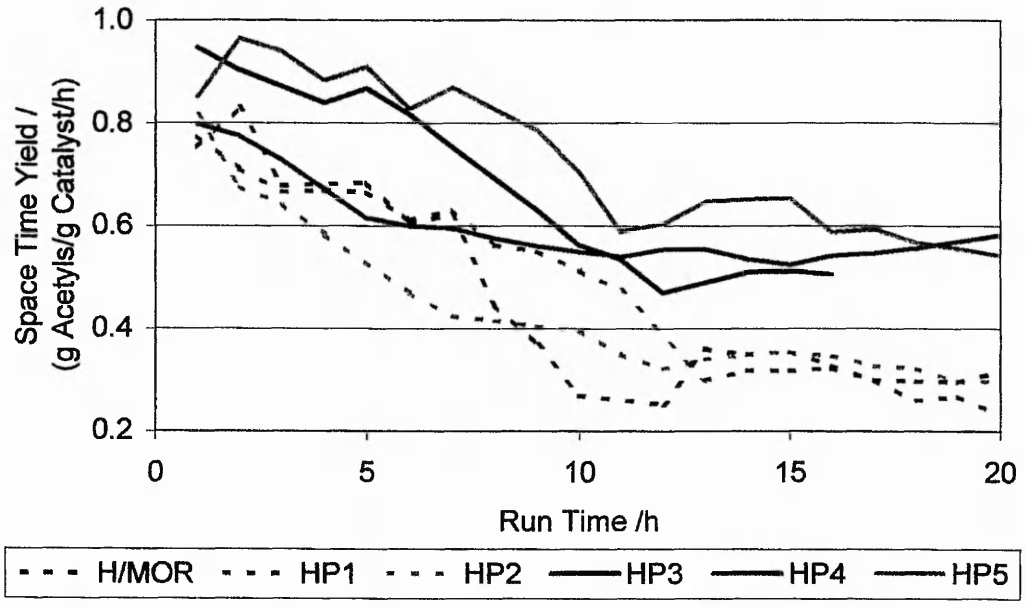

Figure 3.37 Summary showing the acetyls space time yields for all the controlled copper loading samples compared to H/MOR

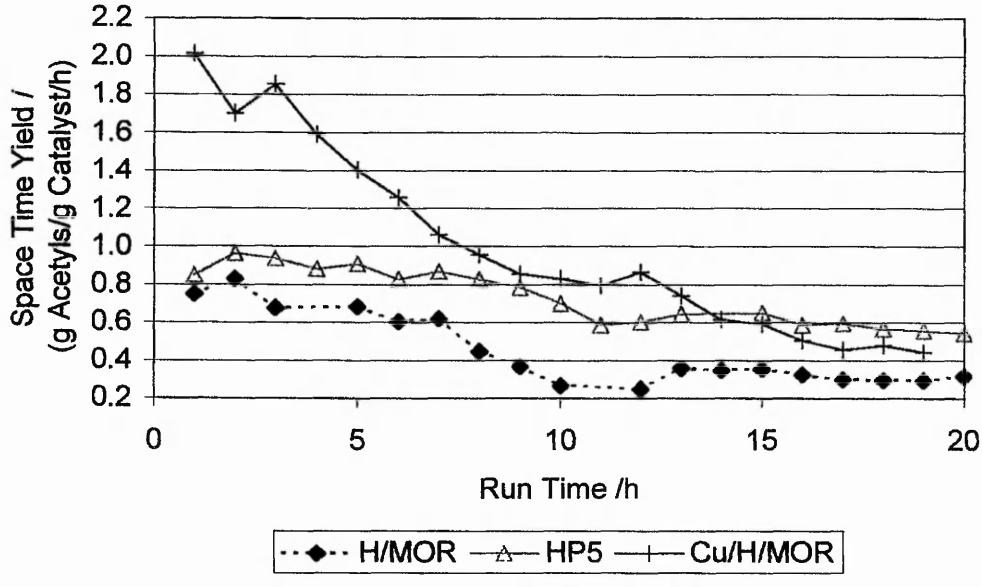

Figure 3.38 Summary showing the acetyls space time yield of HP5 compared to that for H/MOR and Cu/H/MOR SE2

THE OTHER COPPER LOADING TECHNIQUES

Background

The initial level of reactivity observed for the ion-exchanged mordenite is greater than for the controlled loading technique. As the method of incorporation affects the catalyst productivity, it will be useful to study other possible techniques for introducing copper. The following results are for H/MOR (SAR 20) with copper introduced by impregnation, repeated high concentration (1M compared to 0.3M) ion-exchange and solid state exchange, as detailed in Chapter 2. Table 3.2 summarizes the copper loadings for all of the copper mordenite SAR20 samples described in this chapter.

SAMPLE ID	Initial [Cu] of Solution /M	Theoretical Cu Loading /wt%	Cu Loading /wt%
Cu/MOR SE1	0.3	43.26	2.20
Cu/MOR SE2	0.3	43.26	2.59
Cu/MOR SE3	0.3	43.26	(2.45)
Cu/MOR HP1	0.0006	0.32	0.32
Cu/MOR HP2	0.0011	0.65	0.70
Cu/MOR HP3	0.0023	1.28	1.27
Cu/MOR HP4	0.0045	2.51	(2.40)
Cu/MOR HP5	0.0089	4.95	(4.96)
Cu/MOR IMP	0.2971	3.63	-
Cu/MOR [1M]	1.0070	71.63	(2.80)
Cu/MOR SS	N/A	4.73	(4.24)

Table 3.2 Summary of the copper loadings for all the Cu/H/MOR SAR20 samples

Impregnation

Figure 3.39-41 compare a sample of mordenite, impregnated with 3.6 wt% copper, to the H/MOR (SAR 20). The conversion, Figure 3.39a, for the impregnated sample is initially over 95% and steadily falls to a stable 80%. The levels of conversion and carbon balance, for H/MOR and the impregnated sample, are comparable for the first 10 hours of reaction, apart from the first point.

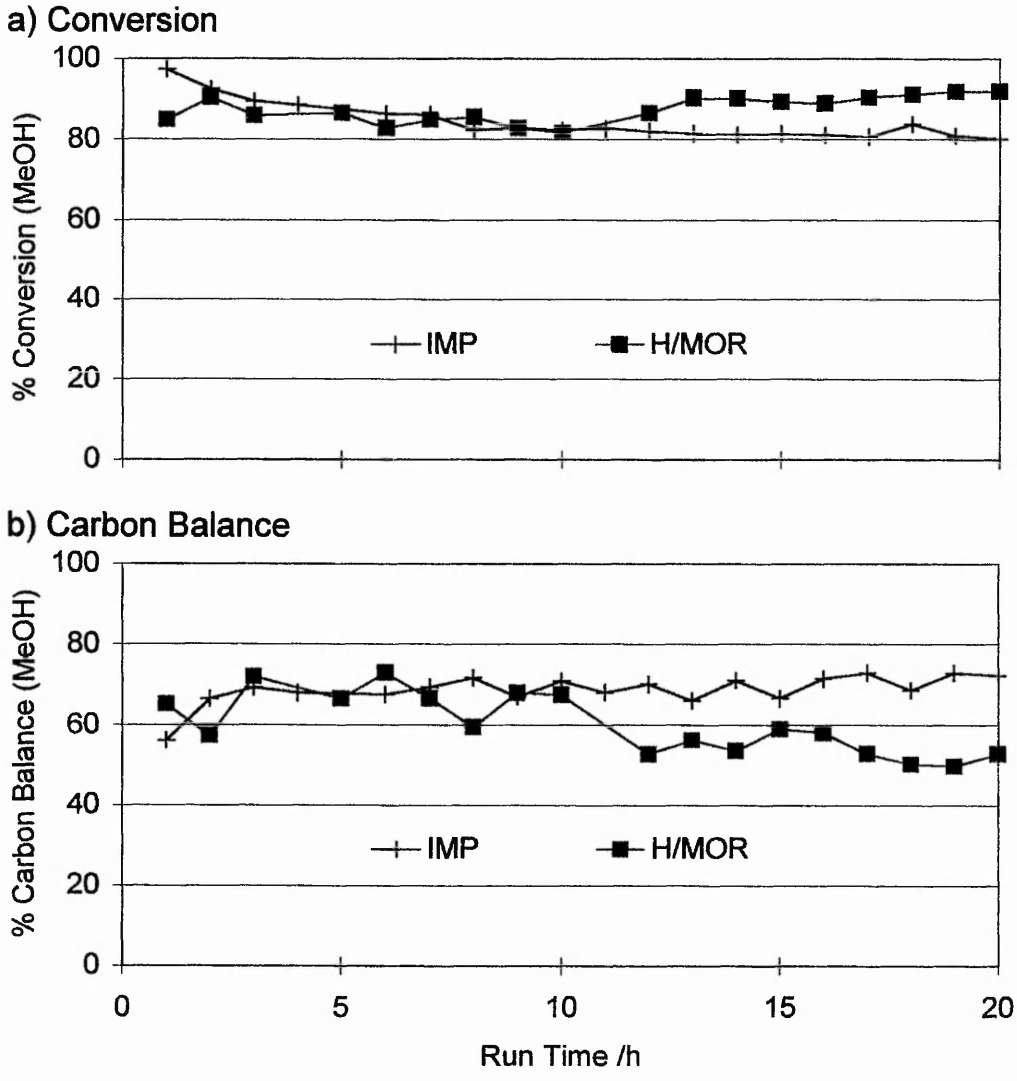

Figure 3.39 The effect of copper impregnation (IMP) on (a) the Conversion and (b) the Carbon Balance compared to H/MOR SAR20

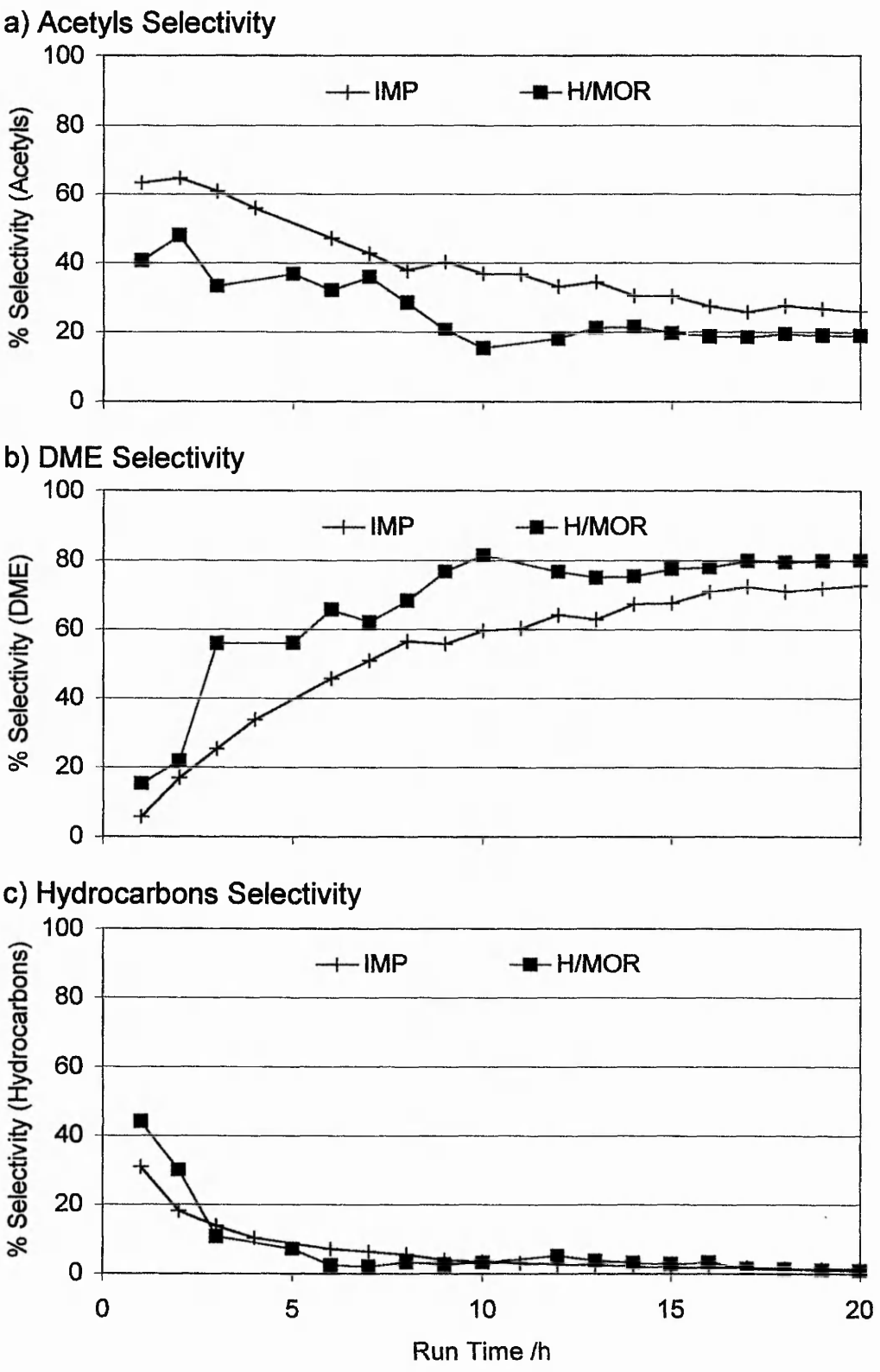

Figure 3.40 The effect of copper impregnation (IMP) on the selectivities to (a) Acetyls, (b) DME and (c) Hydrocarbons compared to H/MOR SAR20

In Figure 3.40a, the acetyls selectivity follows the same trend for both the impregnated and H/MOR samples but is constantly higher for the former sample. Throughout the reaction, the selectivity to DME for the impregnated sample is lower by 10%, than for the H/MOR. For both samples, the selectivity to hydrocarbons is equivalent initially 30-40% it falls rapidly to less than 10% by 5 hours. Therefore, the difference in selectivity for the two samples is solely due to the higher selectivity to acetyls for the impregnated sample, especially over the period 2-10 hours where the levels of conversion are equivalent. The slightly higher yield of acetyls for the copper impregnated sample compared to the H/MOR is shown in Figure 3.41. Impregnation of the high level of copper (3.6 wt%) does not produce a catalyst as productive as Cu/H/MOR SE2 (2.2 wt%).

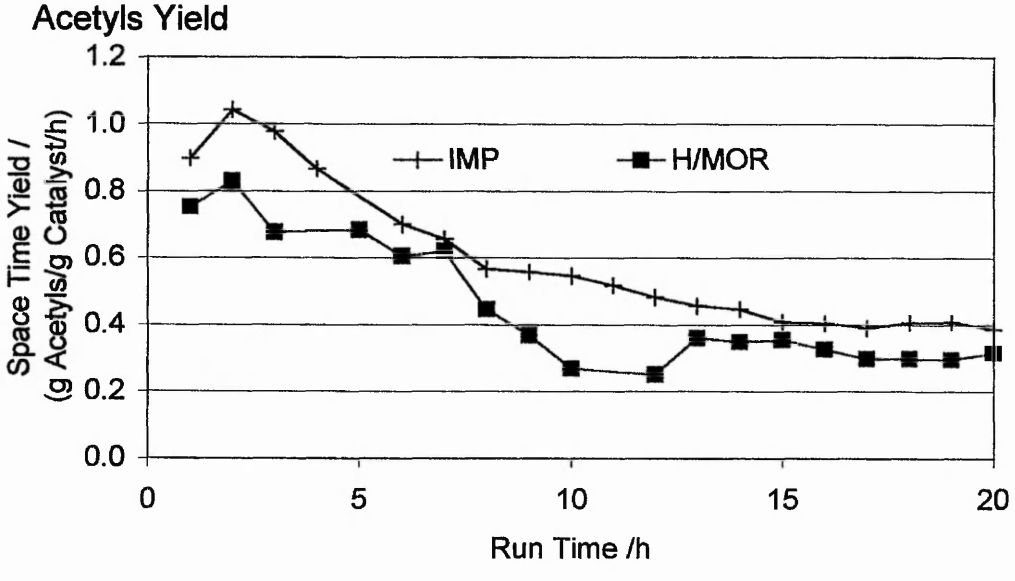

Figure 3.41 The effect of copper impregnation (IMP) on the Acetyls Space Time Yield compared to H/MOR SAR20

High concentration ion-exchange

All the Cu/H/MOR SE samples were prepared using an initial 0.3M copper nitrate solution. The following sample was prepared differently, using an initial concentration of 1.0M copper nitrate, resulting in a copper loading of 2.8 wt% compared to 2.2 wt% for the 0.3M copper solution. An initial conversion of 100% falls by 5 hours to a stable 85%, which is then retained throughout the reaction, as shown in Figure 3.42a. Again the opposite trend to that for H/MOR, which starts low and then rises. During the initial high level of conversion the carbon balance is lower than 40%, but it rises to a stable 60% by 5 hours.

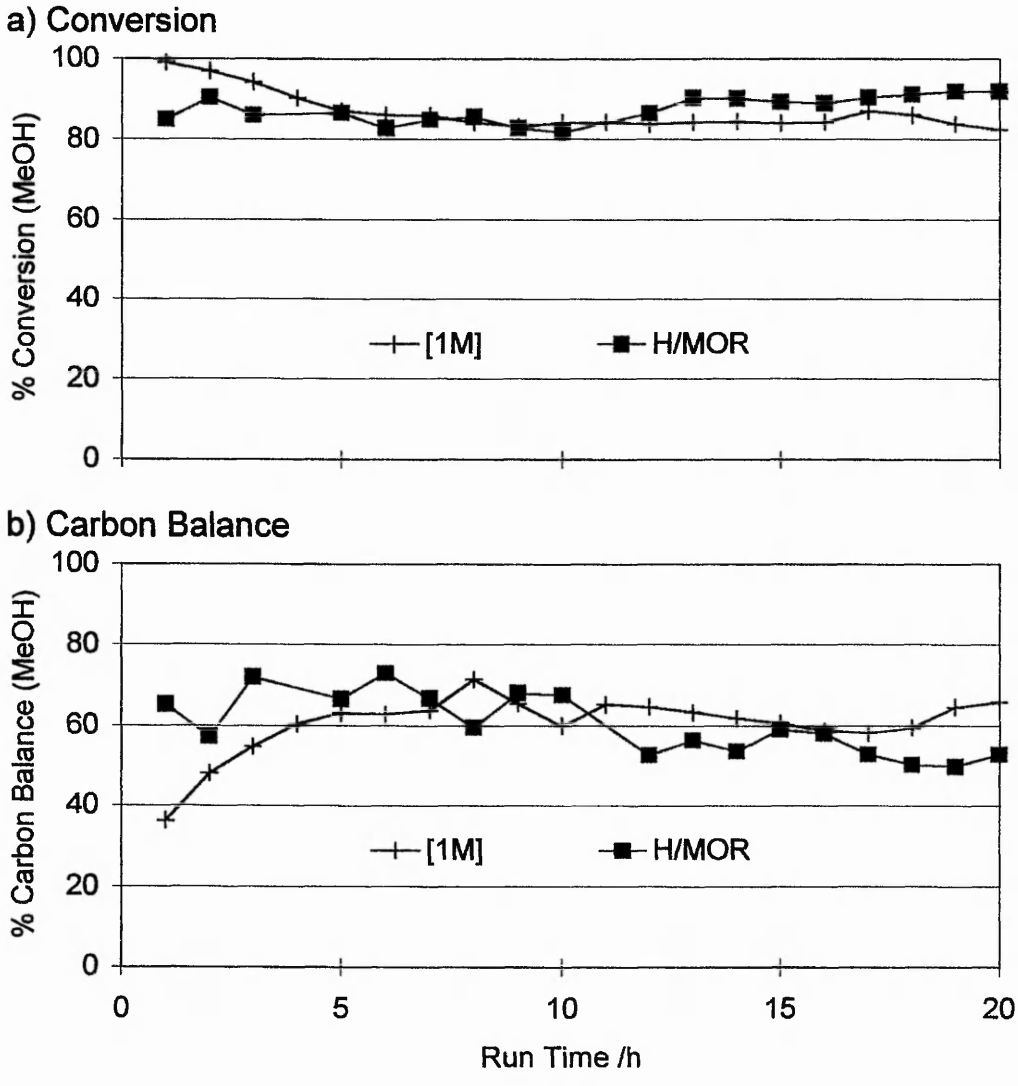

Figure 3.42 The effect of ion-exchange using 1.0M copper solution on (a) the Conversion and (b) the Carbon Balance compared to H/MOR SAR20

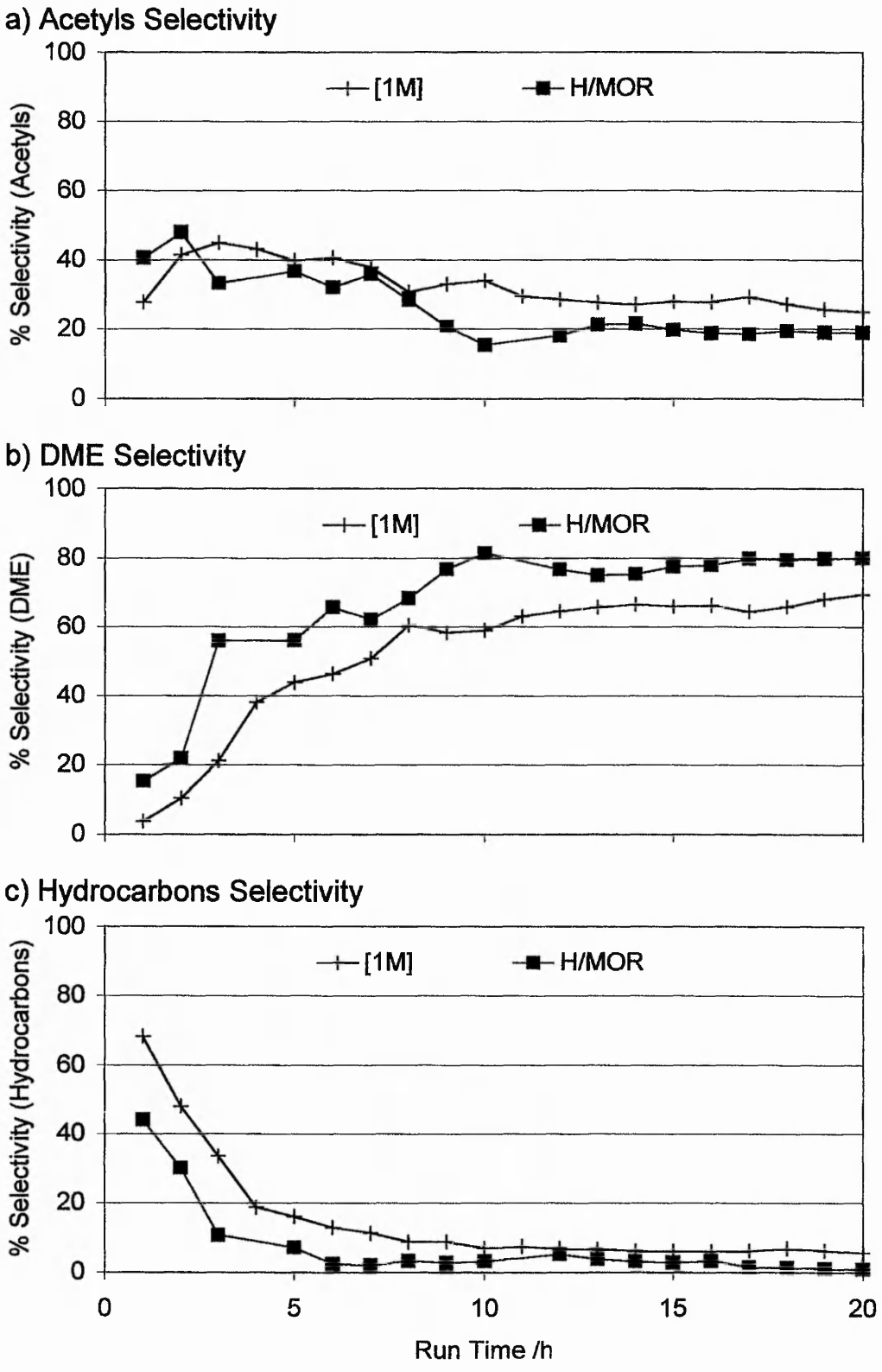

Figure 3.43 The effect of ion-exchange using 1.0M copper solution on the selectivities to (a) Acetyls (b) DME and (c) Hydrocarbons compared to H/MOR SAR20

The product selectivities for the concentrated copper ion-exchange sample follow the same trends as for H/MOR. The initial acetyls selectivity, Figure 3.43a, is low compared to the other copper loaded samples tested, but is comparable to that for the H/MOR sample. The selectivity to DME is constantly lower than the H/MOR by at least 10%. Both samples follow the same DME selectivity trend, initially very low and rising within the first 7 hours to a stable value. The selectivity to hydrocarbons is therefore constantly higher than for H/MOR, initially 70% it falls to a stable 10%, again by 7 hours.

As shown in Figure 3.44, there is no initial high acetyls yield for this copper loaded sample. The maximum yield of 0.6 g/g/h occurs after 3-4 hours of the reaction and rapidly falls to around 0.3 g/g/h, as for the H/MOR sample. The maximum yield obtained is later in the reaction, and no greater than observed for H/MOR. This indicates that not only the procedure, but also the preparation conditions used can modify the reactivity of the copper loaded system.

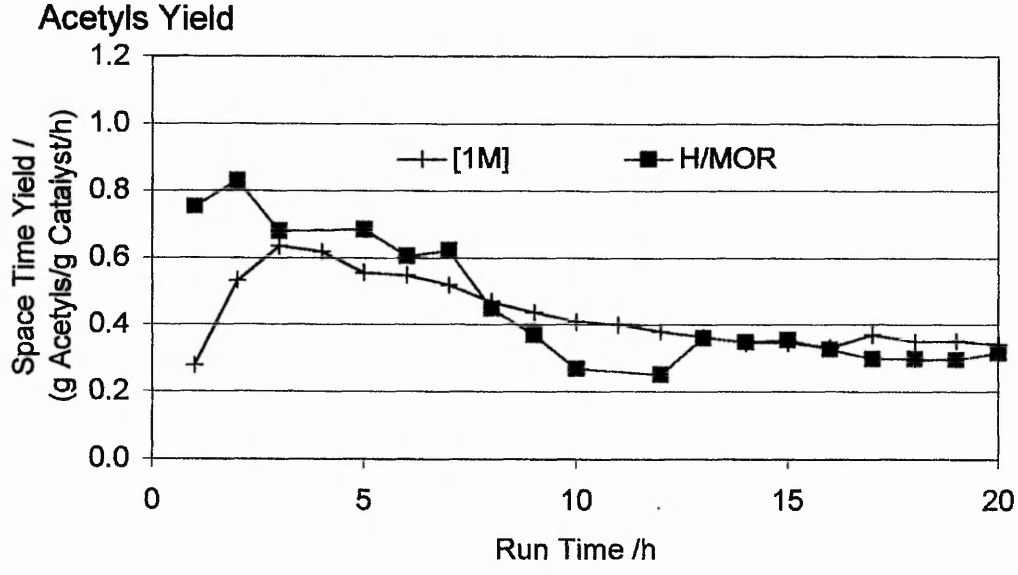

Figure 3.44 The effect of ion-exchange using 1.0M copper solution on the Acetyls Space Time Yield compared to H/MOR SAR20

Solid state exchange with CuO

Solid state exchange was used, to control directly the amount of copper introduced, and as a comparison to the liquid phase controlled method described earlier (page 75). Additionally, if the copper did not completely exchange it would be present as a physical mixture with the zeolite, either as the oxide or the metal. Any promotional effect of copper containing clusters external to the zeolite framework could therefore also be determined.

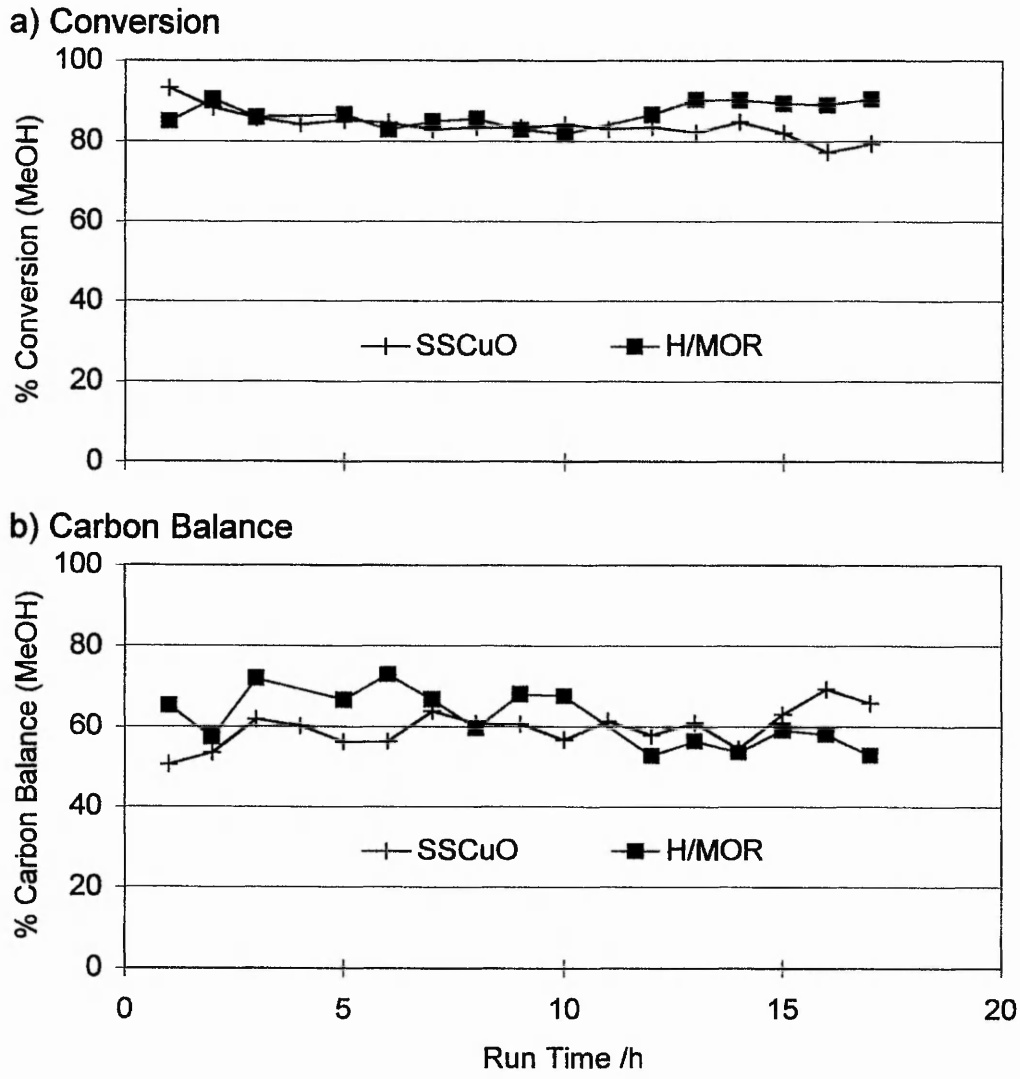

Figure 3.45 The effect of solid state ion-exchange on (a) the Conversion and (b) the Carbon Balance compared to H/MOR SAR20

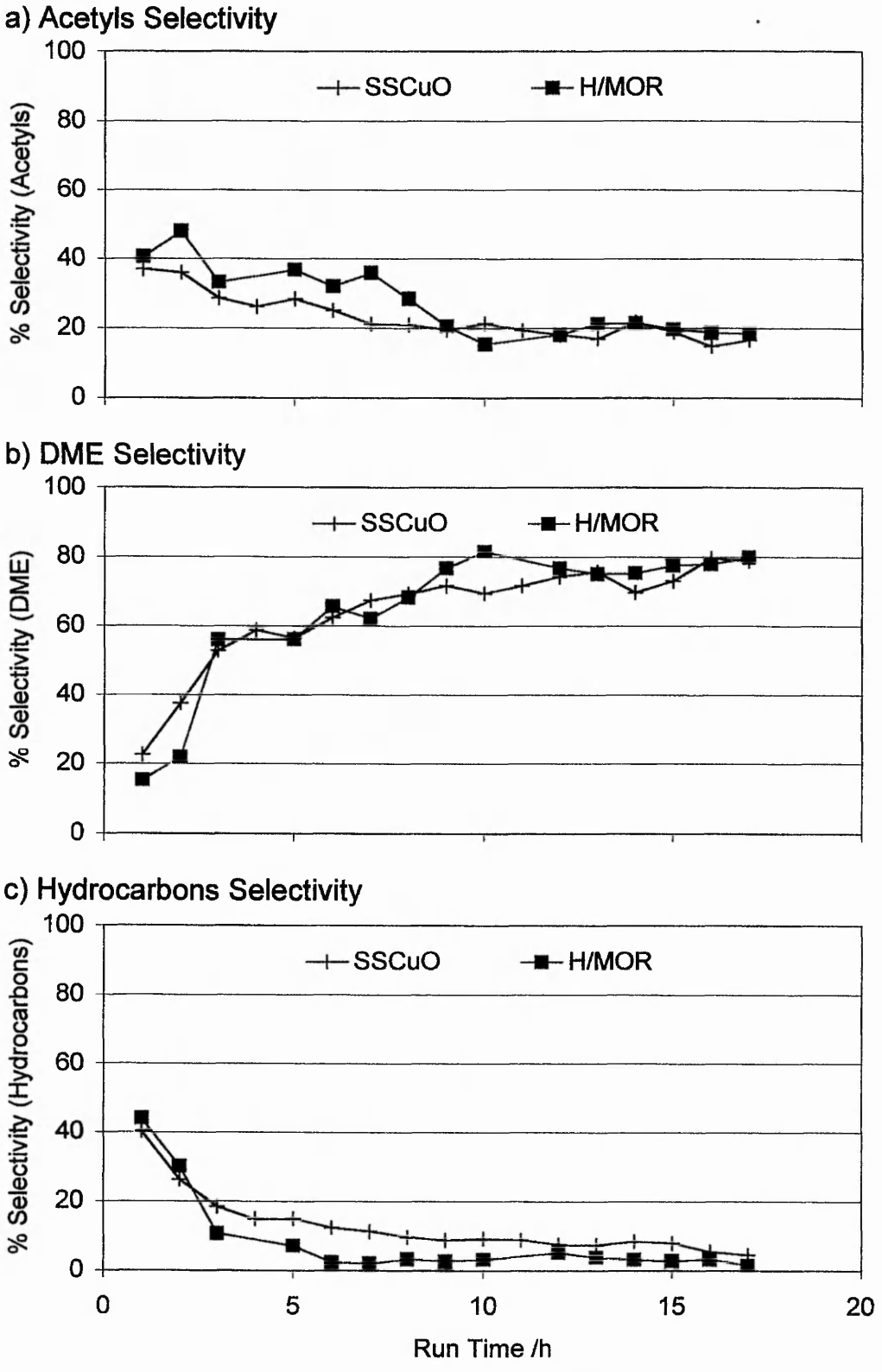

Figure 3.46 The effect of solid state ion-exchange on the selectivities to (a) Acetyls, (b) DME and (c) Hydrocarbons compared to H/MOR SAR20

Figure 3.45a shows that the level of conversion for the solid state exchanged sample is comparable to that for H/MOR, especially between 3-10 hours of the reaction. The initial point is higher and the later periods are lower as the degree of conversion slowly decreases after 10 hours. For the majority of the reaction, the carbon balance for the copper loaded sample is lower than for the H/MOR sample.

During the period of comparable conversion, the selectivity to acetyls for the solid state exchanged sample is lower than for the H/MOR by 10%, as shown in Figure 3.46. The selectivities to DME are comparable throughout. The hydrocarbon selectivity is therefore higher for the solid state exchanged sample compared to H/MOR, especially during the period 3-10 hours of reaction.

Figure 3.47 shows the lower acetyls yield for the solid state exchanged sample. The initial yield of only 0.5 g/g/h steadily falls to 0.2 g/g/h by 10 hours reaction. Solid state ion exchange therefore does not introduce copper into the framework in a form that promotes the reactivity of the mordenite system.

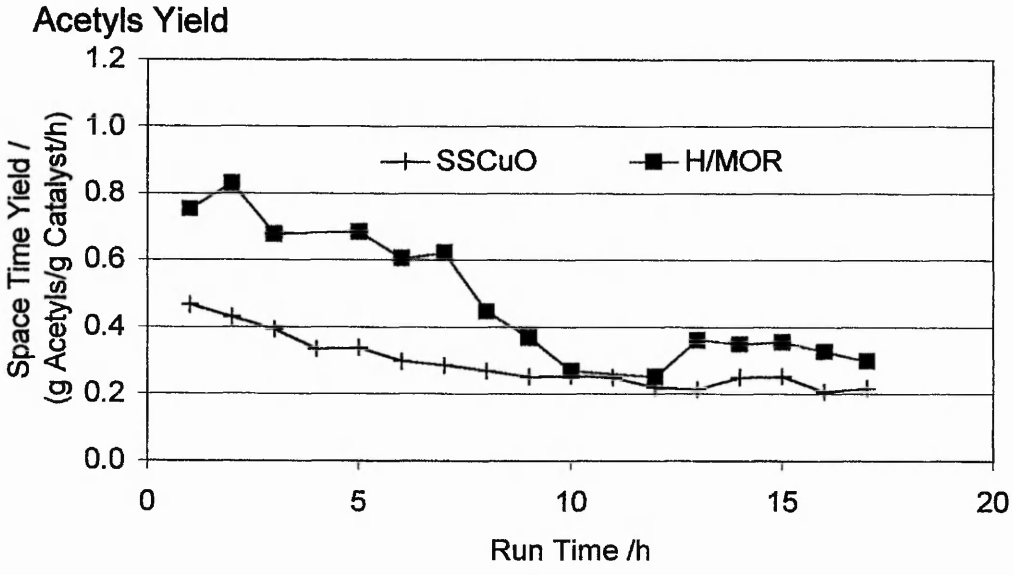

Figure 3.47 The effect of solid state ion-exchange on the Acetyls Space Time Yield compared to H/MOR SAR20

THE EFFECT OF TEMPERATURE

In an attempt to prolong the high initial yield of acetyls over the Cu/H/MOR SE3 (SAR20), the effect of raising the temperature in a series of steps was studied. The results are presented in the standard format, but with an additional axis to the right to show the temperature. The temperature, after an initial 5 hours at 350°C, was programmed to rise at 5°C min^{-1} in steps of 25°C every 3 hours. It should be noted that the reactor was at the new temperature for 55 minutes before the first of three injections, not with the ramp taking the full hour as represented on the plots.

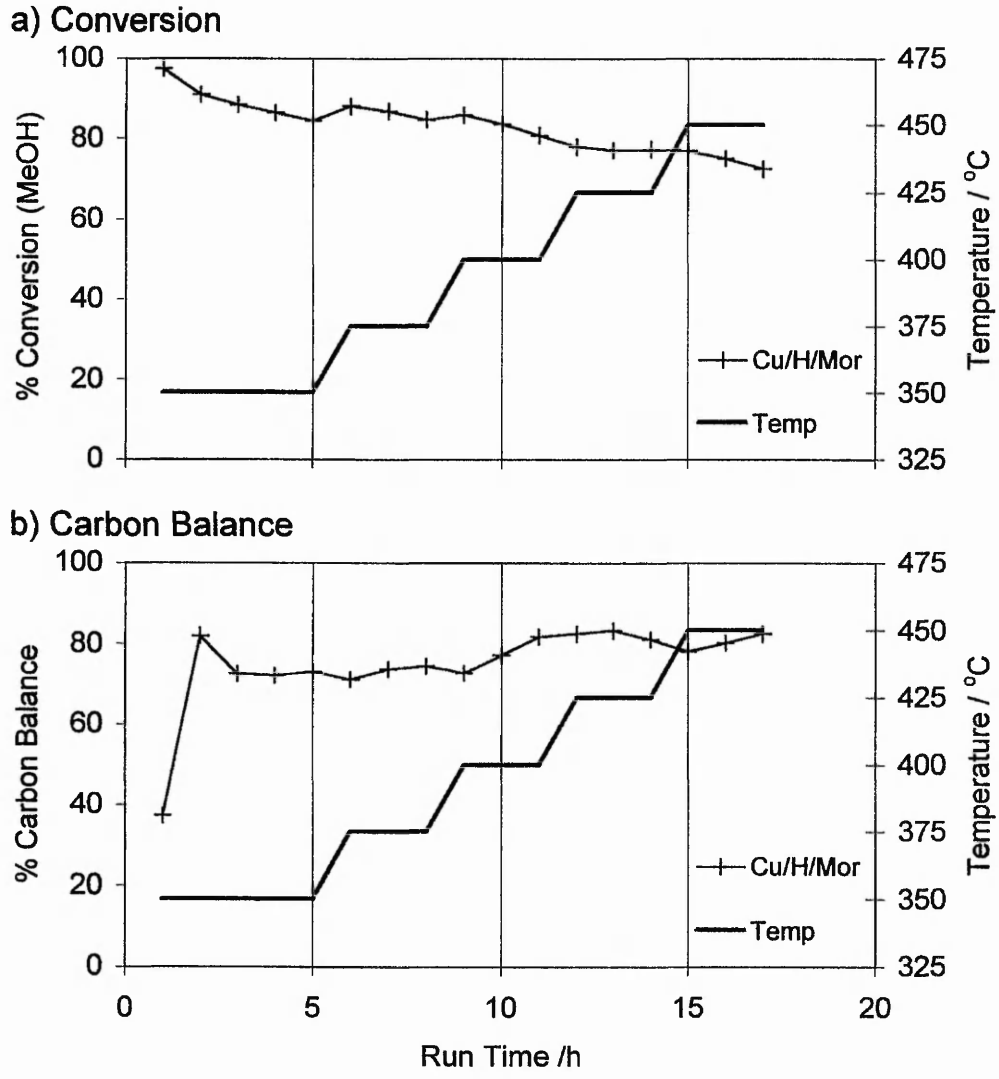

Figure 3.48 Effect of Increasing the Temperature on (a) the Conversion and (b) the Carbon Balance for Cu/H/MOR SE3

The level of methanol conversion is not changed by any significant degree, on increasing the temperature, as shown in Figure 3.48a. The overall trend as a function of run time is of the conversion decreasing from 100% to 70%. There are very small increases in conversion at the 350-375 °C and 375-400 °C temperature jumps.
The initial carbon balance is only 40%, as shown in Figure 3.48b, within the following hour the carbon balance reaches its peak of over 80% and then subsequently falls to 70%, with a general trend of increasing as a function of run time. On raising the temperature, the carbon balance is not disturbed greatly but falls slightly after each step, e.g. 375-400°C, before rising again at a similar rate.
Figure 3.49a clearly shows the selectivity to acetyls maintains a level of 30% even on raising the temperature. After each temperature increase, the selectivity rises slightly but then returns within the following hour. In comparison, without the temperature ramp it is found (Figure 3.8 page58) that the initial acetyls selectivity is high but drops to a stable level around 20%. For DME, its selectivity is seen to rise rapidly for a given temperature, as found previously, until a selectivity of 60% is obtained where it stabilises. Each time the temperature is raised, the DME selectivity is seen to fall. The overall effect of the temperature programming is therefore to prolong the time it takes for the DME selectivity to stabilise at the high value.
The Cu/H/MOR SE3 gives an initial high hydrocarbon selectivity of 70%, which as a function of run time decreases rapidly. However, the first two temperature jumps increase the initial hydrocarbon selectivity of 30% by a further 20% and 10% respectively. The further temperature increases are not accompanied by any significant change in the hydrocarbon selectivity, which falls off to around 5%.
The constant levels of conversion and carbon balance indicate that the variations in selectivities to DME and hydrocarbons are a result of increasing the temperature.

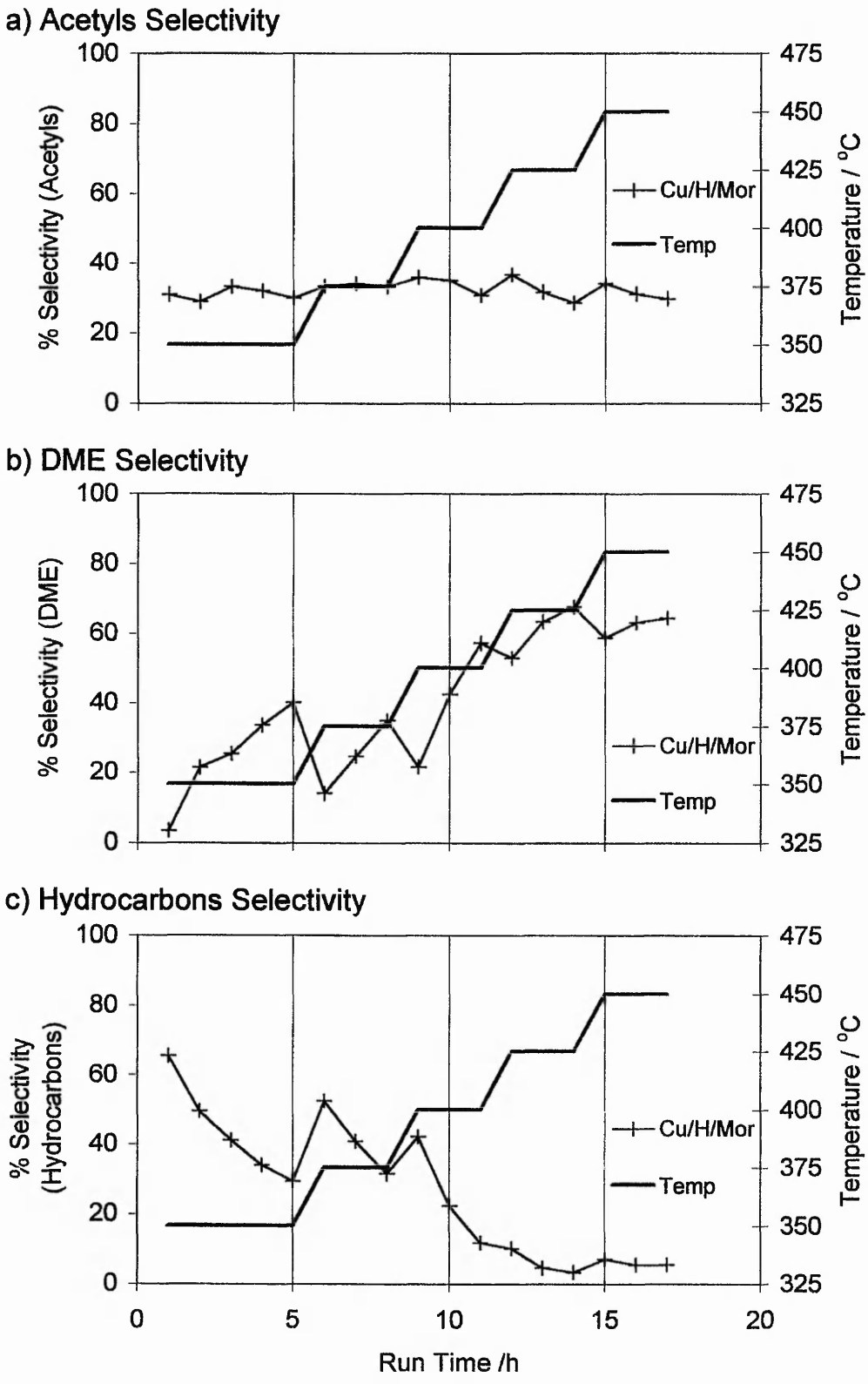

Figure 3.49 Effect of increasing the Temperature on the Selectivities to (a) Acetyls, (b) DME and (c) Hydrocarbons for Cu/H/MOR SE3

The effect of the temperature programming, on the acetyls space time yield, is seen in Figure 3.50a. The yield of 0.6 g/g/h of acetyls is maintained throughout. At any given temperature the acetyls yield is seen to fall, but after the first three steps it recovers. At 425 °C, the yield is seen to fall off steeply and is not recovered significantly when the temperature reaches 450 °C, instead it is seen to stabilise at 0.5 g/g/h.

Therefore, the overall effect of the temperature programming is to maintain the higher acetyls yield for longer. However, the yield still decreases after every temperature rise. Figure 3.50b&c show that the acetic acid yield is not affected by the increasing temperature, but remains stable at 0.2-0.1 g/g/h yield. It is therefore the methyl acetate yield that is modified as a function of temperature, maintaining the higher 0.5 g/g/h yield. Each temperature rise corresponds to a drop in the DME selectivity with equally split increases in the acetyls and hydrocarbon selectivities.

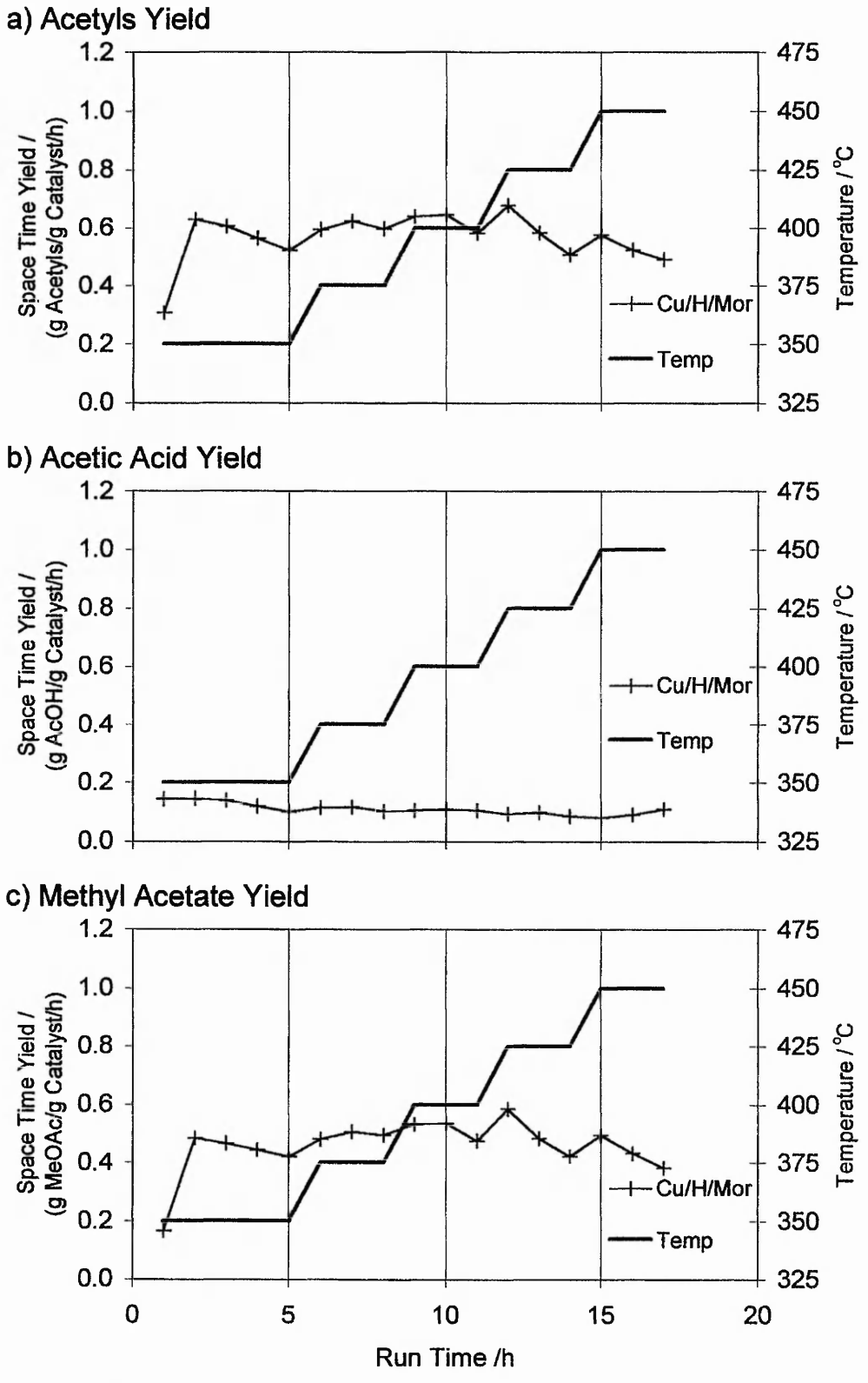

Figure 3.50 Effect of increasing the Temperature on the Space Time Yields to (a) Acetyls, (b) Acetic Acid and (c) Methyl Acetate for Cu/H/MOR SE3

DEALUMINATION OF MORDENITE

Background

As detailed in Chapter 2, three different preparations of dealuminated mordenite were tested for their reactivity towards methanol carbonylation. The overall effect of dealumination, as detailed in Chapter 1, is to reduce the concentration of Bronsted acid sites by removing the framework aluminium. Additionally, reducing the acid site concentration further increases the acid strength, until the remaining Bronsted acid sites are isolated. The removal of the framework aluminium also opens up the framework structure, introducing mesoporous regions into the microporous channel structure. All of these effects may increase the reactivity of the mordenite framework. The starting material Na/MOR SAR12.8 was assumed to be converted to the proton form during the acid washing process. No copper was introduced into these samples and so they are compared here with the H/MOR SAR20 sample. Table 3.3 below, summarizes the effect of the three procedures on the SAR ratio, as determined by XRF.

SAMPLE ID	Initial Si/Al_2 Ratio (SAR)	Final Si/Al_2 Ratio (XRF)
Na/MOR BP1 ST	12.8	13.94
Na/MOR BP1 AW	12.8	19.55
Na/MOR BP2 ST	12.8	19.51
Na/MOR BP2 AW	12.8	-
Na/MOR NTU 1	12.8	-
Na/MOR DOW 1	12.8	-

Table 3.3 Summary of the mordenite framework composition after dealumination

BP steam and acid wash

For the sample prepared using the steaming apparatus at BP (Sunbury), the cycle of steaming and acid washing was carried out twice on one batch, BP1 is after the first cycle, and BP2 after the second. The steaming removes the aluminium from the framework to form extraframework alumina species. The following acid wash then dissolves the extraframework species out from the sample. This can be clearly seen, for the BP1 sample in Table 3.3, by the SAR ratio determined by XRF. After the first

steaming, BP1 with a SAR 13.9 is similar to the as supplied Na/MOR SAR 12.8, when compared to the increase to SAR 19.5 after the acid washing. Further steaming does not change the SAR further, however the acid washing causes a further increase. The samples were tested in the reactor only after the acid washing steps.

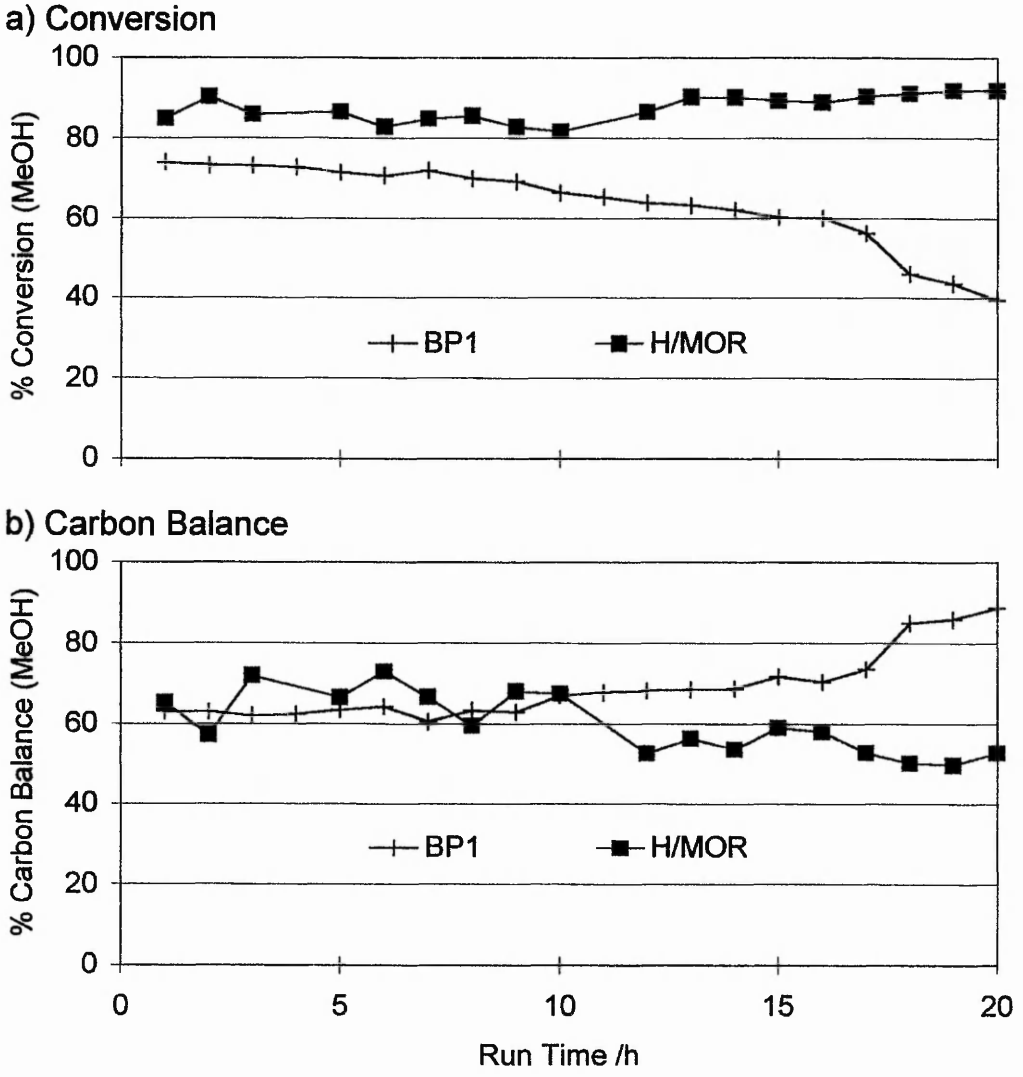

Figure 3.51 The effect of dealumination for BP1 on (a) the Conversion, and (b) the Carbon Balance compared to H/MOR SAR20

The level of conversion after the first cycle of steaming and acid washing, is low compared to that for the H/MOR, initially 75% it steadily falls to 60% by 15 hours reaction. The initial carbon balance is similar to that for the H/MOR, being between 60-70% for the first 10 hours.

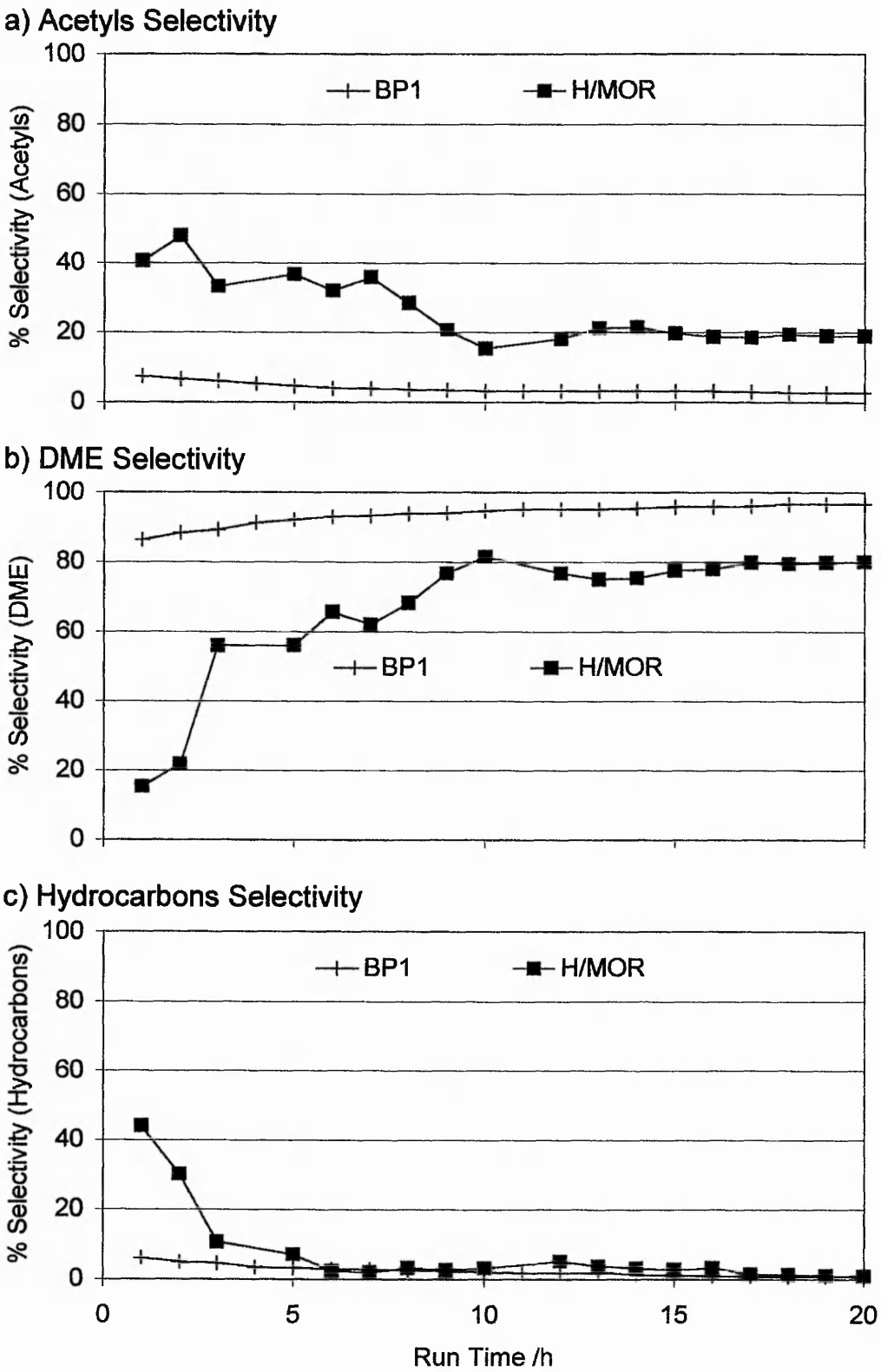

Figure 3.52 The effect of dealumination for BP1 on the Selectivities to (a) Acetyls, (b) DME and (c) Hydrocarbons compared to H/MOR SAR20

Figure 3.52b clearly shows that of the 70% methanol converted, at least 90% of it is converted to DME. The selectivities to acetyls and hydrocarbons never rise higher than their initial combined total of 10%. This indicates that the reactivity of the dealuminated sample is no greater than that for the as supplied Na/MOR SAR12.8.
The reactivity of BP1 is 10% that of the H/MOR, the acetyls never rising above the initial 0.1 g/g/h yield.

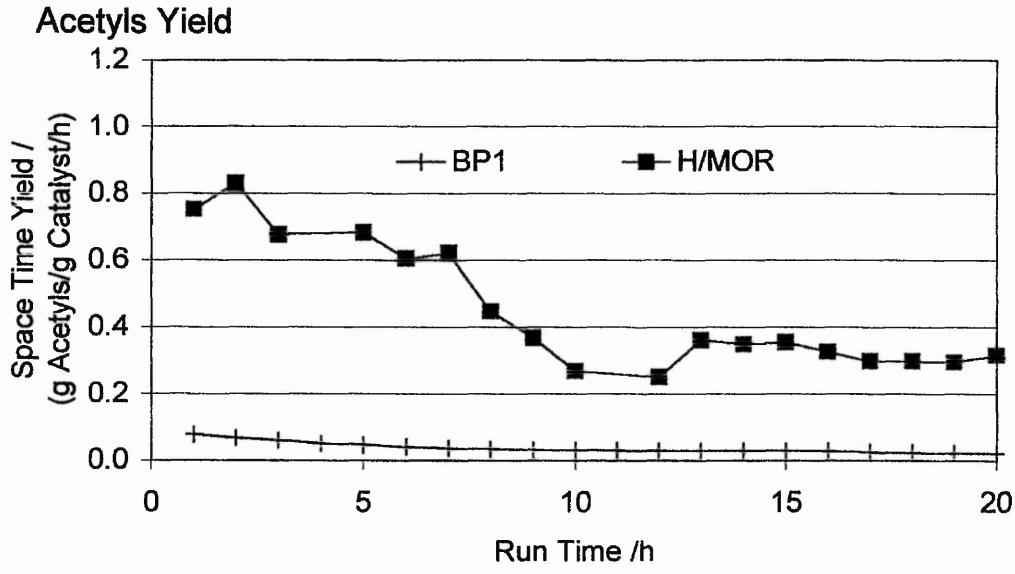

Figure 3.53 The effect of dealumination for BP1 on the Acetyls Space Time Yield as compared to H/MOR SAR20

In contrast Figure 3.54-56 show the results for BP2, after the second cycle of steaming and acid washing of Na/MOR SAR 12.8. The conversion is seen to be virtually 100% throughout the reaction, whilst the carbon balance is initially lower than 50%. The rapid rise in the carbon balance after 15 hours of reaction indicates that a build up of hydrocarbon residues blocked the reactor. The initial low carbon balance is due to the conversion of methanol to the formation of undetected non-volatile hydrocarbons. The selectivities, shown in Figure 3.55, support the low carbon balance detected. The acetyls selectivity is low throughout, never rising above 10% until after the reactor is blocked. The DME selectivity is seen to be virtually at zero throughout the reaction. Therefore, the hydrocarbons form over 90% of the detected products. This high selectivity to the volatile hydrocarbons suggests that undetectable heavy hydrocarbons will be formed simultaneously, which accounts for the low carbon balance observed. The acetyls yield of around 0.1 g/g/h rises at the onset of the rising carbon balance, due to the increase in sample size due to the higher pressures of the blocked reactor.

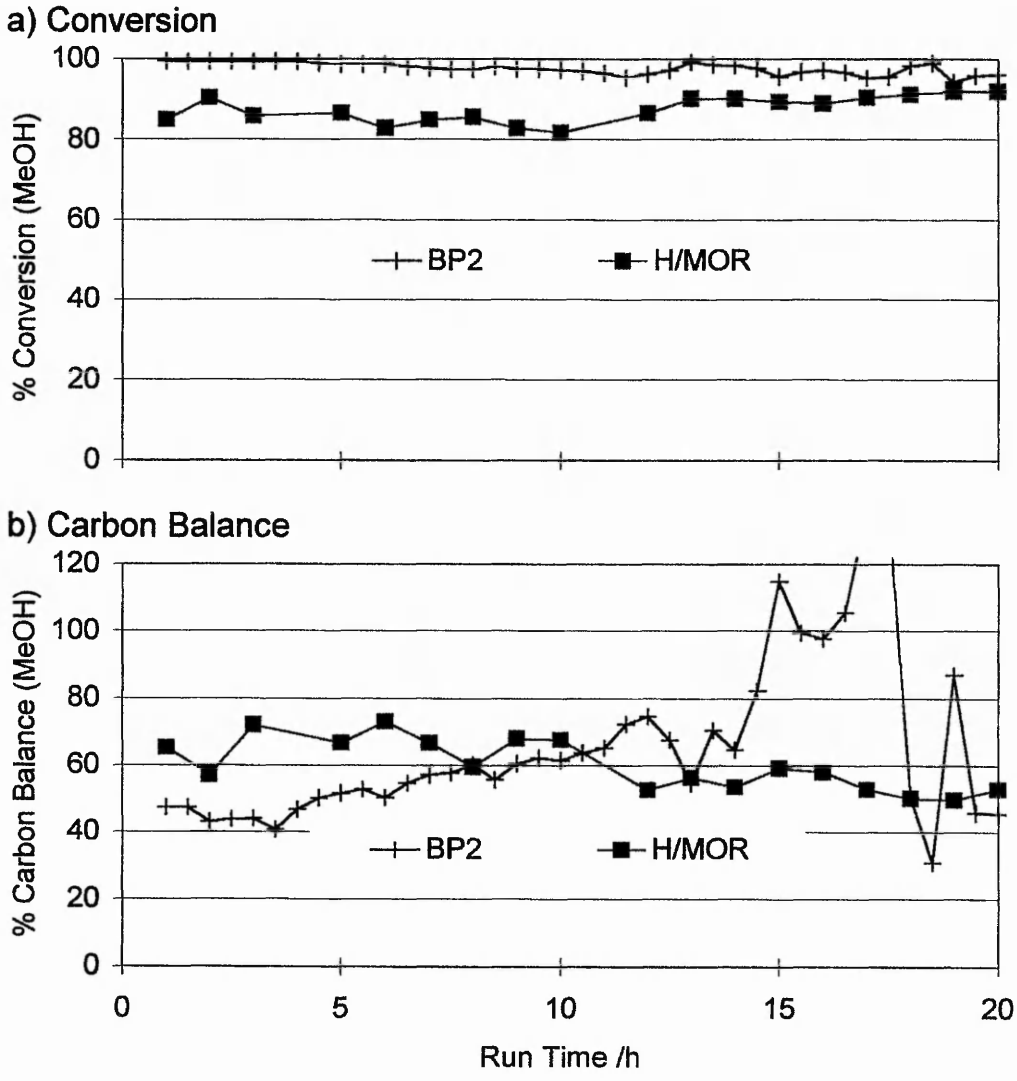

Figure 3.54 The effect of dealumination for BP2 on (a) the Conversion, and (b) the Carbon Balance compared to H/MOR SAR20

Therefore, the slight increase in acetyls yield over that for BP1, comes at the cost of a loss in DME selectivity, giving rise to a broad range of byproducts being formed, which result in the blocking of the reactor. Comparing the results for BP1 and BP2 indicates that the further dealumination removes the sites responsible for the formation of DME. However, the second cycle creates, or allows access to, sites capable of forming the hydrocarbons without greatly affecting the acetyls yield.

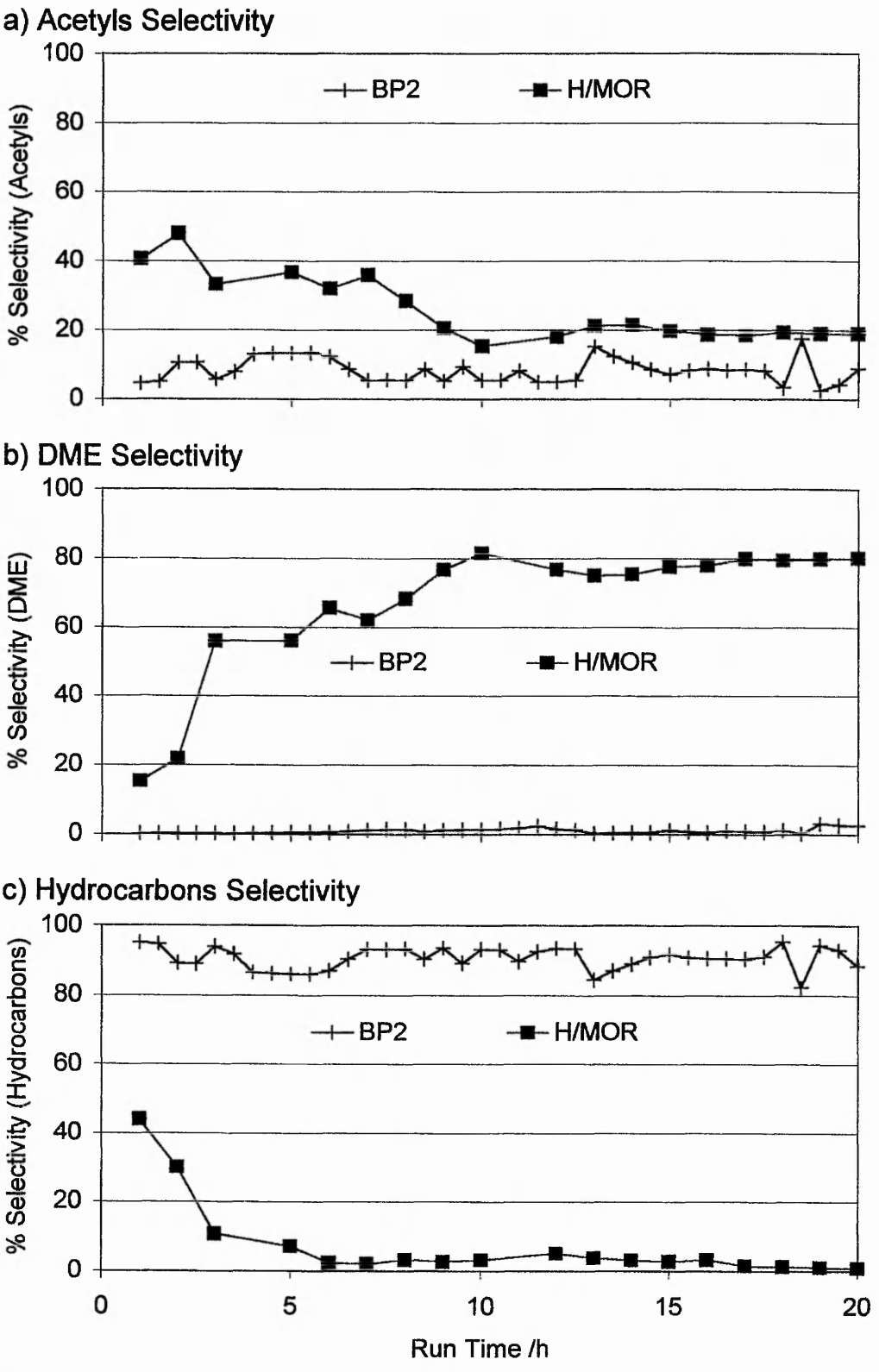

Figure 3.55 The effect of dealumination for BP2 on the Selectivities to (a) Acetyls, (b) DME and (c) Hydrocarbons compared to H/MOR SAR20

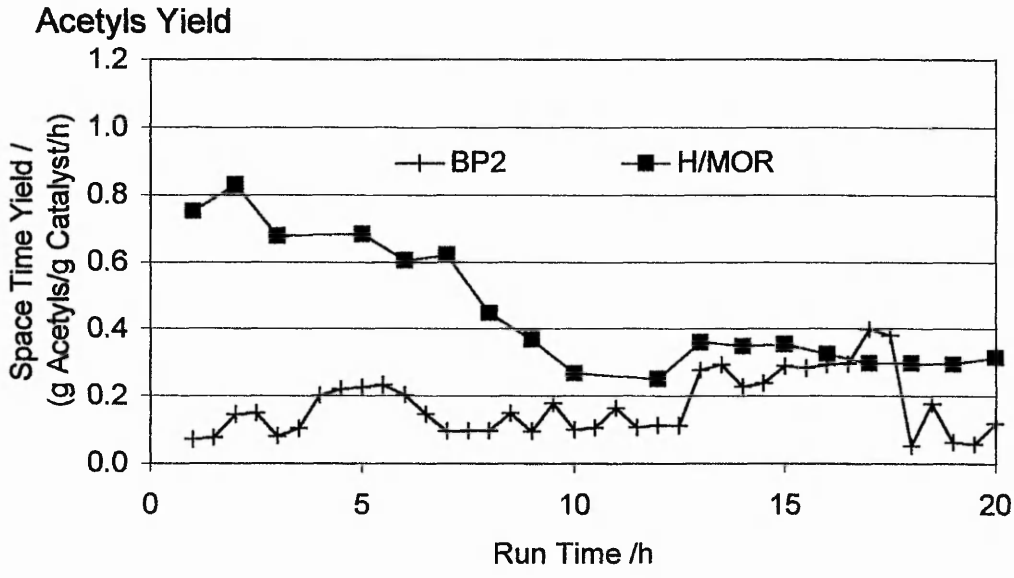

Figure 3.56 The effect of dealumination for BP2 on the Acetyls Space Time Yield as compared to H/MOR SAR20

NTU steam and acid wash

To repeat the preparation carried out whilst at BP (Sunbury), a similar, but smaller scale procedure was adopted on returning to NTU, see Chapter 2 for details.

The reaction for the sample NTU1, calcined under the normal conditions after the first cycle of steaming and acid washing, was seriously disrupted by the reactor becoming blocked, similar to the BP2 sample above. Figure 3.57-59 show the results for this sample for the first 15 hours of reaction. The level of conversion is less than 50% for the majority of the reaction. The carbon balance is unstable, initially 60% during the highest conversion period, but peaking at 120% at the low point in conversion after 5 hours of reaction. The carbon balance falls quickly back to 60% but then starts to increase again as the conversion falls. Selectivities in Figure 3.58 show that hydrocarbons are the major product formed throughout, especially during the initial period of highest conversion. The blockage causes the selectivities to be unstable, but the general trend is of the hydrocarbon selectivity falling as the DME dominates. The selectivity to acetyls is less than 20% throughout, and is only effected slightly by the blockage. The low acetyls space time yield of 0.2 g/g/h acetyls, is comparable to the BP2 sample and solely due to the formation of methyl acetate.

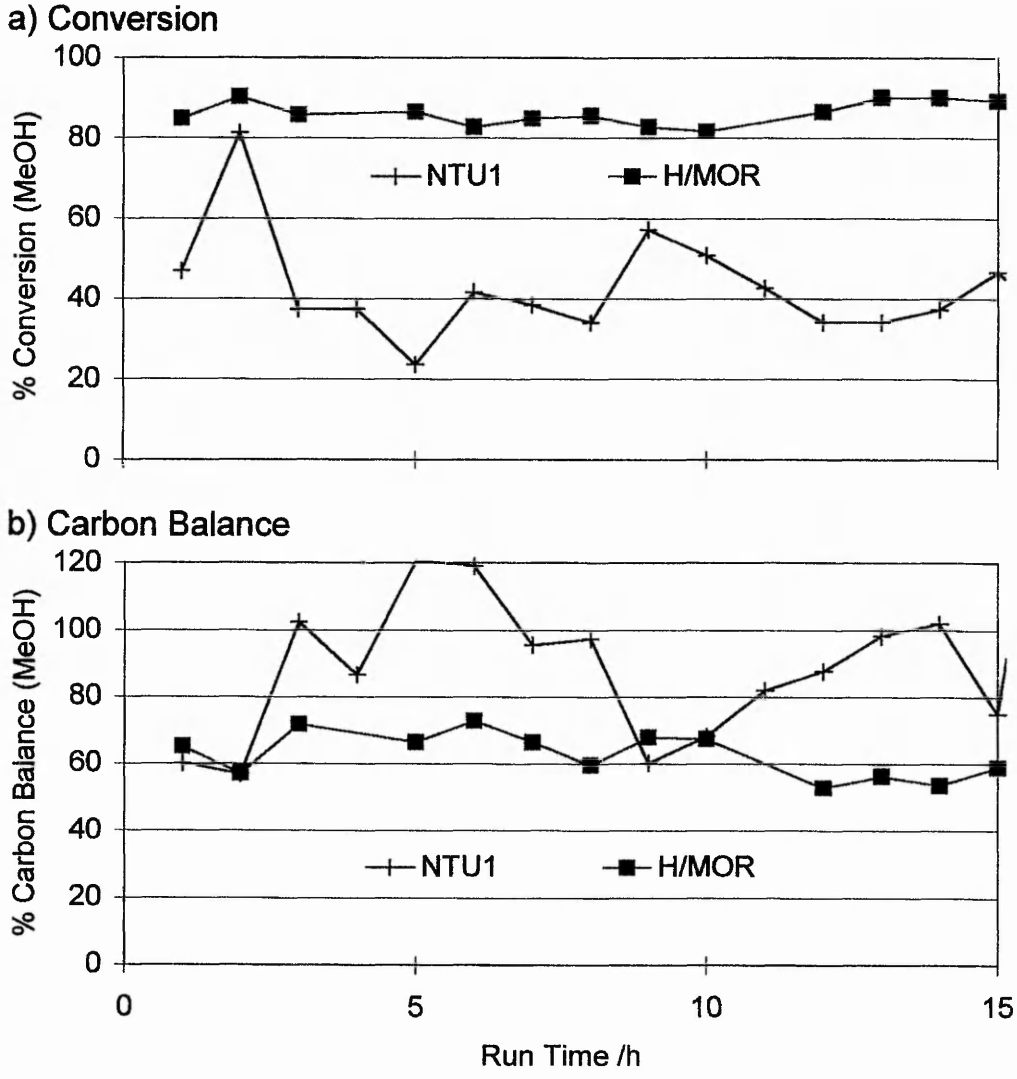

Figure 3.57 The effect of dealumination for NTU1 on (a) the Conversion and (b) the Carbon Balance as compared to H/MOR SAR20

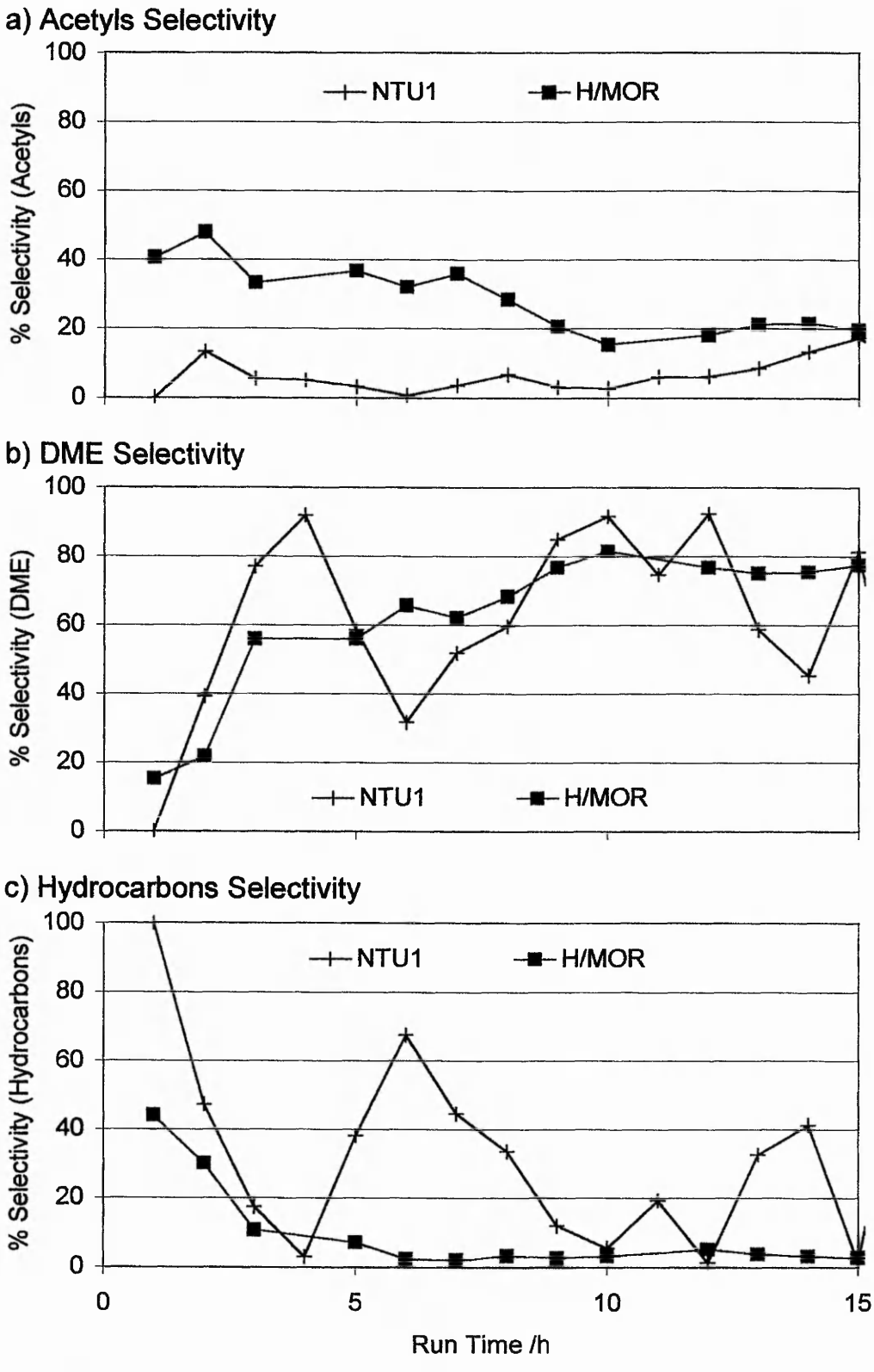

Figure 3.58 The effect of dealumination for NTU1 on the Selectivities to (a) Acetyls, (b) DME and (c) Hydrocarbons as compared to H/MOR SAR20

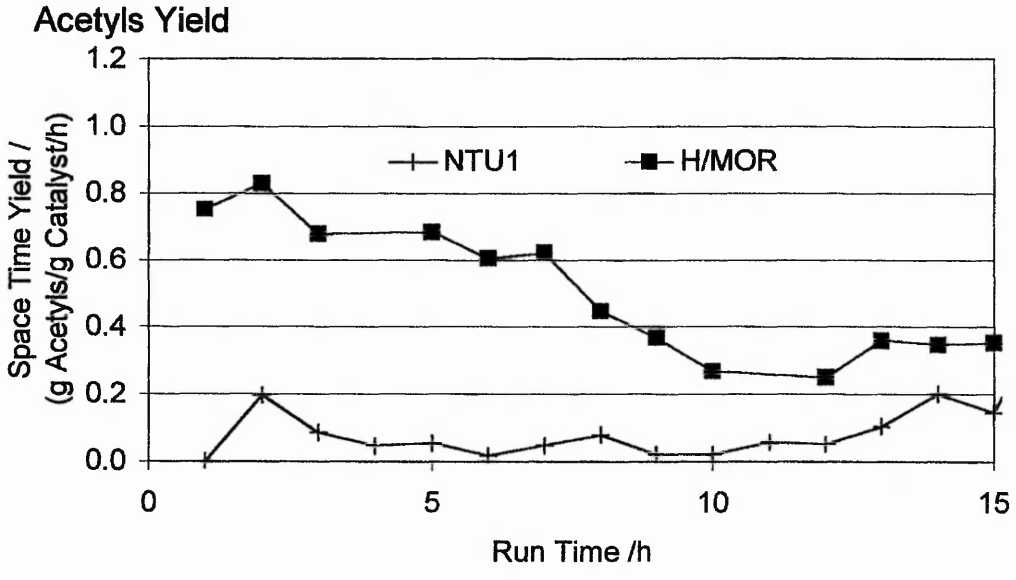

Figure 3.59 The effect of dealumination for NTU1 on the Acetyls Space Time Yield as compared to H/MOR SAR20

The effect, of the steaming and acid washing, on the mordenite framework is shown by the following XRD traces after the different stages. The as supplied Na/MOR SAR 12.8, presented in Chapter 2, shows sharp peaks and is clearly crystalline. In Figure 3.60 there is no major decrease in the crystallinity after, both the steaming and acid washing stages of the dealumination. The framework is therefore dealuminated, without any migration of the remaining tetrahedrally coordinated atoms. The framework should therefore contain mesoporous cavities rather than a modified siliceous framework. However in Figure 3.61a, crystallinity is lost after calcination under the standard conditions of 500 °C. Indicating that the resulting mesoporous framework structure is unstable under high temperature conditions. The sample NTU1 after calcination is therefore equivalent to an amorphous silica alumina. The unselective conversion of methanol to hydrocarbons over NTU1 is due to the loss of steric control induced by the mordenite framework structure. The similar conditions to the BP preparation used on this smaller sample are equivalent to repeating the BP cycle.

To retain the dealuminated structure, milder calcination conditions of 200 °C, after extensive drying under flowing helium at room temperature, were used. As shown in Figure 3.61 the structure is still affected, but not to the same degree. The reactor results for this sample NTU 200C follow.

(a) NTU ST Na/MOR(12.8) Steamed

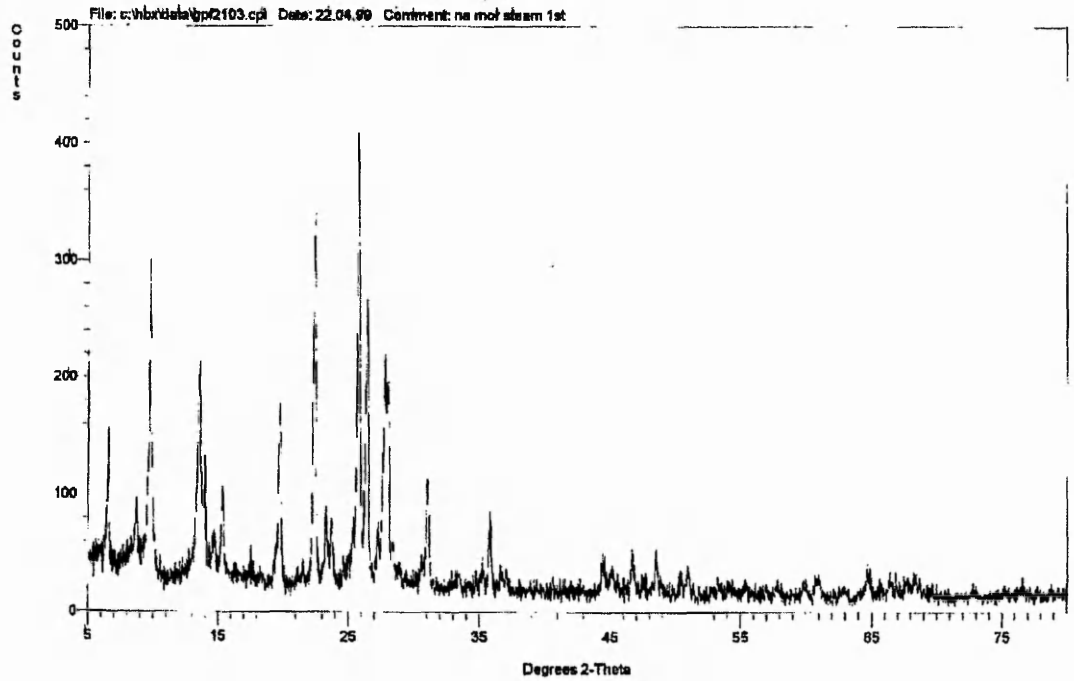

(b) NTU NC Na/MOR(12.8) Steamed & Acid Washed Uncalcined

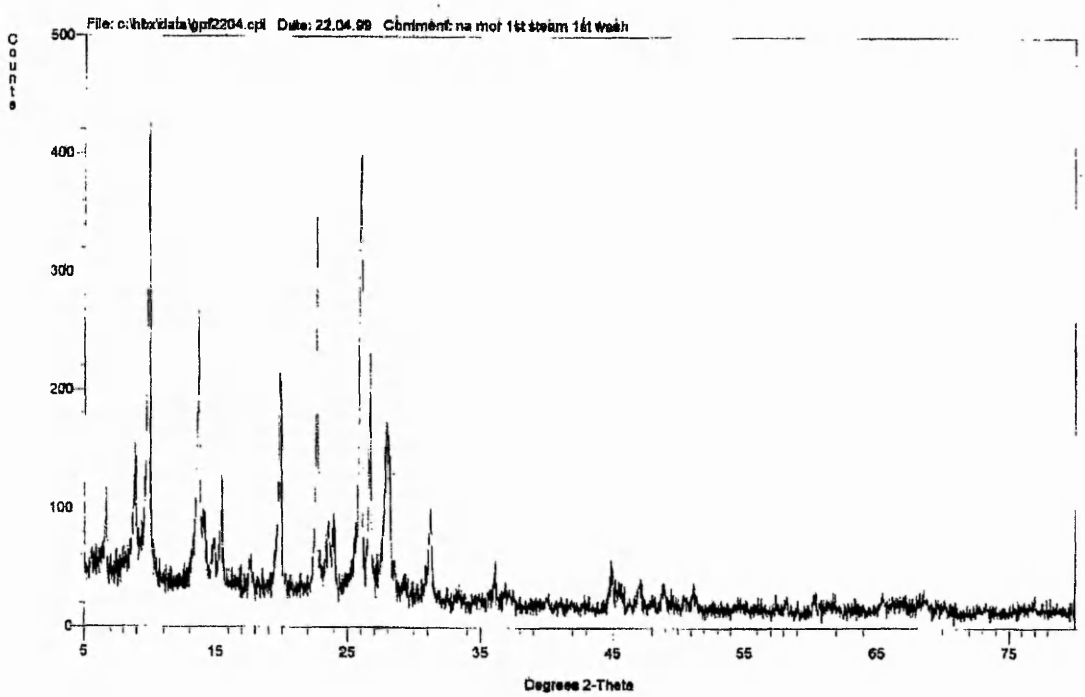

Figure 3.60 XRD Traces confirming that the crystallinity of mordenite was retained after (a) steaming and (b) acid washing under the NTU dealumination conditions

(a) NTU1 Na/MOR(12.8) Steamed & Acid Washed Calcined 500°C

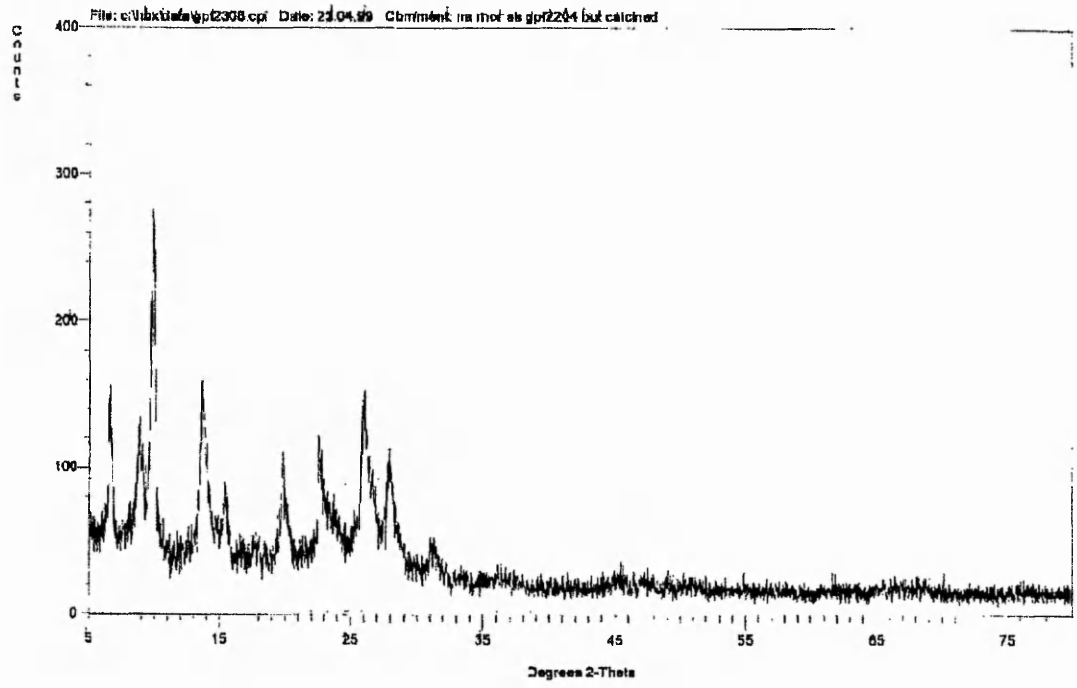

(b) NTU 200C Na/MOR(12.8) Steamed & Acid Washed Calcined 200°C

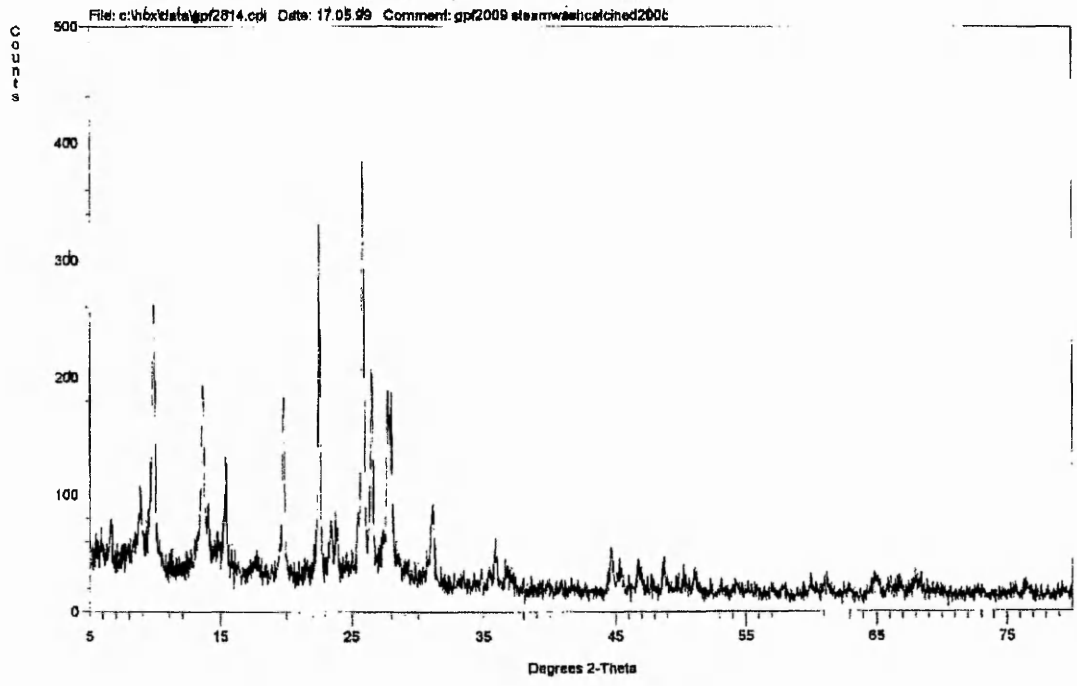

Figure 3.61 XRD Traces confirming that the crystallinity after calcination at (a) 500°C was lost and (b) 200°C was retained after steaming and acid washing under the NTU dealumination conditions

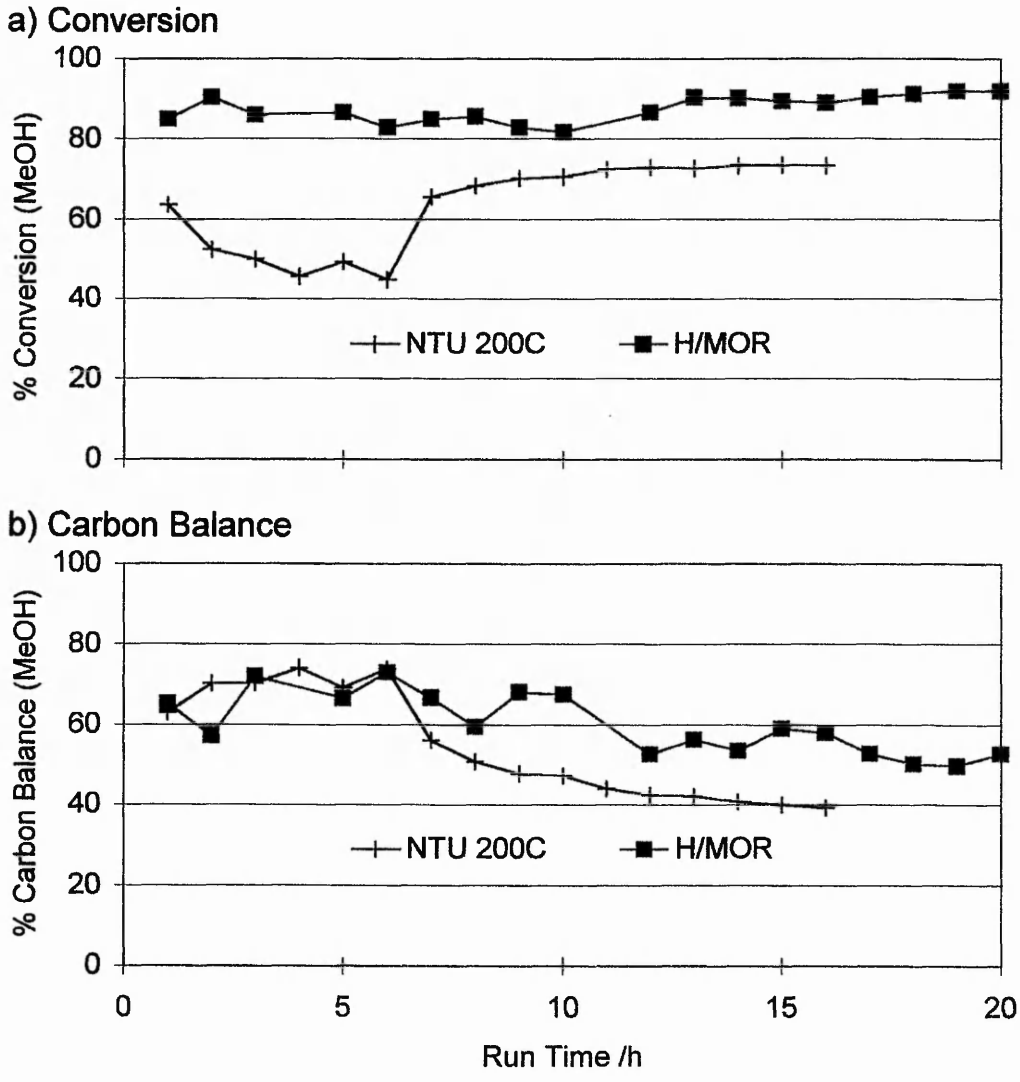

Figure 3.62 The effect of dealumination for NTU200C on (a) the Conversion and (b) the Carbon Balance as compared to H/MOR SAR20

The conversion for this mildly calcined sample is lower than for H/MOR, averaging around 60% throughout the reaction time of 15 hours. The carbon balance is seen to be stable between 60-70% for the first 6 hours before dropping to 40% which is closely matched to the trend for H/MOR. The major product throughout is DME, with a selectivity of greater than 95% throughout. Apart from a slightly higher initial hydrocarbon selectivity, both the acetyls and hydrocarbons are effectively zero throughout. Consequently, the yield of acetyls is virtually zero throughout the reaction.

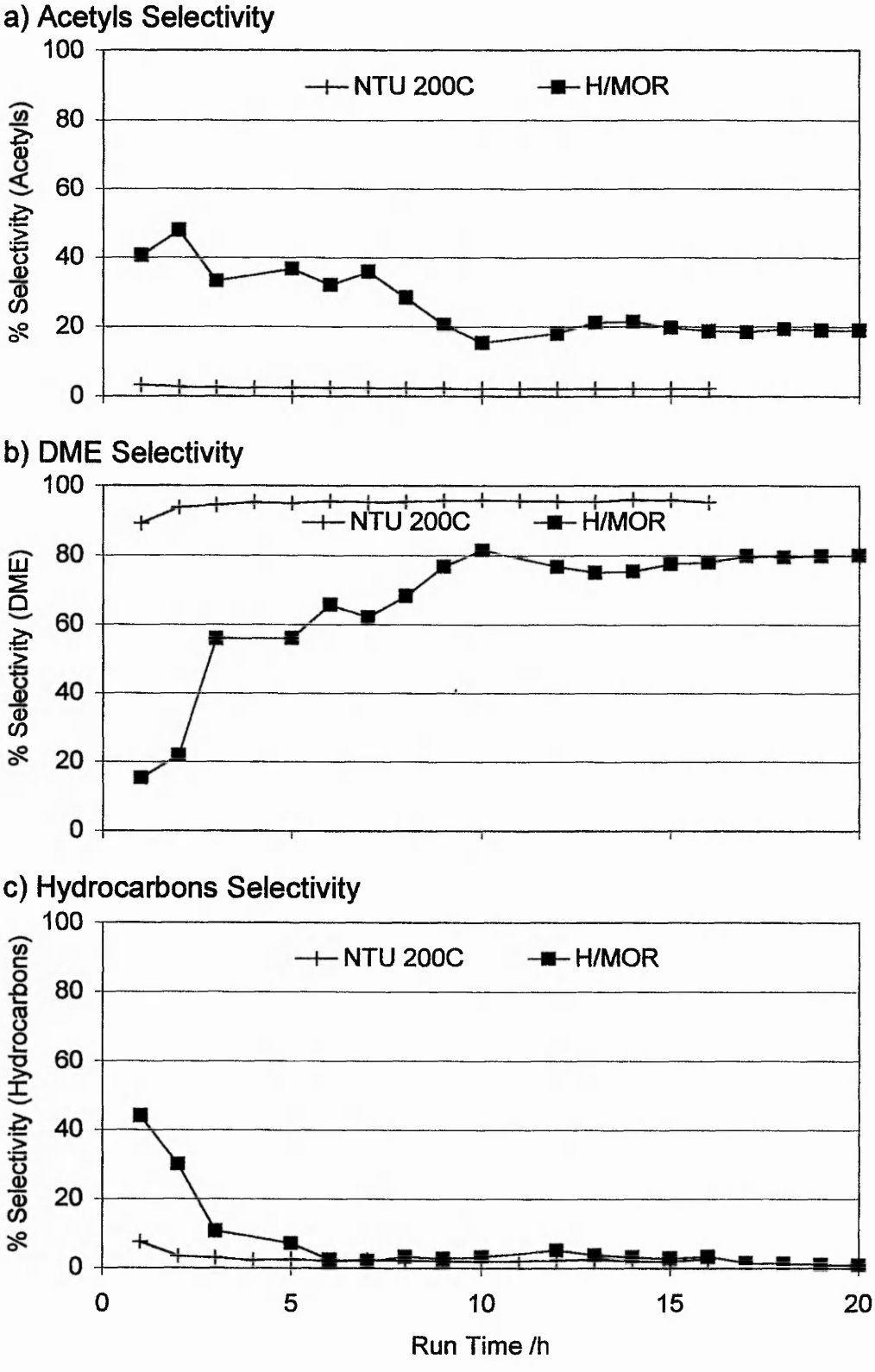

Figure 3.63 The effect of dealumination for NTU200C on the Selectivities to (a) Acetyls, (b) DME and (c) Hydrocarbons as compared to H/MOR SAR20

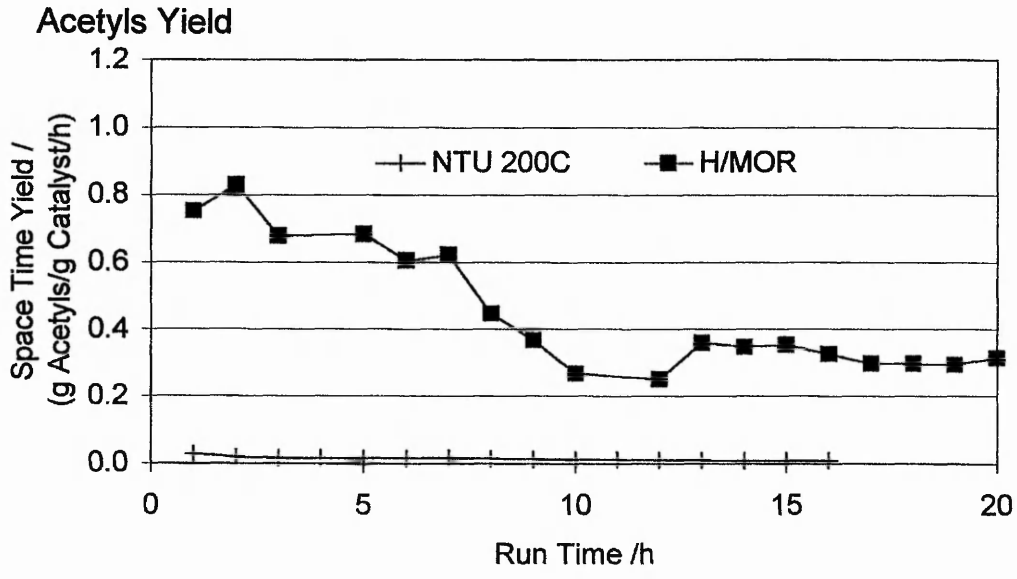

Figure 3.64 The effect of dealumination for 200C on the Acetyls Space Time Yield as compared to H/MOR SAR20

The results after mild calcination are comparable to results obtained without prior calcination, which are therefore not shown.

The dealumination of the framework by combined steaming and acid washing has been shown here to remove the large majority of the active sites. The incorporation of the mesoporous regions into the framework causes it to become thermally unstable. The activation of the catalyst by calcination causes the remaining framework to break down. Initially in the sodium form, acid sites are introduced by the acid washing and calcining as indicated, for the BP2 sample, by the uniquely low selectivity to DME that was previously seen to dominate over the sodium form. However the loss of the structural integrity of the zeolite framework means that the acid sites introduced are under no steric control from the framework and give rise to a broad spectrum of the hydrocarbon byproducts.

The DOW prep

Instead of dealuminating the mordenite by steaming, this third preparation initially involved acid washing the sample followed by calcination under severe conditions. The procedure was carried out according to a patent of DOW, as detailed in Chapter 2. To maintain any level of reactivity for the DOW sample, temperature programing was found necessary, so the reaction data is not compared directly to any other sample.

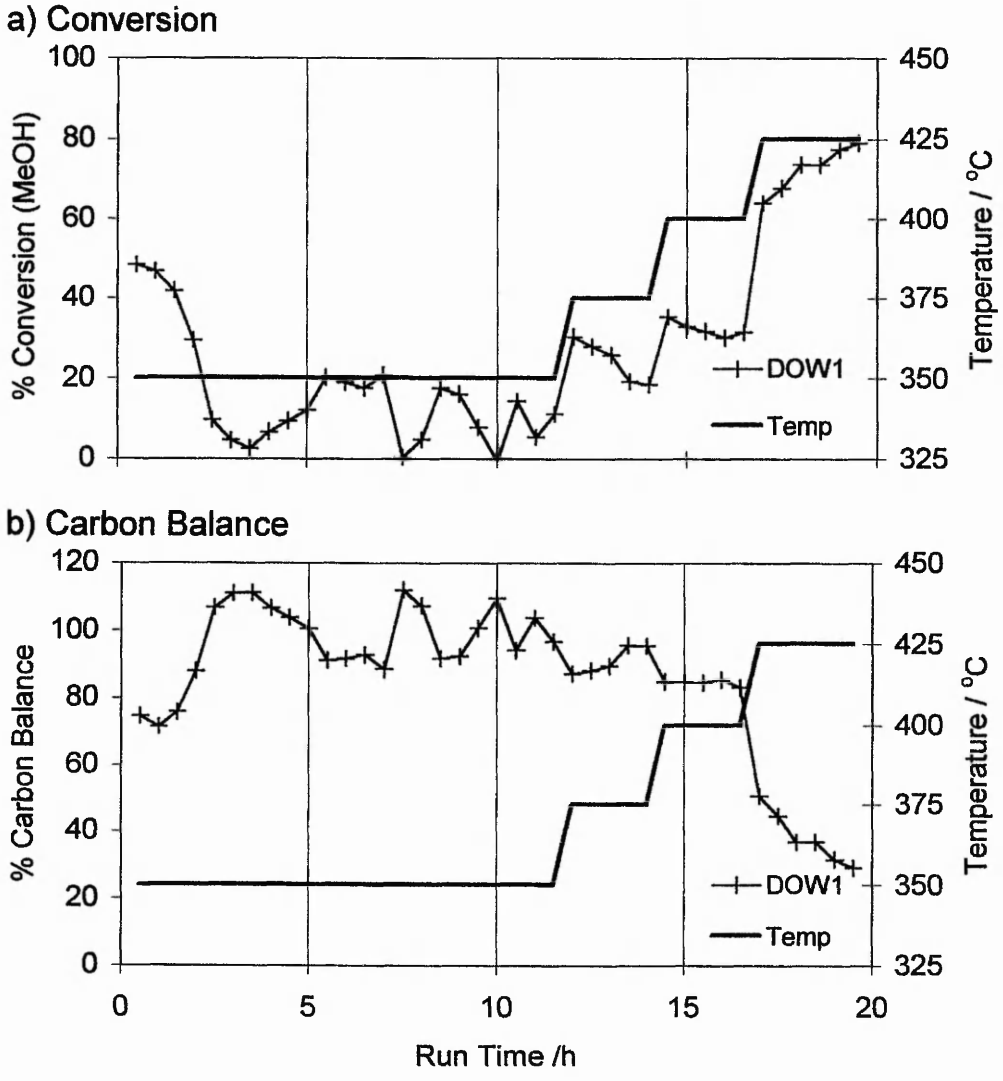

Figure 3.65 The level of (a) the Conversion and (b) the Carbon Balance for the sample prepared by the DOW dealumination patent

The level of conversion for the DOW sample can be seen in Figure 3.65a to be very low, initially at 50% it rapidly drops to an average of 10%, whilst the temperature is held at 350 °C.

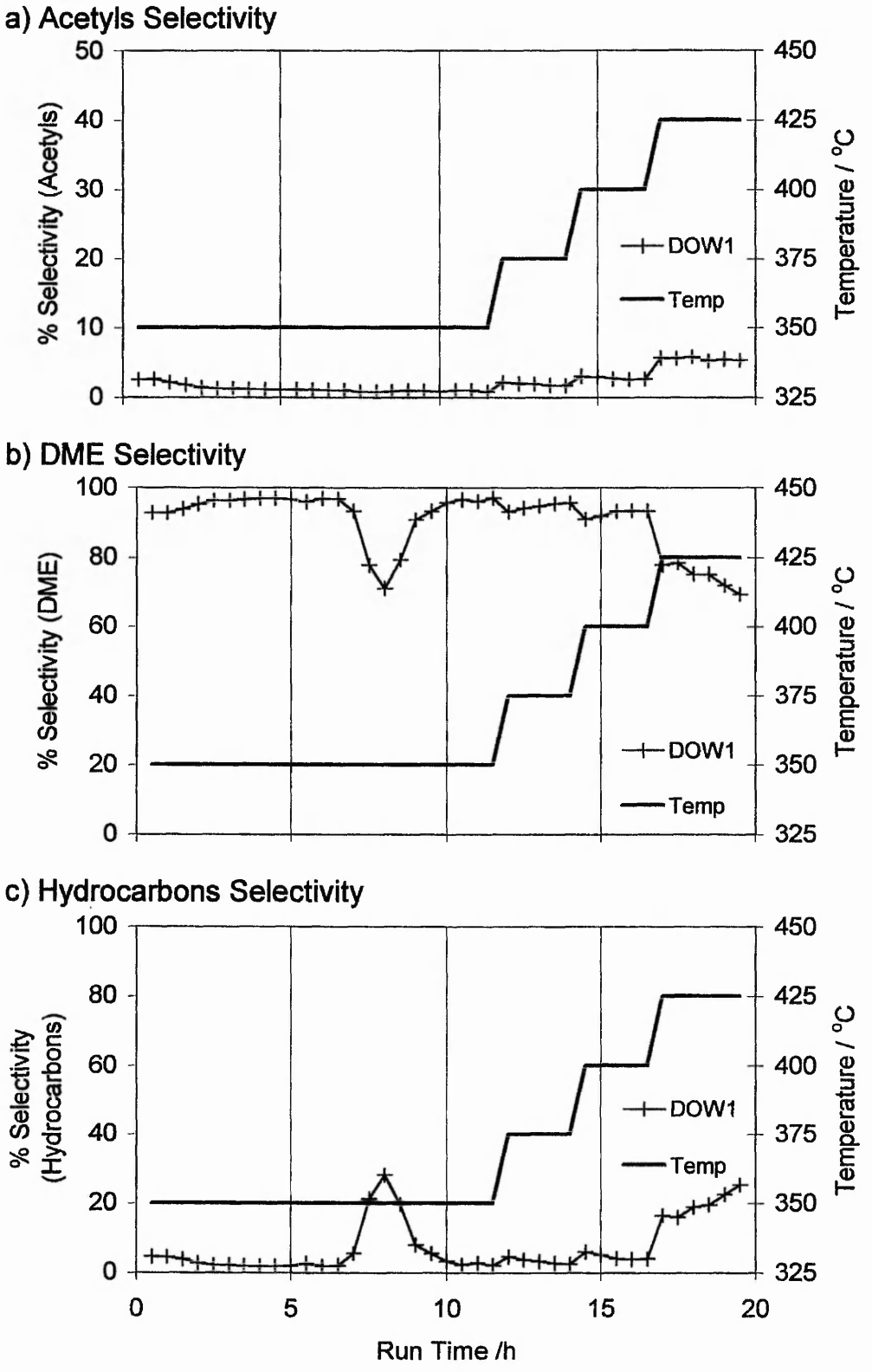

Figure 3.66 The Selectivity to (a) the Acetyls, (b) DME and (c) the Hydrocarbons for the sample prepared by the DOW dealumination patent

On raising the temperature by 25 °C, the conversion rises to 30% but quickly returns to 20%. A further 25 °C rise causes the conversion to return to 30%, which is retained whilst the temperature is held at 400 °C. The last temperature rise to 425 °C causes the conversion to jump to 60% from where it continues to rise. Due to the low level of conversion at 350 °C, the majority of the methanol detected is unconverted giving rise to the high carbon balances. There was no evidence of the pressure building up, due to the reactor becoming blocked by products. On increasing the temperature, each increase in conversion is accompanied by a similar decrease in the carbon balance, especially at 425 °C when a decrease from ~90% to 50% is observed.

The selectivities in Figure 3.66 show that the initial conversion of 50% corresponds to a combined selectivity, to the acetyls and hydrocarbons, of less than 10% being quickly replaced by DME as the conversion falls further. The initial selectivity to acetyls is seen in Figure 3.67 to be an insignificant space time yield of 0.02 g/g/h.

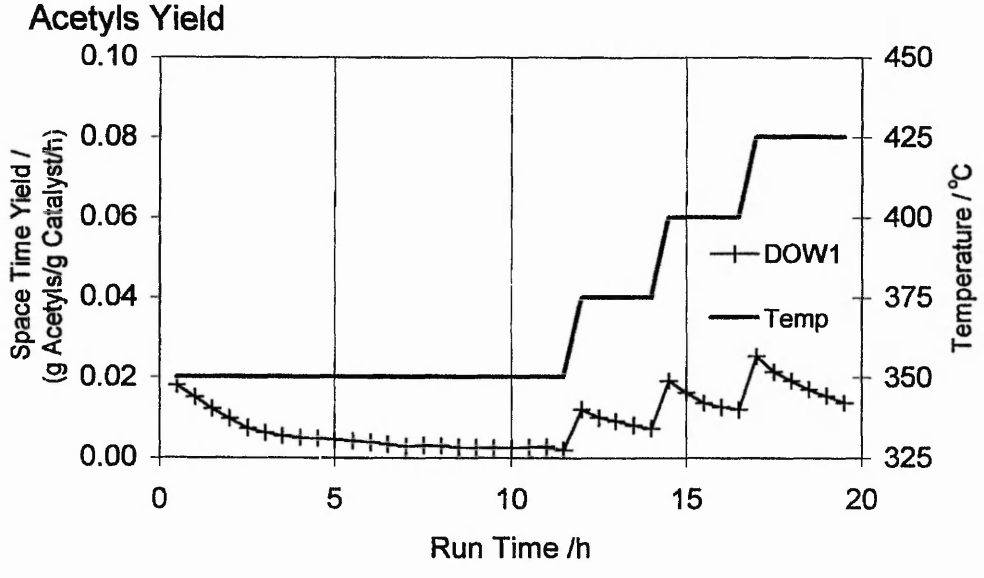

Figure 3.67 The Acetyls Space Time Yield for the sample prepared by the DOW dealumination patent

The dealumination of mordenite by all three procedures appears to remove the significant acetyls productivity of the proton form.

CHAPTER 4

THE MORDENITE FRAMEWORK

Introduction – Aims of the chapter

This chapter aims to interpret the results highlighted in Chapter 3, in terms of the structure and acidity of the mordenite catalysts used, additionally a mechanism for the carbonylation of methanol is postulated. Firstly, a summary of the results is listed followed by a detailed description of the mordenite structure.

Introduction – Summary of the reactor results

1) The sodium exchanged mordenite converts methanol only to dimethyl ether (DME).
2) The proton form of mordenite does convert methanol in the presence of carbon monoxide into acetyls. The higher framework concentration of aluminium, and hence the greater number of Bronsted acid sites, produces the lower acetyls yield.
3) Ion-exchanged copper increases the acetyls yield irrespective of the aluminium concentration. Additionally, the introduction of high concentrations of copper into the sodium form also produces a significant acetyls yield.
4) No acetyls are formed when the carbon monoxide is replaced by nitrogen.
5) The acetyls yield is prolonged by incremental temperature increases.
6) The increase in acetyls yield in the presence of copper is dependent on the preparation technique used.
7) Dealumination destroys the acetyls reactivity of the mordenite framework.

The framework structure of mordenite

The pore structure of mordenite (Structure Type Code MOR) is briefly described as a one-dimensional array of 12-T-ring channels [1], however its actual framework structure is more involved.

The straight 12-T-ring channels (free diameter 6.5 x 7.0 Å) run parallel to the *c*-direction in a 2 dimensional *fcc* array. A section in the *ab* plane in Figure 4. 1 shows that running parallel, between the adjacent 12-T-ring channels, there are elliptical 8-T-

ring cavities (free diameter 2.6 x 5.7 Å). Additionally, running in the *b*-direction only there are circular double 8-T-rings that connect the adjacent 12 & elliptical 8-T-ring channels together. Passage via these double 8-T-rings between adjacent 12-T-ring channels is severely restricted because of their staggered connection across the elliptical 8-T-ring cavity[2], as shown in Figure 4. 2.

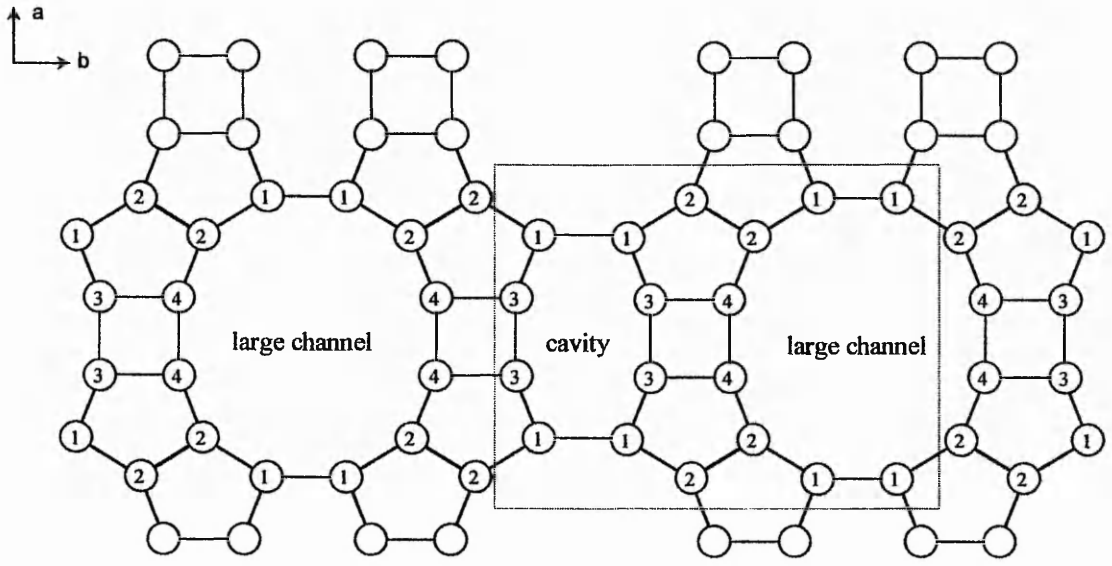

Figure 4. 1 A section through the mordenite framework in the *ab* plane showing the elliptical 8-T-ring cavity running parallel to the large 12-T-ring channels in the *c*-direction. The dashed outline highlights the cross section in *Figure 4. 3* below. Adapted from reference 2.

The unit cell formula for mordenite is $Na_x(Al_xSi_{48-x}O_{96}).24\ H_2O$. The 48 Si and aluminium atoms are located in 4 distinct crystallographic positions T1 – T4, as labelled 1 to 4 in the figure above, with populations of 16:16:8:8 per unit cell respectively. Positions T1 & T2 correspond to distorted 6-T-ring sheets that run parallel to the *bc* plane. These distorted hexagonal sheets are terminated either side the *bc* plane, by 5-T-rings containing the positions T3 & T4. The three dimensional framework is formed in the *a*-direction by two adjacent sheets being connected directly at the T3 & T4 positions, giving rise to single 4-T-rings[3]. The 6-T-rings form two sides of the 12-T-channels and the 4-T-rings form the sides of the linking circular double-8-T-ring channels.

Aluminium in the mordenite framework

From the results for the mordenite catalysts, it is evident that the carbonylation of methanol requires specific reaction sites to be present. The production of acetyls with the proton form indicates that Bronsted acid sites appear to be a necessity. However, the observed dependence on aluminium content indicates a more stringent requirement.
It has been determined experimentally[4,5] and theoretically that the maximum number of strong Bronsted acid sites in a zeolite framework corresponds to each aluminium present having a second coordination sphere solely of silicon. The maximum concentration is therefore dependent on the framework density and for mordenite corresponds to ~4 aluminium per unit cell or a SAR ~19. It may therefore be suggested that the carbonylation of methanol requires the strongly acidic sites.
Alternatively, rather than the acid strength being critical, the Bronsted acid sites may require a particular site geometry. The location of the bridged Bronsted acid Si-OH-Al group is dependent on the location of the aluminium within the framework. For aluminosilicate structures the average bond length, determined from single crystal XRD, for Al – O is 1.75 Å and that for the Si – O bond is 1.62 Å. The positioning of aluminium in the lattice can therefore modify the unit cell significantly enough to be detected via XRD. The determination of the 3 unit cell constants by XRD enables the location of aluminium to be distinguished. This has been carried out for a mordenite sample after several stages of aluminium removal.[6] It was concluded that aluminium was preferentially removed from T2 then from T1 and that removal from T4 & T3 resulted in collapse of the remaining framework. That work further concluded that, from the rate of change in the three unit cell constants, for a unit cell initially containing 8 aluminium atoms the population of T1:T2:T3&T4 was 4:2:2 respectively. Several authors[7] report the aluminium distribution for the mordenite framework to be T3>T1>T4>T2, which has been found to be independent of the mordenite's origin.
The 4-T-rings contain the sites T3 & T4, the preferential occupation of T3 by aluminium therefore results in a high probability of the 4-T-rings containing one aluminium, its Bronsted acid site being located in the restricted elliptical 8-T-ring. This is thought to arise because of the increased stability of the longer Al – O bond in the smaller ring, with Si preferring to occupy the uniform sheets of the 6-T-rings[3].
However, the most productive sample, of SAR 20, contains 4 aluminium per unit cell and even with one located within the elliptical channel there are certainly going to be

Bronsted acid sites also located at the T1 positions in the readily accessible large 12-T-ring channels. The even distribution of the aluminiums throughout the channel structure is assured by the further restrictions observed that, additional to Lowenstein's Rule,[7] the 4 and 5-T-rings can only contain one aluminium.

The cation locations in mordenite

In contrast to the Bronsted acid sites, the location of ion-exchanged metal cations is determined by the equilibrium between the negative electrostatic field of the framework and the positive charge on the cations.[2] Furthermore the degree of cation hydration, controlled by the history of thermal treatment, affects the extent of their interaction. Eight possible locations, occupied by both uni and divalent cations, within the mordenite framework have been determined by single crystal XRD and are shown, as compiled by W. Mortier, in Figure 4. 2.

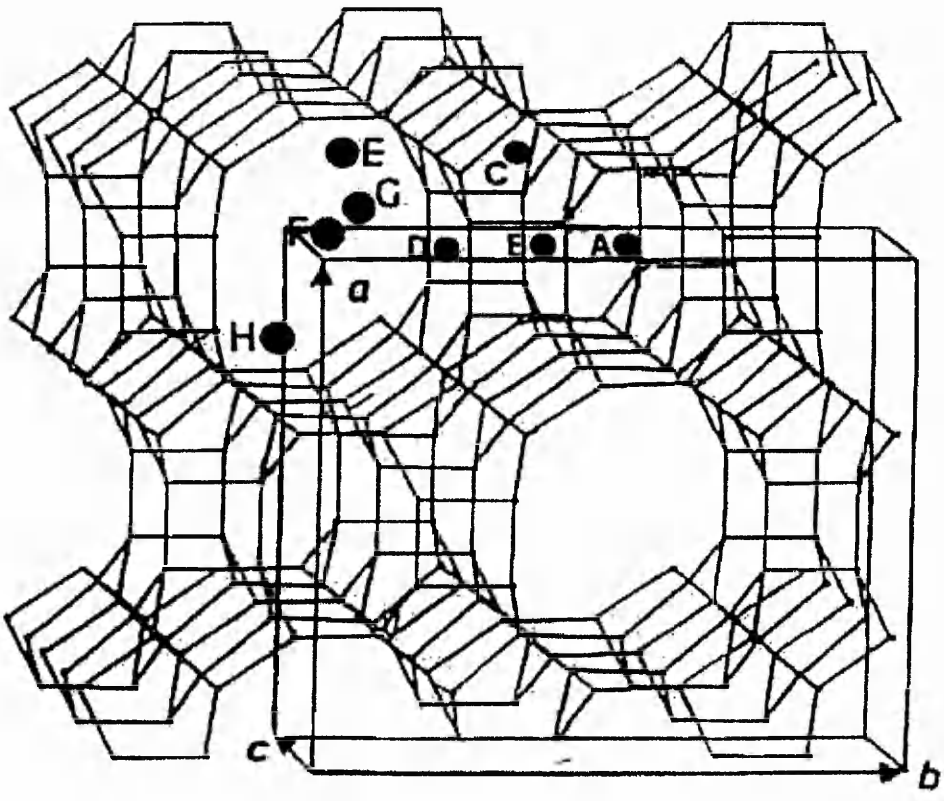

Figure 4. 2 The framework structure for the unit cell of mordenite showing the eight possible cation locations A – H (alternatively labelled I – VIII) as compiled by W. Mortier. Adapted from reference 2.

Site A is located in the elliptical 8-T-ring channel, centrally between two of the circular 8-T-ring channels that are staggered in the *b* direction. A cation in Site A is coordinated with six, virtually planar, framework oxygens of one elliptical 8-T-ring. Furthermore, a water molecule located in each Site B, located at the mouth of the circular 8-T-ring channel, if present, can increase the coordination of a Site A cation further to eight. Due to the short range cationic repulsion, Site B can not be occupied by a cation if Site A is already occupied. Site C is coordinated to four framework oxygens, all located to one side of the circular 8-T-ring channel, giving rise to a coordinatively unsaturated site. Site D, coordinated to six oxygens, is located centrally in the circular 8-T-ring at the mouth with the large 12-T-ring channel. Site E is coordinated to four framework oxygens of a 6-T-ring that forms the side of the large 12-T-ring channel. Site F is at the centre of the large 12-T-ring channel and tends to be occupied only when the cation is fully hydrated. Sites G & H are structurally equivalent to Site E but in symmetrically different locations with respect to the channel structure. The sites of further interest are shown in the cross section Figure 4. 3.

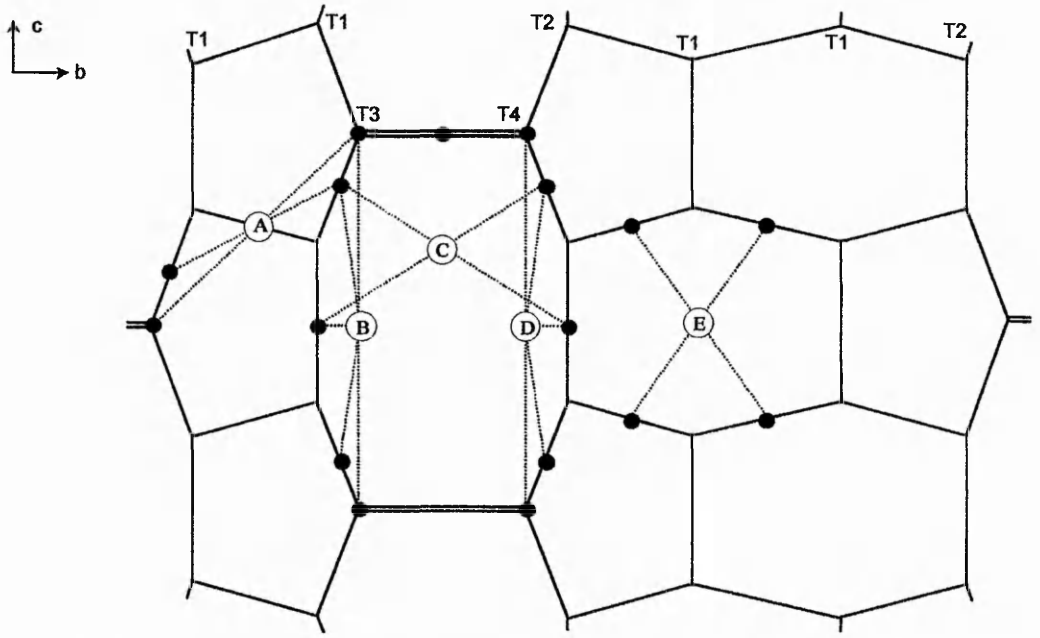

Figure 4. 3 A cross section, in the bc plane, of the mordenite framework including the Sites; A, C, D & E, determined by W. Mortier to be those occupied by calcium. Site B is only occupied by water stabilising Site A. The double lines indicate the 4-T-rings perpendicular to the page. The infilled circles show where possible the coordinated framework oxygens. Adapted from reference 3.

The framework has been cut down the *bc plane* through the T3-O-T3 and T4-O-T4 oxygens in the 4-T-rings, to show one side of the internal channel structure and the coordination of the cations with the framework oxygens.

To illustrate the effects due to the different levels of framework coordination, and the varying levels of cation hydration, the stability of the sites for a calcium containing mordenite was studied using single crystal XRD, by W. Mortier,[3] as a function of temperature. As the temperature increased, Site A became the more populated, because of its greater extent of coordination directly to the framework, and was therefore assumed to be the most stable. For the dehydrated calcium mordenite below 350°C the population was found to be in the order A > E > D > C with the stability of D & C reversing at higher temperatures. It is of interest to note that for the sample held at 350°C, in the presence of water, the sites A & D were the most stable due to water further increasing the degree of coordination of the cation.

The introduction of copper into the proton form by ion-exchange causes a significant increase in the initial acetyls yield. It is therefore of interest to consider the possible location of copper in the framework. A single crystal XRD[8] study, carried out at room temperature, reported two different copper sites for the hydrated form. The first site, in the centre of the elliptical 8-T-ring, equivalent to Site A, and including two waters in the adjacent Site B's. The second site, was located at the centre of the main 12-T-ring opposite the mouth of the circular 8-T-ring, octahedrally coordinated to six waters, equivalent to Site F. After increasing the temperature in stages and holding at 475°C for 36 hours under vacuum, only partial dehydration was achieved. For this crystal, returned to room temperature, three copper sites were determined. The first again equivalent to Site A and the coordinated waters at Site B accounted for those remaining after the high temperature treatment. The second site was coordinated to four oxygens of a 6-T-ring of the main channel equivalent to Site E. The least stable site was located on the side of the circular 8-T-ring channel equivalent to Site C.

These two single crystal XRD studies confirm that both the degree of framework coordination and the hydration of a cation influence its preferred location within the framework. Although calcium and copper are both divalent they occupy different sites apart from the preferred Site A. The high probability of Site A being occupied is consistent with the preferential occupation of T3 by aluminium.[2]

ESR[9,10] has confirmed the preferred location of copper in the Sites A and E for sodium mordenite ion-exchanged with copper. However, one ESR study[11] found the sites

occupied by copper, when introduced into a proton mordenite, to be different. It concluded that in the presence of water, copper prefers Site D coordinated to three water molecules. However, on heating the copper dehydrates and migrates to the more stable Site A. Although poorly occupied, an additional unidentified site was also present. The difference in initial cation location observed is accounted for by the extent of framework interaction exhibited by the counter cation present.

XRF analysis of the most productive Cu/H/MOR SE sample studied here indicates the copper loading to be 2.2 wt%. The aluminium content is 4.0 wt%, therefore the copper loading corresponds to 1 copper ion per 4 aluminium of one unit cell. Prepared by aqueous exchange, the divalent copper may initially be located in Site F, being stabilised by water of hydration. However, it can be assumed that after calcination at 500°C for four hours in static air the system will be, at least, partially dehydrated and the copper relocated into Site A, the most stable site for a dehydrated divalent cation. There is a large body of literature confirming that on calcination in air the copper[12] remains in oxidation state (+2). For every divalent cation introduced, two protons are removed. The electrostatic interactions ensure that the two protons removed should be those closest to the position of the divalent cation. Considering the high proportion of aluminium at T3, it is most probable that the protons are removed from two neighbouring 4-T-rings across an elliptical 8-T-ring channel, rather than two unequivalent protons being removed. The overall result of calcination is copper in oxidation state (+2) being concentrated in the elliptical 8-T-rings, with the Bronsted acid sites in the large 12-T-rings, at the mouths of the circular 8-T-rings.

The active site for carbonylation

The further high temperature treatment in carbon monoxide, prior to the introduction of methanol, promotes the initial acetyls selectivity over that to hydrocarbons for the catalyst Cu/H/MOR SE. As already stated, in the absence of copper, Bronsted acid sites, rather than sodium Lewis sites, promote the carbonylation of methanol. However, all the protonated catalysts were pretreated at 500°C under an atmosphere of carbon monoxide, this may cause the partial dehydroxylation of the framework to create framework Lewis sites. If these were the only sites required then productivity would be proportional to the aluminium content, which is not observed. Therefore, Bronsted acid

sites must still be present and required for the carbonylation of methanol. Additionally, in the presence of carbon monoxide, especially at 500°C, copper (II) cations should be reduced to copper (I), coupled with the formation of carbon dioxide.

$$Cu^{2+}2\,[Si\text{-}O\text{-}Al]^{-} + CO = Cu^{+}[Si\text{-}O\text{-}Al]^{-} + [Si\text{-} \text{-}Al] + CO_2$$

Alternatively, reduction may occur by the formation of a copper carbonyl bond.

$$Cu^{2+}2\,[Si\text{-}O\text{-}Al]^{-} + CO = OC\text{-}Cu^{+}[Si\text{-}O\text{-}Al]^{-} + [Si\text{-}O\text{-}Al]^{-}$$

By either mechanism, it is expected that copper (I) would not migrate from the stable Site A position. There is uncertainty in the literature[13] as to the exact structure around the second aluminium, whether it forms an extraframework species e.g. $(AlO)^{+}$ or remains as a 3 coordinate framework Lewis site. Under these reaction conditions, it is suggested that extraframework species would be favoured to allow the restabilisation of the uncoordinated silicon by the formation of a bridging Si – O – Si bond[14]. However, the removal of aluminium from a 4-T-ring is considered to be unfavourable, leading to the destruction of the framework. It is proposed that one of the remaining protons will migrate from the 12-T-channel to retain the aluminium, and also a Bronsted acid site, within the 4-T-ring and therefore create the extraframework species in the 12-T-channel. The creation of any positively charged extraframework species requires the presence of a neighbouring anionic framework site created during dehydroxylation. For the most productive catalyst containing four aluminiums and one copper per unit cell, the two active sites are proposed to be (i) the copper (I) cation close to a Bronsted acid site in the 8-T-channels, and (ii) an extraframework species coupled with an anionic framework site located in the 12-T-ring channels.

The formation of DME over sodium mordenite indicates that, under the reaction conditions adopted, methanol condenses to its ether in the presence of sodium Lewis acid sites. The constant formation of DME for this catalyst further indicates that the sites responsible are not modified in the presence of water. Therefore, framework Lewis acid sites are not responsible or present, as they would be re-hydroxylated to create Bronsted acid sites capable of producing hydrocarbons. However, extraframework sites are irreversibly formed, even in the presence of water,[13] and could give rise to the

formation of DME. The low level of methanol conversion over the sodium system may indicate that only a low concentration of the required sites is present.

The literature of methanol to gasoline chemistry[15] reports that methanol readily converts to DME and that the two compounds can be considered as equivalent reagents. Therefore the high DME selectivity observed, after only a few hours of reaction in most cases, suggests that one of the possible active sites for DME, proposed to be the extraframework Lewis acid sites, is not the site singularly responsible for the formation of the acetyls. Furthermore, it is proposed that the sites responsible for DME are present at the start, with the DME initially formed being subsequently converted into the acetyls.

The sequential conversion of methanol to acetyls via DME is supported by the initially observed preferential formation of acetic acid over that of methyl acetate in the case of Cu/H/MOR SE. The condensation of methanol to the ether provides the required water for the formation of the acid, and the low concentration of detected DME indicates its further conversion. The conversion of methanol is constantly high (greater than 80%), and therefore it is present only in a low final concentration throughout the reaction time. As the active sites responsible for carbonylation are deactivated with time, the further conversion of DME starts to decline and consequently its concentration increases. The observed increase in the formation of methyl acetate indicates the combined concentration of DME and methanol becomes greater than that of the water. Furthermore, as the concentration of DME and methanol increases, acetic acid is more likely to interact with either them, causing the facile conversion under these conditions, of acetic acid to methyl acetate with the formation of either water or methanol respectively.

With the carbon monoxide replaced by nitrogen, the major products are DME and the hydrocarbons. The production of hydrocarbons supports the presence of Bronsted acids. The first step involves interaction of methanol with the Bronsted acid site. The first experimentally observable intermediate, by FTIR[16] and C^{13} MASNMR[17], is the silyl methyl ether resulting from the condensation of methanol.

$$CH_3OH + [Si\text{-}OH\text{-}Al] = [Si\text{-}OCH_3\text{-}Al] + H_2O$$

The stability and the degree of charge separation, of the intermediate, have been widely debated[18], but it is assumed to be reactive under the current reaction conditions. The

strong Bronsted acid sites are postulated to introduce a high degree of charge separation. Further reaction of the CH_3^+ groups occurs with methanol or DME, and by a number of postulated intermediates forms the first C – C bond, giving rise to small unsaturated hydrocarbons or aromatic species. Once different cationic hydrocarbon species form there are a whole host of possible secondary reactions. Aided by the strongly Bronsted acidic framework, the continued formation of a wide range of hydrocarbons occurs. Some products are unable to diffuse out of the crystallite and are the beginnings of the coke that causes the blockage of the pores and eventually the reactor. Even in the presence of large amounts of entrapped coke, the mordenite framework remains active towards the formation of acetyls after 20 hours on-line, which suggests that a significant proportion of the active sites are readily maintained and remain accessible within the framework, as was observed in the previous work[19].

The weaker Bronsted acid sites give rise to a covalent intermediate. The interaction with a second methanol gives rise to a second mechanism for the formation of DME, as supported by the observation that the frameworks of higher aluminium content produce an overall lower methanol conversion but still a high selectivity to DME.

$$CH_3OH + [Si\text{-}OCH_3\text{-}Al] = CH_3OCH_3 + [Si\text{-}OH\text{-}Al]$$

Methanol and DME are again considered to be equivalent, in the presence of nitrogen, with DME being formed throughout, as is evident from the slow rise in DME with reaction time resulting from the decrease in the formation of hydrocarbons.

The formation of the hydrocarbon byproducts, in the presence of carbon monoxide, is assumed to occur via a competing mechanism that is also promoted by the presence of strong Bronsted acid sites, as evident from the lower selectivity to hydrocarbons for the case of higher aluminium content.

Further insight into the preferred active site structure is given by the reactivity of the catalysts prepared from the different cation precursors. As previously discussed, the initial location of copper introduced by ion-exchange from aqueous solution is determined by the counter cation present and during calcination, and hence dehydration, the cations are presumed to re-establish equilibrium. In both cases, the divalent copper cations preferentially occupy Site A, with it having the strongest interaction with the framework.

However, the initially surprising finding, is that more than DME is formed in the presence together of both sodium and copper. The high level of methanol conversion attained strongly contrasts that for the sample containing solely sodium. It is therefore proposed[20], from the literature, that during the aqueous phase ion-exchange, the waters of hydration are able to create Bronsted acid sites, most probably during the calcination period. Initially divalent copper requires two framework aluminium sites to retain neutrality. For the sample with over five aluminiums per unit cell (SAR 12.8), the higher loading corresponds to divalent copper occupying two thirds of the framework aluminium, see Table 4. 1. It is expected, under this high level of exchange, that the charge balancing required will destabilise the divalent cations and that in the presence of water, copper (II) will prefer to form[21] either the species $[CuOH]^{+}$ and one Bronsted acid site, or a bridging oxygen species $[CuOCu]^{2+}$ and two Bronsted acid sites. Both oxygen containing species will readily be reduced, with the formation of carbon dioxide, during the carbon monoxide pretreatment. Further stability, is expected to arise during the dynamic exchange process, from the complete removal of the remaining sodium cations in favour of the formation of the localised Bronsted acid sites, especially in the solution of pH 4 - 5. This interpretation is supported by the reactivity observed for the catalyst with a low copper loading of 0.18 aluminium per unit cell. Similar levels of methanol conversion and selectivity to hydrocarbons indicate the presence of Bronsted acid sites introduced during the exchange procedure. The lower loading of copper does not force the formation of the oxygen containing species, especially the $[CuOCu]^{2+}$, but retains the hydrated copper (II) cation, that on calcination locates preferentially in Site A. On reduction the extraframework aluminium should be formed. The low acetyls yield corresponds to the low copper content being in the presence of a high concentration of Bronsted acid sites.

For the two samples of framework (SAR 12.8) containing very similar copper loadings, initially in the sodium and proton forms, the final catalysts should be equivalent in both structure and productivity if the above deductions are correct.

It is not apparent why the catalysts originating from the sodium form give rise to a higher selectivity to hydrocarbons, especially considering that in its proton form, a very low selectivity to hydrocarbons is observed. However, a similar reactivity was observed in the first reported work[22] of K. Fujimoto et al.

SAMPLE	SAR (XRF)	Al /Unit Cell	Cu /Unit Cell	Cu / Al_2
Cu/Na/MOR (0.9) SAR 12.8	14.03	5.99	0.54	0.18
Cu/Na/MOR (3.4) SAR 12.8	14.93	5.67	1.87	0.66
Cu/H/MOR (2.2) SAR 20	18.59	4.66	1.10	0.48

Table 4. 1 Summary of the elemental compositions, determined by XRF characterisation, for the copper ion-exchanged mordenite samples.

It is suggested that the higher concentration of strong Bronsted acid sites are promoted towards the formation of hydrocarbons when only in the presence of the copper in oxidation state (+1). Whereas, a few strong Bronsted acid sites in the presence of copper in oxidation state (+1) and the previously formed extraframework Lewis acid sites promote the carbonylation products. It is therefore suggested that a multifunctional active site is required, rather than one specific acid centre. But it has to be remembered that the proton form is also able to produce the acetyls, and that the framework of lower aluminium concentration favours it. These pieces of evidence together, again suggest that isolated strong Bronsted acid sites in the presence of extraframework Lewis acid sites favour carbonylation, and are further promoted by copper (I) cations. This promotional effect is most probably due to the Lewis centres controlling the approach of methanol, or DME, by attracting the oxygen lone pairs.

In the presence of isolated and therefore strong Bronsted acid sites, methanol forms hydrocarbons with nitrogen as the inert carrier. However, the same site concentration in the presence of carbon monoxide produces the acetyls. The evidence presented above suggests that acetyls are promoted by the presence of the extraframework aluminium sites. The formation of these by dehydroxylation occurs both in the calcination stage and during the high temperature carbon monoxide pretreatment, especially when ion-exchanged copper is being reduced. Copper (I) in the presence of the extraframework sites further promotes the acetyls formation because of its strong affinity for carbon monoxide[23]. Furthermore, there is evidence reported of Bronsted sites regenerating copper (I) from metallic copper.

Once the CH_3^+ group has formed from either methanol or DME it is proposed that in the presence of excess carbon monoxide, aided by the presence of Lewis acid sites, an insertion mechanism occurs with the resulting formation of the CH_3CO^+ group. It is thought that the presence of Lewis acid sites is able to concentrate the carbon monoxide around the CH_3^+ group preventing the onset of hydrocarbon formation. Copper (I) is known to form carbonyl complexes[24].

It has also been determined[13] that methanol interacts with the ion-exchanged copper of the zeolite. Furthermore, the location of the copper determined both the number and orientation of the methanol molecules adsorbed. Under the reaction conditions adopted here, it is expected that any adsorption complex formed, would be short lived, but indicates that copper may control the structure of the intermediates and transition states involved.

The mechanism for methanol carbonylation

The following mechanism for the formation of the acetyls is proposed. Methanol, or more probably DME, reacts with the isolated strong Bronsted acid group to produce the CH_3^+ group. In the excess carbon monoxide present, the relatively stable CH_3CO^+ group forms by insertion, which then in the presence of water forms acetic acid and restores the acid site. In the presence of methanol, or DME, methyl acetate is the preferred product. Additionally, with DME the CH_3^+ group is reformed directly, rather than the Bronsted acid group.

$$CH_3OH + [Si\text{-}OH\text{-}Al] = [Si\text{-}OCH_3\text{-}Al] + H_2O$$

$$[Si\text{-}OCH_3\text{-}Al] + CO = [Si\text{-}O(COCH_3)\text{-}Al]$$

$$[Si\text{-}O(COCH_3)\text{-}Al] + H_2O = CH_3COOH + [Si\text{-}OH\text{-}Al]$$

$$[Si\text{-}O(COCH_3)\text{-}Al] + CH_3OH = CH_3COOCH_3 + [Si\text{-}OH\text{-}Al]$$

$$[Si\text{-}O(COCH_3)\text{-}Al] + CH_3OCH_3 = CH_3COOCH_3 + [Si\text{-}OCH_3\text{-}Al]$$

This mechanism only requires the presence of Bronsted acid sites. It is proposed that the role of both the copper and the extraframework aluminium sites is to aid in orientating

the reagents at the Bronsted site and in removing the products, avoiding the possibility of secondary reactions.

The specific requirement for ion-exchanged copper

The initial acetyls selectivity is enhanced significantly in the presence of ion-exchanged copper. The process of ion-exchange introduces copper cations into the zeolite channel structure that are capable of interacting with the remaining Bronsted acid sites, as discussed earlier. The slightly acidic (pH 5 - 6) copper nitrate solution used for the ion-exchange preparation retains the hydrated cations in solution[25]. Whereas the drop wise addition of ammonia solution causes the immediate precipitation of a polymeric $Cu(OH)_2$ gelatinous precipitate[26]. The insoluble precipitate deposits onto the external surface of the zeolite crystallites causing the light blue colouration observed and the complete removal of hydrated copper from the solution. Calcination in static air dehydrates the precipitate with the possible formation of surface copper oxide clusters and causes the colour change to a white/grey. The carbon monoxide pretreatment may cause reduction of the deposited copper oxide species with the formation of carbon dioxide. Compared to the proton form there is no significant promotional effect on the initial acetyls yields for the copper loaded catalysts prepared at higher pH. It is therefore proposed that virtually no ion-exchange has taken place, but that the majority of copper is concentrated at the near surface. However, the stable acetyls yield, after 10 hours reaction, is increased significantly by copper loadings of 1.27 wt% (HP3) and greater. It is postulated therefore that the deposited copper reduces any secondary reactions, especially of the exiting acetyls, to keep the channel mouths free of coke.

Impregnation by incipient wetness allows a minority of the copper to ion-exchange into the channels as shown by the promotion of the initial acetyls yield. The maintained stable yield, similar to that observed for the high pH preparations, suggests that the majority of the copper is deposited at the near surface of the mordenite.

The 1M copper solution introduces more copper than the 0.3M solution and reduces the Bronsted acid site concentration too far.

The greater degree of dehydroxylation and hence the significant loss of Bronsted acid sites that occurs during the high temperature solid state exchange account for the reduced acetyls yield observed.

Comparison with the previous work

As outlined in Chapter 1, this project is a continuation of work that screened a large number of different materials[19]. The reaction conditions used here are comparable to the prior ones, apart from the use of a smaller sample giving rise to a higher Gas Hourly Space Velocity. There are significant differences in the observed reactivities. The prior work exhibits three clear regions of different reactivities, (I) MTG, (II) Acetyls and (III) DME, whereas here only regions (II) & (III) can be distingusihed. No carbon monoxide pretreatment at 500°C was used routinely in the prior work, but it was reported to increase the acetyls productivity. It is proposed from comparing the results that the Bronsted acid site concentration is reduced by this pretreatment. Supported by the formation of acetyls being delayed in the run where no pretreatment was carried out. It can also be concluded that the MTG and acetyls mechanisms are in direct competition. The higher concentration of Bronsted acid sites in the prior work initially promotes the hydrocarbon formation, especially with the longer residence time in the catalyst bed. Once the concentration of sites is reduced by coke formation, the remaining sites are able to form acetyls, unhindered by secondary reactions.

The copper loading by ion-exchange (3.4 wt%) of the prior work is significantly greater than here (2.2 wt%). The copper particulates observed in the prior work by XPS of the active sample suggests that the higher loading of ion-exchanged copper may be detrimental for acetyls productivity. Too many ion-exchanged coppers reduce the Bronsted acid concentration too far. The maintained yield reported there was 0.3 g/g/h whilst here an initial peak of 2.0 g/g/h falling to 0.5 g/g/h has been observed. The prior work reports equivalent yields were observed for samples prepared by both ion-exchange and impregnation. Impregnation introduces the copper particulates whilst retaining the active proton sites within the channel structure producing an equivalent sample. Optimum productivity relies on the maximum number of Bronsted acid sites being isolated from each other by neighbouring Lewis acid sites, preferentially of copper species but alternatively extraframework aluminium species.

References

1. Kuroda, Y., Kotani, A., Uemura, A., Yoshikawa, Y., Morimoto, T., *J. Chem. Soc. Chem. Commun.*, 1989, 1631-1632.
2. Tyburce, B., Kappenstein, C., Cartraud, P., Garnier, E., *J. Chem. Soc. Faraday Trans.*, 1991, **87(17)**, 2849-2853.
3. Mortier, W.J., *J. Phys. Chem.*, 1977, **81**(13), 1334-1338.
4. Stach, H., Janchen, J., *Zeolites*, 1992, **12**, 152-154.
5. Trung Tran, M., Gnep, N.S., Szabo, G., Guisnet, M., *J. Catal.*, 1998, **174**, 185-190.
6. Olsson, R.W., Rollmann, L.D., *Inorg. Chem.*, 1977, **16(3)**, 651-654.
7. Takaishi, T., Kato, M., Itabashi, K., *Zeolites*, 1995, **15**, 21-32.
8. Attfield, M.P., Weigel, S.J., Cheetham, A.K. *J. Catal.*, 1997, **170**, 227-235.
9. De Tavernier, S., Schoonheydt, R.A., *Zeolites.*, 1991, **11**, 155-163.
10. Oliva, C., Selli, E., Ponti, A., Correale, L., Solinas, V., Rombi, E., Monaci, R., Forni, L., *J. Chem. Soc. Faraday Trans.*, 1997, **93(15)**, 2603-2608.
11. Sass, C.E., Kevan, L., *J. Phys. Chem.*, 1989, **93**, 4669-4671.
12. Kucherov, A.V., Kucherova, T.N., Slinkin, A.A., *Catal. Lett.*, 1991, **10**, 289-296.
13. Jacobs, P.A., Beyer, H.K., *J. Phys. Chem.*, 1979. **83(9)**, 1174-1177.
14. Chen, N.Y., Smith, F.A., *Inorg. Chem.*, 1976, **15(2)**, 295-297.
15. Stocker, M., *Microporous Mesoporous Mat.*, 1999, **29**, 3-48.
16. Jiang, X.Z., *J. Molec. Cat. A-Chem.*, 1997, **121**, 63-68.
17 Ivanova, I.I., Corma, A., *J. Phys. Chem. B.*, 1997, **101**, 547-551.
18. Stich, I., Gale, J.D., Terakura, K., Payne, M.C., *J. Am. Chem. Soc.*, 1999, **121**, 3292-3302.
19. Ellis, B., Howard, M.J., Joyner, R.W., Reddy, K.N., Padley, M.B., Smith, W.J., *Stud. Surf. Sci. Catal.*, 1996, **101**, 771-779.
20. Connerton, J., Joyner, R.W., Padley, M.B., *J. Chem. Soc. Faraday Trans.*, 1995, **91(12)**, 1841-1844.
21. Iwamoto, M., Hoshino, Y., *Inorg. Chem.*, 1996, **35**, 6918-6921.
22. Fujimoto, K., Shikada, T., Omata, K., Tominaga, H., *Chem. Lett.*, 1984, 2047-2050.
23. Sarkany, J., d'Itri, J.L, Sachtler, M.H., *Catal. Lett.*, 1992, **16**, 241-249
24. Souma, Y., Iyoda, J., Sano, H., *Inorg. Chem.*, 1976, **15(4)**, 968-970
25. Blint, R.J., *J. Phys. Chem.*, 1996, **100**, 19518-19524.
26. Valyon, J., Hall, W.K., *Catal. Lett.*, 1993, **19**, 109-119.

CHAPTER 5

THE EFFECT OF THE FRAMEWORK

Introduction – Aims of the chapter

The mordenite framework, as detailed in Chapters 3&4, has been found to be active for the carbonylation of methanol to the acetyls, acetic acid and methyl acetate, under the reaction conditions adopted. Furthermore, the performance of the mordenite framework is improved by the presence of copper, especially when it is introduced by the ion-exchange procedure. To determine whether this reactivity is unique to mordenite, several other frameworks have been tested using the experimental conditions summarised in Table 2.1.

The frameworks, indicated in Table 5.1, vary in both their pore size and the dimensionality of their main channel. Only ZSM-5 has been previously studied in this reaction (see Chapter 1).

Framework Name	Channel Structure	Channel Diameter /Å	SiO_2/Al_2O_3 (SAR)
Theta-1	1 Dimensional 10-T-Ring	4.4 x 5.5 Straight	54.5
ZSM-5	3 Dimensional 10-T-Ring	5.6 x 5.4 Straight 5.5 x 5.1 Sinusoidal	50.0
Mordenite	1 Dimensional 12-T-Ring Side Pockets 8-T-Ring	6.5 x 7.0 Straight	20.0
Beta	3 Dimensional 12-T-Ring	7.6 x 6.4 Straight 5.5 x 5.5 Sinusoidal	25.0
MCM-22	Isolated 10 & 12-T-Ring	7.1 Ø x 18.21 Supercages	35.7

Table 5.1 Summary of the physical characteristics for the frameworks tested

Each framework structure is briefly described and the performance of the proton form is directly compared with the H/MOR (SAR20) sample. The effect of ion-exchanged copper is then compared to that for the respective proton form. One of the frameworks, Theta-1, is then studied further by varying the conditions to optimise its performance.

H/Theta-1

The zeolite Theta-1 was the first unidimensional zeolite structure to be synthesised[1]. It is the parent of the structure type code TON, to which there have been subsequent members assigned; Nu-10, KZ-2, ISI-1, ZSM-22. The Theta-1 structure illustrated in Figure 5.1 consists of 10-T ring channels, of elliptical cross section 4.4 x 5.5 Å, running parallel with the *c*-direction. Theta-1 is synthesised directly as a high Si framework as for the sample studied with a SAR 54.5, as measured by x-ray fluorescence.
Theta-1 was chosen for this work as it consists of small non-intersecting channels of a size similar to the side pockets of the mordenite framework.

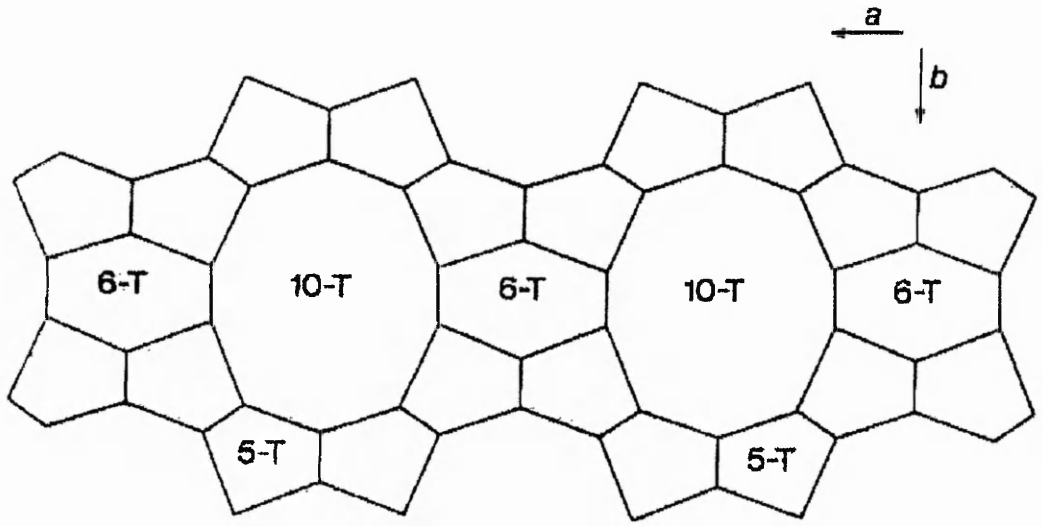

Figure 5.1 Projection in the a-b plane of Theta-1 to show the elliptical 10-T ring channels running parallel (into the page) to the c direction. Reproduced from reference [1].

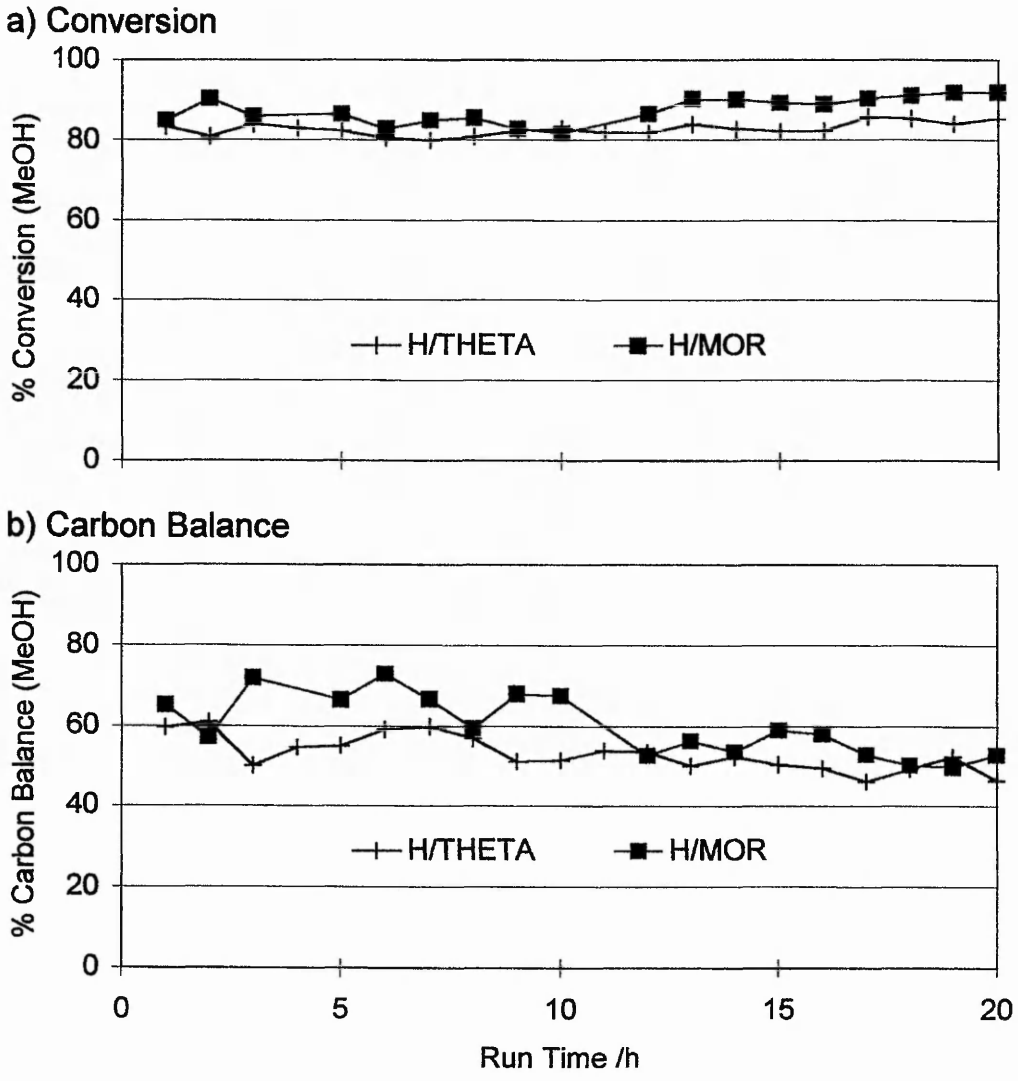

Figure 5.2 Comparison for H/Theta-1 of (a) the Conversion and (b) the Carbon balance with H/MOR SAR20

Under the standard reaction conditions, Figure 5.2a shows that the level of conversion of methanol is similar for both the H/Theta-1 and H/MOR, it being constantly above 80% throughout the 20 hours of reaction. The general trend in the carbon balance for H/Theta-1, as shown in Figure 5.2b, is also very similar to that for H/MOR, initially 60% for 7 hours before falling to 50%. There was no evidence of the reactor being blocked by heavy hydrocarbons, but the spent catalyst was coked.

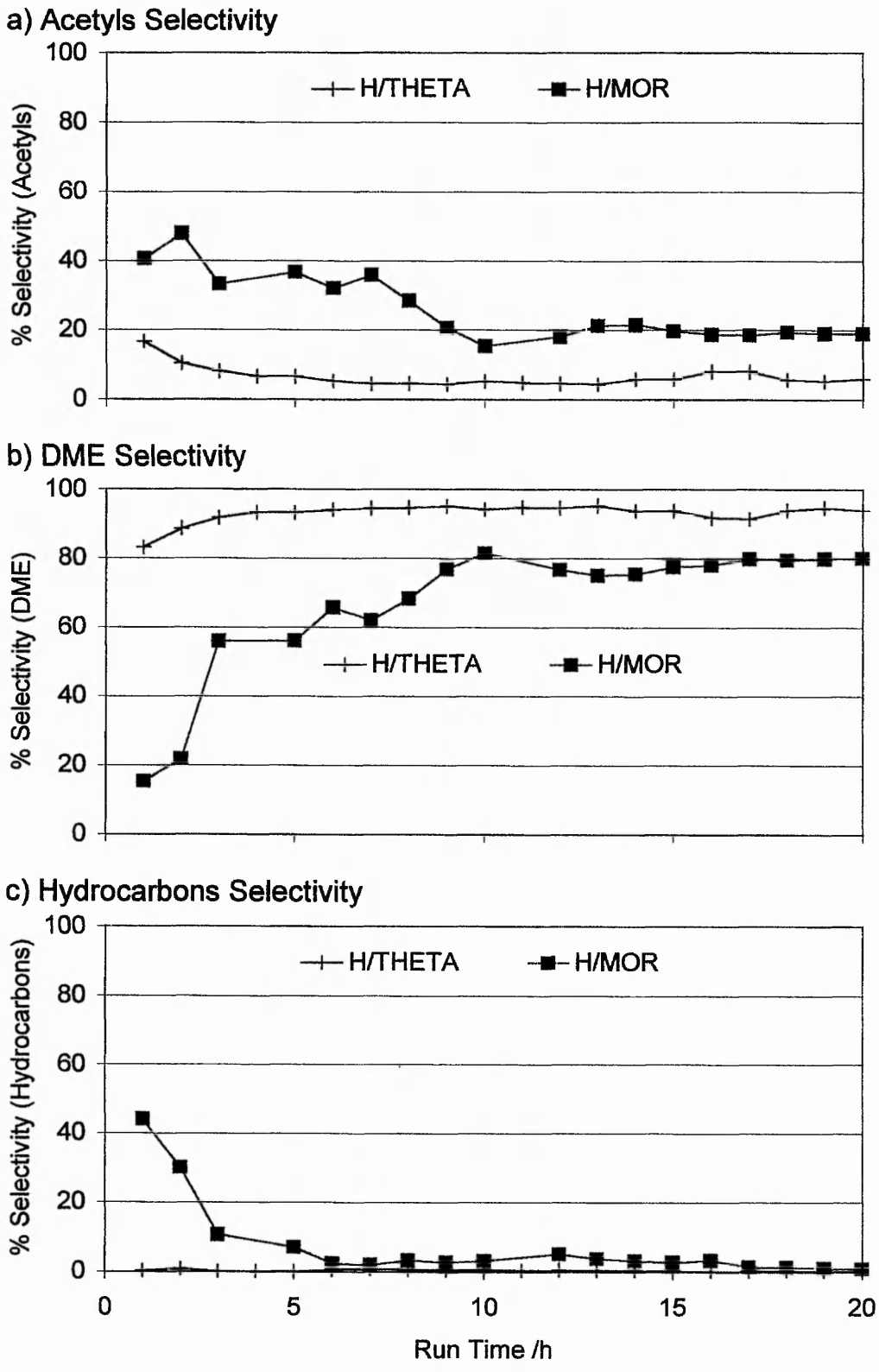

Figure 5.3 Comparison for H/Theta-1 of the Selectivities to (a) Acetyls (b) DME and (c) Hydrocarbons with H/MOR SAR20

The selectivities are shown in Figure 5.3a-c. For the high level of conversion observed, the acetyls yield is low, initially 20% it quickly falls to less than 10% compared to H/MOR being initially at 40% and falling to a stable 20%. DME is seen to dominate throughout the reaction, initially 80% and rising to a stable 95% compared to that for H/MOR being initially zero and rising to 80%. The selectivity to hydrocarbons is virtually zero throughout the reaction in contrast to that for H/MOR. The low acetyls selectivity corresponds to an acetyls space time yield of of 0.1 g/g/h after an initial high of 0.3 g/g/h yield. The low acetyls yield consists entirely of methyl acetate with recyclable DME as the only other product.

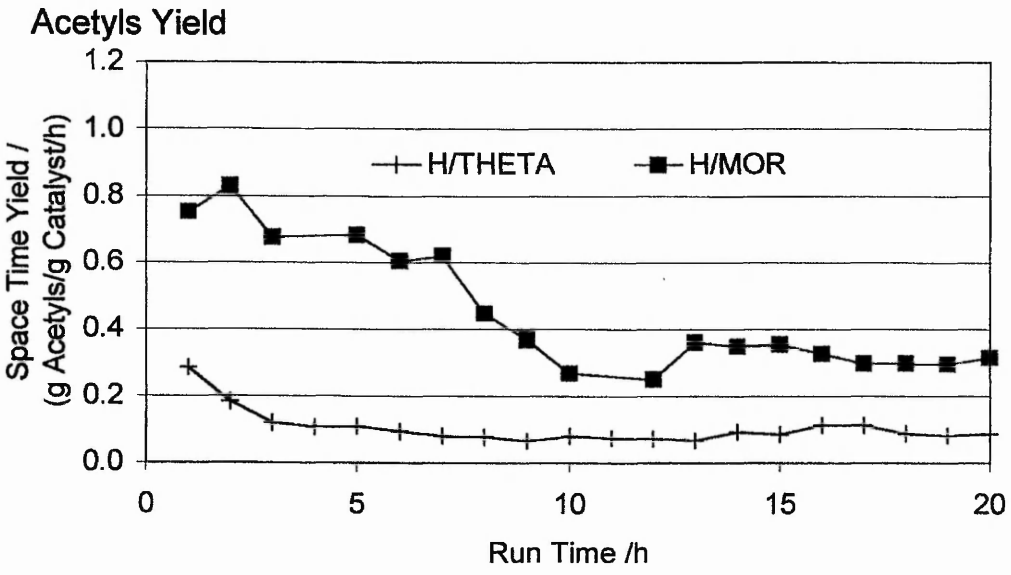

Figure 5.4 Comparison for H/Theta-1 of the Acetyls Space Time Yield with H/MOR SAR20

H/ZSM-5

ZSM-5 is a well known medium pore zeolite[2] and has been assigned the Structure Type Code MFI. It can be synthesised directly over a large range of SAR. The ZSM-5 structure, similar to mordenite, is a member of the pentasil family built from 5-1 secondary building units. The pore structure, as shown in Figure 5.5 below, is three dimensional with intersecting straight and sinusoidal channels, both constructed from 10-T rings with dimensions of 5.6 x 5.4Å and 5.5 x 5.1Å respectively[3]. The channels formed are similar to those in Theta-1 but the three dimensionality of the structure additionally gives rise to larger voids at the channel intersections.

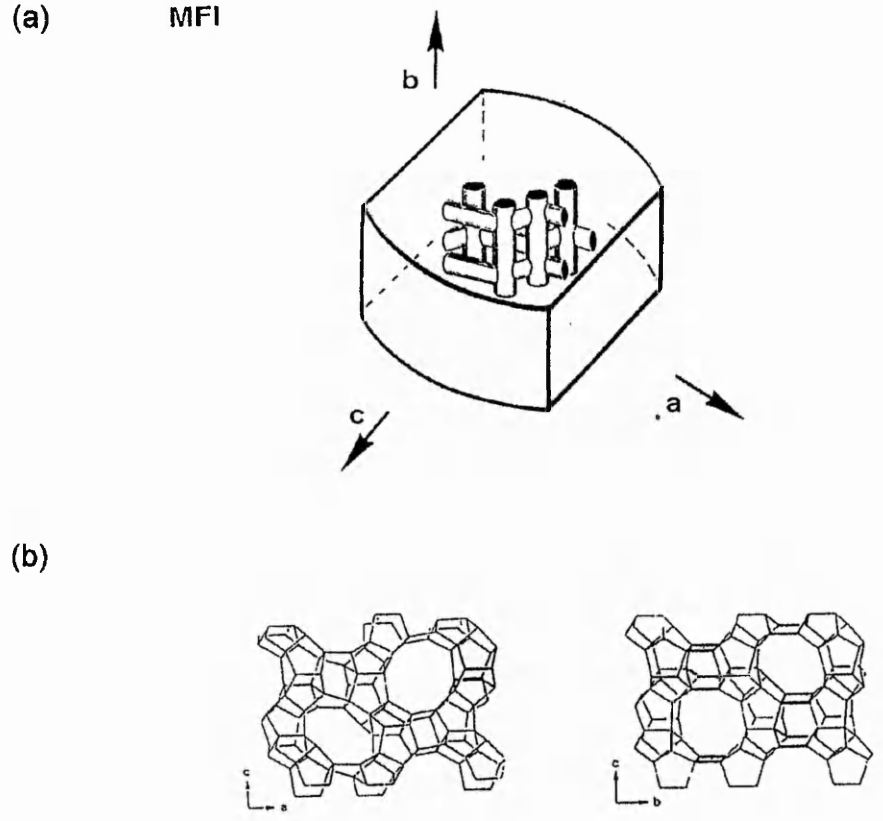

Figure 5.5(a) The idealised ZSM-5 (MFI) structure showing the straight channels parallel to the b-direction with the sinusoidal ones in the a-c plane. (b) Detailed sections in the a-c and b-c planes showing the structures of the two types of pore. Reproduced from reference [3].

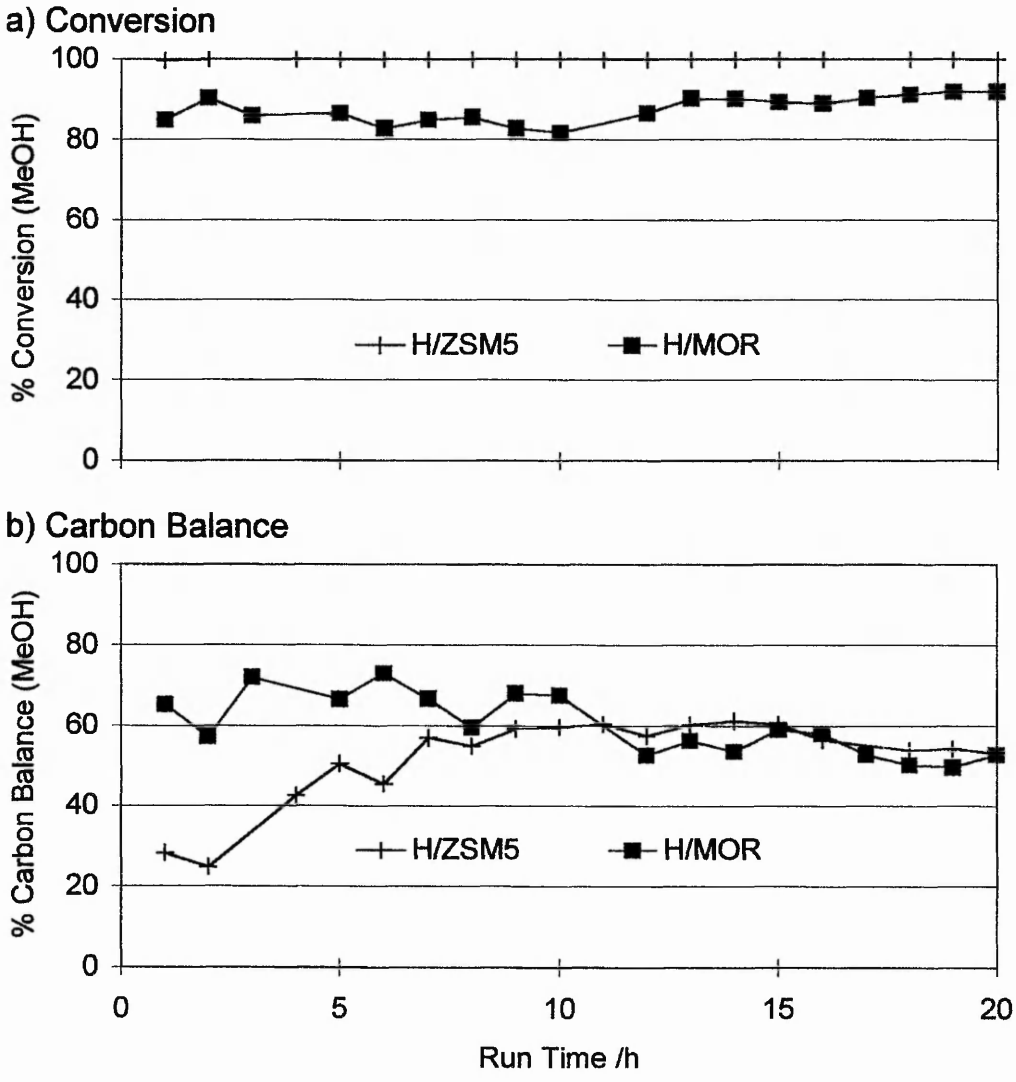

Figure 5.6 Comparison for H/ZSM-5 of (a) the Conversion and (b) the Carbon balance with H/MOR SAR20

The level of conversion for H/ZSM-5, seen in Figure 5.6a, is 100% throughout the reaction time. Figure 5.7a-c show that virtually all the methanol is converted to hydrocarbons rather than to acetyls or DME. On comparing Figure 5.3a & Figure 5.7a it can be seen that the selectivity to acetyls is virtually the same, for both Theta-1 and ZSM-5, after accounting for the 20% difference in conversion. However, ZSM-5 converts the remaining methanol to hydrocarbon by-products whereas Theta-1 only forms recyclable DME.

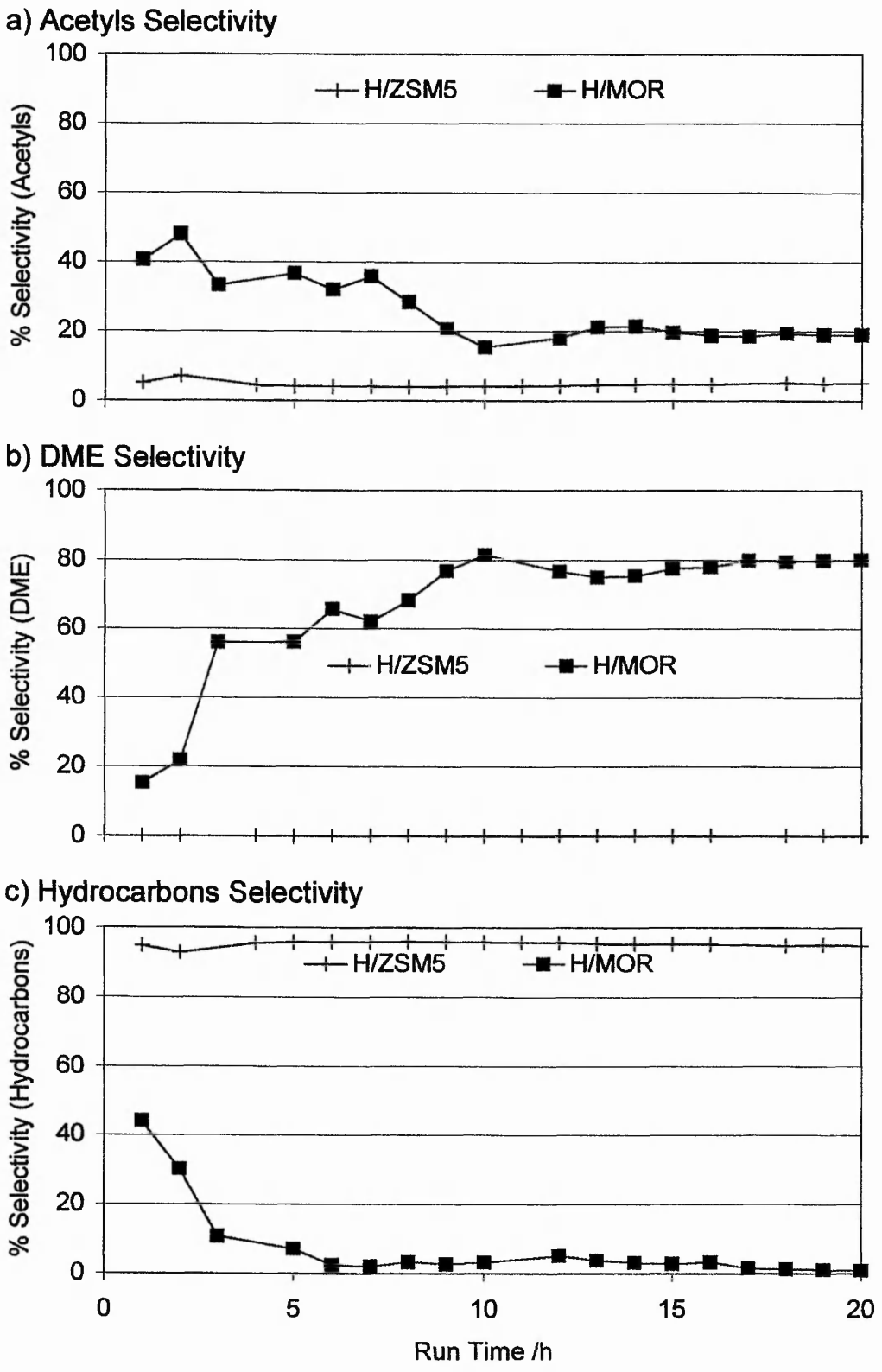

Figure 5.7 Comparison for H/ZSM-5 of the Selectivities to (a) Acetyls (b) DME and (c) Hydrocarbons with H/MOR SAR20

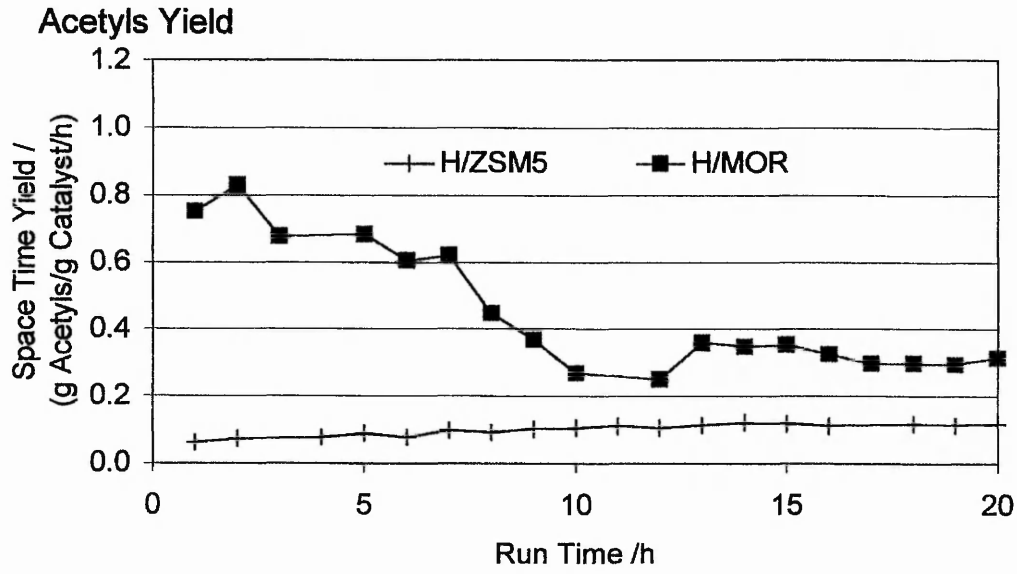

Figure 5.8 Comparison for H/ZSM-5 of the Acetyls Space Time Yield with H/MOR SAR20

On comparing Figure 5.8 with Figure 5.4, both ZSM-5 and Theta-1 produce a stable yield of between 0.2 and 0.1 g/g/h acetyls. However, for Theta-1 the yield is initially higher and falls to the stable yield, whilst for ZSM-5 the yield is initially lower and only stabilises after 10 hours of reaction. Similarly, for both of the frameworks, the acetyls yield consists totally of methyl acetate.

H/Beta

Beta, assigned the Structure Type Code BEA, is a three dimensional, 12-T-ring channel structure. Detailed structural determination [4] has shown that it consists of an intergrowth of two distinct, but closely related 12-T ring structures. Beta exhibits unique Lewis acidic properties related to the local defects created by the edge dislocations of these two distinct structures.

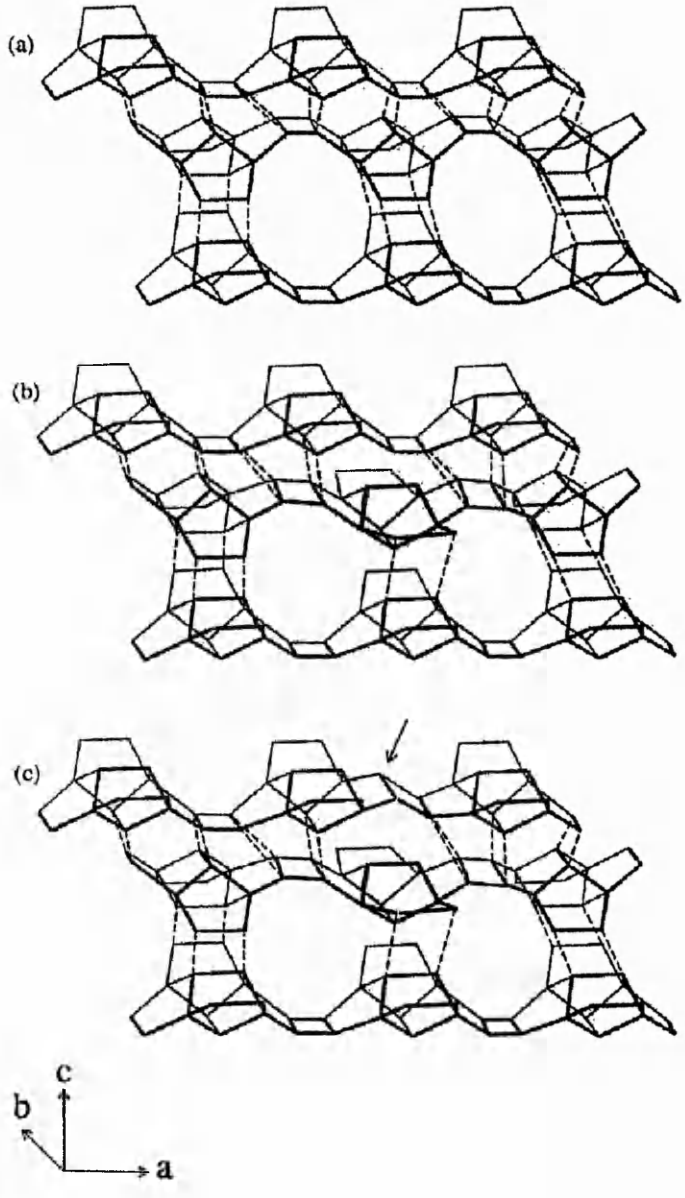

Figure 5.9 The formation of the defect sites in the Beta framework

The resulting pore structure is of two mutually perpendicular and connected channels. The first a straight channel, with a cross section 7.6 x 6.4 Å, runs in both the a & b directions and the second a smaller sinusoidal channel, of cross section 5.5 x 5.5 Å, runs parallel to the c-direction.

The level of conversion over catalyst H/Beta is shown in Figure 5.10a. Initially 100%, the conversion falls to between 70-80% after 5 hours reaction. In contrast, the carbon balance in Figure 5.10b is initially low at 40% and after 5 hours has increased to between 80-90%. This confirms that the higher level of conversion is to products that are not detected.

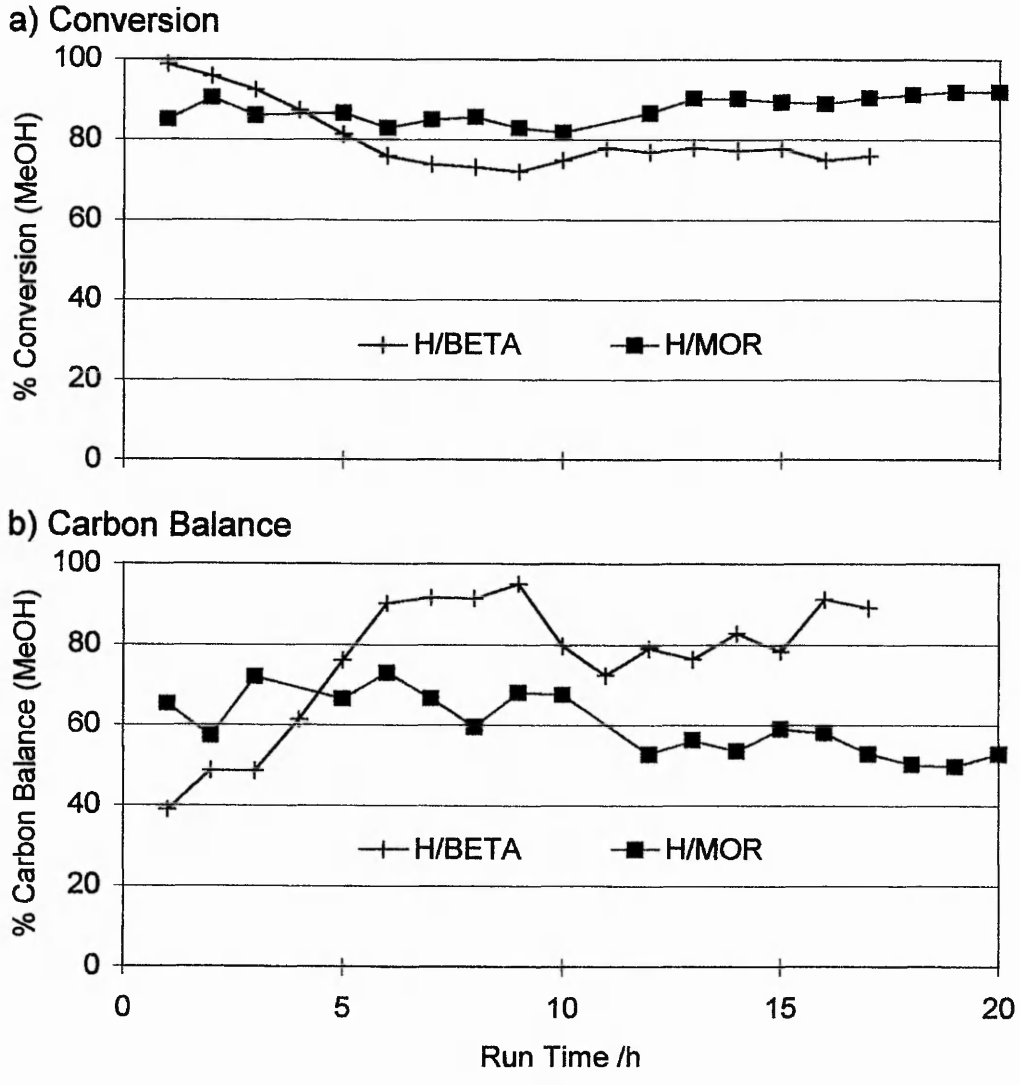

Figure 5.10 Comparison for H/Beta of (a) the Conversion and (b) the Carbon balance with H/MOR SAR20

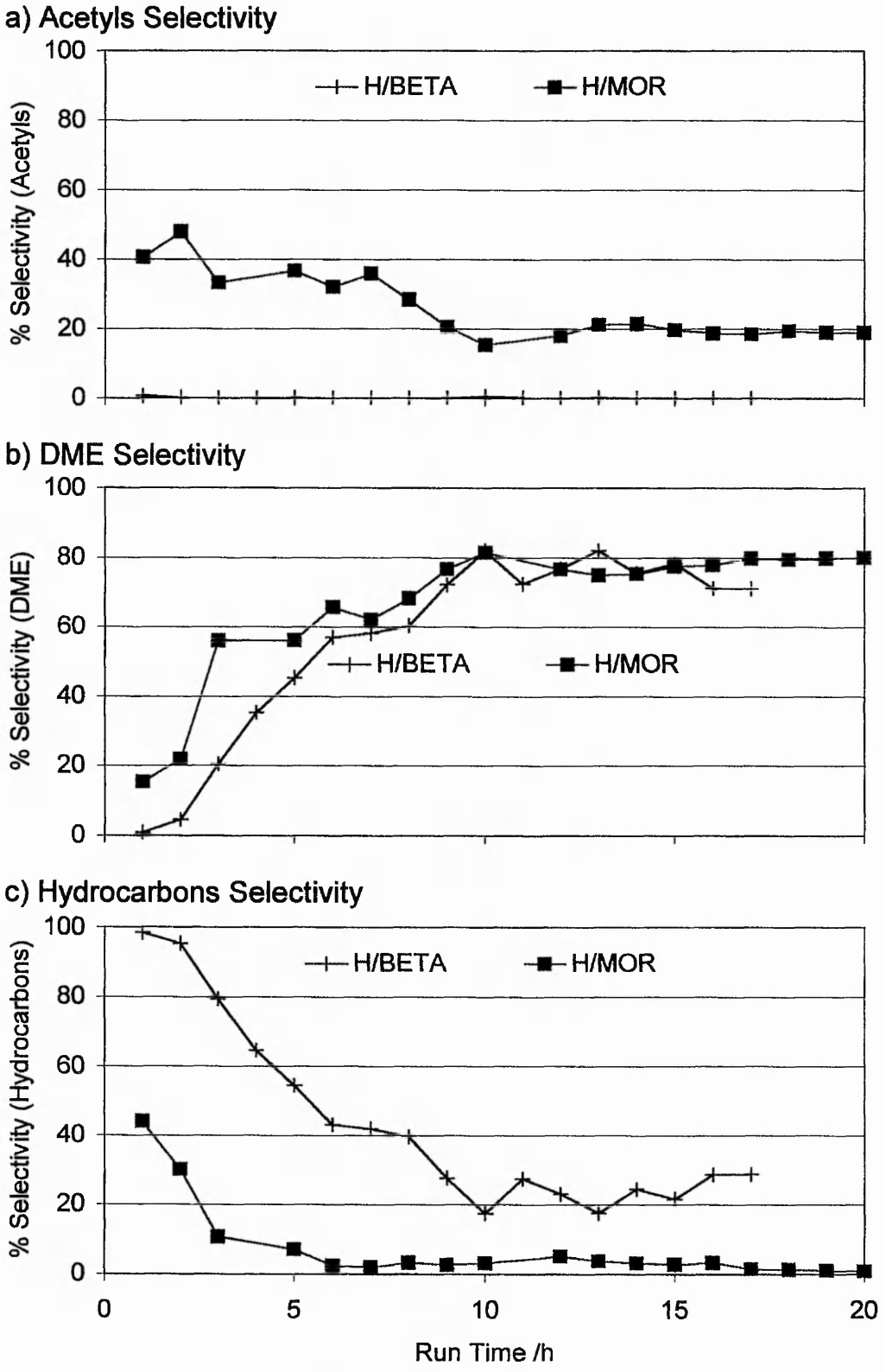

Figure 5.11 Comparison for H/Beta of the Selectivities to (a) Acetyls (b) DME and (c) Hydrocarbons with H/MOR SAR20

Under the high level of methanol conversion, the selectivity to, and yield of, acetyls over H/Beta is effectively zero. In contrast the selectivity to DME is similar to that for H/MOR, so assuming equivalent levels of methanol conversion, the yields of DME for H/Beta and H/MOR are similar. For H/Beta the initial hydrocarbon selectivity is 100% (compared to 50% over H/MOR) falling steadily to 20% after 10 hours reaction as the DME selectivity increases. This indicates that the large cavities present at the intersection of the 12-T-ring channels are unfavourable for carbonylation of methanol as found for the smaller ones of ZSM-5.

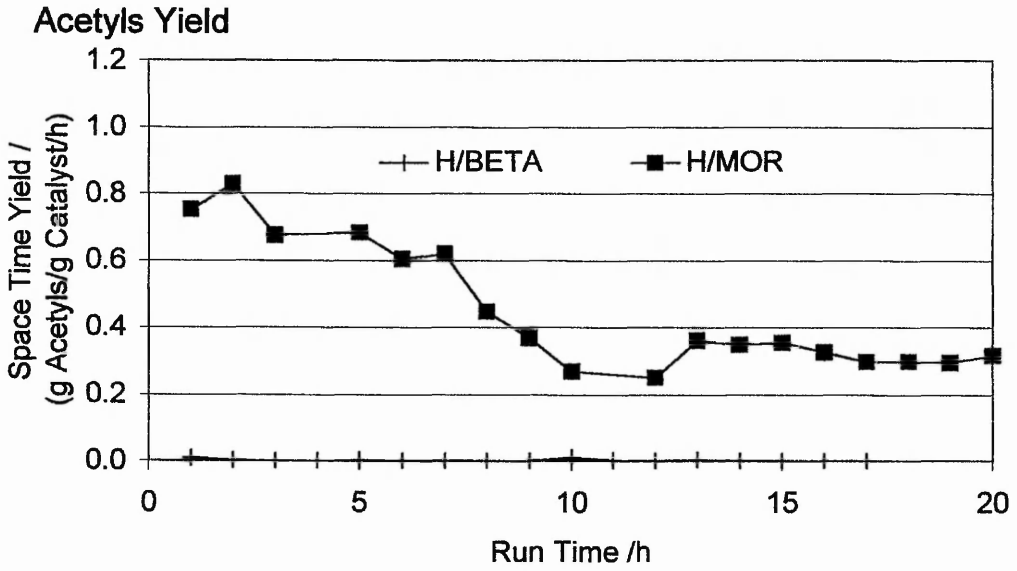

Figure 5.12 Comparison for H/Beta of the Acetyls Space Time Yield with H/MOR SAR20

The quoted SAR 25 for the H/Beta supplied is significantly higher than the SAR 5 observed by the XRF characterisation. The sample, supplied as pellets, is suspected to have been mixed with an alumina binder prior to pelleting.

THE PROMOTIONAL EFFECT OF COPPER

Background

The previous results compare the frameworks: Theta-1, ZSM-5 and Beta with mordenite in their proton forms. The proton forms are now compared to copper ion-exchanged samples studied under the same conditions. The copper loadings of each sample are summarised below in Table 5.2.

Designation	Source	SAR*	Cu wt%*,†	Cu/Al_2*
H/Theta	BP (Sunbury)	54.5	N/A	N/A
Cu/Theta SE	H/Theta BP (Sunbury)	54.6	0.10 (0.12)	0.06
Cu/Theta HP	H/Theta BP (Sunbury)	79.4	1.82	2.58
Cu/Theta SS	H/Theta BP (Sunbury)	-	(4.54)	-
H/ZSM-5	H/ZSM-5 Catal	50.0‡	N/A	N/A
Cu/ZSM-5 SE	H/ZSM-5 Catal	-	(1.23)	-
H/Beta	H/Beta PQ	25.0‡	N/A	N/A
Cu/Beta SE	H/Beta PQ	-	(1.43)	-
Cu/Beta HP	H/Beta PQ	5.5	2.60 (2.67)	0.19
Cu/MCM-22	BP (Sunbury)	35.7	5.90	2.80

Table 5.2 Summary of the copper loadings of the different frameworks tested

*Values from XRF by BP (Sunbury)

†Values in brackets determined by AA from dilute nitric acid solutions of lithium borate fusions.

‡Value quoted when supplied.

Cu/H/Theta

The level of conversion, shown in Figure 5.13a, is not affected significantly by the incorporation of ion-exchanged copper, maintaining a level of at least 80% throughout. Similarly the carbon balance, Figure 5.13b, is not modified by the presence of copper, other than it appearing at a more stable level of 55% throughout the reaction.

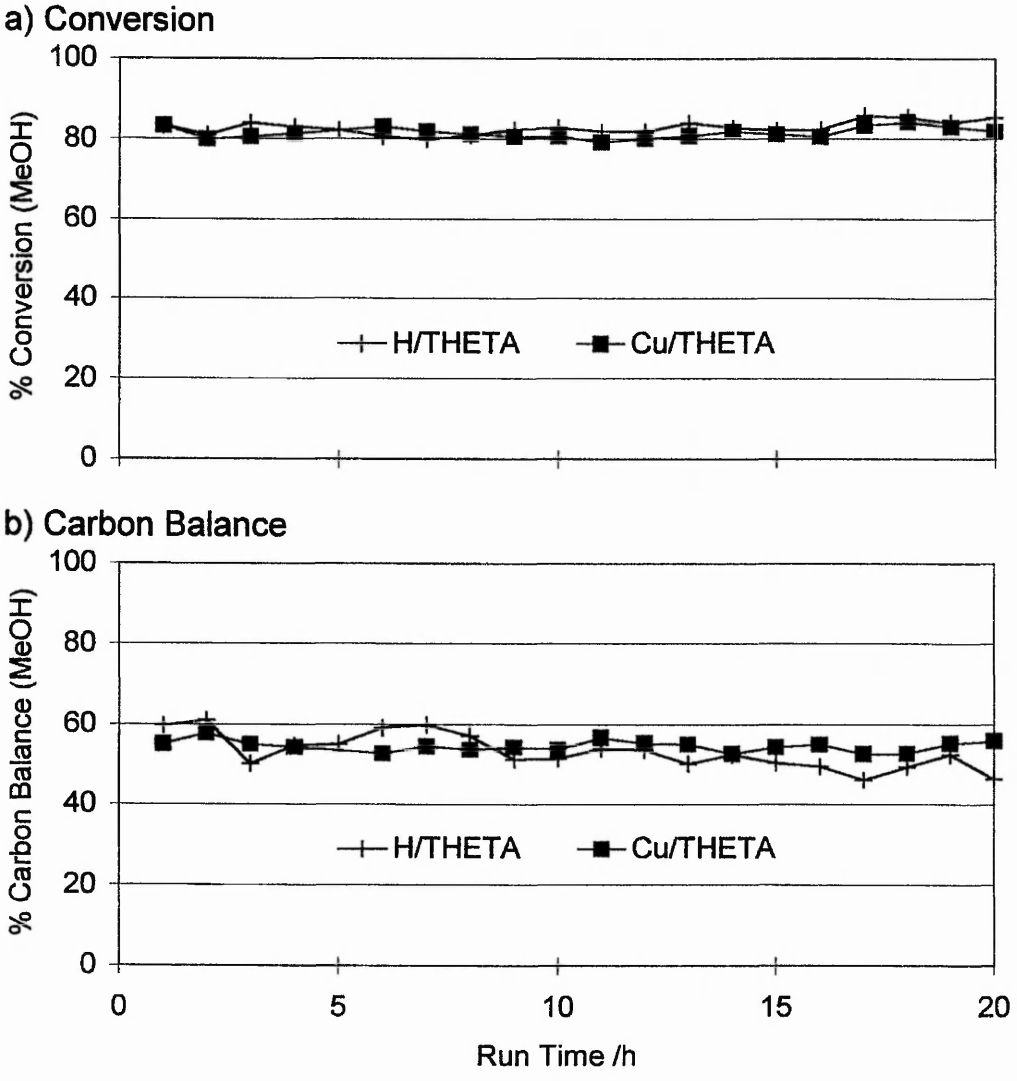

Figure 5.13 The effect of ion-exchanged copper on (a) the Conversion and (b) the Carbon Balance for H/Theta-1

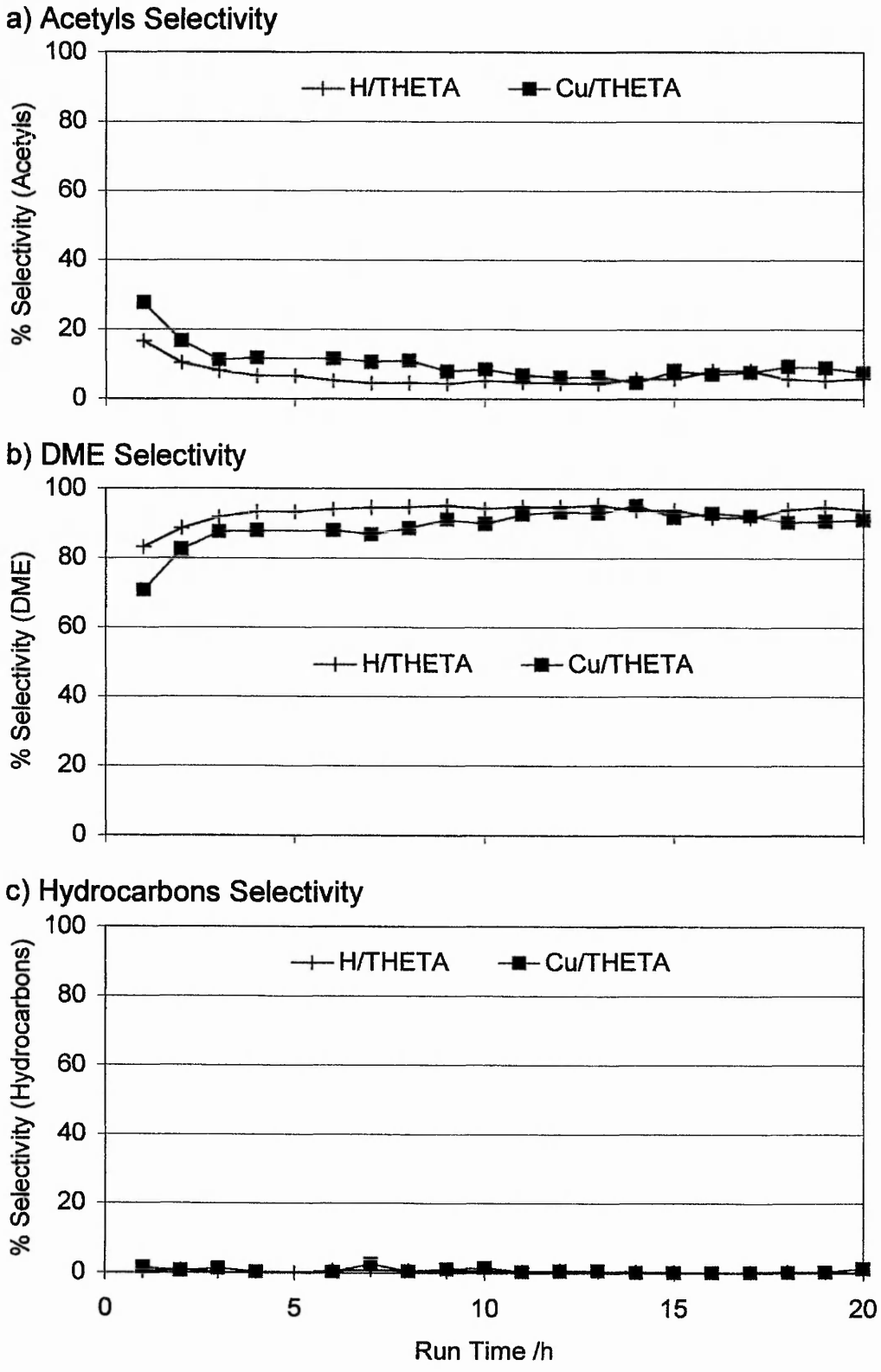

Figure 5.14 The effect of ion-exchanged copper on the Selectivities to (a) Acetyls, (b) DME and (c) Hydrocarbons for H/Theta-1

For the similar levels of conversion and carbon balance the initial selectivity to acetyls, Figure 5.14a, is seen to be greater in the presence of copper. Initially at 30%, the acetyls fall in the first 3 hours to maintain a stable 10% selectivity, compared to being initially at 20% and falling, over the same period, to 10% for the proton form. The difference in acetyls selectivity is made up entirely by a lower DME selectivity for the copper loaded form.

For both samples, the selectivity to hydrocarbons remains zero throughout. The slightly higher selectivity to acetyls for the copper form corresponds to a yield, greater by approximately 0.05 g/g/h, making an initial high of 0.35 g/g/h which then falls to a stable 0.1 g/g/h yield for the remaining reaction.

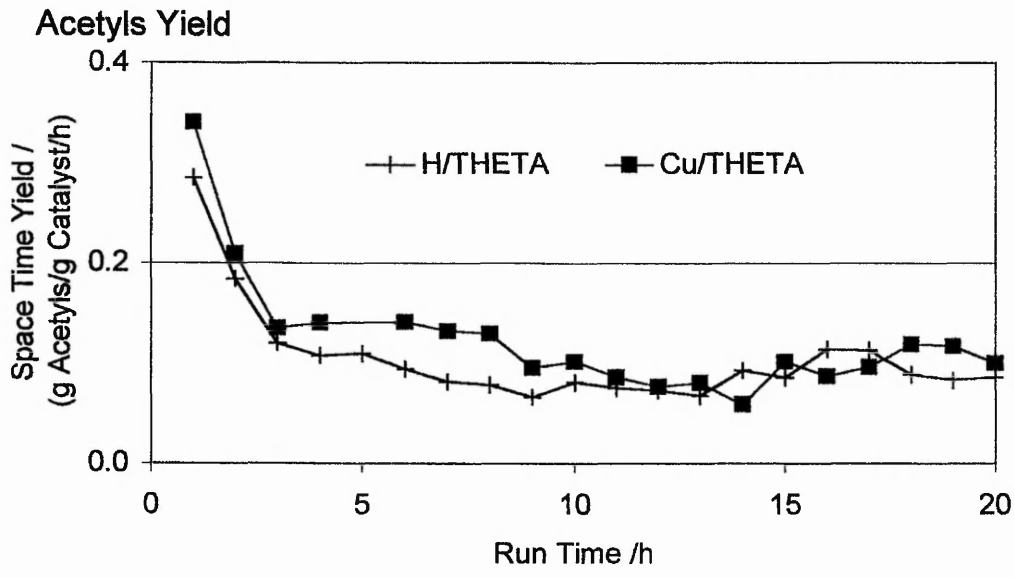

Figure 5.15 The effect of ion-exchanged copper on the Acetyls Space Time Yield for H/Theta-1

The improvement in the initial acetyls yield for the copper form is only slight. However, the actual loading of copper in the sample is also very low. From the XRF, of the as prepared sample, only 0.1 wt% of copper is present. The other techniques of introducing copper were used, to increase the level of loading in the Theta-1 framework, the effects of which are presented later in this chapter.

Cu/H/ZSM-5

For ion-exchanged copper in H/ZSM-5 the initial level of conversion, see Figure 5.16a, has been reduced, compared to the 100% conversion for the proton form, to between 80-90% with a steady decline with reaction time. The carbon balance, Figure 5.16b, is initially between 60-70% and is seen to increase up to 80% by 20 hours reaction that corresponds to the decrease in the level of conversion observed.

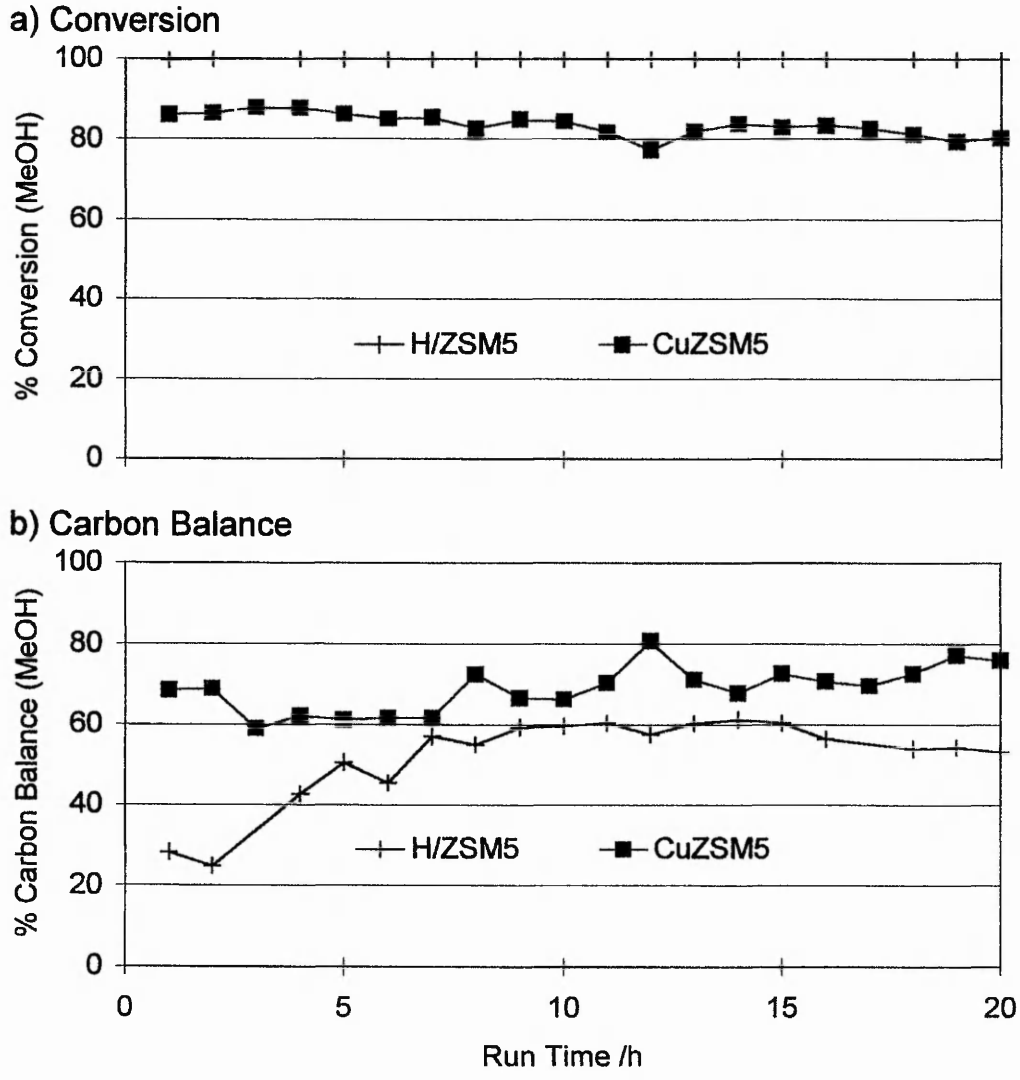

Figure 5.16 The effect of ion-exchanged copper on (a) the Conversion and (b) the Carbon Balance for H/ZSM-5

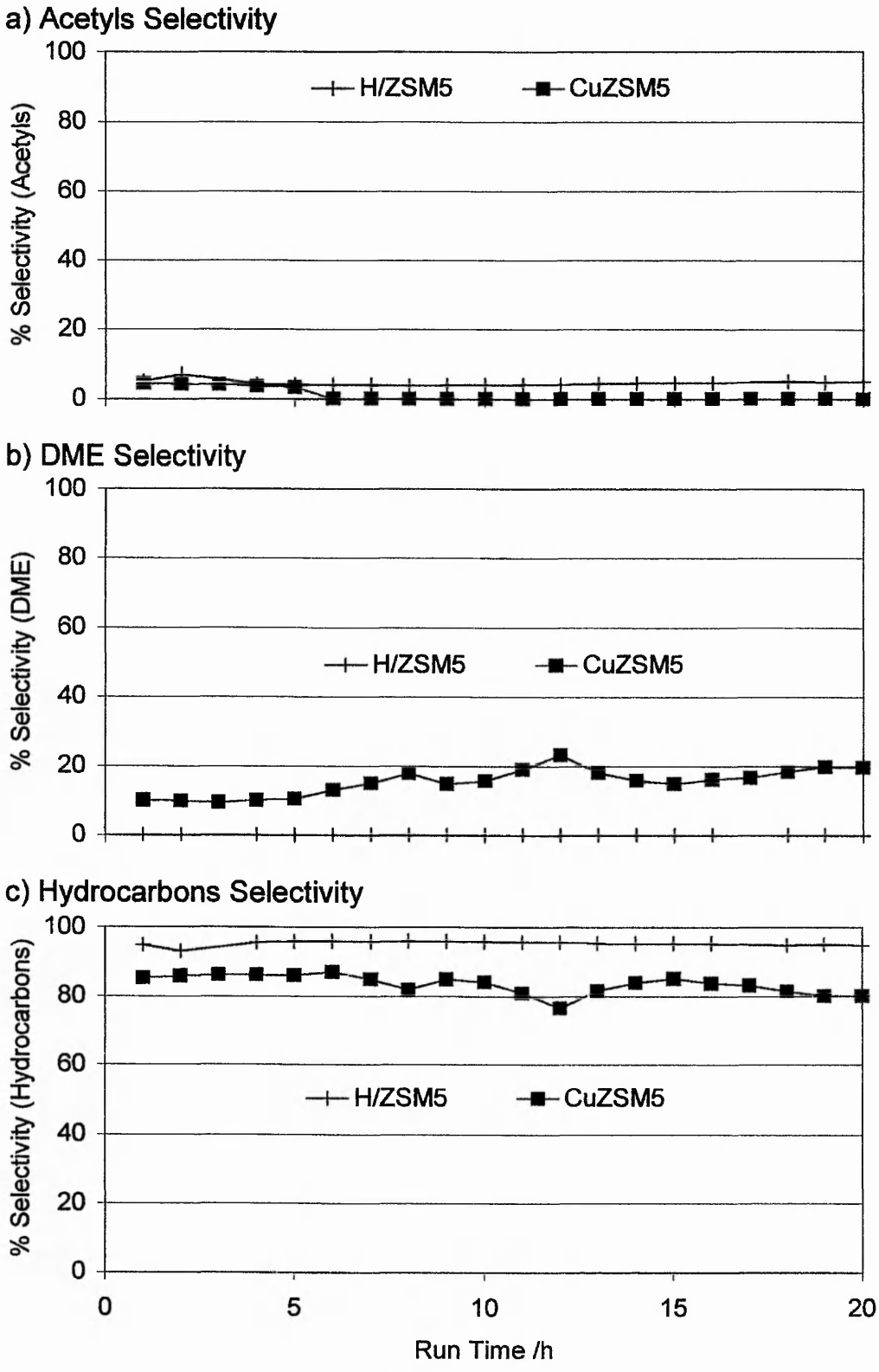

Figure 5.17 The effect of ion-exchanged copper on the Selectivities to (a) Acetyls, (b) DME and (c) Hydrocarbons for H/ZSM-5

There is only a degree of acetyls formation during the first 5 hours of reaction, solely of methyl acetate, it accounts for a selectivity of less than 10%. The initial acetyls selectivity is similar to that continuously observed for the proton form. In the presence of copper the initial selectivity to DME is 10% which has risen to 20% by 12 hours, compared to a constant DME selectivity of zero for the proton form. The hydrocarbon selectivity for the copper form is lower by a constant 10%, as expected from the difference in DME selectivity. The yield of acetyls consists solely of methyl acetate for both catalysts. The yield is very similar for the first 5 hours of reaction, but in the case of the copper form appears to suddenly disappear, as shown in the selectivity.
From the activity that is present it appears that the acetyls yield is decaying for the copper form, compared to a small rise to a stable yield for the proton form.

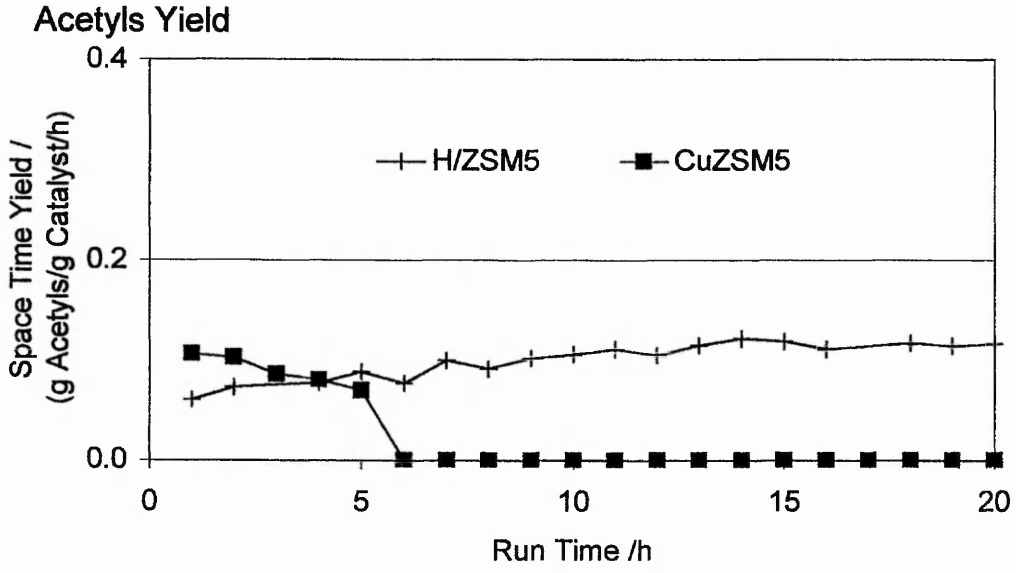

Figure 5.18 The effect of ion-exchanged copper on the Acetyls Space Time Yield for H/ZSM-5

The copper introduced by ion-exchange, into the ZSM-5 framework, is seen here not to promote the acetyls formation compared to the proton form. However, the copper does decrease the total methanol conversion to hydrocarbons and promotes the formation of DME.

Cu/H/Beta

The introduction of copper by ion-exchange into H/Beta has no significant effect on the level of methanol conversion, Figure 5.19a, initially 100% it falls in 5 hours to a stable 80%. However the carbon balance is seen to be lower, initially zero it reaches a maximum of 70% by 10 hours before decreasing again to 50%. The carbon balance for the proton form is similarly initially zero but steadily rises to between 90-70%.

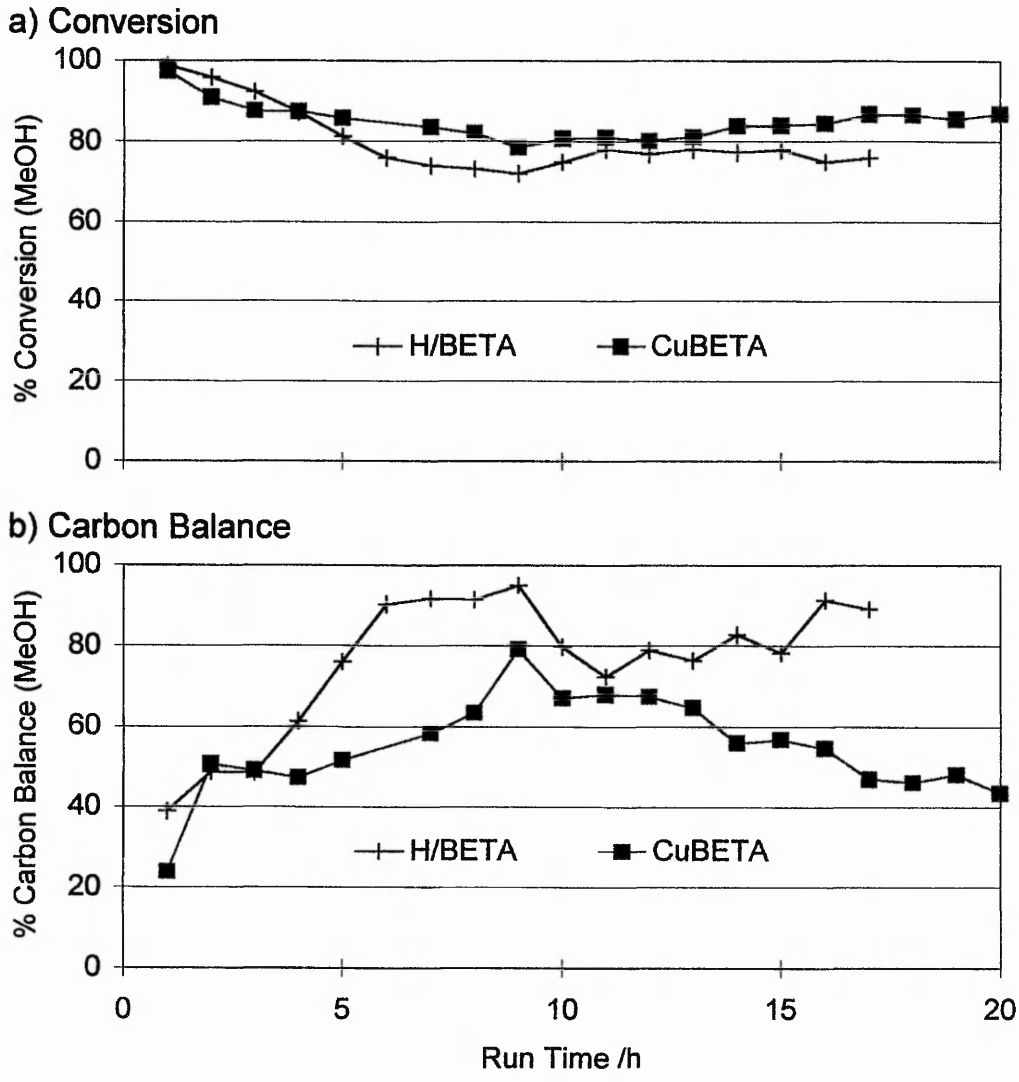

Figure 5.19 The effect of ion-exchanged copper on (a) the Conversion and (b) the Carbon Balance for H/BETA

The acetyls selectivity for both samples is seen in Figure 5.20 to be zero throughout. The DME selectivities are comparable, initially zero they rise to a maximum of 80% by 10 hours reaction. The DME selectivity is seen to rise faster for the copper form.

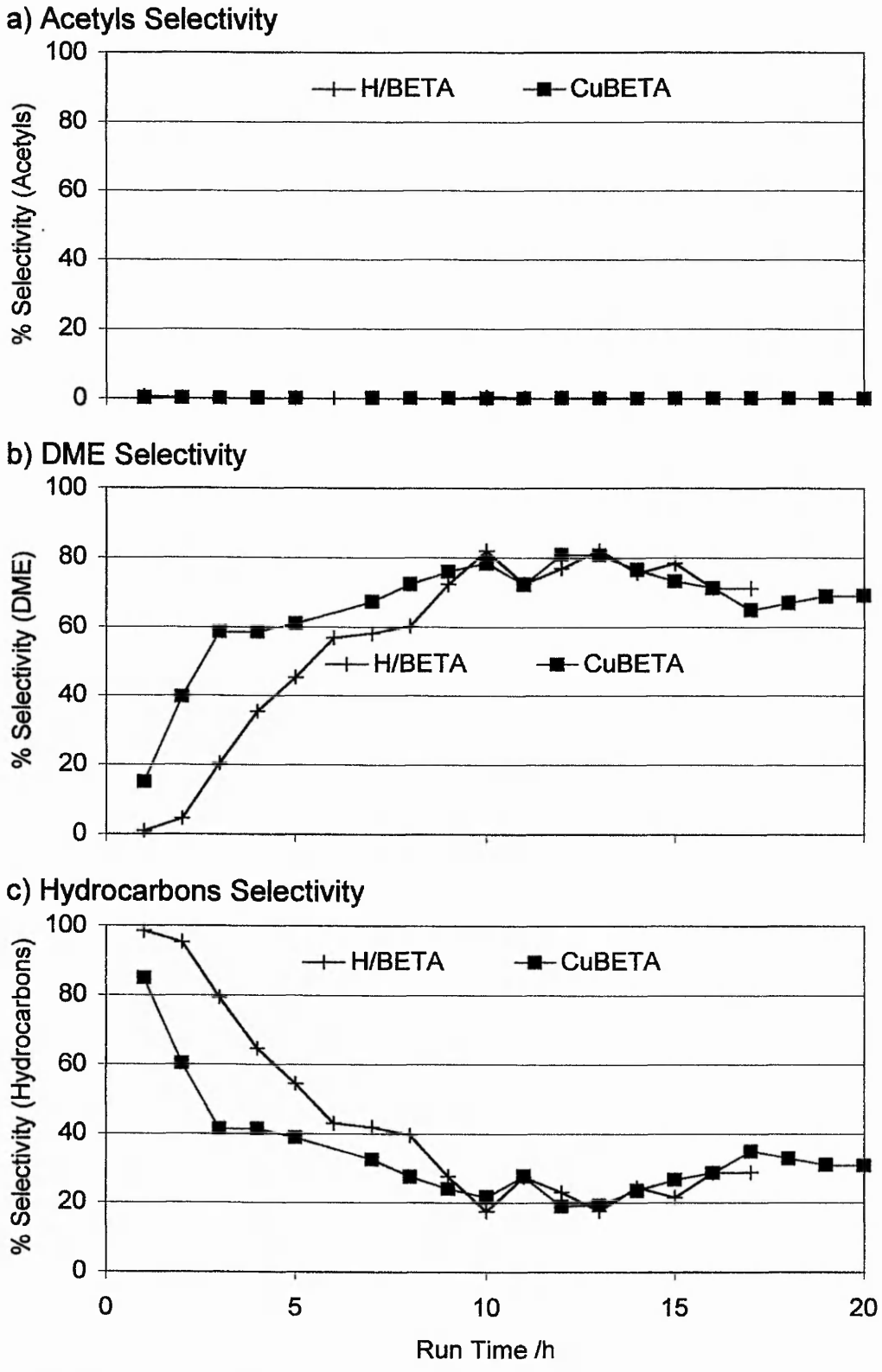

Figure 5.20 The effect of ion-exchanged copper on the Selectivities to (a) Acetyls, (b) DME and (c) Hydrocarbons for H/BETA

The similarity in DME selectivities is mirrored for the hydrocarbons, both initially 100% and falling to 20-30% by 10 hours, with the copper loaded form falling faster. As shown below, zero selectivity to acetyls corresponds to an acetyls space time yield of zero.

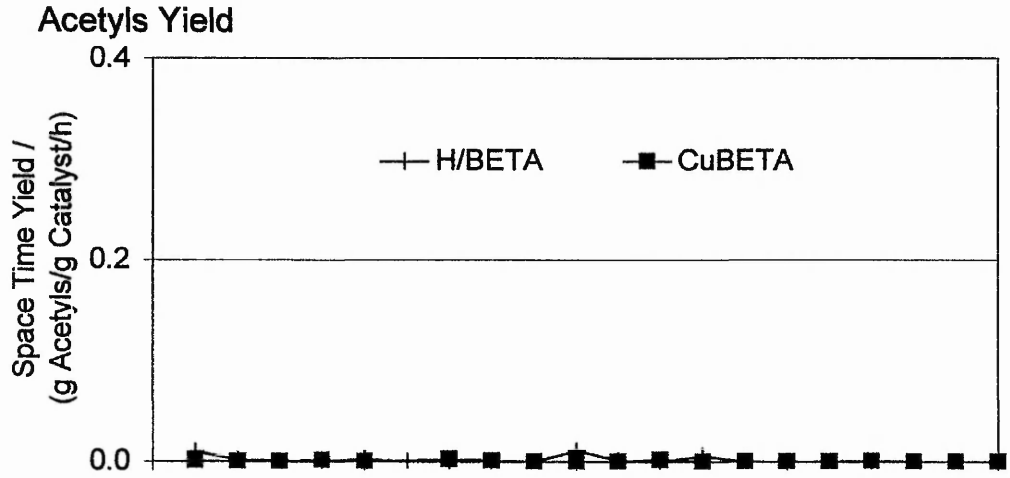

Figure 5.21 The effect of ion-exchanged copper on the Acetyls Space Time Yield for H/BETA

Copper therefore does not promote the formation of acetyls over the Beta framework, however copper does promote, as for ZSM-5, the formation of DME in favour of the hydrocarbons.

Cu/MCM-22

The sample of MCM-22 was supplied directly from BP (Sunbury) already containing copper and its performance is compared here to that for H/MOR SAR20.

The zeolite MCM-22 was first synthesised by Mobil[5] and has been assigned the structure type code MWW. The unique pore structure is one of the few frameworks where the two different channel structures present are not interconnected. The first channel shown in Figure 5.22 consists of large supercage structures, 7.1Å in diameter and 18.21Å in length, terminated by narrow double 6-T ring restrictions.

(a) (b)

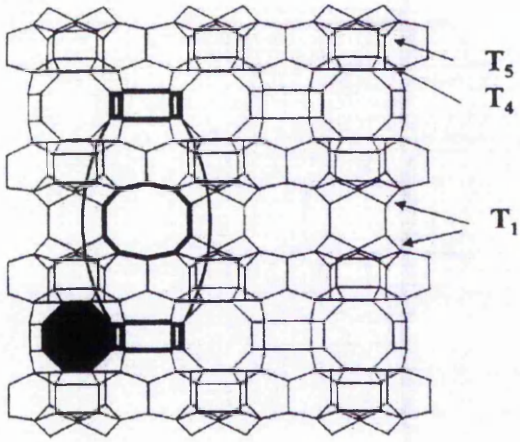

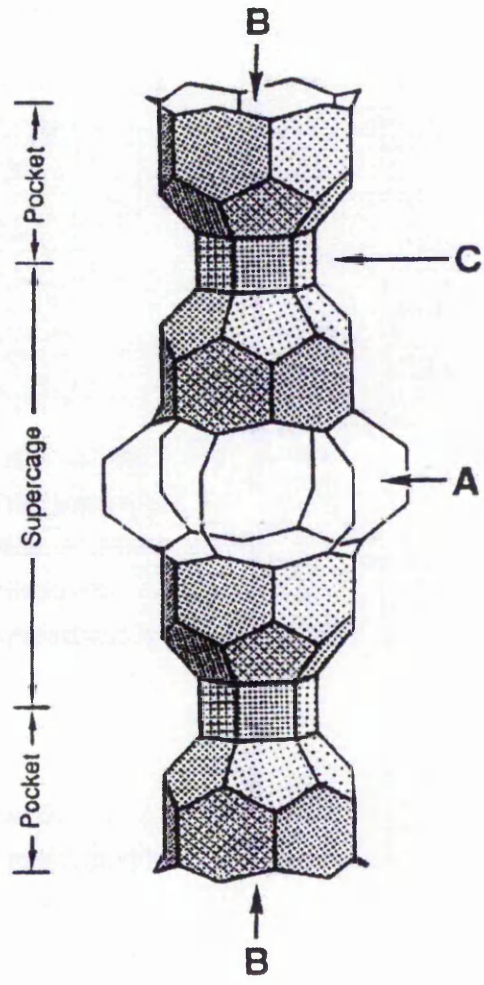

Figure 5.22(a) A Cross section of MCM-22 showing the relative position of the supercage structure to the perpendicular sinusoidal 10-T channel. (infilled 8-T ring adjacent to the double 6-T ring). Access to the supercage is only via the highlighted 10-T ring. Reproduced from reference [6].

(b) A view of the supercage structure showing, (A) the 12-T ring supercage, (B) The structure of the pockets on the external surface, (C) The isolating double 6-T rings. Reproduced from reference [7].

As highlighted in Figure 5.22a, access to the supercages is only via the 10-T ring windows that form the sides of the supercage[6]. The second channel system consists of 10-T ring sinusoidal channels giving rise to a two dimensional array running

perpendicular to the supercage channels around the double 6-T ring restrictions. The MCM-22 crystallites are planar and can be considered[7] to be an **ABAB** layered structure with **A**, the supercage system, and **B** the sinusoidal channel system. The framework terminated by half supercages gives rise to the deep pockets within the external surface, see Figure 5.22b.

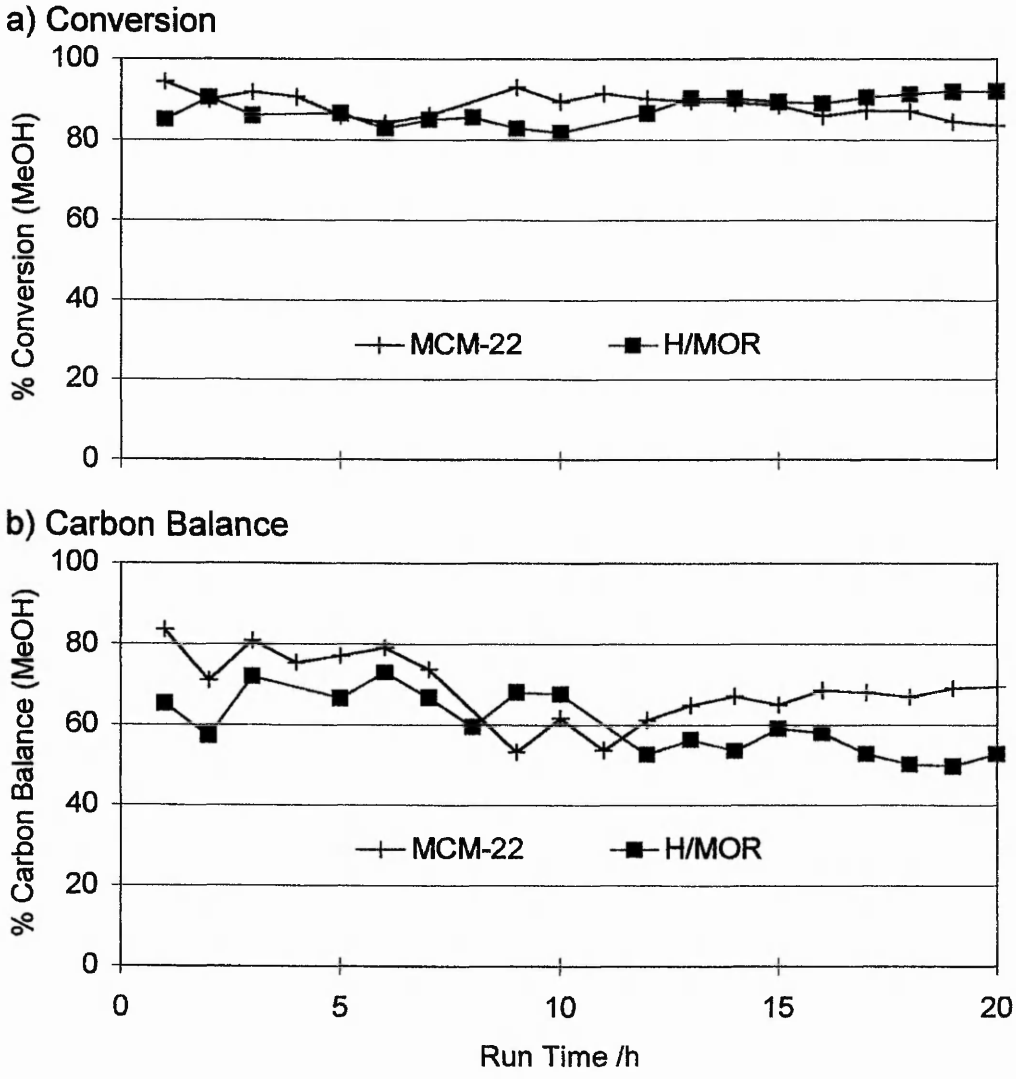

Figure 5.23 Comparison for Cu/H/MCM-22 of (a) the Conversion and (b) the Carbon balance with H/MOR SAR20

The level of methanol conversion over Cu/H/MCM-22 is seen in Figure 5.23a to be directly comparable with that for the H/MOR, never falling below 80% during the 20 hours of reaction. Additionally, the carbon balance in Figure 5.23b is higher overall for the Cu/H/MCM-22 sample, initially 80% and dropping to ~60% after 8 hours of reaction. In contrast, the H/MOR has an initial carbon balance of 70% which falls to 50-60% after 10 hours of reaction.

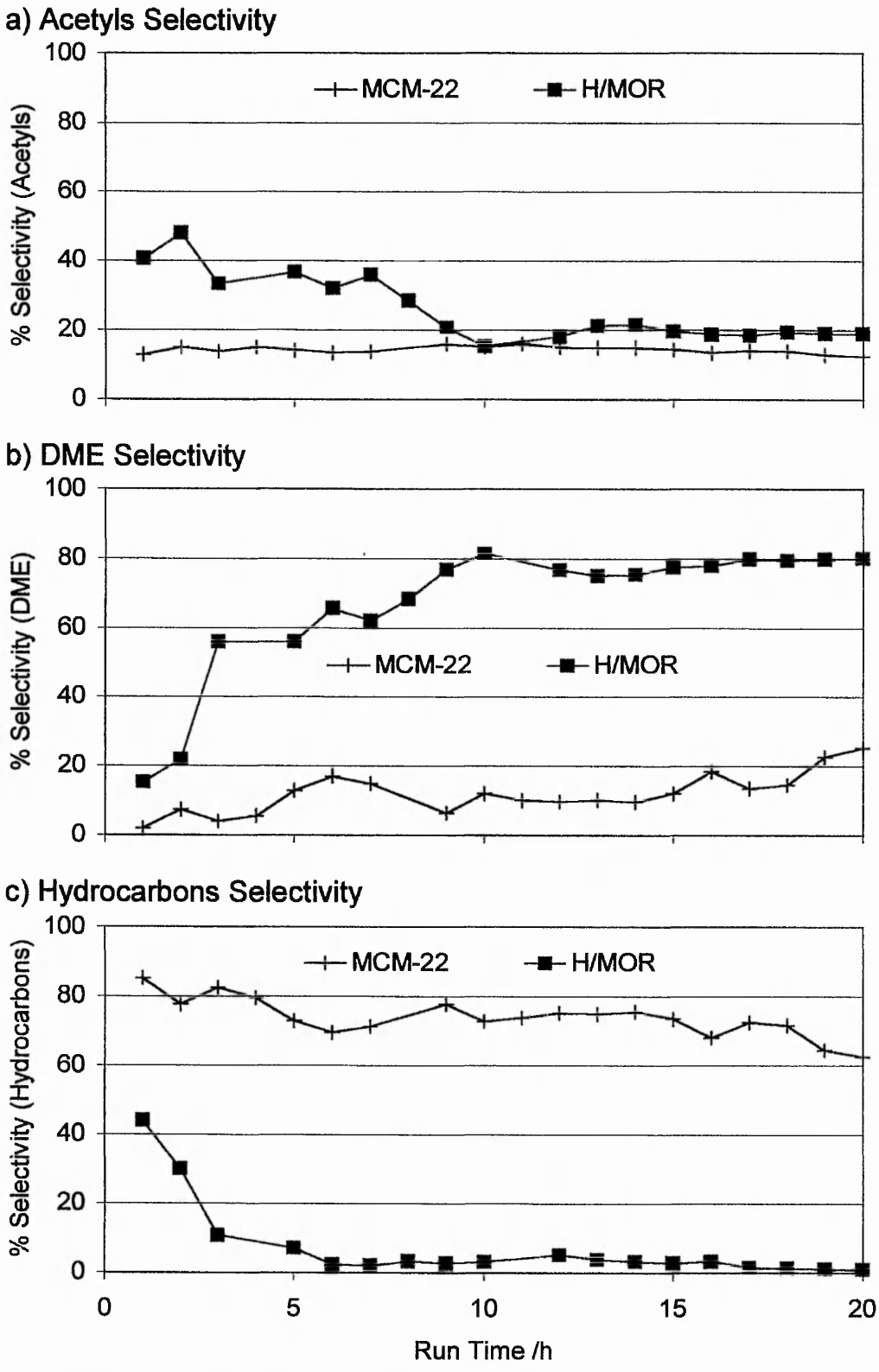

Figure 5.24 Comparison for Cu/H/MCM-22 of the Selectivities to (a) Acetyls (b) DME and (c) Hydrocarbons with H/MOR SAR20

In Figure 5.24a, under comparable levels of methanol conversion Cu/H/MCM-22 maintains a constant, but below 20%, selectivity to acetyls whilst H/MOR has an initial high selectivity of 40% falling to 20% after 10 hours reaction.
Additionally, Cu/H/MCM-22 maintains a low selectivity to DME, rising above 20% only after 18 hours reaction. The selectivity to DME for H/MOR rapidly rises to 80% after 10 hours reaction. There is therefore a high selectivity to hydrocarbons for Cu/H/MCM-22 throughout the reaction, initially greater than 80% falling to 60%, in sharp contrast to H/MOR for which the initial 40% rapidly falls to zero. The constant 20% selectivity to acetyls corresponds to a yield of 0.3-0.2 g/g/h, which is similar to the stable level observed over H/MOR and also Cu/H/MOR. As for the ZSM-5 and Beta frameworks the acetyls yield over MCM-22 is entirely of methyl acetate.

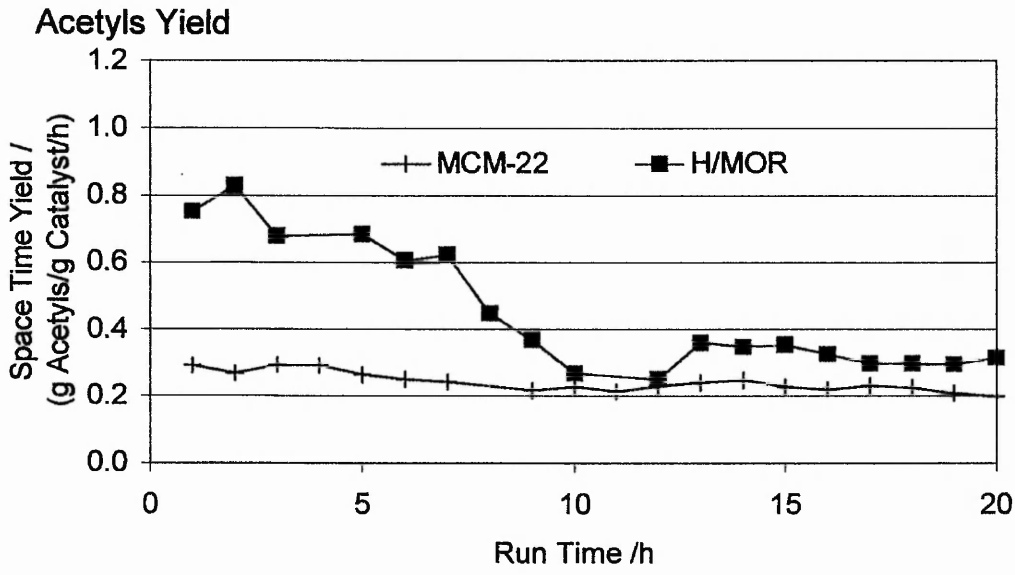

Figure 5.25 Comparison for Cu/H/MCM-22 of the Acetyls Space Time Yield with H/MOR SAR20

The distribution of hydrocarbons formed

For each framework tested, except H/Theta that produced negligible hydrocarbons, the distributions of hydrocarbons formed during the standard conditions are shown in Figure 5.26. For each case the single injection point is during a stable period of hydrocarbon formation.

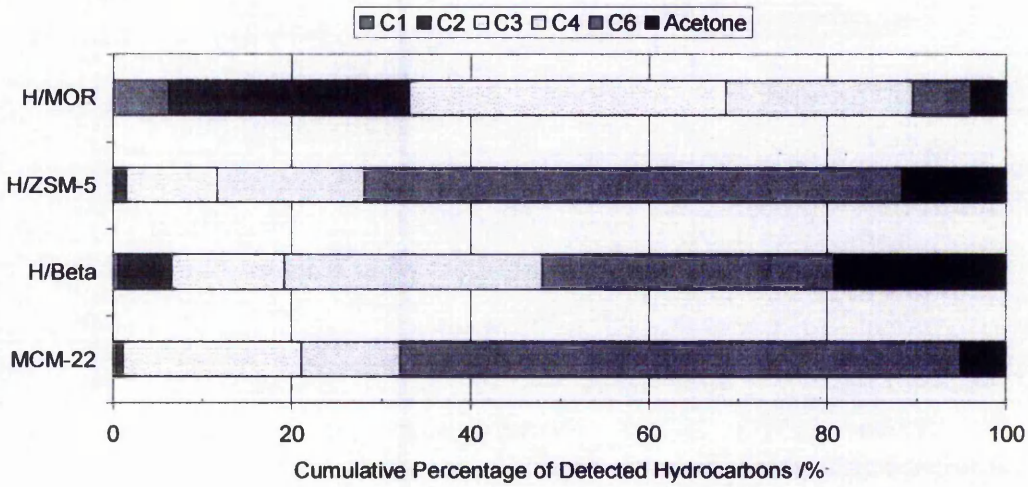

Figure 5.26 Summary of the typical hydrocarbon distributions for the different frameworks tested

The percentages of detected methanol, listed in Table 5.3, correspond to 100% of the hydrocarbon distributions in Figure 5.26. The amount and nature of the hydrocarbons formed over H/MOR are different to those from the other frameworks tested. H/MOR produces a small quantity of the lighter C2 & C3 hydrocarbons whilst the other frameworks produce a much larger quantity of the C6 and heavier hydrocarbons, presumed to be aromatic in nature.

Framework	% Detected MeOH
H/MOR	14
H/ZSM-5	96
H/Beta	87
MCM-22	56

Table 5.3 Percentage of detected methanol corresponding to the hydrocarbons for each of the frameworks tested.

The nature of the coke deposited

Post reactor samples of the catalysts were characterised by standard CHN analysis to determine the amount and nature of the coke deposited. The results in Table 5.4 highlight the effect of each framework, on the nature of the hydrocarbon byproducts formed. The mordenite samples are included for comparison.

Designation	Source	SAR	%wt Coke	H : C
H/MOR(20)	H/MOR(20) Catal	-	14.0	1.0
Cu/MOR 2	H/MOR(20) Catal	18.8	14.2	0.8
Cu/MOR 3(MTG)	H/MOR(20) Catal	-	13.8	0.9
Cu/MOR HP1	H/MOR(20) Catal	18.3	14.1	1.0
Cu/MOR HP2	H/MOR(20) Catal	18.7	14.1	1.0
Cu/MOR HP3	H/MOR(20) Catal	18.0	14.3	1.0
Cu/MOR HP4	H/MOR(20) Catal	-	14.2	0.9
Cu/MOR 1M	H/MOR(20) Catal	-	14.0	0.9
BP 1ST&AW	Na/MOR(12.8) PQ	19.6	11.9	1.0
BP 2ST&AW	Na/MOR(12.8) PQ	-	6.3	1.0
H/Theta	BP (Sunbury)	54.5	3.8	1.7
Cu/Theta	BP (Sunbury)	54.6	3.7	0.9
Cu/Theta HP	BP (Sunbury)	79.4	7.0	0.4
Cu/Theta SS	BP (Sunbury)	-	4.1	0.4
H/ZSM-5	H/ZSM-5 Catal	-	7.3	1.0
Cu/ZSM-5	H/ZSM-5 Catal	-	8.9	1.1
H/Beta	H/Beta(25) PQ	-	7.1	2.0
Cu/Beta	H/Beta(25) PQ	-	6.3	2.0
Cu/Beta HP	H/Beta(25) PQ	5.5	6.6	2.0
Cu/MCM-22	BP (Sunbury)	35.7	13.3	0

Table 5.4 The weight percent and H:C ratio of the coke deposited during catalyst testing, as determined by standard CHN analysis.

THE OPTIMISATION OF FRAMEWORK THETA-1

Introduction

The results, for the proton forms of the different frameworks, suggest that the framework Theta-1 is the most promising for further study. For the standard conditions (Table 2.1) it can be seen from Figure 5.3 that with H/Theta-1, the majority of the methanol introduced is converted only into DME and acetyls. All the other frameworks, formed hydrocarbons as the major products and the introduction of copper did not modify their selectivity by any extent. Furthermore, the introduction of a low loading of copper into Theta-1 by ion-exchange, Figure 5.14, improved the acetyls yield slightly. Two approaches for the optimisation of Theta-1 were taken. Firstly, temperature programing, during the reaction, was used for the proton form. Secondly, different techniques were used to increase the level of copper loading in the framework.

Temperature programing

The results are presented in the standard format, but with an additional axis to the right for the temperature profile used. The temperature was increased at 5°C min^{-1}, and the reactor was allowed to stabilise, for at least 50 minutes, before the first injection at the new temperature. Only the combined acetyls yields are shown, because the changes caused by the temperature profile are equivalent for both acetic acid and methyl acetate.

Profile 1: 350 – 650°C in 50°C steps

Figure 5.27a shows methanol conversion levels of 80 – 90% occur readily from 350°C until the temperature reaches 600°C, at which point no further unreacted methanol is detected. The corresponding carbon balance is around 50% until the temperature reaches 550°C when it starts to fall rapidly. These temperature dependencies indicate that above 550°C the methanol rapidly decomposes to form coke. At the initial temperature of 350°C virtually all the methanol is converted to DME and on increasing the temperature, the DME decreases, as the acetyls selectivity increases.

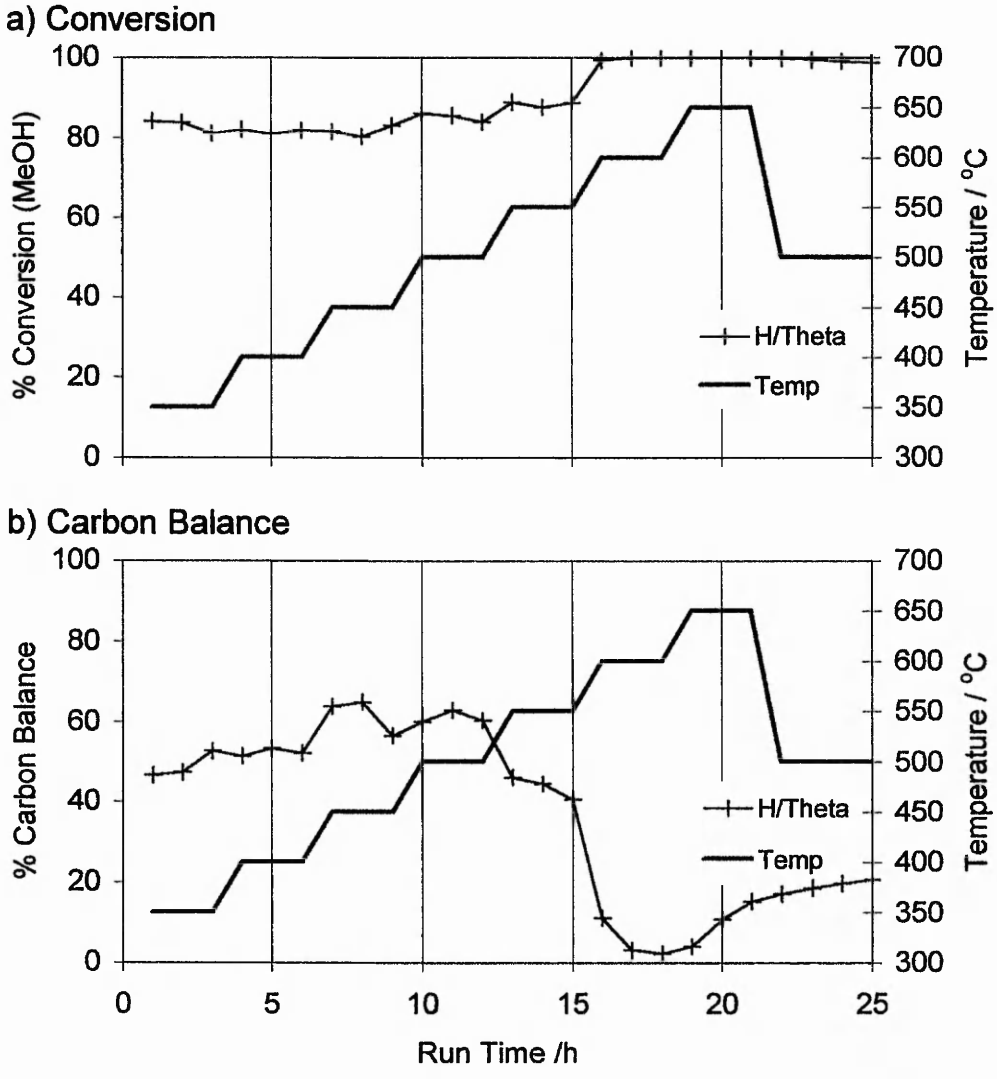

Figure 5.27 The Effect of 50°C steps to 650°C on (a) the Conversion and (b) the Carbon Balance for H/Theta

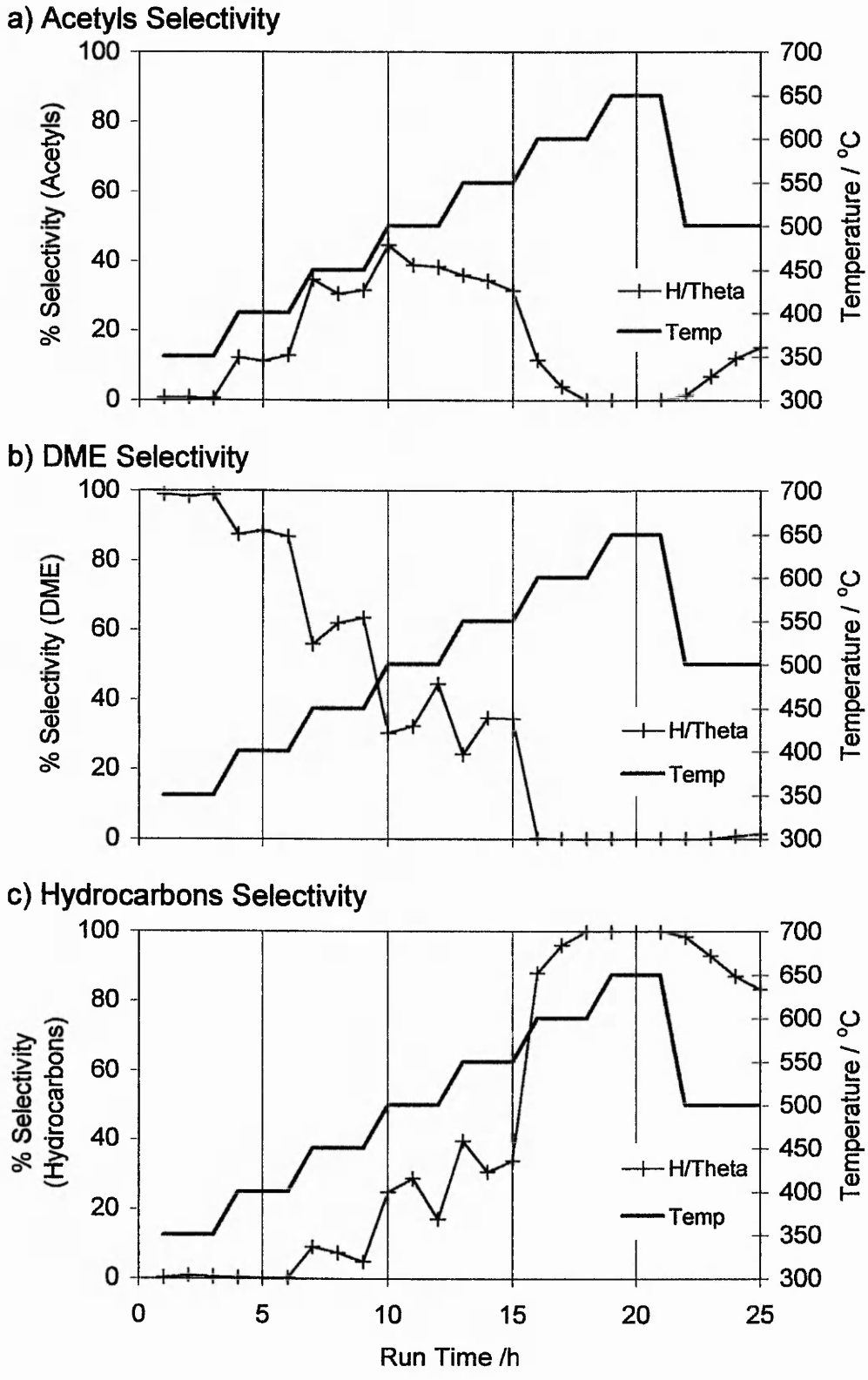

Figure 5.28 The Effect of 50°C steps to 650°C on the Selectivities to (a) Acetyls (b) DME and (c) Hydrocarbons for H/Theta

The maximum selectivity to acetyls of 40% occurs at 500°C and corresponds with a selectivity of 40% DME and 20% hydrocarbons. The initial highest yield of 0.8 g/g/h once 500°C is reached, is not maintained but quickly dies off. Therefore, 500°C is seen to be the maximum temperature at which the carbonylation of methanol occurs. On returning to 500°C from 650°C the acetyls yield begins to recover, suggesting the active sites are neither completely lost nor blocked during the higher temperatures when the hydrocarbons dominate.

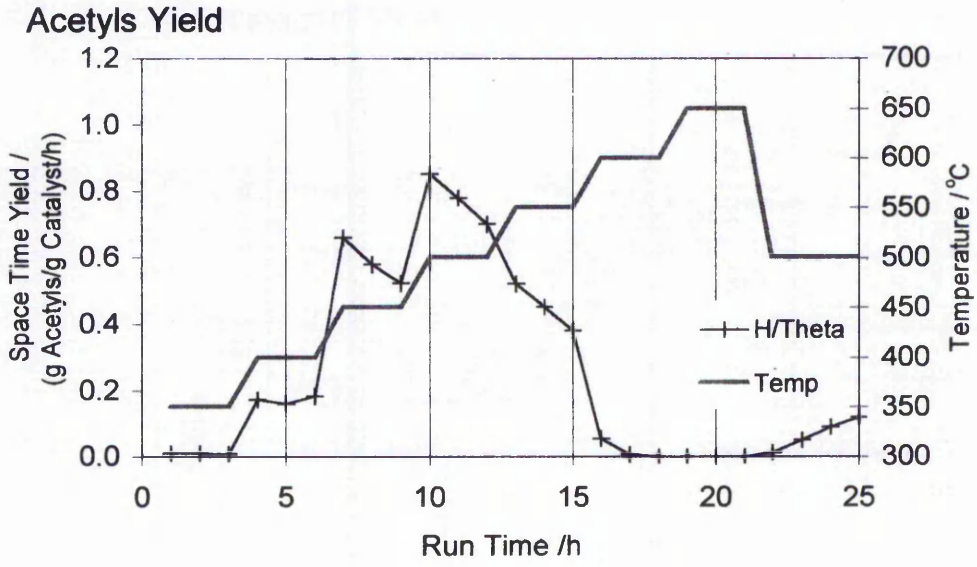

Figure 5.29 The Effect of 50°C steps to 650°C on the Space Time Yield to Acetyls for H/Theta

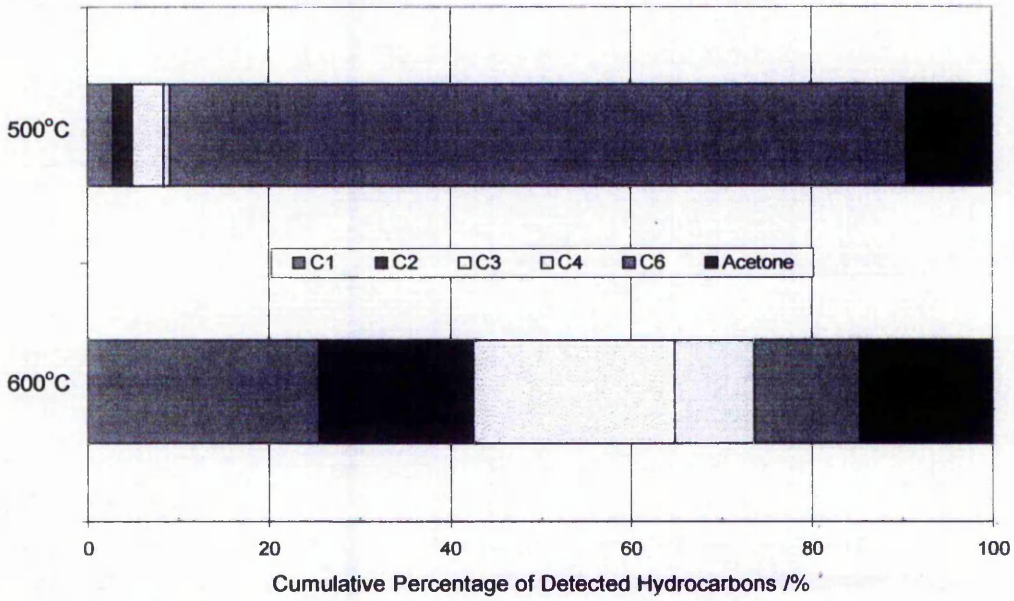

Figure 5.30 Comparison of the Hydrocarbon Distributions at 500°C & 600°C for H/Theta

Profile 2: 350 – 500°C in 25°C steps

Due to the jump in production in profile 1 between 400 and 450°C, the second profile was set at smaller temperature intervals of 25°C to a maximum of 500°C.

The conversion and carbon balance follow exactly the same trends as for profile 1. The Selectivities are also seen to follow similar trends, with the acetyls rising as the DME selectivity decreases. The maximum acetyls selectivity of 50% again occurs when 500°C is attained. Similar to profile 1, the hydrocarbon selectivity only becomes significant around 450°C.

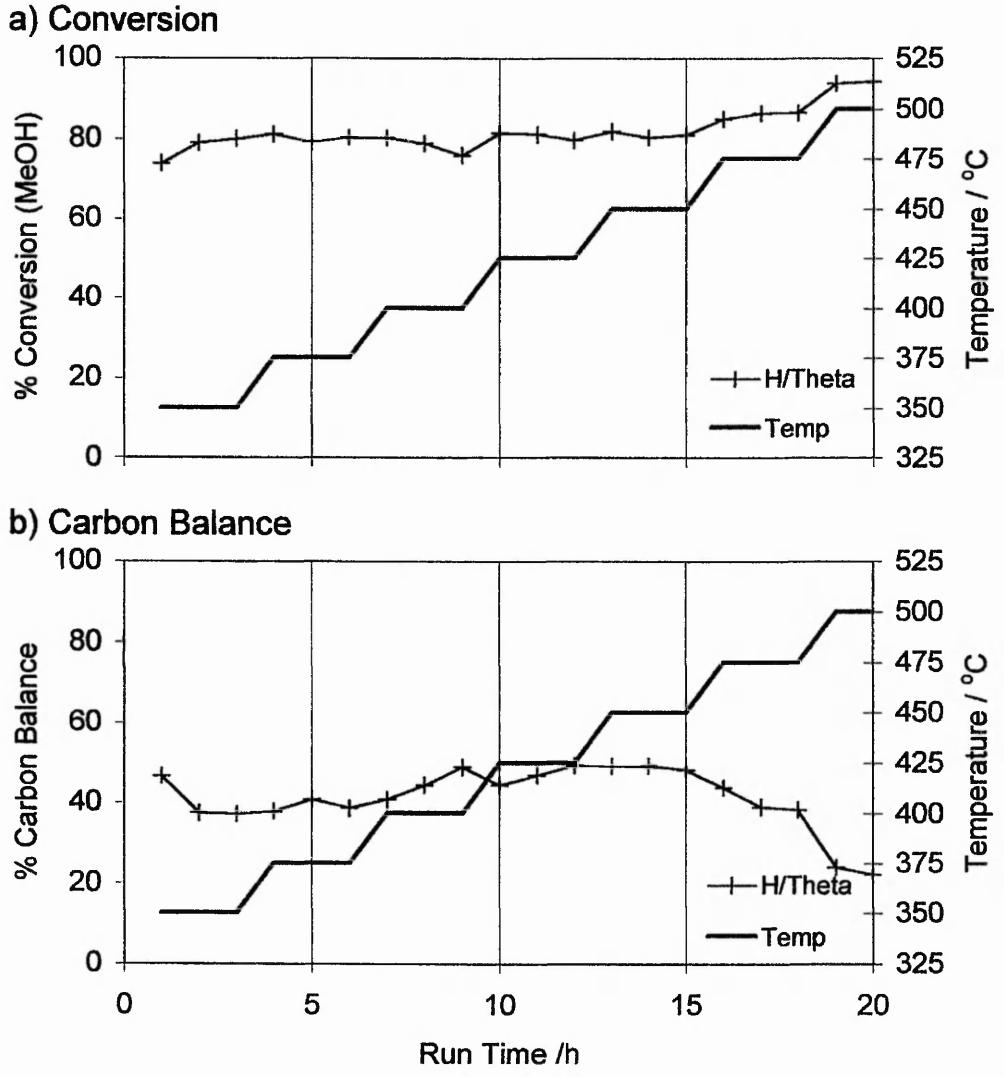

Figure 5.31 The Effect of 25°C steps to 500°C on (a) the Conversion and (b) the Carbon Balance for H/Theta

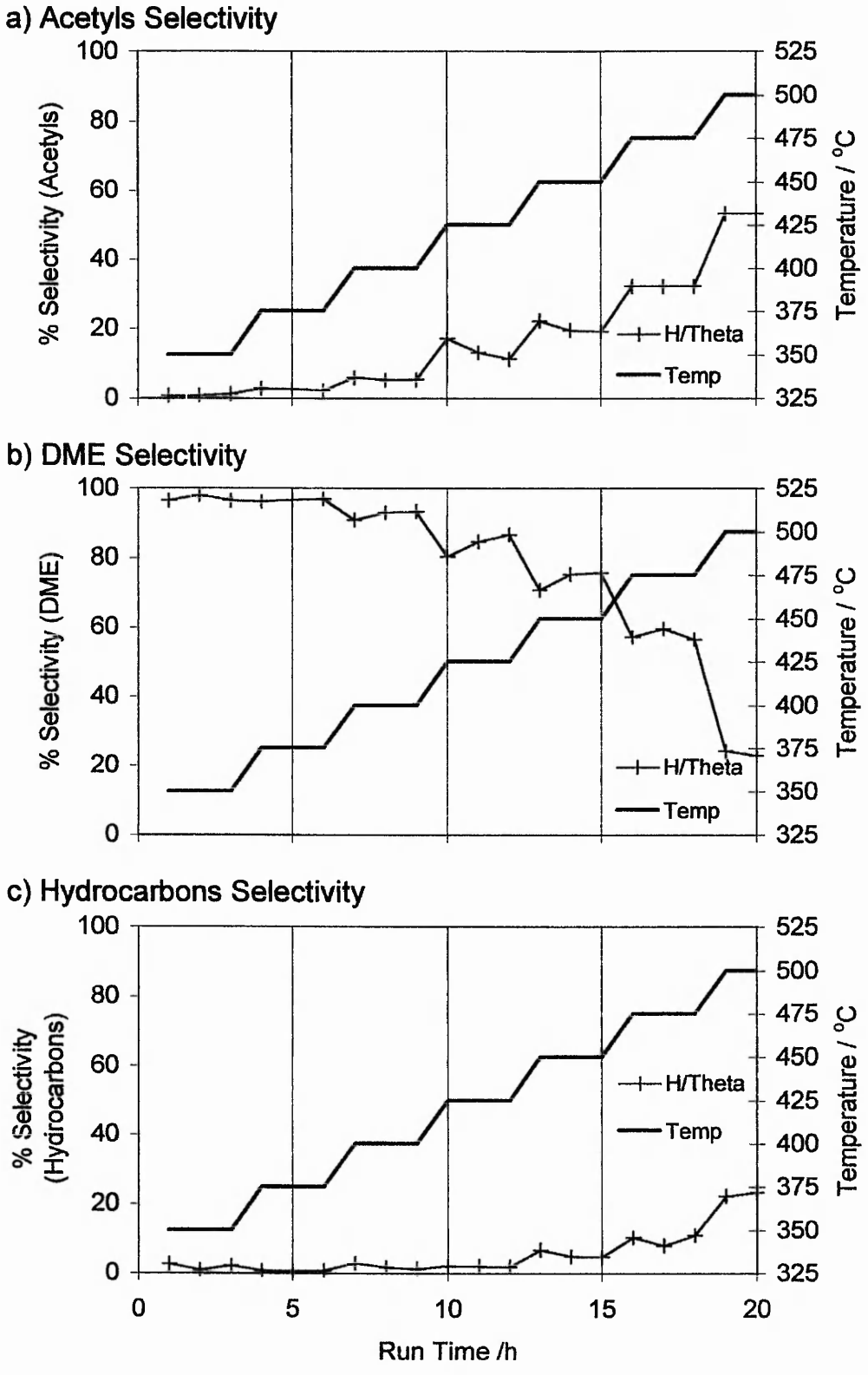

Figure 5.32 The Effect of 25°C steps to 500°C on the Selectivities to (a) Acetyls (b) DME and (c) Hydrocarbons for H/Theta

The maximum acetyls yield is only half that of profile 1 but is achieved at 475°C. Although low, the yield is maintained rather than peaking for just the first hour. The extended lower temperature treatment therefore appears to be detrimental for the production of the acetyls.

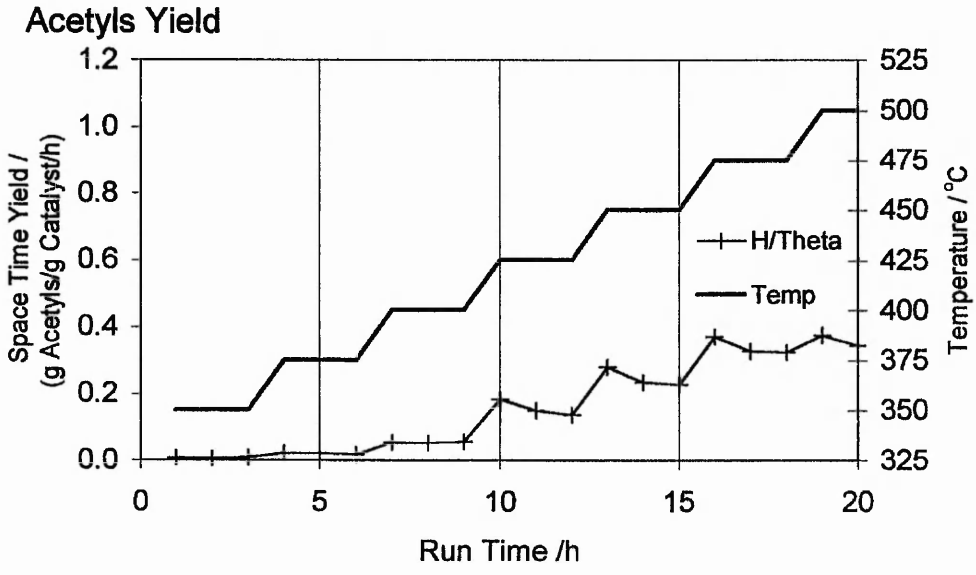

Figure 5.33 The Effect of 25°C steps to 500°C on the Space Time Yield to Acetyls for H/Theta

Profile 3: 500°C

This reaction was started at 500°C to determine whether this temperature immediately gave the maximum yield. It is evident that this is not the case. The level of conversion is virtually 100% from the start and corresponds to a very low carbon balance. The selectivity to hydrocarbons dominates, but decreases with reaction time from 90% to 50% with a corresponding increase in DME selectivity. The acetyls selectivity never rises above 20% and does not start to recover when the temperature is dropped.

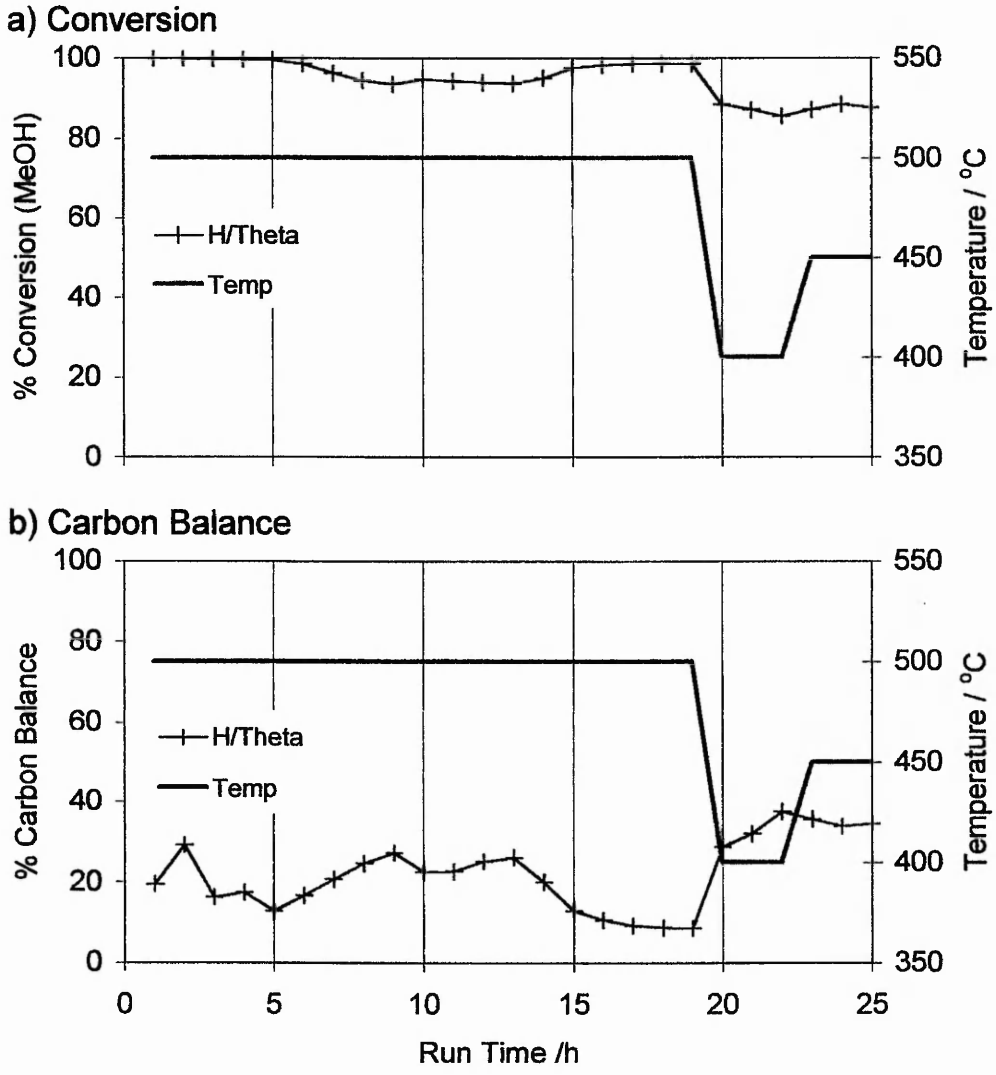

Figure 5.34 The Effect of 500°C on (a) the Conversion and (b) the Carbon Balance for H/Theta

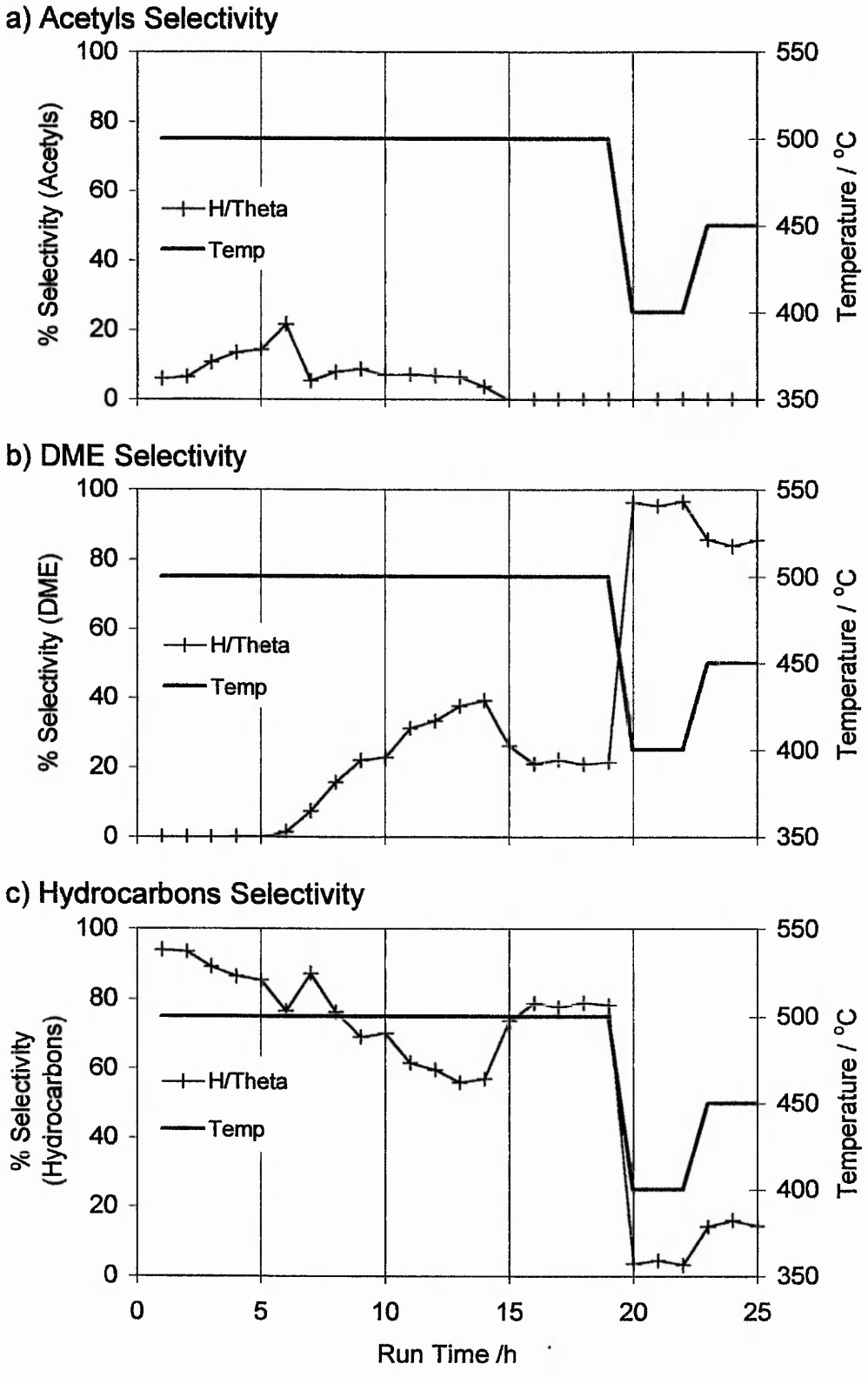

Figure 5.35 The Effect of 500°C on the Selectivities to (a) Acetyls (b) DME and (c) Hydrocarbons for H/Theta

However, the selectivity to DME becomes virtually 100% and dominates over the hydrocarbon formation.

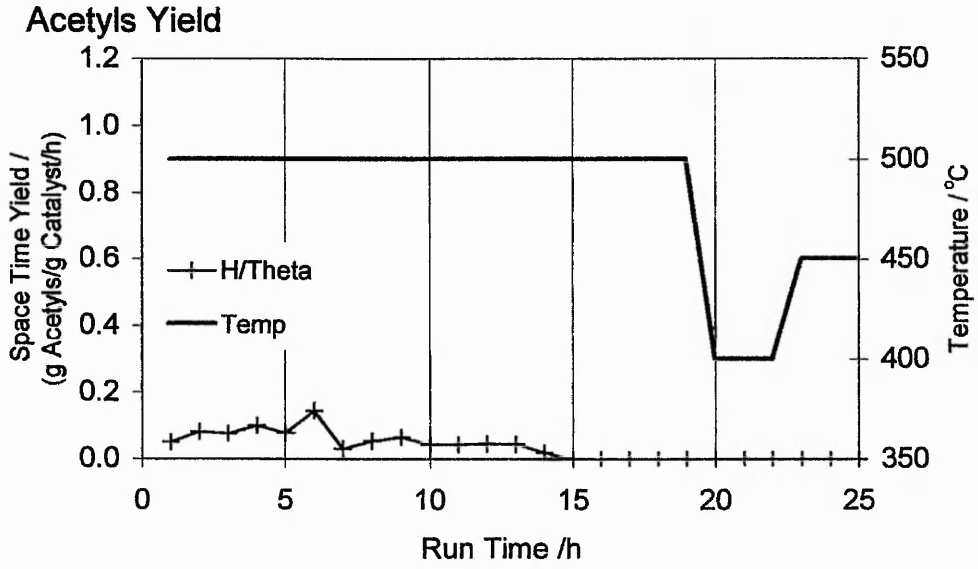

Figure 5.36 The Effect of 500°C on the Space Time Yield to Acetyls for H/Theta

The initial high temperature therefore causes irreversible damage and prevents any significant formation of acetyls. The initial low temperature treatment does not attain the brief maximum yield that occurs following the large temperature rises. For profile 2, the significant yield of acetyls is accompanied by the formation of hydrocarbons, which competes and appears to cause the acetyls yield to decline. To produce a maintained, but smaller yield, the following temperature profiles were maintained below 475°C to prevent the onset of hydrocarbon formation.

Profile 4: 350 – 450°C in 25°C steps

Only the acetyls yields are shown here, as the conversion and carbon balance remain unchanged from those observed in profile 2. The selectivity to acetyls follows the same trend as for the yield, with the higher acetyls selectivity replacing the DME and the hydrocarbons being insignificant below 450°C throughout.

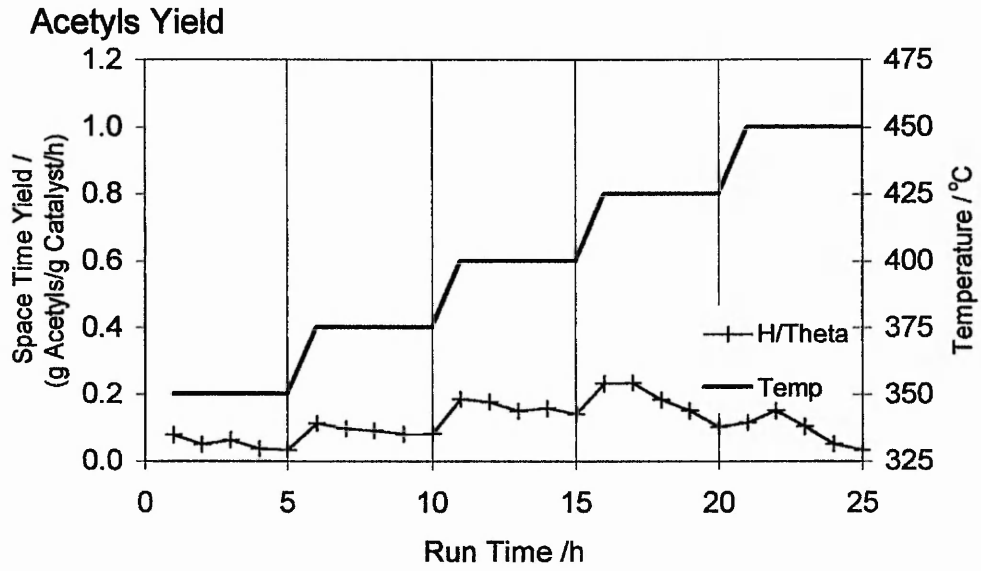

Figure 5.37 The Effect of 25°C steps to 450°C on the Space Time Yield to Acetyls for H/Theta

Again, the maximum yield is not attained as previously observed between 400-450°C. This reaction suggests that with the current temperature profile the maximum yield obtainable may be maintained at 400°C, as a further increase in yield is not observed. The final temperature increase is clearly detrimental and corresponds, as before, to the first significant selectivity to hydrocarbons.

Profile 5: 350 – 400°C in 25°C steps

This reaction shows there is some variation in performance between different reactor loadings of this H/Theta sample. As before, an increase in acetyls yield is seen with each temperature rise. However, the step is larger for this case and the yield is ~0.4 g/g/h at 400°C compared to 0.2 g/g/h produced in profile 4. The higher yield is also maintained for 8 hours before decreasing to a stable 0.2 g/g/h for the remaining 5 hours reaction time.

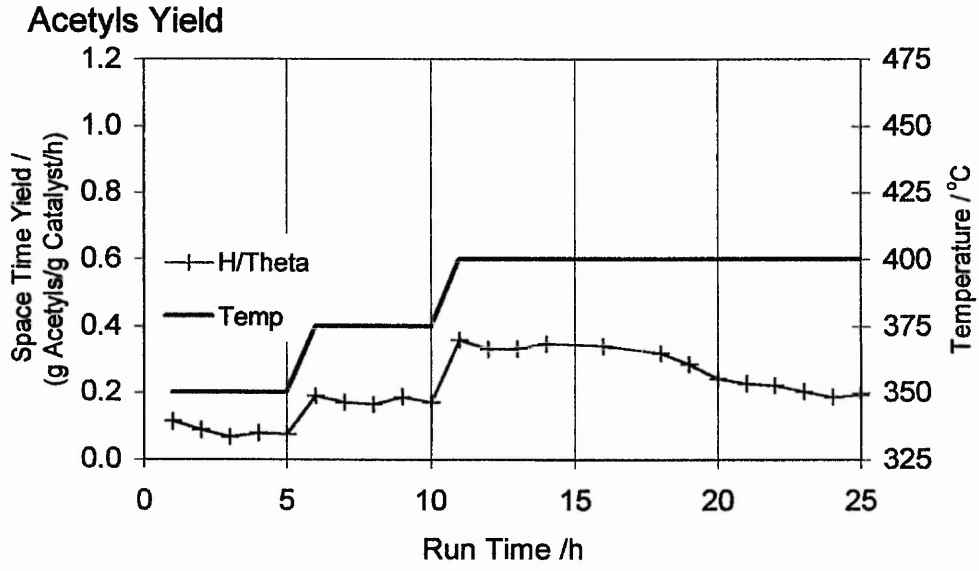

Figure 5.38 The Effect of 25°C steps to 400°C on the Space Time Yield to Acetyls for H/Theta

Although sample dependent, this temperature programing procedure has enabled an equivalent yield to be maintained using H/Theta as was obtained with mordenite, but without the initial production of the hydrocarbons. The only significant by-product is DME, which can be considered to be equivalent to the initial methanol feed.

Introduction of copper

As presented earlier in this chapter, there is a slight increase in the acetyls yield, following the introduction of copper by ion-exchange. Subsequent copper analysis determined a very low loading (0.1 wt%) to be present. It is of interest therefore, to increase the amount of copper incorporated into the framework, and this was done by the techniques previously described (Chapter 2). The amounts of copper present are listed in Table 5.2 page 156.

Again, for the same reasons as earlier, only the acetyls yields will be presented here.

Controlled copper exchange

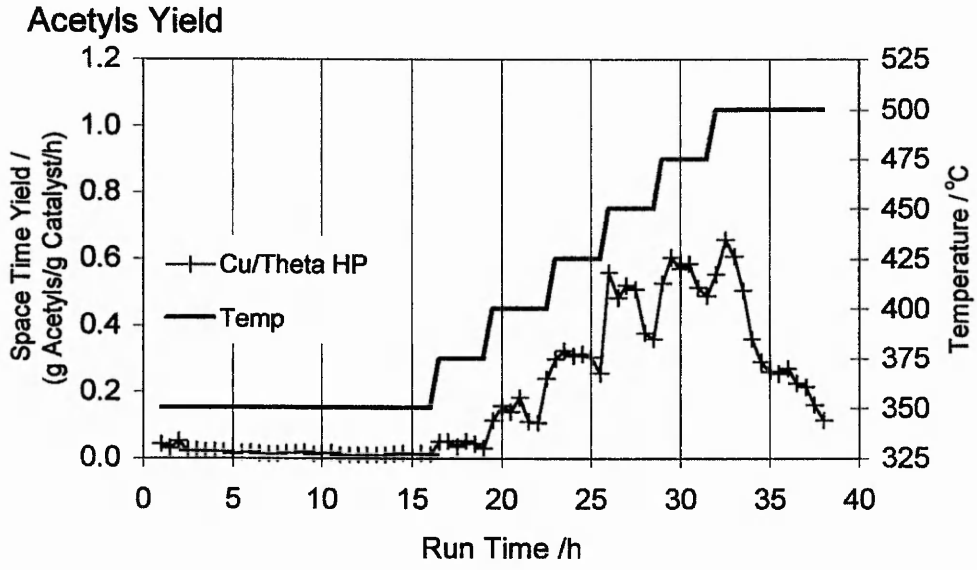

Figure 5.39 The effect of copper on the acetyls yield for Cu/H/Theta HP

Without increasing the temperature, no significant acetyls yield is observed. The maximum yield of 0.6 g/g/h is attained at 450°C. Unfortunately, the yield can not be maintained, without further temperature increases that cause it to decrease faster. The maximum yield observed here is lower than for the temperature programing of H/Theta, but it does occur at a lower temperature.

Solid state copper exchange

A significant yield of 0.2 g/g/h does not occur until the temperature reaches 425°C. The yield is still low and decays to half its initial value after 10 hours, before being restored on raising the temperature further.

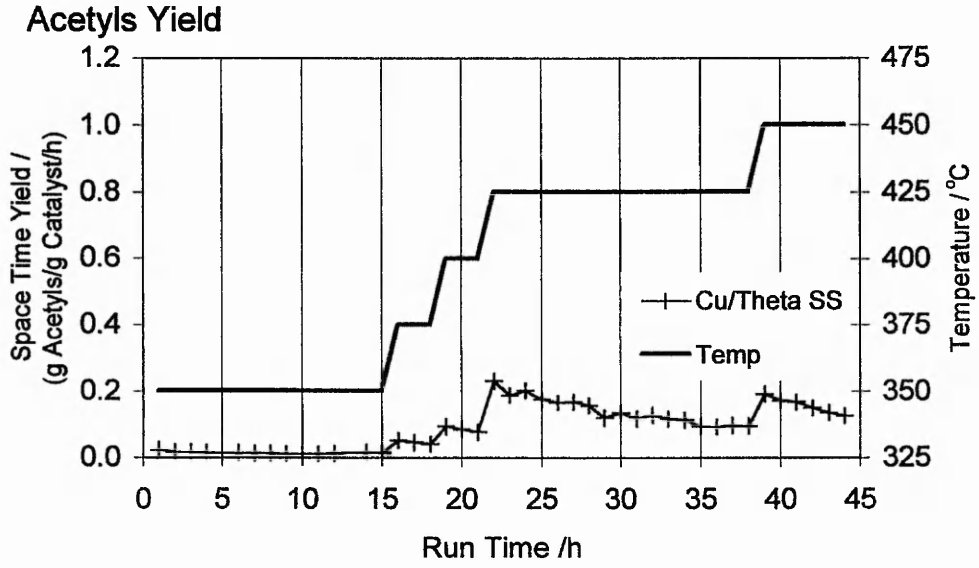

Figure 5.40 The effect of copper on the acetyls yield for Cu/H/Theta SS

References

1. Barri, S.A.I., Smith, G.W., White, D., Young, D., *Nature,* 1984, **312,** 533-534.

2. Masuda, T., Fujikata, Y., Mukai, S.R., Hashimoto, K., *Appl. Catal. A-Gen.*, 1998, **172,** 73-83.

3. *Introduction to zeolite science and practice,* vanBekkum, H., Flanigen, E.M., Jansen, J.C., (Eds.), Elsevier Science Publishers B.V., Amsterdam, 1991, 773.

4. Jansen, J.C., Creyghton, E.J., Njo, S., vanKoningsveld, H., vanBekkum, H., *Catal. Today,* 1997, **38,** 205-212.

5. Rubin, M.K., Chu, P., US Patent 4 954 325, (1990).

6. Corma, A., *Microporous Mesoporous Mater.,* 1998, **21,** 487-495.

7. Lawton, S.L., Leonowicz, M.E., Partridge, R.D., Chu, P., Rubin, M.K., *Microporous Mesoporous Mater.,* 1998, **23,** 109-117.

CHAPTER 6

INFLUENCE OF THE FRAMEWORK ON CATALYTIC REACTIVITY

Introduction – Aims of the chapter

The catalytic results for each framework, presented in Chapter 5, are considered in turn and are interpreted in terms of the mechanism proposed in Chapter 4. Firstly, the mechanism and results are briefly summarised.

Introduction – Summary of the mechanism for mordenite

The activation of methanol, or dimethyl ether (DME), by mordenite requires the presence of Bronsted acid sites. The extent of CH_3^+ formation is uncertain but when the acid site is isolated, the insertion of carbon monoxide can occur to produce the CH_3CO^+ species. Subsequent reaction with methanol, DME or water creates the final acetyls product.

Ion-exchanged copper (II) promotes carbonylation in two possible ways. Firstly, with the creation of a Bronsted acid site on the reduction to copper (I), the neighbouring copper cation increases the concentration of carbon monoxide at the activated methanol. Secondly, creation of the extraframework aluminium species, again during the reduction process, further reduces the acid site concentration and promotes the formation of DME over that to the first carbon – carbon bond of the hydrocarbon byproducts.

Introduction – Summary of the reactor results

1. As the channel intersection volume increases in the order: Theta-1 < MOR < ZSM-5 < Beta, the selectivity of methanol to hydrocarbons increases.
2. Careful temperature programming produces a stable yield of acetyls from H/Theta, equivalent to that from mordenite.
3. ZSM-5 produces a similar stable yield of acetyls as mordenite, with the major byproducts being hydrocarbons in place of DME.
4. Beta does not yield acetyls, but produces both DME and hydrocarbons.
5. The unique framework of MCM-22 gives rise to both acetyls and hydrocarbons.
6. Compared to mordenite, the levels of copper introduced into the other frameworks do not significantly modify their selectivity to acetyls.

Optimisation of H/Theta

Both the one dimensional channel structure of H/Theta and its low aluminium content (SAR 54) cause the acid sites within the channels to be isolated from each other, especially when compared to the frameworks containing interconnecting voids. At best, two sites could be at opposite sides of the same channel, but then they would only be able to interact with the same methanol molecule. The inability of H/Theta to concentrate activated methanol, especially below 450°C, prevents the formation of the first carbon – carbon bond and hence the hydrocarbons. However, methanol adsorbed at the isolated acid sites causes DME to be the major product. Considering the high concentration of DME immediately formed, it is proposed, as for mordenite, that methanol and DME can be considered to be equivalent reagents at the active sites. The extent of CH_3^+ formation is not known, but compared to mordenite, the necessesity for higher temperatures before significant acetyls formation, suggests the extent of the initial charge separation is not as great in H/Theta. Additionally, both selectivities to acetyls and hydrocarbons increase with temperature, this suggests that a similar degree of charge separation is required for both mechanisms to occur. It is the concentration of methanol activated by neighbouring sites, which determines the end product. A low concentration favours the acetyls whilst a high concentration favours the formation of the hydrocarbons.

The regeneration of the acetyls formation immediately after each temperature increase suggests that the active sites become temporarily blocked by a strongly adsorbed species, most likely acetic acid which in Chapter 2 was shown to stick within mordenite. The higher yield of methyl acetate observed for all the reactions using H/Theta may be due to the high concentration of DME and methanol, but the formation of DME from methanol should also give the equivalent concentration of water. It may therefore be proposed that acetic acid is formed, but is retained within the zeolite and only released when it is converted to the more mobile ester.

A change in mechanism is proposed to occur between 450 & 500°C, as indicated by the significant increase in the formation of hydrocarbons, the C6s in particular, in preference to DME. The preferential formation of aromatics from methanol is found at similar temperatures for the Bronsted acid sites of other zeolites[1], e.g. H/ZSM-5. Perhaps 500°C is sufficient to allow the complete dehydration of the adsorbed methanol, or demethanolation of adsorbed DME, to create isolated CH_3^+ species which

subsequently react with further methanol to preferentially produce further carbon – carbon bonds. The constant formation of hydrocarbons at the higher temperatures suggests the active sites responsible are retained, furthermore the same sites are responsible for the return of the acetyls activity on lowering the temperature. The active sites for carbonylation are proposed to be within the channels of H/Theta rather than the relatively low concentration of external surface acid sites present. Carbonylation being promoted by the narrow channel structure further increasing the effective concentration of carbon monoxide around the isolated and activated methanol. All the catalyst samples discharged from the reactor were black with coke, especially after increasing the temperature above 450°C. The internal sites would be rapidly deactivated by the formation of coke blocking the one-dimensional channels, but this is not observed. It is proposed therefore that above 500°C further reactions involving the initially formed aromatic hydrocarbons occur at the unrestricted external surface sites, possibly with methanol, giving the detected lighter hydrocarbon products and coke. The hydrogen content of the coke from profile 1 (H:C ratio 1.2) is too high for pure aromatic species and suggests that the deposited coke is possibly formed of polymethylated/polyaromatic species.

The variation in the maximum acetyls productivity, observed between the temperature profiles 2, 4 & 5, is possibly due to different extents of dehydroxylation occurring during pretreatment, causing, as with mordenite, the formation of extraframework aluminium sites that are inactive for carbonylation.

The comparable stable acetyls yields obtained from mordenite (SAR 20) and H/Theta (SAR 54) suggest that a few isolated Bronsted acid sites are preferable to a high site concentration for efficient methanol carbonylation.

The introduction of copper by ion exchange, although only in a small concentration, promotes the acetyls formation. The low uptake of copper is explained by the isolated nature of the acid sites in the restricted channels making it difficult to stabilise the hydrated divalent copper. It is possible that the hydrated copper coordinates to a ring of framework oxygens, similar to sites B & D in mordenite, equidistant between two framework aluminiums. As for mordenite, it is expected that the copper remains divalent during calcination, possibly forming the $[CuOH]^+$ species and a Bronsted acid site, rather than complete dehydration and dehydroxylation. The further pretreatment in carbon monoxide causes reduction to copper (I) with the creation, or retention, of the

Bronsted acid site at the second aluminium. It is postulated that the intially high SAR 54 for this H/Theta sample makes further dealumination of the framework unfavourable during the pretreatment. The overall result is the creation of an active site, consisting of a copper (I) cation coordinated close to a Bronsted acid site, in a channel of similar diameter to the earlier proposed 8-T-ring channel site in mordenite. The copper (I) cation in close proximity to the Bronsted acid site is thought to increase the concentration of carbon monoxide at the acid site[2], so that the possibility of carbon monoxide insertion at the adsorbed CH_3^+ species is increased. Once the CH_3CO^+ species is formed, a further water or methanol reacts to form acetic acid or methyl acetate respectively and restore the acid site.

The carbonylation productivities for the proton forms of both mordenite and theta are promoted only by the presence of ion-exchanged copper. Copper introduced under similar conditions[3] to the basic ones, during the controlled ion-exchange procedure, are reported to precipitate the copper species onto supports which explains the complete uptake of all the copper in solution by the zeolite. The introduced copper is not coupled with a Bronsted acid site within the channel structure and is detrimental to the productivity. Similarly, the conditions required for the solid state exchange of copper cause the dehydroxylation of Bronsted acid sites, if not dealumination, further reducing the concentration of the active acid sites. In both procedures, copper is preferentially deposited at the external sites of the crystallites, restricting access to the remaining acid sites and requiring the use of the harsher conditions.

H/ZSM-5

Compared to theta, the three-dimensional ZSM-5 structure exhibits a larger pore volume although their channels are of similar cross section. Considering the two frameworks have similar aluminium contents, ZSM-5 (SAR 50) produces a greater proportion of hydrocarbons than H/Theta (SAR 54.5). Furthermore, the hydrocarbon selectivity of ZSM-5 is much greater than for mordenite of similar pore volume and significantly higher aluminium content. Comparing the three frameworks it is concluded that hydrocarbons are preferentially formed in the larger cavities at the channel intersections of the ZSM-5 structure. It has been detemined theoretically that for H/ZSM-5 a significant proportion of the acid sites is present in the channel intersections[4]. Products smaller than the 10-T-ring channels, once formed, rapidly diffuse out whilst larger products are retained within the larger void until they are reconverted into smaller products[5]. This is one explanation given for the higher para-xylene selectivity[6] observed during the methylation of toluene over H/ZSM-5, and secondly for its high resistance to deactivation by coke formation[7].

It is proposed the concentration of acid sites directed into one internal cavity is able to promote the formation of hydrocarbons from methanol. C^{13} MAS NMR has observed that aromatics are directly formed from labelled methanols even in the presence of toluene[8]. If a methanol forms the CH_3^+ group at one Bronsted acid site, it is close enough to other methanols activated by the surrounding framework sites to form the initial carbon-carbon bond. One mechanism for the conversion of methanol does propose that the zeolite is an activated methanol reservoir[9], or 'carbon pool', promoting the production of hydrocarbons. It is therefore not necessary, for all the Bronsted acid sites present to be strong ones to produce a high hydrocarbon yield.

The complete lack of DME suggests two things, firstly DME is equivalent to methanol as a reagent, and secondly, all the methanol and DME interacts with the acid sites present to form intially the CH_3^+ species followed by hydrocarbons or acetyls. The higher concentration of acid sites favouring the hydrocarbons.

Ion-exchanged copper reduces the acid site concentration and therefore the methanol and DME conversion. The redox behaviour of the copper is expected to be the same as for mordenite, but copper is assumed unable to isolate single acid sites.

H/BETA

The reaction of methanol over zeolite Beta has been reported twice[10,11], both using similar conditions as this work. The major volatile product initially detected, in both cases, was iso-butane. The first reported work also used acetic acid as the initial reagent under the same conditions and observed that iso-butene was the major volatile product. In the present work, different C4 by-products could not be quantified separately, under the conditions required for separating methanol from DME. The C4's being a significant fraction (~25%) of the detected hydrocarbons supports, the reported formation of iso-butane from methanol, and also iso-butene from acetic acid. It is therefore proposed that the further conversion of acetic acid to isobutene may account for the observed low acetyls yield. It can not be verified why, of the frameworks tested, only the H/Beta framework would further convert acetic acid to isobutene. It is suspected that a high concentration of acid sites, within the large channels, allows sequential reactions of the acetyls to occur.

The coke deposited within the beta framework has twice the hydrogen content than any of that formed in the pentasil frameworks tested. The coke of the pentasil frameworks (H:C = 1) is assumed to be highly aromatic in nature, with the additional methyl groups balancing the polyaromatic species. The greater hydrogen content of the coke on H/Beta (H:C = 2) strongly suggests the formation of polyaliphatic species. The high C6 content suggests that aromatic species diffuse out of the framework rather than undergo further conversion to produce polyaromatic coke. It is tentatively proposed that the presence of higher concentrations of the unsaturated isobutene, formed from acetic acid, give rise to the formation of aliphatic C8 species which become trapped. The low C1 – C3 content in the hydrocarbon product distribution indicates that neither further scission, nor the sequential reactions of trapped polymethylated benzenes are occurring.

MCM-22 framework

Interest has been shown in this structure because the isolated channels within the same structure allow direct correlation between catalytic activity and pore size[12]. The disproportionation of toluene by propene has been widely studied in this respect[13,14].
A recent theoretical consideration[15] of the MCM-22 framework structure has predicted that aluminium and therefore its related acid sites will be present in both series of channels. Furthermore, one third of the Bronsted acid sites are positioned within the larger supercages with the remainder in the sinusoidal channels. The two experimentally observed IR bands[16] were calculated and both frequencies were found to correlate with different Bronsted acid sites present in each channel. Therefore a single IR frequency may arise from acid sites in more than one location in a framework.
The stable formation of the acetyls and hydrocarbons suggest that one product is preferentially formed in one channel structure. On considering the results, from the other frameworks tested, it is postulated that the hydrocarbons form preferentially in the larger supercage structures, similar to the intersecting voids of beta. Meanwhile, the acetyls form preferentially in the two-dimensional network of sinusoidal 10-T-channels, similar to the straight channels of theta, and without the three-dimensional interconnections of ZSM-5.
The MCM-22 framework produces coke that is solely of carbon, this suggests that large polycyclic species, similar to graphite, are formed in favour of the polymethylbenzenes reported for the pentasil zeolites. Alternatively, the disproportionation of carbon monoxide to coke and carbon dioxide may occur over the high copper loading present in this framework.

References

1. Haw, J.F., Nicholas, J.B., Song, W., Deng, F., Wang, Z., Xu, T., Heneghan, C.S., *J. Am. Chem. Soc.*, 2000, **122**, 4763-4775.

2. Sarkany, J., d'Itri, J.L, Sachtler, M.H., *Catal. Lett.*, 1992, **16**, 241-249

3. Valyon, J., Hall, W.K., *Catal. Lett.*, 1993, **19**, 109-119.

4. Hunger, M., Horvath, T., *J. Am. Chem. Soc.*, 1996, **118**, 12302-12308.

5. Perot, G., Guisnet, M., *J. Molec. Catal.*, 1990, **61**, 173-196.

6. Ribeiro, F.R., Alvarez, F., Henriques, C., Lemo, F., Lopes, J.M., Ribeiro, M.F., *J. Molec. Cat. A-Chem.*, 1995, **96**, 245-270.

7. Dejaifve, P., Auroux, A., Gravelle, P.C., Vedrine, J.C., Gabelica, Z., Derouane, E.G., *J. Catal.*, 1981, **70**, 123-136.

8. Ivanova, I.I., Corma, A., *J. Phys. Chem. B.*, 1997, **101**, 547-551.

9. Goguen, P.W., Xu, T., Barich, D.H., Skloss, T.W., Song, W., Wang, Z., Nicholas, J.B., Haw, J.F., *J. Am. Chem. Soc.*, 1998, **120**, 2650-2651.

10. Hutchings, G.J., Johnston, P., Lee, D.F., Warwick, A., Williams, C.D., Wilkinson, M., *J. Catal.*, 1994, **147**, 177-185.

11. Mikkelsen, O, Kolboe, S., *Microporous Mesoporous Mat.*, 1999, **29**, 173-184.

12. Corma, A., *Microporous Mesoporous Mat.*, 1998, **21**, 487-495.

13. Wu, P, Komatsu, T., Yashima, T., *Microporous Mesoporous Mat.*, 1998, **22**, 343-356.

14. Meriaudeau, P., Tuan, V.A., Nghiem, V.T., Lefevbre, N.F., Ha, V.T., *J. Catal.*, 1999, **185**, 378-385.

15. Sastre, G., Fornes, V., Corma, A., *J. Chem. Soc. Chem. Commun.*, 1999, 2163-2164.

16. Corma, A., Corell, C., Fornes, V., Kolodziejski, W., Perez-Pariente, J., *Zeolites*, 1995, **15**, 576-582.

CHAPTER 7

OVERALL CONCLUSIONS

The heterogeneous carbonylation of methanol to the acetyls, acetic acid and methyl acetate, in the complete absence of a halide promoter, has been carried out over a number of acidic zeolite catalysts.

This work has confirmed for mordenite, (i) the reaction requires the presence of Bronsted acid sites, and (ii) the productivity of the proton form is increased by the presence of copper. Additionally, it is concluded that the carbonylation of methanol, or dimethyl ether, is in direct competition with the formation of hydrocarbons, the outcome being determined by the acid site density of the zeolite.

Two further aims of the work were to determine, (i) the role of copper, and (ii) the effect of the framework's structure.

The role of copper

Of all the frameworks tested, the promotional effect of ion-exchanged copper is the most marked for mordenite.

Ion-exchange, followed by activation, introduces copper adjacent to the remaining Bronsted acid sites. Reduction of the divalent copper cations, by carbon monoxide, increases the concentration of the extraframework aluminium species, and therefore, further decreases the concentration of Bronsted acid sites. Copper promotes the acetyls productivity, of a proton form initially capable of carbonylation, by increasing the effective carbon monoxide concentration around the remaining Bronsted acid sites.

It is concluded, the formation of the acylium cation CH_3CO^+ occurs by the insertion of carbon monoxide at isolated CH_3^+ sites, that are unable to react with further methanols to form carbon – carbon bonds by the competing hydrocarbon mechanism.

The effect of the framework structure

The carbonylation of methanol is sensitive to the framework structure, mordenite being the most productive framework tested. The side pockets of mordenite, and the linear channels of Theta-1, provide the isolated Bronsted acid sites required to activate methanol carbonylation in a high concentration of carbon monoxide.

The channel intersections in the ZSM-5 and beta frameworks allow the interaction of neighbouring activated CH_3^+ species and the preferential formation of hydrocarbons, the incorporation of copper is not sufficient to isolate these Bronsted acid sites.
In the unique MCM-22 framework, the large supercages allow the formation of hydrocarbons, while the narrower channels promote the formation of acetyls.

FUTURE WORK

The ion-exchange of zeolite protons for metal cations replaces Bronsted acid sites with Lewis acid sites[1]. The effect of the resulting combination of Bronsted and Lewis acid sites on catalysis can not be predicted[2]. Characterisation of the active catalysts used in this work is required to determine any synergistic effects caused by the copper introduced[3]. Both the type and concentration of the active sites present can be determined by their interaction with selected probe molecules, e.g. pyridine or carbon monoxide, measured by Fourier Transform Infra Red Spectroscopy (FT-IR)[4,5].
The effect of the methanol concentration needs to be studied further for this reaction. A 1:1 ratio of carbon monoxide to methanol would be the industrially preferred reactor feed for optimal productivity[6]. However, results from this work suggest that the lifetimes and overall productivities of these catalysts could be improved by operating at very low methanol concentrations. Methanol therefore has a strong affinity for the active sites of these catalysts under the operating conditions used here. Further work at low methanol concentrations, by using a pulsed flow reactor[7] or isotopic labelling[8] of the methanol, could determine the extent of methanol's interaction. It may also distinguish whether the first hydrocarbon bond preferentially forms from one or two activated methanols.

Carbonylation is in direct competition with hydrocarbon formation, but the balance is determined by the framework structure. The testing of further structures[9], e.g. ZSM-11 the straight channel variant of ZSM-5 could provide catalysts of higher productivity.

Isolated Bronsted acid sites appear to favour carbonylation. Therefore, the determination of the acid site density to provide isolated Bronsted acid sites within a framework could be tested catalytically by the methanol carbonylation reaction.

References

1. Auroux, A., Gervasini, A., Guimon, C., *J. Phys. Chem. B.,* 1999, **103**, 7195-7205.

2. Coq, B., Tachon, D., Figueras, F., Mabilon, G., Prigent, M., *Appl. Catal. B-Env.,* 1995, **6**, 271-289.

3. Farneth, W.E., Gorte, R.J., *Chem. Rev.* 1995, **95**, 615-635.

4. Lercher, J.A., Grundling, C., Eder-Mirth, G., *Catal. Today,* 1996, **27**, 353-376.

5. Kuroda, Y., Maeda, H., Yoshikawa, Y., Kumashiro, R., Nagao, M., *J. Phys. Chem. B.,* 1997, **101**, 1312-1316.

6. Howard, M.J., Jones, M.D., Roberts, M.S., Taylor, S.A., *Catal. Today,* 1993, **18**, 325-354.

7. Ono, B.Y., Mori, T., *J. Chem. Soc. Faraday Trans. 1,* 1981, **77**, 2209-2221.

8. Mikkelsen, O., Ronning, P.O., Kolboe, S., *Microporous Mesoporous Mat.,* 2000, **40**, 95-113.

9. Ivanova, I.I., Corma, A., *Zeolites: A Refined Tool for Designing Catalytic Sites*, Bonneviot, L., Kaliaguine, S., (Eds.) Elsevier Science B.V., Netherlands, 1995, 27-34.

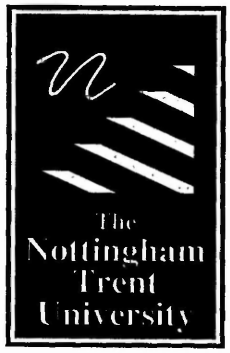

Libraries &
Learning
Resources

The Boots Library: 0115 848 6343
Clifton Campus Library: 0115 848 6612
Brackenhurst Library: 01636 817049